Research Report
High-Performance Computing in Hessen
2007/2008

12. Januar 2009

Inhaltsverzeichnis

1 Vorwort

Der für das Jahr 2008 aktualisierte Forschungsbericht dokumentiert in beeindruckender Art und Weise, in welchem Ausmaß sich die hessischen Hochleistungsrechner zu einem unverzichtbaren Forschungswerkzeug in allen Bereichen der Natur- und Ingenieurwissenschaften an den hessischen Forschungsstandorten entwickelt haben. Neben der enormen Leistungssteigerung der verfügbaren Hardware haben auch die Anstrengungen im Bereich Softwareentwicklung dazu geführt, dass computergestützte Simulationen zur Lösung von chemischen, physikalischen oder technischen Fragestellungen einen exzellenten wissenschaftlichen Reifegrad erreicht haben, so dass die theoretischen Vorhersagen mittlerweile gleichberechtigt neben den Ergebnissen experimenteller Arbeit im Laboratorium oder Technikum stehen. In anderen Fällen liefern Simulationen detaillierte Einblicke in experimentell prinzipiell unzugängliche Zusammenhänge. Entsprechend erweist sich derzeit weltweit die enge Zusammenarbeit von Simulation und Experiment als außergewöhnlich erfolgreich und effizient in der Entwicklung der wichtigsten Forschungsthemen unserer Zeit. Der vorliegende Forschungsbericht liefert eine umfangreiche Darstellung der aktuell an den hessischen Hochleistungsrechnern bearbeiteten Fragestellungen, von denen viele zentrale Bausteine für prestigeträchtige, profilbildende Verbundprojekte mit internationaler Sichtbarkeit darstellen. Wie schon im vergangenen Jahr legen wir diesen Bericht als Beleg für die ausgezeichnete Qualität der computergestützten Forschung an den hessischen Forschungsstandorten vor. Und nicht ohne Stolz präsentieren wir mit der Liste der aus diesen Projekten entstandenen Publikationen das hervorragende Niveau der Forschungsleistungen der beteiligten hessischen Arbeitsgruppen.

Prof. Dr. Max Holthausen
Vorsitzender des Hessischen Beirats für Hochleistungsrechnen
Frankfurt am Main, den 10. Dezember 2008

2 Einleitung

Die Bedeutung des Wissenschaftlichen Rechnens als eine Schlüsseltechnologie für nahezu alle Bereiche von Wissenschaft und Technik ist heutzutage unumstritten. Trotz der enormen Fortschritte im Bereich der Rechnertechnologie ist hierbei in vielen Anwendungsfällen der Einsatz von Hochleistungsrechnern unerlässlich, nicht zuletzt auch aufgrund der stetig wachsenden Komplexität der Problemstellungen. Das Hochleistungsrechnen trägt entscheidend zur Reduktion von Entwicklungszeiten neuer Methoden und Technologien bei. So können Probleme angegangen werden, die aufgrund der hohen Anforderungen an die Rechenleistung anderweitig einer numerischen Simulation nicht zugänglich sind.

Der Verfügbarkeit einer adäquaten Hochleistungsrechnerkapazität kommt damit für den Wissenschaftsstandort Hessen eine große Bedeutung zu, da diese die Grundlage für eine national und international konkurrenzfähige Forschung im Bereich des Wissenschaftlichen Rechnens darstellt. Der Erfolg von Sonderforschungsbereichen, Forschergruppen, Graduiertenkollegs und einer Vielzahl unterschiedlicher Einzelprojekte hängt entscheidend davon ab.

Der Hochleistungsrechenbedarf in Hessen wird durch zentrale Rechenkapazitäten auf Landesebene gedeckt. Aufgrund unterschiedlicher Anforderungen der Nutzer werden zwei größere Systeme mit unterschiedlichen Architekturen betrieben:

- Ein SMP-Cluster an der TU Darmstadt für Anwendungen mit feingranularer Parallelität mit vergleichsweise hohen Anforderungen an die Kommunikationsleistung, wie z.B. Strömungssimulationen oder Strukturrechnungen komplexer Quantensysteme.
- Ein MPP-Cluster an der Universität Frankfurt für Anwendungen mit grobgranularer Parallelität mit vergleichsweise geringen Anforderungen an die Kommunikationsleistung, wie z.B. Vielteilchendynamik in Stoßprozessen.

Dem Darmstädter Forschungszentrum CE und dem Frankfurter CSC kommt die Funktion von Kompetenzzentren im Bereich des Hochleistungsrechnens zu. Die notwendige fachübergreifende Kompetenz ist durch die interdisziplinäre Zusammensetzung der beiden Zentren, sowie durch entsprechende Aktivitäten der Mitglieder in Forschung und Lehre gewährleistet. Damit leisten beide Zentren einen Beitrag zu den folgenden Aufgaben:

- Entwicklung bzw. Weiterentwicklung von Anwendungssoftware für den Hochleistungsrechner in den verschiedenen Anwendungsbereichen
- Unterstützung von Nutzern bei der Portierung von Anwendungssoftware
- Ausbildung von wissenschaftlichem Nachwuchs im Bereich des Wissenschaftlichen Rechnens
- Technologietransfer in die Industrie im Rahmen von Kooperationsprojekten
- Organisation von regelmäßigen Benutzer-Kolloquien, die den Erfahrungsaustausch zwischen allen Nutzern des Rechners ermöglichen

- Kontaktpflege und Zusammenarbeit mit anderen im Bereich des Hochleistungsrechnens tätigen Arbeitsgruppen im In- und Ausland (z.B. Workshops, Forschungsprojekte)

Die Rechenzentren der hessischen Universitäten betreiben den Rechner gemeinsam unter Federführung der Rechenzentren der TU Darmstadt und der Universität Frankfurt, an denen die Rechner installiert sind. Zu den Aufgaben der Rechenzentren an den beiden Standorten gehören:

- Bereitstellung von Räumlichkeiten und der zugehörigen Infrastruktur
- Administration und Operating (24-Stunden-Betrieb)
- Betriebssteuerung und Überwachung der Betriebsvorgaben
- Fehlerverfolgung und -behebung
- Benutzerverwaltung
- Datensicherung

Die Rechner sind für Nutzer aller hessischen Universitäten zugänglich. Die einzelnen Rechenzeitkontingente richten sich nach den finanziellen Beteiligungen der Hochschulen, Fachbereiche bzw. Fachgebiete.

3 Technik und Organisation

3.1 Der HHLR am Forschungszentrum Computational Engineering (CE) in Darmstadt

3.1.1 Systemaufbau

Im Jahren 2007/2008 (bis Novermber 2008) bestand der Hessische Hochleistungsrechner in Darmstadt aus 65 Shared Memory Rechnern (SMP) unterschiedlicher Leistungsfähigkeit mit insgesamt 560 Power5-Prozessoren. Der Zugang erfolgt über einen speziellen Loginknoten. Auf diesem kann der Nutzer seine Programme vorbereiten, sowie Daten analysieren und abholen. Rechenknoten im Backend sind für den Nutzer nicht direkt zugänglich, sondern werden über ein Queuing-System angesprochen. 60 dieser Rechenknoten sind mit jeweils acht Power5 CPUs ausgestattet fünf weitere verfügen über je 16 Power5+ Prozessoren. Die Power5-Prozessoren sind in der Lage, vier Floatingpoint-Operationen pro Takt auszuführen und haben einen internen Cache von 36MB. Ausserdem verfügen diese für Computingaufgaben optimierten Maschinen über eine deutlich höhere Speicherbandbreite als Commodity-Hardware. Damit eignen sie sich besonders gut für HPC-Andwendungen.

Als SMP-Rechner sind die Maschinen prädestiniert für parallele Probleme mit hohem Kommunikationsbedarf. Innerhalb eines Knotens werden Kommunikationsleistungen erreicht, die mit denen der Bundeshöchstleistungsrechner vergleichbar sind. Um auch Programme, die mehr als einen SMP-Knoten benötigen, effektiv ausführen zu können, sind die Rechner untereinander mit einem schnellen, latenzarmen, internen Netzwerk verbunden (IBM High Performance Switch (HPS))

Das Hochschulrechenzentrum (HRZ) der TU Darmstadt betreibt das Rechnersystem im Auftrag des HHLR-Beirats sowie der Kompetenzgruppe wissenschaftliches Hochleistungsrechnen im Forschungszentrum Computational Engineering (CE).

3.1.2 Systemerneuerung im Herbst 2008

Um mit den mit dem technischen Fortschritt wachsenden Anforderungen gerecht zu werden, wurde der Rechner im Oktober/November 2008 durch die TU Darmstadt modernisiert. Das neue System ist identisch mit dem Entwicklungscluster (JUMP) des Bundeshöchtleistungsrechners in Jülich. Auch am Höchstleistungsrechner in Garching (RZG

MPI/IPP) und am Deutsches Klimarechenzentrum (DKRZ) kommt die gleiche Technik zum Einsatz. Das System ist damit bestens geeignet, als Brücke zwischen den PC-Clustern eines Instituts und den deutschen Höstleistungsrechnern zu fungieren.

Das neue System besteht aus einem Cluster von 14 Rechnernknoten mit jeweils 32 Power6-Prozessoren. Bei einer Taktfrequenz 4,7 GHz kommt das Cluster somit auf eine Peakperfomance von 8,5 TFlop/s. Die Rechnenknoten sind mit einem Arbeitsspeicher von 128 GB (einer sogar mit 256 GB) ausgestattet. Auch wenn bei Weitem nicht alle Problemstellungen soviel Speicherplatz benötigen, ist es wichtig, dass gerade die zentralen Rechencluster diese Resourcen vorhalten, da Problemstellungen, die diese Anforderungen haben, auf konvetioneller Hardware nicht lauffähig sind.

Durch die 32 in einem System integrierten Prozessoren können auch sehr kommunikationslastige Programme bis zu 32 CPUs (bisher max. 16 CPUs) nutzen. Ausserdem sind jetzt alle Rechenknoten latenzarm über Infiniband vernetzt. Aufgabenstellungen mit moderateren Anforderungen an die Komunikationsleistung können also auch auf mehrere Knoten verteilt werden.

3.1.3 Auslastung des HHLR

Der Rechner wurde im November 2005 ausgebaut. Bereits im Januar 2006 wurde von den Nutzern mehr Rechenzeit abgerufen, als vor dem Ausbau verfügbar war. Seit März 2007 arbeitet das System mit einer Auslastung von über 80%. Auf vergleichbaren Systemen wird das üblicherweise als defakto vollständig ausgelastet bezeichnet.

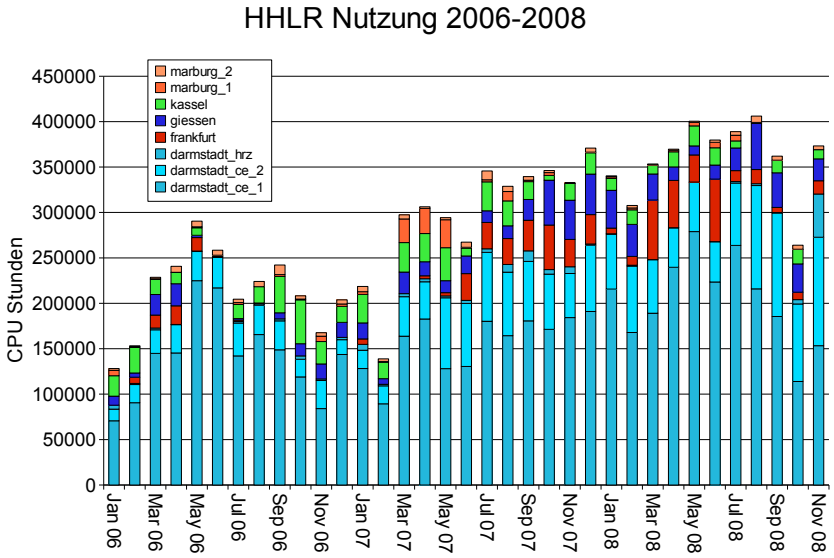

Abbildung 3.1: *Verteilung der Rechnezeit auf die einzelnen Universitäten*

Daher sind wird durchaus stolz darauf, dass es uns im Jahr 2008 gelungen ist, das Scheduling und – in enger Zusammenarbeit mit den Nutzern – auch die Jobstruktur so zu

optimieren, dass seit April eine Auslastung von mehr als 90% erreicht wurde. In den Sommermonaten stieg die Auslastung auf anähernd 95%. Der Abfall im Herbst ist auf die beginenden Umbauarbeiten zurück zuführen.

Die Zuweisung der Rechenzeit an die Wissenschftler der einzelnen Standorte richtet sich nach der Beteiligung der jeweiligen Hochschule an den Investitionskosten. Die TU Darmstadt hat ein Kontinget von 67,5%, der Uni Giessen und Marburg stehen 11,3% bzw. 10,8% zu und die Univesiäten in Franfurt und Kassel haben einen Anspruch auf 5,2% der Rechenzeit. Wenn ein Standort sein Kontingent nicht ausschöpft, so wird die Rechenzeit auf die anderen Standorte verteilt.

2008 wurde der Rechner durch die Uni Marburg kaum noch genutzt. Im Jahresdurchschnitt haben Marburger Wissenschaftler nur 1,4% der insgesammt verfügbaren Rechenzeit abgerufen. Von dieser Zurückhaltung profitiert haben die TU Darmstadt (70%) und die Uni Frankfurt (7,3%), die in 2008 deutlich mehr Rechenzeit in Anspruch nehmen konnten als das Konntingent vorsieht. Die Nutzung durch Wissenschaftler aus Giessen und Kassel liegt mit 8% bzw. 3,7% im Rahmen der Planungen.

3.1.4 HPC-Ausbildung an der TU Darmstadt

Mit dem Bachelor- und Master-Studiengang Computational Engineering sowie der Graduiertenschule Computational Engineering wurde an der TU Darmstadt ein durchgängiges konsekutives Konzept zur interdisziplinären Ausbildung im Bereich des HPC etabliert. Der Bachelor-/Master-Studiengang wird vom fachbereichsübergreifenden Studienbereich Computational Engineering organisiert und betreut, der von den Fach- und Studienbereichen Mathematik, Mechanik, Bauingenieurwesen und Geodäsie, Maschinenbau, Elektrotechnik und Informationstechnik, Informatik und dem Forschungszentrum Computational Engineering getragen wird. Den Studierenden werden mathematische, informationswissenschaftliche und ingenieurwissenschaftliche Kenntnisse, mit denen sie physikalische und technische Systeme modellieren und simulieren können, vermittelt. Methoden des HPC sind hierbei ein wesentlicher Bestandteil. Das Ausbildungskonzept wird durch die Graduiertenschule Computational Engineering komplettiert, in welche die Studierenden bereits nach dem ersten Masterjahr eintreten können, und nach weiteren vier Jahren mit einer Promotion abschließen können. HPC ist ein zentrales Querschnittsthema der Forschungsarbeiten an der Graduiertenschule.

3.2 Linux Cluster am Center for Scientific Computing (CSC) der Uni Frankfurt

Das Center for Scientific Computing (CSC) der Goethe-Universität betreibt einen der beiden hessischen Hochleistungsrechner. Das CSC wurde im Jahr 2002 als gemeinsame Initiative von 15 Forschungsgruppen der naturwissenschaftlichen Fachbereiche der Universität Frankfurt ins Leben gerufen. Ausgangspunkt für seine Gründung war die Erkenntnis, dass in den modernen Naturwissenschaften die Bewältigung komplexer numerischer Aufgaben eine zentrale Rolle einnimmt.

Das CSC bietet daher neben der Bereitstellung einer umfangreichen Rechenkapazität für die Projekte der beteiligten Forschergruppen ein fachübergreifendes Forum auf dem Gebiet Computational Science in Form von interdisziplinären Vorträgen. Darüber hinaus bietet das CSC einen zweijährigen englischsprachigen Masterstudiengang in Computational Science an. Der Studiengang ist in modularer Form konzipiert, so dass alle Studienleistungen in Form von international anerkannten Credit Points gemäß dem European Credit Transfer System bewertet werden. Die durchweg in englischer Sprache gehaltenen Kurse eröffnen auch ausländischen Studierenden eine interdisziplinäre Ausbildung in allen Bereichen der Computer Simulation.

Die Forschungsaktivitäten der am CSC arbeitenden Wissenschaftlern umfassen eine große Zahl von Projekten mit hohem numerischen Aufwand. Die Projekte, die auf dem CSC-Cluster bearbeitet werden, umfassen eine weite Spanne aktueller Themenbereiche. Sie erstrecken sich über so unterschiedliche Gebiete wie die Untersuchung der Strukturen von Proteinen in der Biochemie und die Eigenschaften von Kristallen unter höchstem Druck in der Geophysik. Die Dynamik der Grundbausteine der Materie, der Quarks, und Gluonen, im Urknall und bei Hochenergieexperimenten werden in der theoretischen Physik auf dem CSC simuliert. Wissenschaftler des Frankfurt Institute for Advanced Studies modellieren komplexe atomare Strukturen und untersuchen die Möglichkeiten der Krebstherapie mit Schwerionenstrahlen.

Der Hochleistungsrechner des CSC besteht aus 2 Linux MPP-Clustern (CSCII und CSCIII), die über das schnelle universitätsweite Netz (10Gbit/s) verbunden sind.

Der Cluster CSCII wurde im Jahr 2004 in Betrieb genommen. Die Anlage besteht aus 10 wassergekühlten Racks, die 282 Rechenknoten enthalten, welche jeweils mit 2 64bit Opteron CPUs mit einer Taktrate von 1,8 GHz bestückt sind. Die Knoten sind standardmäßig mit 4 GByte Hauptspeicher ausgerüstet. 15 Knoten wurden auf 8 GByte, weitere 15 auf 16 GByte Speicher aufgerüstet. 64 Knoten sind mit Myrinet schnell vernetzt, die übrigen Knoten mit Gigabit Ethernet verbunden. Das RAID-System verfügt über 10 TByte Plattenplatz.

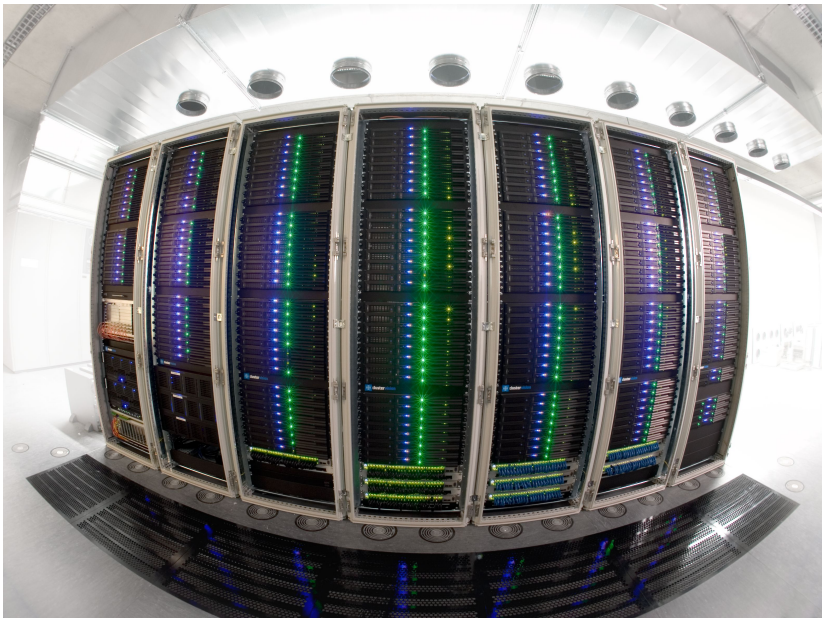

Das Clustersystem CSCIII wurde in 2006 zur Benutzung freigegeben und Anfang 2007 ausgebaut. Es besteht aus 251 Knoten, die jeweils mit 2 DualCore 2GHz Opteron CPUs ausgestattet sind. Jeder Knoten verfügt über 8 GByte Hauptspeicher, zusätzlich sind 44 Knoten auf 16 GByte aufgerüstet worden. 64 der Knoten (und damit 256 Prozessorkerne) sind über Myrinet schnell vernetzt. Ein Raid-System stellt 25 TByte Speicherplatz zur Verfügung.

Durch den stetigen Ausbau verfügt das CSC damit über ein MPP-System aus insgesamt 1568 Prozessoren mit einer theoretischen Rechenleistung von 6 TFlop/s. Der anstehende Ausbau des CSCIII, der bis Mitte 2009 abgeschlossen sein wird, wird die bestehende Rechenkapazität verdoppeln.

Ab Januar 2009 steht allen Mitgliedern des CSC im Rahmen ihrer jeweiligen Rechenkontingente ein kleiner GPGPU-Cluster (Scout) als experimentelles System zur Verfügung. Das System besteht aus 9 Recheneinheiten, wobei jede Einheit aus zwei CPU- und drei GPU- Knoten besteht. Die CPU-Systeme bestehen aus zwei QuadCore Xeon CPUs mit 16 Gbyte Hauptspeicher. Die GPU-Knoten sind Tesla S1070 Systeme von Nvidia. Jeder GPU-Knoten leistet 4 Tflop/s single precision (sp), bzw 345GFlop/s double precision (dp), so dass das Gesamtsystem eine Spitzenleistung von 108 TFlop/s sp, bzw 9.3 Tflop/s dp erreicht. Die Kommunikation innerhalb einer Recheneinheit erfolgt über PCI Express, die Kommunikation zwischen den Recheneinheiten wird ab 2009 durch ein Infiniband-Netzwerk erweitert. Ziel des Scout ist es, allen interessierten Arbeitsgruppen Erfahrungen im Einsatz von GPGPU-Systemen zu ermöglichen.

Den Nutzern wird eine Vielzahl von Softwarepaketen und Compilern zur Verfügung gestellt. Die Datensicherung aller Systeme erfolgt über das Backup-System des Hochschulrechenzentrums der Universität.

Mehr als 450 Wissenschaftler aus über 90 Arbeitsgruppen aus dem Bereich der Naturwissenschaften, Mathematik und Informatik sorgen für eine vollständige Auslastung des Rechners über das ganze Jahr. Etwa ein Viertel der verfügbaren Rechenzeit wird von Gruppen aus Darmstadt, Marburg, Gießen und Kassel verbraucht.

Die Finanzierung der Anlage erfolgte überwiegend durch Beiträge Frankfurter Hochschullehrer und –Institutionen, sowie Zuschüsse des Landes Hessen und des Bundes (im Rahmen des HBFG und Forschungsgroßgeräte-Programms). Über den Verbund der Hessischen Hochleistungsrechner (HHLR) haben Wissenschaftler aller hessischen Hochschulen Zugang zu den Computersystemen des CSC.

4 Projektberichte

4.1 Chemie

4.1.1 Control of the Transmembrane Potential in K^+ Channel Simulations

Stefan M. Kast, Michael Kreim, Gerhard Thiel// Eduard-Zintl-Institut für Anorganische und Physikalische Chemie, Institut für Botanik, Technische Universität Darmstadt

The transmembrane potential represents the electric voltage difference between the interior (cytosol) and the exterior of a cell. Interior and exterior regions are electric conductors whereas the thin separating region, the cell's plasma membrane, is highly resistive. Due to the different ionic composition of cytosol and exterior solution and due to the presence of ion channels and transporters in the membrane, the resting membrane potential is different from zero and is predominantly controlled by K^+ ions. In electrophysiological experiments the transmembrane potential is varied by electrodes and the current response is measured in order to gain insight into the function of membrane channel and transporter proteins.

A molecular dynamics simulation model of the electric currents across membranes must take into account suitable methods for imposing a given transmembrane potential, i.e. the consequence of the presence of electrodes. Frequently, a linearly varying potential corresponding to a constant electric field and force acting on the atoms is employed which can lead to serious artifacts. Related to the methodology of ref. [1] we have established a physically more realistic model of the membrane potential by creating a slight charge imbalance (different numbers of cations and anions) between cytosol and exterior solution in simulations of the Kcv potassium channel [2,3] (Abb. 1.1).

In such a double-bilayer system the transmembrane potential follows from inverting Poisson's equation, taking the charge density that is averaged over the trajectory as input.

Extensive molecular dynamics simulations over several tens of nanoseconds revealed a number of key parameters that influence the statistical properties of the resulting potentials and the voltage range as a response to an imposed charge imbalance. Relevant parts of the channel protein that are responsible for a particular potential distribution have been identified. The role of the protein's interior cavity which acts as a concentration buffer has been characterized.

References

1. J. N. Sachs, P. S. Crozier, T. B. Woolf, *J. Chem. Phys.* **121**, 10847-10851 (2004).

2. M. Kreim, Diplomarbeit, Darmstadt 2007.

3. S. Tayefeh, T. Kloss, M. Kreim, M. Gebhardt, D. Baumeister, B. Hertel, C. Richter, H. Schwalbe, A. Moroni, G. Thiel, S. M. Kast, *Biophys. J.*, in press.

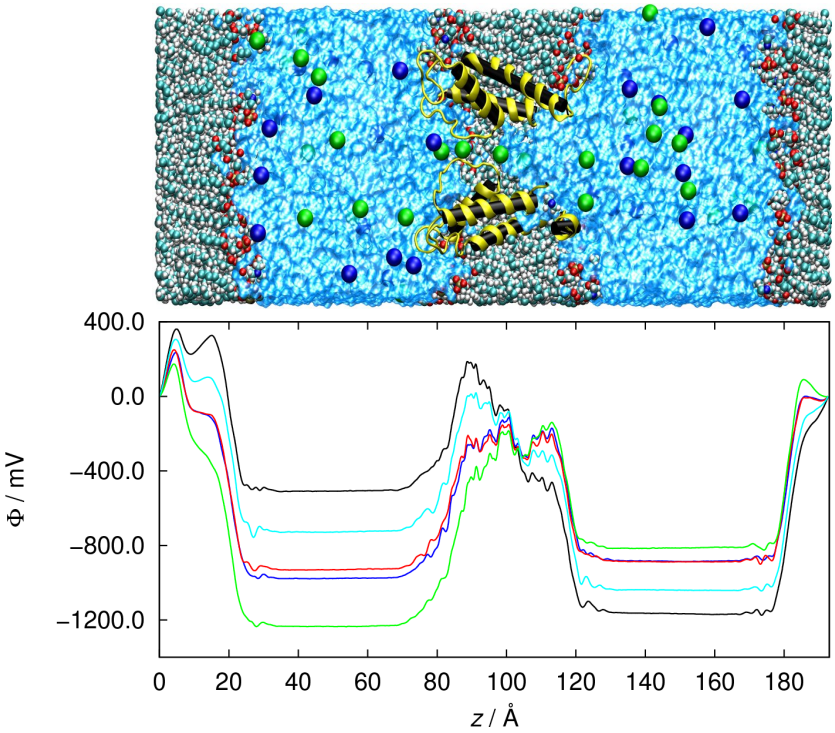

Abbildung 1.1: *Simulation system of the Kcv channel embedded in a lipid membrane, cytosol and exterior bath are separated by a pure lipid membrane (top); transmembrane potentials (bottom).*

4.1.2 Molecular Dynamics Simulation of the Kcv Potassium Channel

Stefan M. Kast, Sascha Tayefeh, Gerhard Thiel
Eduard-Zintl-Institut für Anorganische und Physikalische Chemie, Institut für Botanik, Technische Universität Darmstadt

Potassium channels are membrane-bound proteins that enable the cell to selectively exchange potassium ions with the environment. Exploring the relation between amino acid sequence and channel functionality is important for understanding design principles of channel proteins, which will be relevant, e.g., for creating novel biosensors. The Kcv channel from the plant virus PBCV-1 represents the smallest functional channel known and therefore serves as an ideal model system for studying structure-functions relationships. Ion conduction characteristics can be tuned by site-directed mutagenesis. However, a crystal structure has not been obtained yet.

In order to understand mechanistic features on an atomic scale, several molecular dynamics simulation models have been constructed based on the experimentally available KirBac1.1 structure [1-3]. Functional analogues (truncated KirBac1.1) and Kcv homology models have been simulated in a realistic environment (Abb. 2.1) over several tens of nanoseconds in order to extract structural, thermodynamic and dynamical data. Structures were further analyzed by employing a three-dimensional integral equation theory which provides information about ion binding sites (Abb. 2.2). The results lead to a coherent picture of the influence of key amino acids on ion permeation.

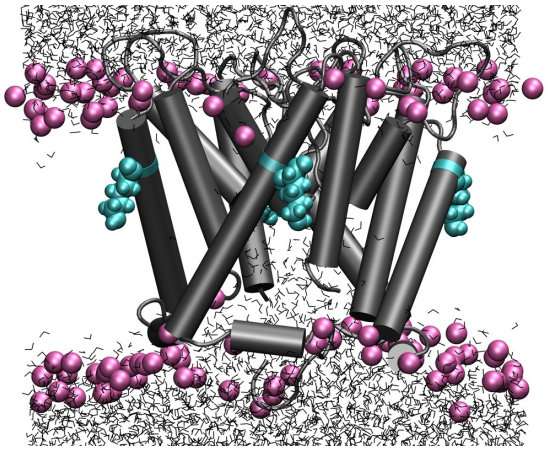

Abbildung 2.1: *Cartoon representation of the Kcv simulation system, showing the protein, lipid head groups, and solvent molecules.*

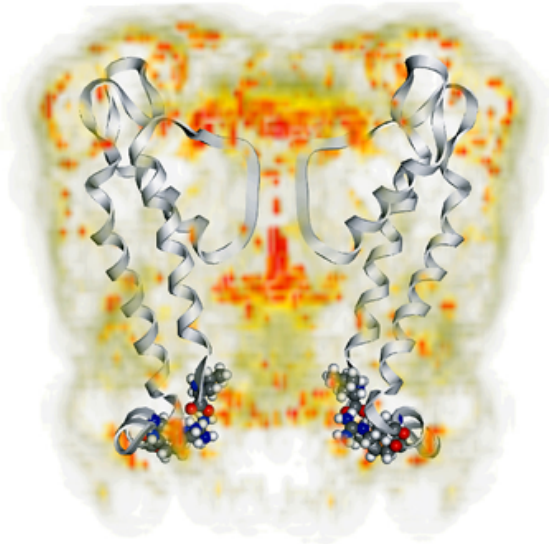

Abbildung 2.2: *Color-coded 3D K^+ ion density (grey: small, red: large) around the Kcv channel from 3D integral equation theory.*

References

1. S. Tayefeh, T. Kloss, G. Thiel, B. Hertel, A. Moroni, S. M. Kast, *Biochemistry* **46**, 4826-4839 (2007).

2. S. Tayefeh, Dissertation, Darmstadt 2007.

3. S. Tayefeh, T. Kloss, M. Kreim, M. Gebhardt, D. Baumeister, B. Hertel, C. Richter, H. Schwalbe, A. Moroni, G. Thiel, S. M. Kast, *Biophys. J.*, in press.

4.1.3 Quantum Chemistry in Solution by Combining 3D Integral Equation Theory with a Cluster Embedding Approach

Stefan M. Kast, Thomas Kloss, Jochen Heil// Eduard-Zintl-Institut für Anorganische und Physikalische Chemie, Technische Universität Darmstadt

Understanding and predicting chemical equilibria and reactivity in solution is a complex problem due to the many degrees of freedom on the atomic scale and due to the difficulty of choosing suitable approximations. In particular, a realistic model has to take into account the mutual response of the electronic structure of the solvated reactants and the solvent structure, which have to be computed self-consistently. Established dielectric continuum solvent models have difficulties to account, e.g., for hydrogen bonding or for heterogeneous environments. A granular, i.e. atomically resolved solvent model is advantageous in such a situation.

To this end, we have developed a hybrid method for the simultaneous solution to the electronic structure problem by quantum chemistry and to the solvent structure by the 3D reference interaction site model (RISM). The electronic structure of the solute is computed self-consistently with the solvent structure by mapping the charge distribution of the solvent onto a set of discrete background point charges that are added to the molecular Hamiltonian, corresponding to an *embedding cluster* (EC-RISM). The EC-RISM procedure yields chemical accuracy in predictions of reaction free energies for several benchmark systems without adjusting empirical parameters [1,2]. A particularly important area of current research is the treatment of acidity (protonation equilibria) in water, characterized by aqueous pK_{a} values [3]. This is supported by a number of methodological developments concerning conceptual and numerical features of 3D-RISM theory [4,5].

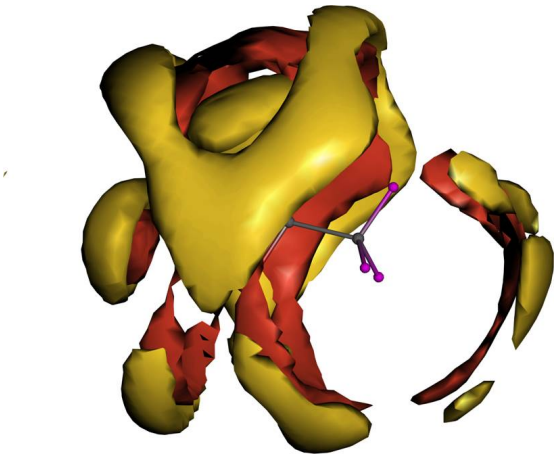

Abbildung 3.1: *Isosurfaces of self-consistent water atom densities around trifluoroacetic acid, red: hydrogen, yellow: oxygen.*

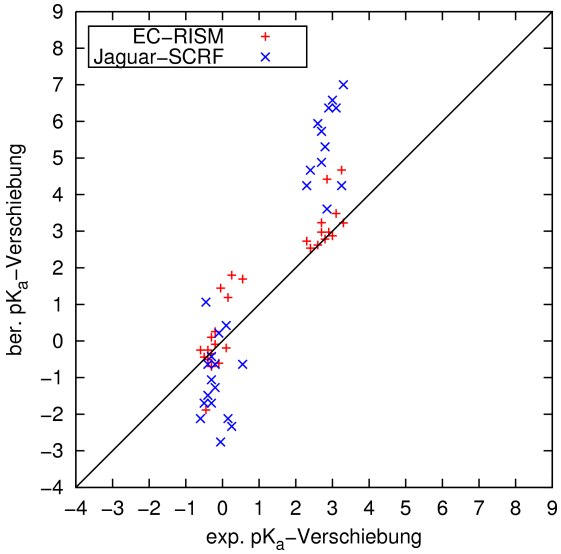

Abbildung 3.2: *Comparison of two different models for predicting pK_a differences among several phenol derivatives.*

References

1. T. Kloss, J. Heil, S. M. Kast, *J. Phys. Chem. B* **112**, 4337-4343 (2008).
2. T. Kloss, Dissertation, Darmstadt 2007.
3. J. Heil, Diplomarbeit, Darmstadt 2008.
4. T. Kloss, S. M. Kast, *J. Chem. Phys.* **128**, 134505 (2008).
5. S. M. Kast, T. Kloss, *J. Chem. Phys.*, in press.

4.1.4 Fast dynamics in coarse-grained polymer models: The effect of the hydrogen bonds

Hosein Ali Karimi-Varzaneh, Paola Carbone, and Florian Müller-Plathe
Eduard-Zintl-Institut für Anorganische und Physikalische Chemie, Technische Universität Darmstadt, Petersenstr 20, D-64287 Darmstadt, Germany

In this contribution we study a coarse-grained (CG) model of polyamide-66 focusing on the dynamics and thermodynamics of the hydrogen bond, which is one of the intermolecular interactions that is responsible for the structure, function, and dynamics of a vast number of chemical systems from inorganic to biological compounds.

Among the common thermoplastic polymers, polyamides are noted for their outstanding properties, including high tensile strength, excellent abrasion, chemical and heat resistance, and low coefficient of friction.

In polymer science numerical simulations can help in establishing the correlation between molecular mechanism and macroscopic properties. In spite of recently available computer power, atomistic simulations of macromolecules have still limitations in investigating properties that require large time and length scale. Hence, the development of CG models for polymers can be of help in overcoming this problem. However, due to the simplification of the CG model, the atoms directly involved in the hydrogen bonding are usually lumped with other atoms in beads. Therefore, the reinsertion of the atomistic details in the CG model after long simulations is important to test the CG force field and the mapping scheme.

As a result of our study, we formulate a simple algorithm for reinserting the atomistic details neglected in the CG description. The resulting coarse-grained and detailed models are tested successfully against several structural properties including the number of hydrogen bonds (1).

Future work: A general way to describe the hydrogen bond interactions in coarse-grained model of polymeric materials will be developed. As first application, the crystallization mechanism of a series of polyamides will be studied.

Reference

1. Fast dynamics in coarse-grained polymer models: The effect of the hydrogen bonds, The Journal of Chemical Physics 129, 154904, 2008.

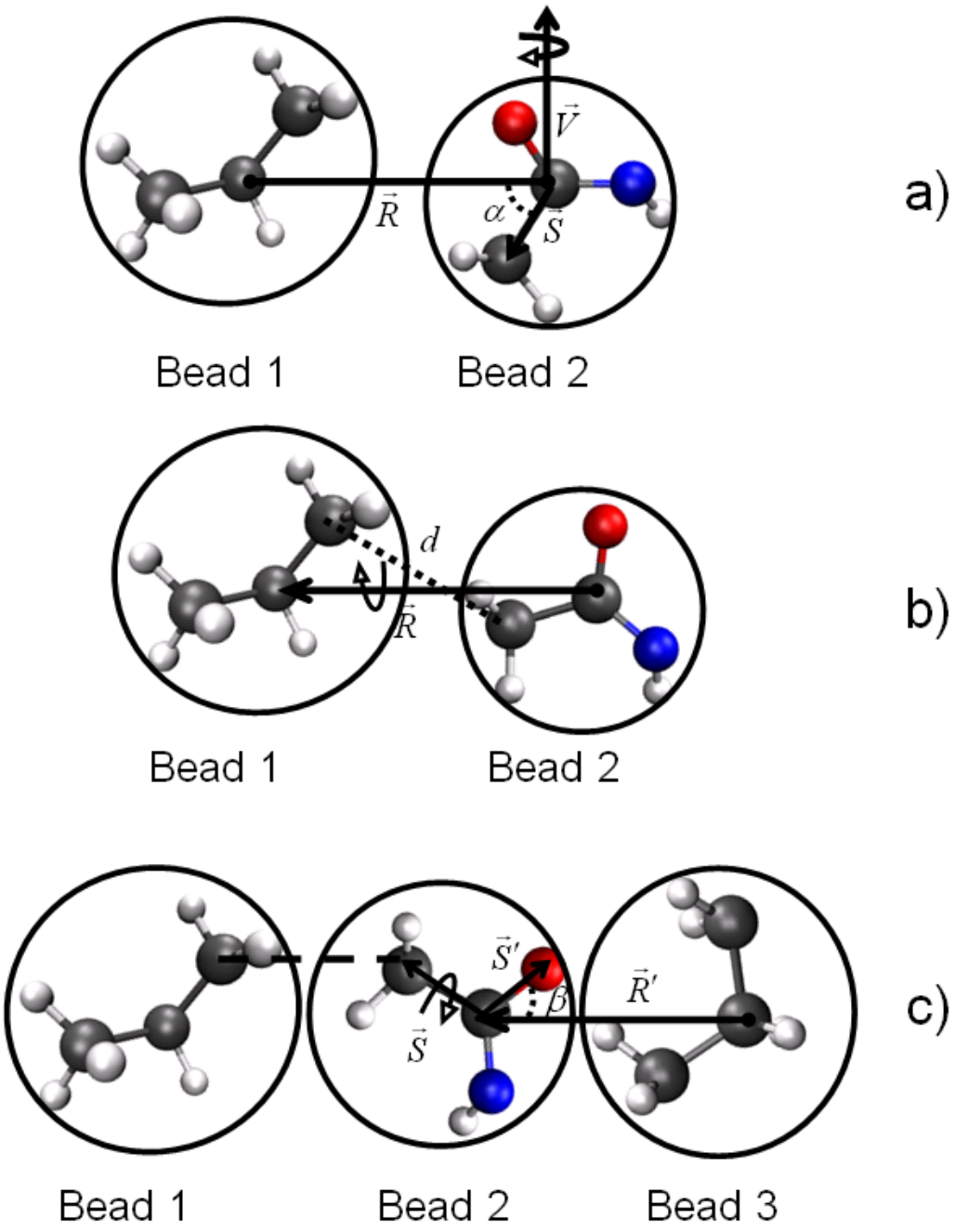

Abbildung 4.1: *Scheme of the backmapping algorithm*

4.1.5 Shear Viscosity of the Ionic Liquid 1-n-Butyl 3-Methylimidazolium Hexafluorophosphate [bmim][PF] Computed by Reverse Nonequilibrium Molecular Dynamics

Wei Zhao, Frederic Leroy, Sundaram Balasubramanian, and Florian Müller-Plathe
Eduard-Zintl-Institut fuer Anorganische und Physikalische Chemie, Technische Universität Darmstadt, Petersenstrasse 20, D-64287 Darmstadt, Germany

The development of ionic liquids has attracted scientific and industrial attention during the past decade. Because of their unique properties such as low melting point, near-zero volatility, high thermal and electrochemical stability, and electrical conductivity, ionic liquids are considered to be ideal replacements of industrially used organic solvents, which are often not environmentally benign and which are less efficient in production as well as in recycling of materials.

There are, however, still impediments to further industrial use of ionic liquids, and one impediment is their high viscosity. On the one hand, the high viscosity of ionic liquids leads to difficulties in handling them practically as in processes of pumping, mixing, or stirring. On the other hand, a low viscosity may cause emulsion formation. It is therefore of industrial relevance to design ionic liquids whose viscosity is under control.

It has been suggested that the viscosity of ionic liquids is determined by their molecular properties such as their tendency to form hydrogen bonds. However, a detailed understanding of the relation between structural and dynamic properties of ionic liquid is still missing, hampering the rational design of low-viscosity products. In recent years, molecular dynamics simulations have been performed to obtain fundamental understanding of various properties of ionic liquids.

In this study, reverse non-equilibrium molecular dynamics and equilibrium molecular dynamics simulations were carried out to compute the shear viscosity of the pure ionic liquids system [bmim][PF6] at 300K. The two methods yielded consistent results which were also compared to experiments (1).

In the future, viscosity of ionic liquids will be studied using both computer simulation and numerical QSPR studies. The purpose of our research efforts is to understand the relationship between viscosity and chemical architecture which is supposed to provide insights into designing ionic liquids of desired viscosities.

Reference

1. Shear Viscosity of the Ionic Liquid 1-n-Butyl 3-Methylimidazolium Hexafluorophosphate [bmim][PF] Computed by Reverse Nonequilibrium Molecular Dynamics
Journal of Physical Chemistry B, 112(27), 8129-8133, 2008.

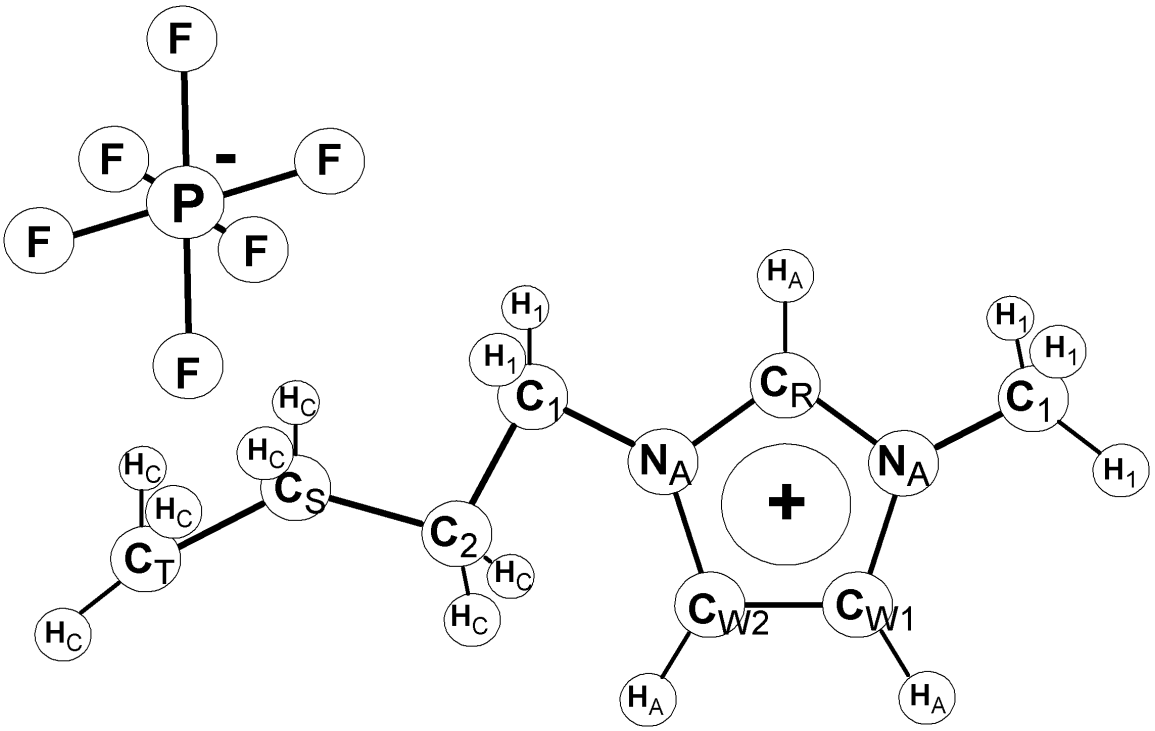

Abbildung 5.1: *Chemical structures of 1-n-butyl-3-methylimidazolium ([bmim];bottom) and hexafluorophosphate*

4.1.6 Thermal Conductivity and Thermal Rectification of Carbon Nanotubes by Reverse Non-equilibrium Molecular Dynamics Simulations

Mohammad Alagemandi, Elena Algaer, Michael C. Böhm, and Florian Müller-Plathe
Eduard-Zintl-Institut fuer Anorganische und Physikalische Chemie, Technische Universität Darmstadt, Petersenstrasse 20, D-64287 Darmstadt, Germany

It is now widely accepted that the thermal management in nanosized devices becomes increasingly important with decreasing size parameters. New thermal management strategies are thus of considerable importance to guarantee high performance and lifetimes. These strategies include the development of novel carbon nanotube materials with high thermal conductivity. Due to the experimental difficulties in synthesizing high-quality and well-ordered nanotubes, it is still challenging to perform perfect thermal conduction measurements. An alternative and supplement to experimental activities are theoretical approaches which have the advantage that the structures generated are clean, defect-free and perfectly characterized.

We have investigated the thermal conductivity of single-walled and multi-walled carbon nanotubes by non-equilibrium molecular dynamics simulations as a function of the tube length, temperature and chiral index (1).

Carbon nanotubes are a possible candidate for thermal rectifiers which are significant for modern electronics, such as nanoscale calorimeters, microelectronic processors, and macroscopic refrigerators.

The thermal rectification effect in nanotubes has been investigated by gradually changing the atomic mass in the tube-axial direction as well as by doing extra masses on the terminal sites of the tube (1).

Future work:

The mechanism of thermal conductivity in soft matter systems will be investigated.

The thermal rectification effect in nanotubes as a function of temperature, length and dimensionality will also be investigated.

Reference

1. Thermal Conductivity and Thermal Rectification of Carbon Nanotubes by Reverse Non-equilibrium Molecular Dynamics Simulations
Submitted toNanotechnology, 2008.

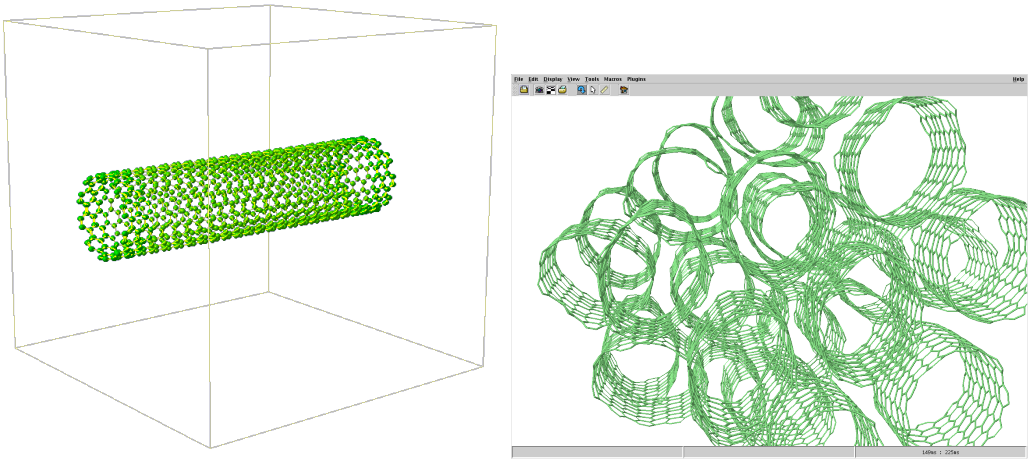

Abbildung 6.1: *left: a (10,10) single-walled carbon nanotube, right: a bulk of short carbon nanotubes.*

4.1.7 Quantum chemical studies on bioinorganic models for dinuclear copper proteins

Max C. Holthausen, Philipp Spuhler, Elixabete Rezabal, Yong Wang
Institut für Anorganische Chemie der Goethe-Universiät Frankfurt am Main

In the past three decades, major research activities have been devoted to the understanding of structure/activity relationships associated with binding and activation of dioxygen by copper-based metalloproteins like tyrosinase or dopamine [F062?]-hydroxylase. Related bioinorganic research has led to a number small synthetic Cu(I) complexes, which contain a $[Cu_2O_2]$ core as a key structural motif to mimic the biocatalytically active paragons. Based on massive use of the mainframe computers provided by the CSC Frankfurt and HLR Darmstadt we employed quantum chemical calculations to uncover the details of the reaction mechanisms of aromatic and aliphatic hydroxylation reactions of mono- and dinuclear copper-oxygen complexes. In the following we compile the some results of our most relevant recent work.

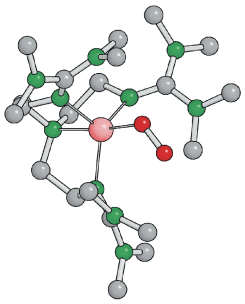

(a) Mononuclear 2:1 Cu/O_2 adducts have been proposed as reactive species for copper-proteins enzymes like PHM. In close cooperation with experimental partners (S. Schindler, Universität Giessen, J. Sundermeyer, Universität Marburg, F. Tuczek, Universität Kiel, K. Karlin, Johns-Hopkins University Baltimore) we were able do provide unequivocal evidence for the existence of an end-on bound Cu-O_2 species. Using low temperature stopped-flow and/or resonance Raman techniques, the initial formation of labile 1:1 Cu/O_2 adducts has been detected as a process which occurs prior to the rapid formation of dinuclear complexes. A number of experimental studies along these lines have impressively demonstrated that dinuclear copper cores can indeed mediate the selective hydroxylation of aliphatic and aromatic C-H bonds. We thus succeeded to unambiguously characterize the structure, spectroscopy, and reactivity of an end-on copper(II)superoxo complex for the first time. [1-3]

(b) We found that the aliphatic hydroxylation in Itoh's system involves a rate-limiting C-H bond activation step, which leads to formation of the product alcohol in a nonsynchronous concerted process [2]. We were able to show that the C-H activation process is a concerted, but non-synchronous step that solely occurs on the singlet surface, i.e., without the occurrence of radical intermediates usually proposed. Based on these results, a general mechanistic scenario is developed to explain experimental observations for several related systems.[4]

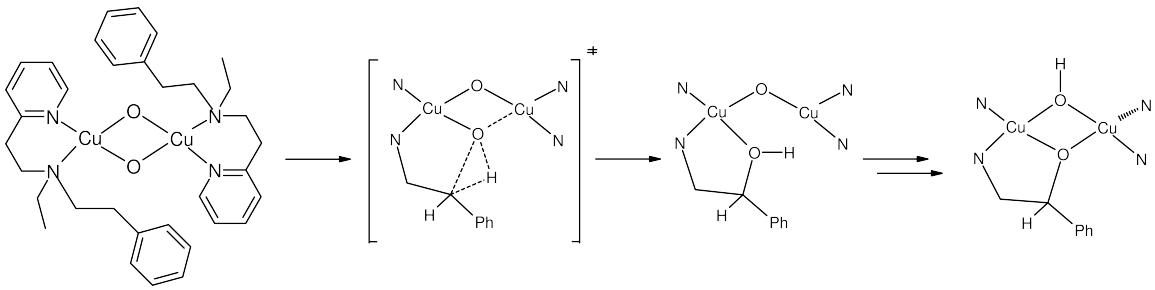

(c) We also investigated structures and reactivities of mononuclear Cu-O complexes. In a recent combined experimental and quantum chemical study we were able to characterize for the first time the reactivity of a copperoxo-species with alkanes in the gas phase, which exhibits a pronounced two-state-reactivity scenario.[5]

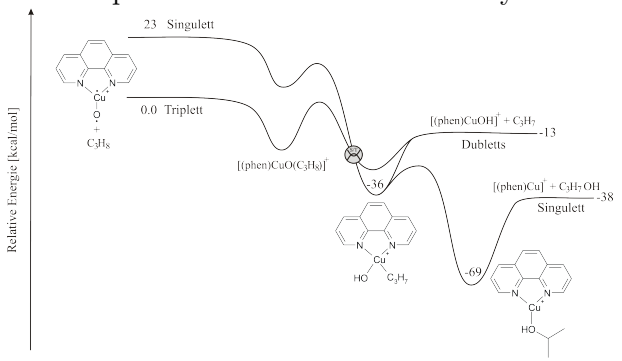

(d) Aromatic hydroxylation in Tolman's system involves a rate-limiting electrophilic attack of the aromatic system in the context of a prominent two-state-reactivity scenario. We propose a dienone species as key intermediate occuring en route to product formation. We extended these studies recently as part of our ongoing cooperation with our experimental partners. [6]

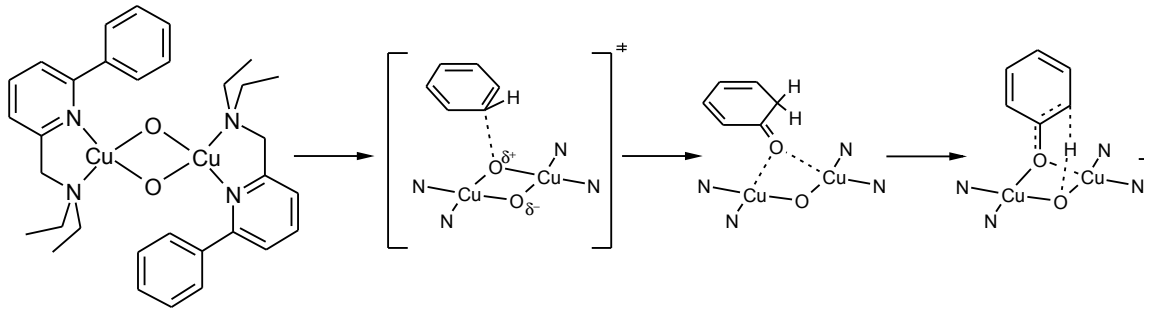

Relevant Publications

[1] Schatz, Raab, Foxon, Brehm, Schneider, Reiher, Holthausen, Sundermeyer, Schindler, *Angew. Chem.* **116**, 4460 (2004).

[2] Würtele, Gaoutchenova, Harms, Holthausen, Sundermeyer, Schindler, *Angew. Chem.* **118**, 3951 (2006).

[3] Maiti, Lee, Gaoutchenova, Würtele, Holthausen, Narducci Sarjeant, Sundermeyer, Schindler, Karlin, Angew. Chem. 120, 88 (2008).

[4] Spuhler, Holthausen, Angew. Chem. 115, 6143 (2003).

[5] Schröder, Holthausen, Schwarz, *J. Phys. Chem. B.,* **108**, 14407 (2004).

[6] Sander, Henß, Näther, Würtele, Holthausen, Schindler, Tuczek, *Chem. Eur. J.* 14, 9714 (2008).

4.1.8 Investigation of molecular structure and dynamics in the gas-phase by ultrafast coherent spectroscopy

Prof. Dr. Bernhard Brutschy and Maksim Kunitski
Institut für Physikalische und Theoretische Chemie, Goethe-Universität Frankfurt am Main

Research Project: Femtosecond Chemistry

Our group studies the dynamical behaviour of large molecules and molecular clusters with ultrafast laser spectroscopy. One aspect concerns the structure of molecules with large amplitude motions. We utilized femtosecond degenerate four-wave mixing (fs DFWM) as an ultrafast pump-probe laser technique, which in its many implementations enables to study different kinds of molecular dynamics.[1] As Rotational Coherence Spectroscopy, fs DFWM has proven to be a powerful tool for investigating the structure of large molecular systems, even if these are bare of a permanent dipole moment.[2,3] The method allows one to study molecular motions (pseudorotation, puckering, torsion) at room temperature by the rotational & centrifugal distortion constants, polarizabilities and energy barriers of the molecules. These data are deduced by means of fitting simulated fs DFWM transient spectra to the measured ones.

Using the example of pyrrolidine (PY) molecule we have recently shown[4] that the fs DFWM spectroscopy can be utilized for studying large amplitude intramolecular dynamics. The PY molecule belongs to the saturated five-membered ring com-pounds. In these molecules a special large amplitude vibration, called pseudo-rotation, takes place. This motion involves the skeletal atoms of the ring and causes the transformation of the molecular conformations into each other (Fig. 8.1). Utilizing the fs DFWM technique we were able to determine the energetics and the structural changes of PY along the pseudorotational path.

The saturated five-membered rings are an essential ingredient of several biologically very important molecules such as the amino acid proline, of nicotine and DNA sugars and therefore the study of this system is of great importance.

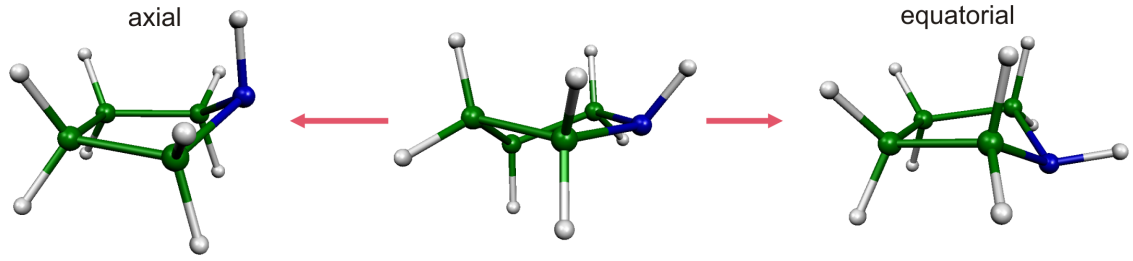

Abbildung 8.1: *Exchange of the two conformers of pyrrolidine: axial and equatorial during pseudorotation.*

System requirements:

The fitted procedure is based on the Differential Evolution minimization algorithm developed by R. Storn and K. Price.[5] It allows one to find a global minimum in a complex fitness landscape at the cost of computational time. Thus for the fit of the fs DFWM spectrum one needs to perform approximately 200 iterations of quantum chemical calculations. In turn each iteration in the worst case requires half a day of CPU time. Consequently the complete fit requires 100 days or 2,400 hours. Usually more than one fit (with different initial parameters) is required for one molecule. For this reason the estimated CPU time for one molecule is roughly 10,000 hours. For one year the number of investigated molecules may be higher than five. Currently we are working on the development of the parallel code in order to minimize the timed required for one fit.

- CPU-time per year: ˜ 50.000 hours
- Typical number of CPUs for parallel calculations: 1
- Network: Gigabit
- Main memory requirements per job: ˜ 1 GByte
- Disk space requirements: ˜ 5 Gbyte

Members of the group

Prof. Dr. Bernhard Brutschy, Maksim Kunitski (PhD student), Dr. Yevgeniy Nosenko

Literature

[1] M. Motzkus, S. Pedersen, A. H. Zewail, *J. Phys. Chem.* **1996**, *100*, 5620-5633.

[2] H. M. Frey, P. Beaud, T. Gerber, B. Mischler, P. P. Radi, A. P. Tzannis, *Appl. Phys. B-Lasers Opt.* **1999**, *68*, 735-739.

[3] C. Riehn, *Chem. Phys.* **2002**, *283*, 297-329.

[4] M. Kunitski, C. Riehn, V. V. Matylitsky, P. Tarakeshwar, B. Brutschy, *submitted* **2008**.

[5] `http://www.icsi.berkeley.edu/~storn/code.html`.

4.1.9 Hydroxy Carbenes: Tunneling Marvels

Peter R. Schreiner
Institute of Organic Chemistry, Justus-Liebig University, Heinrich-Buff-Ring 58, 35392 Giessen, Germany

Hydroxycarbenes (R–C–OH, **1**, Scheme 1) are prototypical donor-substituted carbenes that play a fundamental role in the class of synthetically valuable heterosubstituted carbenes as reagents and metal ligands. Paying tribute to the discoverer of such metal-carbene complexes, these types of structures are now referred to as Fischer carbenes.[1] Yet, attempts to prepare free alkoxycarbenes through thermal decomposition of metal carbenes have failed. The parent hydroxycarbene, **1a** (R=H) also plays an important role in deciphering the organic chemistry of small organic molecules in prebiotic earth and extraterrestrial environments because **1a** is implied in the thermal decomposition of glyoxylic acid (**2a**, R=H) that also gives rise to formic acid, CO, CO_2, H_2, and H_2O. We have shown recently that hydroxycarbenes **1** can be generated in a general fashion (R=OH, CH_3, OCH_3) thermally through high-vacuum flash pyrolysis (HVFP), subsequently be trapped in an argon matrix at 10 K, and be fully characterized spectroscopically.[2, 3]

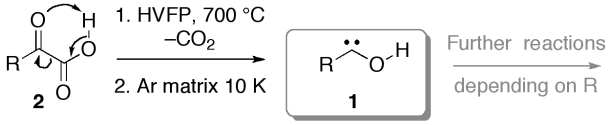

Theory firmly identified **1** as the key structure to rationalize the high-energy chemistry of **6** and indicated that **1** "does appear to rest in a relatively deep potential minimum, and eventual characterization by spectroscopic means seems inevitable".[4] Exceptionally high H/D kinetic isotope effects were predicted theoretically for the tautomer equilibrium of **1** and **6**.[5, 6] Due to the limited amount of experimental spectral information, one needs highly accurate variational (ro)vibrational computations to unambiguously assign spectral features to novel carbenes of sometimes fleeting existence. Such studies require nuclear dynamics techniques. Furthermore, quantum reaction dynamics, based on the same time-independent machinery as the variational (ro)vibrational computations, aid in the determination of microcanonical rate constants for at least some of the tunnelling processes. With a further planned development of the "direct" and "correct" calculation of microcanonical rate constants,[7] full-dimensional computations can be carried out, for example, for **1** and dihydroxycarbene (R=OH),[8] exhibiting drastically different tunnelling characteristics. The full-dimensional results can be compared with results of more traditional one-dimensional treatments (*e.g.*, those based on Eckart or Wigner barriers) and thus establishing what really determines the tunnelling propensities of various hydroxycarbene derivatives and perhaps shedding light on new or only partially explored tunneling phenomena (*e.g.*, resonant tunneling and non-exponential decay).

References

[1] A. de Meijere, H. Schirmer, M. Duetsch, *Angew. Chem.* **2000**, *112*, 4124.
[2] P. R. Schreiner, H. P. Reisenauer, *ChemPhysChem* **2006**, *7*, 880.
[3] P. R. Schreiner, H. P. Reisenauer, F. Pickard, A. C. Simmonett, W. D. Allen, E. Matyus, A. G. Csaszar, *Nature* **2008**, *453*, 906.
[4] C. F. Pau, W. J. Hehre, *J. Phys. Chem.* **1982**, *86*, 1252.

[5] J. R. Sodeau, E. K. C. Lee, *Chem. Phys. Lett.* **1978**, *57*, 71.
[6] W. H. Miller, *J. Am. Chem. Soc.* **1979**, *101*, 6810.
[7] W. H. Miller, *J. Phys. Chem. A* **1998**, *102*, 793.
[8] P. R. Schreiner, H. P. Reisenauer, *Angew. Chem. Int. Ed.* **2008**, *47*, 7071.

4.2 Physik

4.2.1 Gittersimulationen von effektiven Modellen für SU(N) Eichtheorien bei hohen Temperaturen

Prof. Dr. Stefan Schramm, Dipl. Phys. Dominik Smith
Institut für Theoretische Physik, Johann Wolfgang Goethe-Universität

Die Arbeitsgruppe beschäftigt sich mit der Untersuchung von Z(N) symmetrischen drei dimensionalen effektiven Theorien für SU(N) Wilson Schleifen. Ziel ist eine Beschreibung der stark gekoppelten Phase knapp oberhalb des Deconfinement Phasenübergangs, welche sowohl die pertubativen als auch die nicht-pertubativen Aspekte der Quantenchromodynamik erfasst. Die übliche Beschreibung stark Wechselwirkender Systeme als Quasiteilchen verliert ihre Gültigkeit wenn die Kopplung nicht hinreichend klein ist. In Bereichen mittlerer Temperetur ist eine Beschreibung sinnvoll, die stattdessen die Wilson Schleife als effektiven Freiheitsgrad verwendet Die Wilson Schleifen verhalten sich in starker Analogie zu einem Spin Modell.

Unsere Gruppe fürt Gittersimulationen eines solchen Modells mit der Symmetriegruppe SU(2) durch. Dabei werden Observablen wie der Erwartungswert des Polyakov Loop, Suszeptibilitäten, Stringspannung und räumliche Korrelationslängen gemessen. Zur Erzeugung der Gitterkonfigurationen wird der Algorithmus von Metropolis et al verwendet. Heatbath und Overrelaxation werden ebenfalls eingesetzt.

Schwerpunkt der Arbeit ist die Untersuchung der Eigenwertverteilung und der zugehörigen Potentiale. Es soll ermittelt werden, ob durch die Dynamik des Systems Beiträge zum Potential entstehen, die von dem reinen Potential im Lagrangian und dem Vandermonde Potential des Gruppenmaßes verschieden sind.

Mitglieder der Arbeitsgruppe

Prof. Dr. S. Schramm,
Prof. Dr. A. Dumitru,
D. Smith (Doktorand).

Publikationen

A. Dumitru, D. Smith
"Eigenvalue repulsion in an effective theory of SU(2) Wilson lines in three dimensions"
Phys. Rev. D 77, 094022
2008
D. Smith
"Lattice simulation of a center symmetric three-dimensional effective theory for SU(2) Yang Mills" Proceedings of the Conference for Strong and Electroweak Matter 2008 (SEWM08), Amsterdam,
arXiv:0810.1129
2008

4.2.2 Parton dynamics and hadronization from the strongly-coupled QGP

W. Cassing[a] and E. L. Bratkovskaya[b]
[a]Institut für Theoretische Physik, JL Universität Gießen
[b]Frankfurt Institute for Advanced Studies, JWG Universität Frankfurt am Main

The hadronization of an expanding partonic fireball is studied within the Parton-Hadron-Strings Dynamics (PHSD) approach which is based on a dynamical quasiparticle model (DQPM) [1,2] matched to reproduce lattice QCD results in thermodynamic equilibrium. Apart from strong parton interactions the expansion and development of collective flow is driven by strong gradients in the parton mean-fields. An analysis of the elliptic flow v_2 demonstrates a linear correlation with the spatial eccentricity ε as in case of ideal hydrodynamics. The hadronization occurs by quark-antiquark fusion or 3 quark/3 antiquark recombination which is described by covariant transition rates. Since the dynamical quarks become very massive, the formed resonant 'pre-hadronic' color-dipole states (q-qbar) or (qqq) are of high invariant mass, too, and sequentially decay to the groundstate meson and baryon octets increasing the total entropy. This solves the entropy problem in hadronization in a natural way. The resulting particle ratios turn out to be in line with those from a grandcanonical partition function at temperature T=170 MeV rather independent from the initial temperature and indicate an approximate strangeness equilibration.

The details can be obtained from [3].

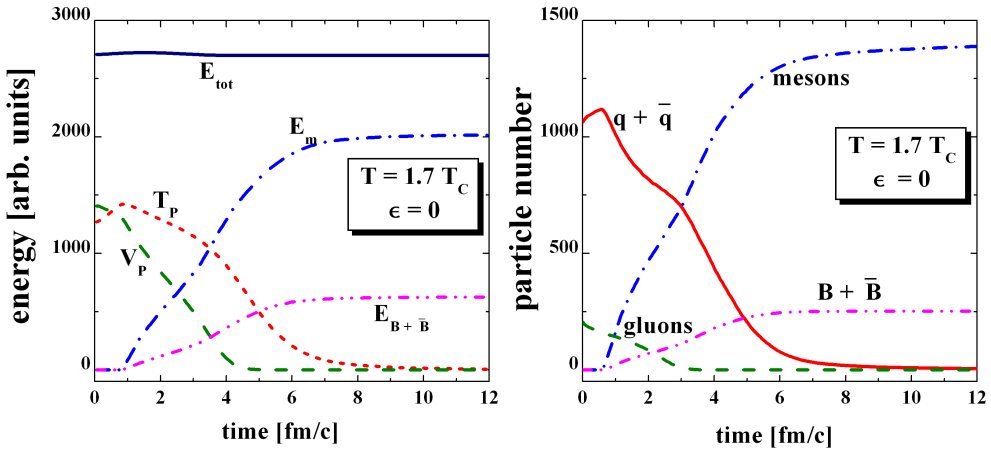

Abbildung 2.1: *Left part: Time evolution of the total energy E_{tot} (upper line), the partonic contributions from the interaction energy V_p and the energy of time-like partons T_p in comparison to the energy contribution from formed mesons Em and baryons (+ antibaryons) E_{B+Bbar}. Right part: Time evolution in the parton, meson and baryon number for an expanding partonic fireball at initial temperature T=1.7 T_c with initial eccentricity $\varepsilon = 0$.*

[1] W. Cassing , Dynamical quasiparticles properties and effective interactions in the sQGP. Nucl. Phys. A795 (2007) 70.

[2] W. Cassing, *QCD thermodynamics and confinement from a dynamical quasiparticle point of view. Nucl. Phys. A791 (2007) 365.*

[3] W. Cassing and E.L. Bratkovskaya, Parton transport and hadronization from the dynamical quasiparticle point of view, Phys. Rev. C 78 (2008) 034919.

4.2.3 Exotische hadronische Materie und Atomkerne

Prof. Dr. Stefan Schramm, Dr. Detlef Zschiesche, Verônica Dexheimer, Jan Steinheimer
Center for Scientific Computing, Frankfurt Institute for Advanced Studies und Institut für Theoretische Physik der Johann Wolfgang Goethe-Universität, Max-von-Laue-Straße 1, D-60438 Frankfurt am Main

Die Arbeitsgruppe "Hadronische Materie" beschäftigt sich seit einer Reihe von Jahren mit der Untersuchung von selbstkonsistenten hadronischen Modellen zur Beschreibung stark wechselwirkender Materie unter extremen äuß eren Bedingungen von Dichte, Temperatur und Isospin.

Ein Schwerpunkt ist die Untersuchung der Isospinabhängigkeit der starken Wechselwirkung, die relativ wenig verstanden ist. Diese Abhängigkeit wird besonders in extremen hadronischen Zuständen sehr wichtig, wenn etwa die Zahl der Neutronen

erheblich höher ist als die Protonzahl. Ein System mit nahezu maximaler Isospinasymmetrie ist der Neutronenstern. Ein anderer Bereich ist die Physik exotischer neutronenreicher Kerne.

Wie es sich in ursprünglichen detaillierten Studien gezeigt hat [1-3], kann man mit einem auf chiraler und Flavor-SU(3)-Symmetrie basierenden Modell eine quantitativ sehr gute Beschreibung von Kernmaterie im Grundzustand als auch von wesentlichen Eigenschaften von Atomkernen über ein groß es Gebiet von Proton- und Neutronzahlen erreichen. Weitere Rechnungen zeigen weiterhin gute Beschreibungen hochangeregter hadronischer Materie [4] sowie der Struktur von Neutronensternen [5]. Das erlaubt insbesonders die Untersuchung der Isospinabhängigkeit der Kernkraft, wie sie speziell in sehr neutronenreichen Umgebungen wichtig ist. Dazu gehört zum einen Neutronensternmaterie als auch die Eigenschaften exotischer Kerne in der Nähe der Stabilitätsgrenze bezüglich Neutronemission („neutron drip line“). Die Kenntnis des Verlaufs dieser Grenze ist auch für das Verständnis der stellaren Nukleosynthese entscheidend. Sowohl die Struktur der Isospinkräfte als auch Deformationseffekte haben entscheidenden Einfluss auf diesen Bereich exotischer Kerne. Eine systematische Untersuchung der Stabilitätsgrenze, ihre Isospinabhängigkeit als auch deren Korrelation mit Neutronensterneigenschaften ist eine wichtige, weitgehend unerledigte Aufgabe, die erheblichen numerischen Aufwand erfordert. Erste, wichtige Resultate

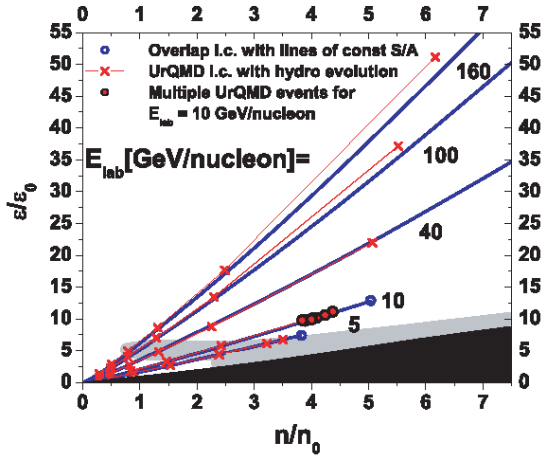

Abbildung 3.1: *Berechnung der Energiedichten ε und Dichten n in der Expansion der heißen Stoßsysteme für unterschiedliche Strahlenergien von 5, 10, 40, 100 und 160 GeV pro Nukleon. Die graue Fläche beschreibt das Phasenkoexistenzgebiet der chiral symmetrischen und gebrochenen Phasen. Die blauen Linien beschreiben eine vereinfachte Abschätzung des Expansionsverhaltens, die roten Linien sind das Ergebnis der mikroskopischen Simulationsrechnung.*

wurden hier kürzlich erzielt [6]. Auf experimenteller Seite besteht ein großes Interesse an der Physik exotischer Kerne, die eines der zentralen Forschungsgebiete der neuen FAIR-Beschleunigeranlage an der GSI, Darmstadt, darstellt.

Mit demselben Ansatz lassen sich hochangeregte Zustände beschreiben, die in ultrarelativistischen Schwerionenstößen erzeugt werden. Die in dem Modell erzeugte Zustandsgleichung der Materie bei gegebener Temperatur und chemischen Potential wird dazu in numerisch sehr anspruchsvolle relativistische molekulardynamische und dreidimesnionale hydrodynamische Simulationen integriert, womit Nichtgleichgewichts-studien der heißen und dichten hadronischen Materie möglich sind. Damit lässt sich die Phasenstruktur des Übergangs von einem Quark-Gluon-Plasma-Zustand zu der kalten hadronischen Materie beschreiben, was das zentrale Thema der Schwerionen-Forschungen an den Beschleunigern am RHIC, USA, an der GSI in Darmstadt und am CERN in Genf, darstellt. Erste Ergebnisse sind in der Figur dargestellt, wobei als Ergebnis numerischer Berechnungen gezeigt wird, wie man experimentell je nach Strahlenergie unterschiedliche Bereiche des Phasenübergangs ausloten kann [7].

References

1. S. Schramm, Phys. Rev. C **66**, 064310 (2002).
2. S. Schramm, Phys. Lett. B**560**, 164 (2003).
3. Ch. Beckmann, P. Papazoglou, D. Zschiesche, S. Schramm, H. Stöcker, and W. Greiner, Phys. Rev. C **65**, 024301 (2002)
4. D. Zschiesche, S. Schramm, H. Stöcker and W. Greiner, Phys. Rev. C **65** (2002) 064902.
5. V. Dexheimer and S. Schramm, Astrophys. Journal, in print.
6. Khin-Nyan Linn, Doktorarbeit, Universität Frankfurt, 2008.
7. J. Steinheimer, M. Bleicher, H. Petersen, S. Schramm, H. Stöcker, D. Zschiesche, Phys. Rev. C **77**, 034901 (2008).

4.2.4 Open and hidden charm in proton-nucleus and heavy-ion collisions.

O. Linnyk[a], E. L. Bratkovskaya[a], W. Cassing[b]
[a] Frankfurt Institute for Advanced Studies, JWG Universität Frankfurt am Main;
[b] Institut für Theoretische Physik, JL Universität Gießen.

We present the results of our calcualtions on the collectivity and the suppression pattern of charmed mesons in heavy-ion collisions based on the microscopic Hadron-String Dynamics (HSD) transport approach for different scenarios of charm interactions with the surrounding matter.

Our findings suggest that the charmonium dynamics in heavy-ion reactions is dominantly driven by hadronic interactions in the SPS energy regime. Since energy densities above 1 GeV/fm3 are reached in central nucleus-nucleus collisions at 158 A·GeV, our observation indicates that hadronic correlators (with quantum numbers of the familiar hadrons) still persist above the critical energy density for the formation of a QGP. In contrast, the study of the formation and suppression dynamics of charmonia within the HSD transport approach for Au+Au reactions at the top RHIC energy has demonstrated that the hadronic 'comover absorption and recreation model' fails severely at $\sqrt{s}$=200 GeV. This is found in the J/Ψ rapidity distribution, in the differential elliptic flow of J/Ψ and the charmonium nuclear modification factor R_{AA} as a function of transverse momentum p_T. Only when including pre-hadronic degrees in the early charm reaction dynamics, the general suppression pattern of charmonia may be reasonably described; though, the elliptic flow v_2 is still (slightly) underestimated. On the other hand, $R_{AA}(p_T)$ for J/Ψ mesons cannot be described appropriately in the comover approach even when incorporating the early pre-hadron interactions. The latter observable indicates that at least part of the final J/Ψ's are created by coalescence of c+cbar pairs in the hadronization phase. Our analysis demonstrates that the dynamics of c+cbar quarks in heavy-ion reactions at RHIC energies are dominated by partonic interactions in the sQGP.

More information on our research can be obtained from [3].

1. PHENIX, A. Adare et al., Phys. Rev. Lett. 98, 172301 (2007).
2. O. Linnyk, E. L. Bratkovskaya, and W. Cassing, Nucl. Phys. A807, 79 (2008).
3. O. Linnyk, E. L. Bratkovskaya, and W. Cassing, Int. J. Mod. Phys. E17, 1367 (2008).

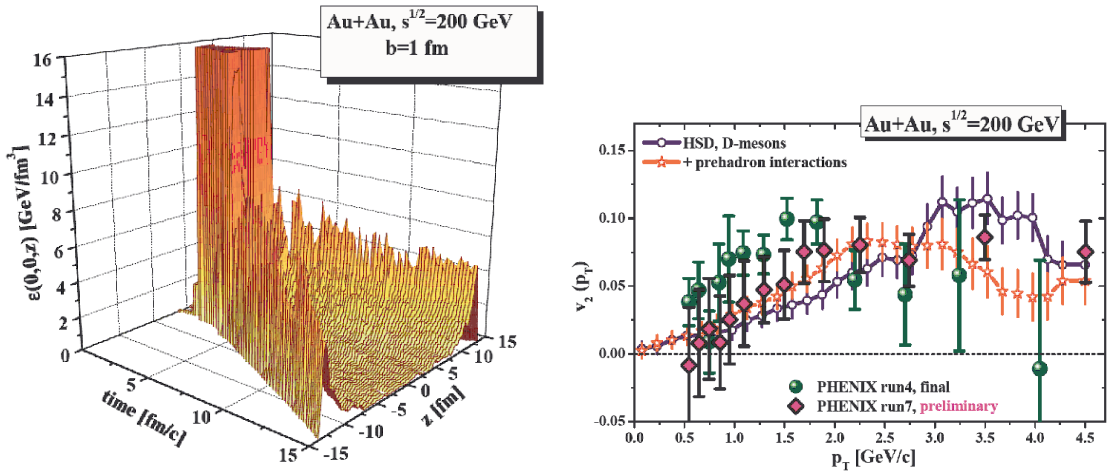

Abbildung 4.1: Left panel: *The energy density from HSD for a central Au+Au collision at* $\sqrt{s}$ *=200 GeV. The time t is given in the nucleon-nucleon center-of-mass system.* ***Right panel:*** *Elliptic flow of D mesons produced in Au+Au collisions at* $\sqrt{s}$ *=200 GeV as a function of* p_T *from HSD (solid blue line with open circles) in comparison to the PHENIX data [2] on* v_2 *of non-photonic electrons. The red line with open stars shows the HSD result for the* v_2 *of D -mesons when including additionally pre-hadronic charm interactions. The figures are taken from Ref. [2].*

4.2.5 Self-consistent calculations of nuclear matter properties at nonzero temperature and density

Chistian Beckmann, Francesco Giacosa, Achim Heinz, Dirk H. Rischke, Dirk Röder, Jörg Ruppert, Stefan Strüber
Institut für Theoretische Physik, J.W. Goethe Universität Frankfurt

Relativistic heavy-ion collisions as studied at experimental facilities like GSI, BNL and CERN can provide insight into the modification of nuclear matter properties at nonzero density and/or temperature. At sufficiently large energies and system sizes they can therefore even offer the opportunity to study the deconfining and chiral phase transitions of QCD matter. We investigate such problems in an effective field-theory framework using many-body approximations. Since the coupling con stant is not small, many-body resummation techniques have to be employed. A thermodynamically consistent framework is provided by Baym's Φ-functional approach. We use it in the form of the approach of Cornwall, Jackiw and Tomboulis, in which self-consistently coupled (Dyson-Schwinger) integral equations for the spectral functions of the physical degrees of freedom are derived. Their iterative solution requires considerable parallel computing power which is provided by the CSC. We have completed various projects along this line of work: broadening of the spectral function of the ρ-meson [1], studying chiral symmetry restoration in a linear sigma model with O(N) symmetry beyond the Hartree-Fock approximation [2], a self-consistent study of the Walecka model at nonzero density and temperature [3], calculation of various temperature dependent meson masses around the chiral phase transition within a gauged linear sigma model [4] and the mixing of a tetraquark with a quarkonium state and its impact on the chiral symmetry restauration at nonzero temperature [5].

Examples of our results from [5]:

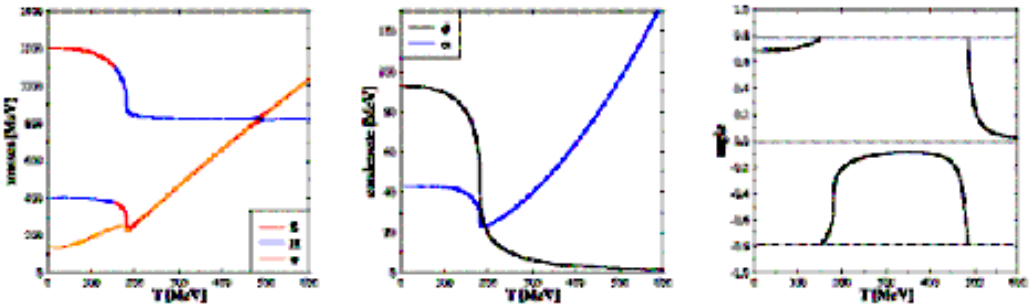

[1] J. Ruppert, T. Renk:
Non-perturbative finite T broadening of the rho meson and dilepton emission
in heavy ion-collisions,
Phys. Rev. C71:064903, 2005,
[2] D. Röder, J. Ruppert, Dirk H. Rischke:
Selfconsistent calculations of spectral densities in the O(N) model: Improving the Hartree-Fock
approximation by including nonzero decay widths,
Nucl.Phys.A775:127-151, 2006,
[3] C. Beckmann:

Self-consistent calculations of hadron properties at nonzero temperature,
Dissertation, Frankfurt, 2005
[4] S. Strüber, D. Rischke:
Vector and axialvector mesons at nonzero temperature within a gauged linear sigma model,
Phys.Rev.D77:085004, 2007
[5] A. Heinz, S. Strüber, F. Giacosa, D. Rischke:
Role of the tetraquark and the chiral phase transition,
arXiv:0805.1134[hep-ph].

4.2.6 Fluctuations in A+A collisions within the HSD transport approach

V. P. Konchakovski, E. L. Bratkovskaya
Frankfurt Institut for Advanced Studies, Johann Wolfgang Goethe Universität, Frankfurt am Main

An ambitious experimental program for the search of the QCD critical point has been started by the NA61 Collaboration at the SPS, CERN (Geneva, Switzerland). The program includes a variation in the atomic mass number A of the colliding nuclei as well as an energy scan. One expects to "locate" the position of the critical point by studying its "fluctuation signals". High statistics multiplicity fluctuation data will be taken for p+p, C+C, S+S, In+In, and Pb+Pb collisions at bombarding energies of E = 10, 20, 30, 40, 80, and 158 AGeV.

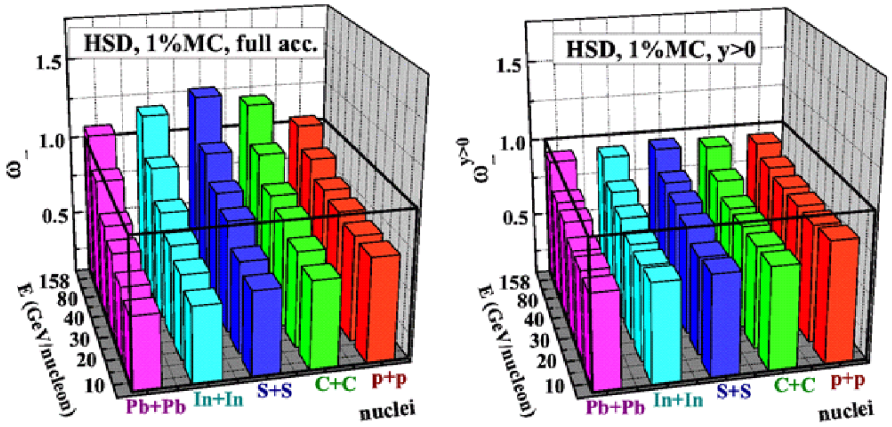

Abbildung 6.1: *HSD results for multiplicity fluctuations in 1% most central A+A collisions at SPS energies.*

The study has been performed in full correspondence to the future NA61 experimental program. Thus we have considered central C+C, S+S, In+In, and Pb+Pb collisions with the energy per nucleon in the lab frame E = 10, 20, 30, 40, 80, 158 AGeV. The results shown in the figure correspond to full 4π acceptance and forward hemisphere (y>0) what should be close to experimental acceptance. The influence of participant number fluctuations on hadron multiplicity fluctuations has been emphasized and studied in detail. To make these "trivial" fluctuations smaller, one has to consider the most central collisions.

Our findings should be helpful for the optimal choice of collision systems and collision energies for the experimental search of the QCD critical point.

[1] V. P. Konchakovski, B. Lungwitz, M. I. Gorenstein, E. L. Bratkovskaya: Multiplicity fluctuations in nucleus-nucleus collisions: Dependence on energy and atomic number, Phys. Rev. C78, 024906 (2008)

4.2.7 Electrohydrodynamic effects in polyelectrolyte solutions

Kai Grass and Christian Holm
Frankfurt Institute for Advanced Studies, Goethe University Frankfurt

We study the importance of hydrodynamic interactions during free-solution electrophoresis of linear polyelectrolytes by means of coarse-grained molecular dynamics simulations including full electro-hydrodynamic interactions.

Starting with the static chain properties of the polyelectrolyte and the counterion distribution around the chain, the influence of hydrodynamics and electrostatics is investigated, especially with respect to the screening due to a finite salt concentration in the solution. Additionally, the perturbation by an external electric field is studied and it is shown that, within the linear response regime, static and dynamic properties are not affected by the electric field. The dynamic properties of flexible polyelectrolyte chains are determined in dependence of the chain length. The comparison of the simulations to existing theories and experiments underlines the importance of hydrodynamic interactions. The simulations can be quantitatively matched to available experimental data and specifically show the experimentally observed maximum in the electrophoretic mobility for intermediate chains, currently not covered by existing theories.

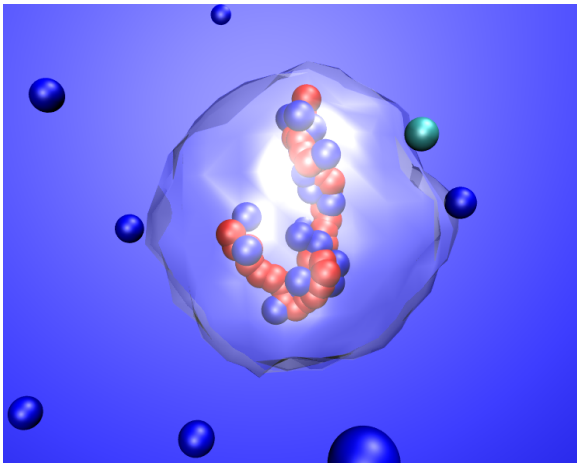

To understand this interesting behaviour on a microscopic level, five independent estimators are formulated and used to determine the effective charge of the polyelectrolyte. The estimators are analyzed with respect to their accuracy, as well as their applicability and efficiency in simulations and their transferability to experiments. The effective charge of the polyelectrolyte turns out to be reduced by counterions surrounding the chain and moving with the polyelectrolyte. An important observation in this context is the fact that the effective charge is not depending on hydrodynamic interactions. Additionally, it is shown that the counterions have a crucial influence on the effective friction of the polyelectrolyte complex during electrophoresis. Based on the mobility measurements and on the charge estimates, the length-dependence of the effective friction is quantified and exhibits a sharp decrease in the friction per monomer due to hydrodynamic shielding. This shielding is reduced as the chain length is increased, indicating an equal exposure of all parts of the chain to the fluid. The results clearly show a screening of hydrodynamic interactions, which is explained by the presence of counterions creating a fluid flow inside the polyelectrolyte coil. The associated screening length is similar to the Debye length for electrostatic screening, emphasizing the role of counterions.

With the analysis of the effective charge and the effective friction a detailed picture of the dynamic behaviour of charged macromolecules during electrophoresis is created. The previously unexplained mobility maximum is shown to be a direct consequence of a different scaling of charge and friction. Similarly, the constant free-solution mobility of

long polyelectrolyte chains, the free-draining behaviour, can be attributed to the linear dependence on chain length of both properties for sufficiently long chains.

Publications

K. Grass, U. Böhme, U. Scheler, H. Cottet, and C. Holm.
Importance of hydrodynamic shielding for the dynamic behavior of short polyelectrolyte chains.
Physical Review Letters, 100(9):096104, 2008
2008
K. Grass and C. Holm.
On the importance of hydrodynamic interactions in polyelectrolyte electrophoresis.
J. Phys.: Condens. Matter, 20(494217), 2008
2008
K. Grass and C. Holm.
Polyelectrolytes in electric fields: Measuring the dynamical effective charge and effective friction.
Submitted to Softmatter, 2008
2008
K. Grass
Towards realistic modelling of free-solution electrophoresis: a case study on charged macromolecules
PhD thesis, 2008
2008

4.2.8 Simulations of magnetic fluids

Joan J. Cerdà and C. Holm
FIAS, Frankfurt Institute for Advanced Studies, Uni. Goethe, Frankfurt am Main

Dipolar magnetic fluids (also known as ferrofluids or ferrocolloids), are colloidal suspensions of ferromagnetic nanoparticles (typical sizes 10-20nm), usually stabilised by steric coatings (in non electrolyte carrier liquids) or by electrical double layers (in aqueous solutions). Due to their size, ferrofluid particles can be considered as magnetic single-domains with a permanent magnetic moment. The singular properties of ferrofluids in external magnetic fields have found application in many areas, ranging from engineering, to biomedical applications. Even in the absence of external fields, ferrofluids have a very complex microstructure, it is crucial to understand the mechanisms behind such structures in order to make a deep progress in the area of science and engineering of ferrofluids. Our current interest focuses on the peculiarities of the aggregation processes in both quasi-two dimensional (monolayers) and bulk ferrofluid systems. We make use of extensive Molecular dynamics (MD) simulations using the software package Espresso [1]. The microstructure formation and phase behaviour are studied thoroughly through a comparison of the theoretical, and computational results. We have studied different mono- and bi-dispersed systems in presence/absence of an external magnetical field. We have observed and characterized the strong dependence of aggregate topologies on particle sizes and area fractions.

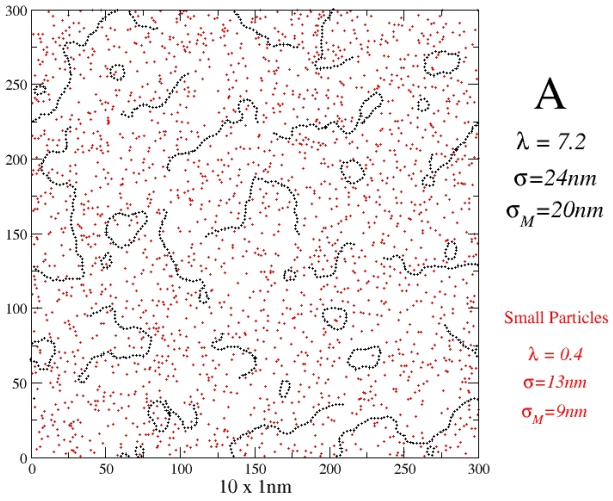

Abbildung 8.1: *Our simulations able to mimic the behavior found in monodiperse and bidisperse experimental monolayers including the formation of rings and other structures observed in experiments.In bidisperse systems our simulations show that for certain ratios of particle sizes there exists a shortening effect for both chains and rings. Similar shortening effects have been predicted by theory, and lately observed in experimental monolayers.*

A bottle neck in simulations dealing with long-range interactions like for instance those found in dipoles is the slowliness of current algoritms. In our group we have recently developed a new dipolar-P3M algorithm able to boost the speed in such calculations [2]. This

algorithm (used in combination with a dipolar layer correction in the case of monolayers) have proved to be very efficient in the simulation of ferrofluid systems, allowing for simulations with a large number of particles in it. Due to the lack of conclusive experiments, the understanding of how dipole-dipole interactions influence the clustering process and determine the subsequent microstructure and phase behaviour of ferrofluids is a challenge [3,4].

Literaturverzeichnis

[1] H. J. Limbach, A. Arnold,B. A. Mann,C. Holm. *Comp. Phys. Comm.* 174(9)(704-727), **2006**.

[2] Juan J. Cerdà, V. Ballenegger, O. Lenz, Ch. Holm. JCP (in press) (see arXiv:0805.4783)

[3] S. Kantorovich, Juan J. Cerdà, C. Holm, *Phy. Chem. Chem. Phy.* 10(14)(1883-1895), **2008**.

[4] Juan J. Cerdà, Sofia Kantorovich, C. Holm, *J.Physics-Condensed Matter* 20(204125), **2008**.

4.2.9 Thermodynamics of Polymer-Chain Stretching Ensembles

Mehmet Süzen, Marcello Sega and Christian Holm
Frankfurt Institute for Advanced Studies, Goethe University, Frankfurt am Main

The physics of small objects is quite fascinating, due to fact that interactions are dominated by thermal fluctuations [1]. The development of recent novel micromanipulation techniques nowadays enable researchers to obtain directly quantitative information about single molecules, such as forces in the nanoscale. Widely used methods are AFM or Optical Tweezers, collectively known as Single Molecule Experiments (SMEs) [2].

However, the outcome of SMEs is quite sensitive to the choice of which control parameter are held fixed. There might be differences in the thermodynamic interpretation between the standard ensemble experiments that are performed with a very large number of molecules (components) and single molecule measurements recently discussed, providing scaling laws for ensemble differences [2,3]. Conflicting views exist in the literature even for the simple case of a Gaussian chain [2,4].

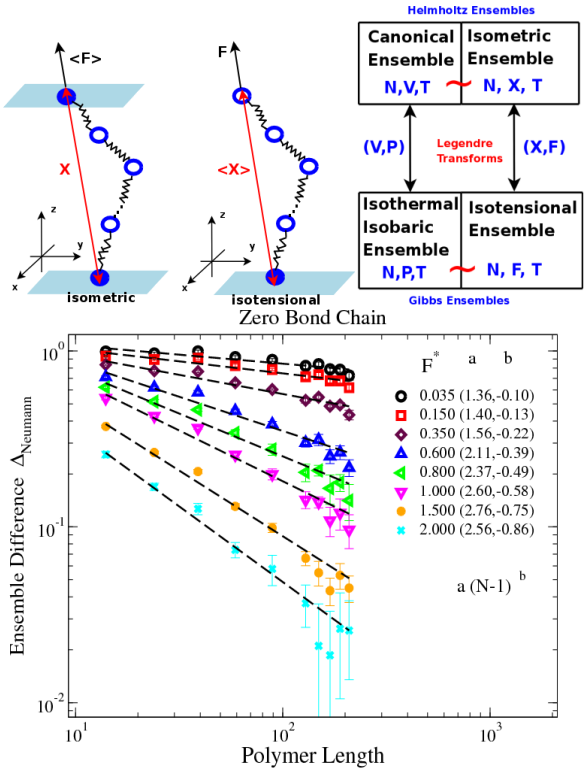

We have performed a large number of coarsed-grained Langevin dynamics simulations with the parallel molecular dynamics suite *ESPResSo* [5]. We have investigated this phenomenon with an isometric and an isotensional chain ensemble for a large range of force-regimes. Our findings [6] suggest that ensemble equivalence indeed can not be reached in the zero force limit regardless of the chain length i.e. even in the thermodynamic limit. Hence, our findings support the arguments given in Ref. [4].

References

1. Bustamante, C. and Liphardt, J. and Ritort, F., *The Nonequilibrium Thermodynamics of Small Systems*, Physics Today, 58, 7, 43-48, *2005*

2. F Ritort, *Single-molecule experiments in biological physics: methods and applications*, Journal of Physics: Condensed Matter, 18, 32, R531-R583, *2006*

3. Keller, D. and Swigon, D. and Bustamante, C., *Relating Single-Molecule Measurements to Thermodynamics*, Biophysical Journal, 84, 2, 733—738, *2003*

4. Neumann, R.M., *On the Precise Meaning of Extension in the Interpretation of Polymer-Chain Stretching Experiments*, Biophysical Journal, 85, 5, 3418—3420, *2003*

5. *H.J. Limbach, A. Arnold, B.A. Mann and C. Holm, ESPResSo--an extensible simulation package for research on soft matter systems, Computer Physics Communications,174,,704-727,2006*

6. M. Suzen, M. Sega, C. Holm, *Ensemble Inequivalence in Single Molecule Experiments,* arXiv:0810.3407, submited.

4.2.10 Ultrakalte Atome in optischen Gittern & elektronische Nanostrukturen

Walter Hofstetter, Michiel Snoek, Irakli Titvinidze, Denis Semmler, Julia Wernsdorfer, Falk May, Ulf Bissbort, David Roosen, Andreas Hubener
Institut für Theoretische Physik, Goethe-Universität Frankfurt am Main

In unserer Arbeitsgruppe wird an verschiedenen Themen aus dem Bereich der theoretischen Physik der kondensierten Materie geforscht. Neben der Beschreibung physikalischer Phänomene, die in ultrakalten Atomen in optischen Gittern beobachtet werden können, beschäftigen wir uns mit Effekten, welche im Transport durch elektronische Nanostrukturen auftreten.

Ultrakalte Atome in optischen Gittern

Ultrakalte Atome in optischen Gittern erlauben eine direkte experimentelle Realisierung von stark korrelierten Quanten-Vielteilchensystemen. Dabei kann ein Großteil der Modellparameter im Labor eingestellt werden, um eine Vielfalt an unterschiedlichen Szenarien realisieren und Quanten-Phasenübergänge direkt beobachten zu können. Unser besonderes Interesse gilt hierbei folgenden Themen:

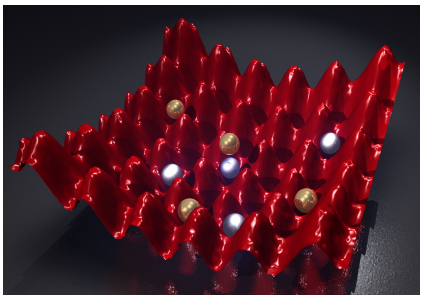

Abbildung 10.1: *Optisches Gitter mit ultrakalten Atomen.*

In zahlreichen Experimenten werden ***Mischungen verschiedener bosonischer Atome*** (z. B. ^{87}Rb und ^{41}K) in einem optischem Gitter untersucht [1]. Um das reichhaltige Phasendiagramm auch bei endlichen Temperaturen besser verstehen zu können benutzen wir eine Weiterentwicklung des Gutzwiller Ansatzes, die bosonische dynamische Molekularfeldtheorie. Des weiteren untersuchen wir die Dynamik in einem solchen System beim „Anschalten“ des optischen Gitters mit Hilfe eines dynamischen Gutzwiller Ansatzes. Dies ermöglicht eine realistische Abschätzung der Zeitskalen, bei denen die „Schaltvorgänge“ noch als adiabatisch angesehen werden können. Diese „Adiabazität“ wird bei Experimenten, bei denen die Wechselwirkung einer zweiten Spezies von Bosonen auf den Superfluid – Mott-Isolator Übergang untersucht wird, immer vorausgesetzt.

Wir studieren ***resonante SupraFluidität*** ultrakalter Fermionen, indem wir eine Mischung aus Fermionen und Bosonen betrachten [2]. Diese Art von Systemen wird durch das Bose-Fermi-Hubbard Modell beschrieben, welches sowohl die ortsabhängige Wechselwirkung der Fermionen untereinander, der Bosonen untereinander, als auch die Wechselwirkung zwischen Fermionen und Bosonen berücksichtigt. Zusätzlich zu diesen Wechselwirkungen enthält das betrachtete Modell auch einen Feshbach-Term, mittels welchem zwei Fermionen in ein Boson umgewandelt werden und umgekehrt. Da diese verschiedenen Wechselwirkungen jeweils anziehend oder abstoßend sein können, ergibt sich ein reichhaltiges Phasendiagramm. Je nach Wahl der Parameter erhält man eine suprafluide Phase, eine antiferromagnetische Phase, Ladungsdichtewellen, Mott Isolatoren, metallische Phasen oder auch Phasenseparation.

Außerdem studieren wir ***Fermionen in inhomogenem Umfeld,*** wie z. B. einem harmonischen Potential. Um die auftretenden inhomogenen Quantenzustände beschreiben zu

können, benötigen wir theoretische Methoden, welche ohne Translationsinvarianz, also ohne den Impuls als Quantenzahl, auskommen. Hierzu haben wir eine verallgemeinerte Version der dynamischen Molekularfeldtheorie (DMFT) entwickelt, welche eine positionsabhängige Selbstenergie zulässt [3]. Die Ortsraum-DMFT erlaubt uns außerdem eine Mischung verschiedener Fermionen zu untersuchen und dort den Effekt der Wechselwirkungsstärke auf die Ausdehnung der Atome, welche sich in Experimenten einfach messen lässt, zu berechnen.

Unordnung in optischen Gittern verändert das Verhalten der Atome drastisch. In Systemen ultrakalter, wechselwirkender Bosonen kann eine beliebig schwache Hinzugabe von Unordnung beispielsweise zu Anderson-Lokalisierung führen. Bei „angeschalteter“ Unordnung und Wechselwirkung zwischen den Bosonen tritt neben den bisher gut erforschten Mott Isolator und kondensierten Phase eine neue exotische Bose-Glas Phase auf. Eine Beschreibung dieser Phase bei T=0 mittels der in unserer Arbeitsgruppe entwickelten stochastischen Molekularfeldnäherung [4] dient als Ausgangspunkt zur weiteren Analyse komplizierterer Systeme. Neben Effekten bei endlichen Temperaturen und ultrakalten Atomen in dreidimensionalen Gittern mit anisotroper Unordnung, die von unmittelbarem Interesse für aktuelle Experimente sind [5], untersuchen wir auch Systeme wechselwirkender Fermionen und Mischungen von Bosonen und Fermionen in ungeordneten optischen Gittern. Hierbei kommen verschiedene numerisch anspruchsvolle Methoden, wie die statistische Dynamische Molekularfeldtheorie oder auch die stochastische Greensfunktionsmethode zum Einsatz.

Elektronische Nanostrukturen

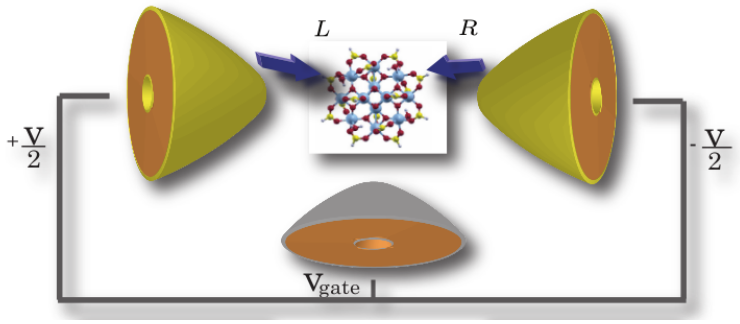

Abbildung 10.2: *Darstellung eines an metallische Leiter gekoppelten molekularen Magneten.*

In unserer Arbeitsgruppe wird neben den obigen Themen die Physik von Quanten-Störstellen-Modellen untersucht. Wir sind hierbei insbesondere an Phänomenen interessiert, welche bei sehr tiefen Temperaturen in diesen Systemen auftreten. Motiviert durch Experimente, bei denen es erstmals möglich war, isolierte molekulare Magneten (z. B. Mn_{12} mit einem Gesamtspin S = 10) an metallische Leiter zu binden und Stromtransport durch sie zu messen [6], untersuchen wir den zeitabhängigen Kondo-Effekt sowie die Beeinflussung des Stromtransport durch Vibrationsanregungen des Moleküls.

Bei Temperaturen in der Nähe des absoluten Nullpunktes reicht eine störungstheoretische Beschreibung der Systeme oftmals nicht mehr aus. Dies macht es notwendig, nicht-perturbative numerische Verfahren, wie z. B. die Numerische Renormierungsgruppe (NRG) [7], zu benutzen. Unser Ziel ist es, mit Erweiterungen dieser Methode auch Nicht-Gleichgewichtsphänomene zu studieren.

Verweise

1. I. Bloch, Physics World, **17**, 25-29 (2004).
2. I. Titvinidze, M. Snoek, and W. Hofstetter , Phys. Rev. Lett. **100**, 100401 (2008).
3. M. Snoek, I. Titvinidze, C. Tőke, K, Byczuk, and W. Hofstetter, New Journal of Physics **8**, 093008 (2008).
4. U. Bissbort and W. Hofstetter, arXiv:0804.0007.
5. J. Catani *et al.*, Phys. Rev. A **77**, 011603 R (2008).
6. H. Heersche *et al.*, Phys. Rev. Lett. **96**, 206801 (2006).
7. K. G. Wilson, Rev. Mod. Phys. **47**, 773 (1975).

4.2.11 Parton Cascade simulating ultrarelativistic heavy ion collisions

I. Bouras, A. El, O. Fochler, C. Greiner, H. Stöcker, J. Uphoff, and Z. Xu
Institut für Theoretische Physik, Goethe-Universität Frankfurt

We have developed a new 3+1 dimensional relativistic Monte Carlo parton cascade Boltzmann Approach of MultiParton Scatterings (BAMPS), which solves the kinetic on-shell Boltzmann equations for quarks and gluons including the elastic as well as the inelastic $gg \leftrightarrow ggg$ pQCD bremsstrahlung processes with full detailed balance. With this tool we simulate the space time evolution of partons and explore the important issue about the existence and the properties of a Quark-Gluon-Plasma (QGP) in an ultrarelativistic heavy ion collision. There are strong hints for the formation of such a new state of matter from experiments at BNL Relativistic Heavy Ion Collider (RHIC) in USA. Comparisons between the calculated elliptic flow v_2 from ideal (viscous) hydrodynamics and the measured v_2 from the experiments at RHIC support the creation of a nearly equilibrated quark-gluon system flowing with a small shear viscosity to entropy density ratio η/s in Au+Au collisions at RHIC energy.

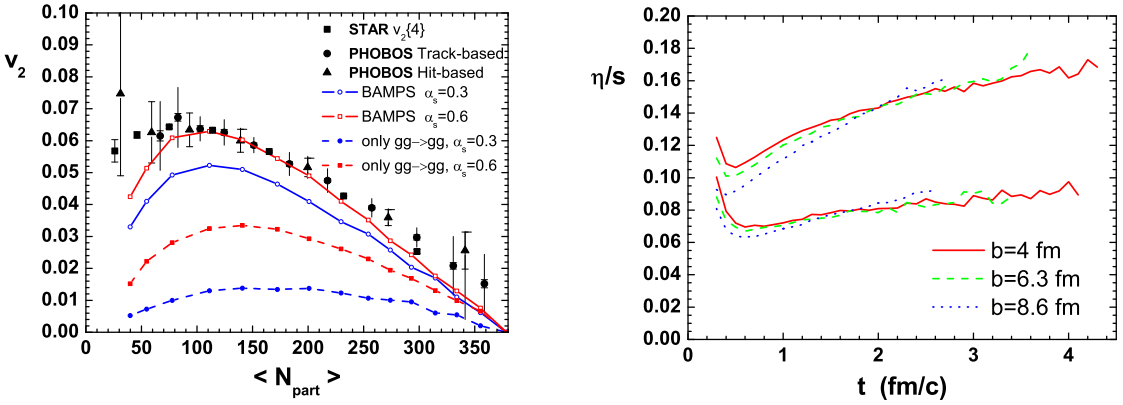

Abbildung 11.1: *Left panel: elliptic flow v_2 as a function of the number of participating nucleons in Au+Au collisions at RHIC. Right panel: the shear viscosity to the entropy density ratio.*

Although the initial conditions of partons just after their production in a heavy ion collision are not known yet, speculations show that they are definitely far from thermal distribution due to the subsequent rapid longitudinal expansion. How quarks and gluons thermalize within a short time scale $\leq$ 1 fm/c as assumed in hydrodynamical calculations is an important issue. This is not only because the thermalization time scale has to be theoretically determined, but also because the mechanism that drives the system toward equilibrium should respond to the smallness of the η/s value and the buildup of the collective flow of the QGP.

Transport calculations employing BAMPS give a transparent way to look at the dynamical processes which drive system to thermal equilibrium. We showed that the pQCD bremsstrahlung process and its back reaction ($gg \leftrightarrow ggg$) make the dominant contribution to thermalization, compared with the contribution from the elastic scatterings. The time

scale of full thermalization is about 1 fm/c in a simulation of a central Au+Au collision at RHIC energy. Whereas the cross section of the pQCD bremsstrahlung process is smaller than that of the elastic scattering, the inelastic processes seem very efficient for momentum isotropization. The large efficiency of the bremsstrahlung stems mainly from its large momentum deflection due to the present implementation of Landau-Pomeranchuk-Migdal effect. This is quantitatively investigated by introducing the transport rate of gluon drift and the transport collision rates of elastic as well as inelastic processes. We showed that for the gluon matter at RHIC pQCD $gg \leftrightarrow ggg$ bremsstrahlung processes isotropize the momentum five times more efficiently than elastic scatterings. Studies on the initial conditions dependence of parton thermalization are in progress.

Also the way thermalization occurs has been investigated and compared with the famous "Bottom-Up" scenario for thermalization of a color glass condensate. We demonstrate that the tremendous production of soft gluons via $gg \rightarrow ggg$, which is shown in the "Bottom-Up" picture as the dominant process during the early preequilibration, will not occur in heavy ion collisions at RHIC and LHC energies, because the back reaction $ggg \rightarrow gg$ hinders the absolute particle multiplication. Moreover, different from the "Bottom-Up" scenario, soft and hard gluons thermalize at the same time. The time scale of thermal equilibrium, as obtained from BAMPS calculations, is of order $\alpha_s^{-2}(\ln \alpha_s)^{-2} Q_s^{-1}$.

Recently, the elliptic flow v_2 of the gluon matter produced in Au+Au collisions at the RHIC energy is calculated by employing the parton cascade BAMPS.

We found that when using a QCD coupling constant of $\alpha_s = 0.6$, the calculated v_2 matches the experimental data. With $\alpha_s = 0.3$ the results are about 20% smaller than the data. Hence, pQCD interactions can explain the buildup of collectivity at RHIC. In addition, the shear viscosity to the entropy density ratio η/s from the transport calculations was extracted and it was found that η/s is between 0.15 for $\alpha_s = 0.3$ and 0.08 for $\alpha_s = 0.6$. These findings are similar to those obtained from viscous hydrodynamical calculations.

On the other hand, whereas the total gluon v_2 from the calculations agree well with the data, the transverse momentum dependence $v_2(p_T)$ are $20 - 50\%$ lower then the data in each centrality class. The final gluon transverse momentum spectra are harder than the data and also the final gluon mean transverse momenta are $40 - 100\%$ larger than the data. However, the final gluon transverse energy per rapidity at midrapididy agrees with the data. This indicates that the hadronization process via the parton-hadron duality is not justified. A realistic hadronization that transforms a gluon to $1.5 - 2$ pions on average would be expected for low p_T gluons, whereas at intermediate p_T, quark recombination shall be a better scenario of hadronization. In addition, the inclusion of quark degrees of freedom would reduce the final parton mean p_T and would lead to a better agreement between the calulated and measured $v_2(p_T)$. Adding quarks into the dynamical evolution of the QCD matter with a detailed understanding of the hadronization of gluons and quarks will be helpful in explaining the viscous facets of the final hadron elliptic flow and in extracting the shear viscosity to the entropy density ratio of the QGP. These works will be done in the near future.

Since the Quark-Gluon-Plasma has a large geometrical size, high energy particles will lose their energy when travelling through the medium. This phenomenon is named "Jet-Quenching" and manifested by the experimental measurement. Employing the parton cascade BAMPS the gluonic contribution to the nuclear modification factor, R_{AA} , is investigated for central Au+Au collisions at $\sqrt{s} = 200$A GeV. Energy loss of jets is mainly due to their bremsstrahlung. Our result is in good agreement with results from the GLV

formalism. We demonstrated that the present microscopic transport description is able, for the first time, to explain both jet-quenching and a strong buildup of elliptic flow in terms of the same standard pQCD interactions. A detailed study of the dependence of the pQCD bremsstrahlung process on the Landau-Pomeranchuck-Migdal suppression has to be done. This is one of our future projects.

Heavy quarks are very important hard probes for extracting properties of the QGP. Investigations on thermalization, ellipitic flow and energy loss of heavy quarks are in progress.

Experimentally a significant and exciting structure in the two-particle and three-particle correlations of associated particles of a high energy jet has been observed, which might be the result of the conical emission of propagating Mach shocks created by a jet crossing the expanding medium. A particular simpler case of a to be created shock wave represents the well established (relativistic) Riemann problem. Using the parton cascade BAMPS dissipative shocks in the Riemann problem are nicely produced (see Fig. 11.2). Whether Mach cone-like behaviour can be observed within realistic simulations for RHIC is an exciting issue, as the QGP life time is not long and the medium is indeed viscous. Works are in progress. Such simulations need very intensive computing time. In addition, cascade simulations provide an execellent basis for testing numerical algorithms for the various developing dissipative hydrodynamical theories. First results show when the Israel-Stewart second order viscous hydrodynamics breaks down. Further investigations will be done in the near future.

1. Z. Xu and C. Greiner: Shear viscosity in a gluon gas, Phys.Rev.Lett.100:172301,2008

2. Z. Xu, C. Greiner, and H. Stöcker: Perturbative QCD Calculations of Elliptic Flow and Shear Viscosity in Au+Au Collisions at $\sqrt{s_{NN}} = 200$ GeV, Phys.Rev.Lett.101:082302,2008

3. A. El, Z. Xu, and C. Greiner: Thermalization of a color glass condensate and review of the "Bottom-Up" scenario, Nucl.Phys.A806:287-304,2008

4. Z. Xu, C. Greiner, and H. Stöcker: QCD plasma thermalization, collective flow and extraction of shear viscosity *Proceedings of Quark Matter 2008*, J.Phys.G35:104016,2008

5. A. El, Z. Xu, and C. Greiner: Review of the "Bottom-Up" scenario *Proceedings of Quark Matter 2008*, J.Phys.G35:104072,2008

6. O. Fochler, Z. Xu, and C. Greiner: Towards a unified understanding of jet-quenching and elliptic flow within perturbative QCD parton transport, e-Print: arXiv:0806.1169 [hep-ph], submitted to Phys.Rev.Lett.

7. Z. Xu and C. Greiner: Elliptic flow of gluon matter in ultrarelativistic heavy-ion collisions, e-Print: arXiv:0811.2940 [hep-ph], submitted to Phys.Rev.C

8. I. Bouras, L. Cheng, A. El, O. Fochler, J. Uphoff, Z. Xu, and C. Greiner: Viscous Effects on Elliptic Flow and Shock Waves *Proceedings of the 2008 Erice School on Nuclear Physics*, e-Print: arXiv:0811.4133 [hep-ph]

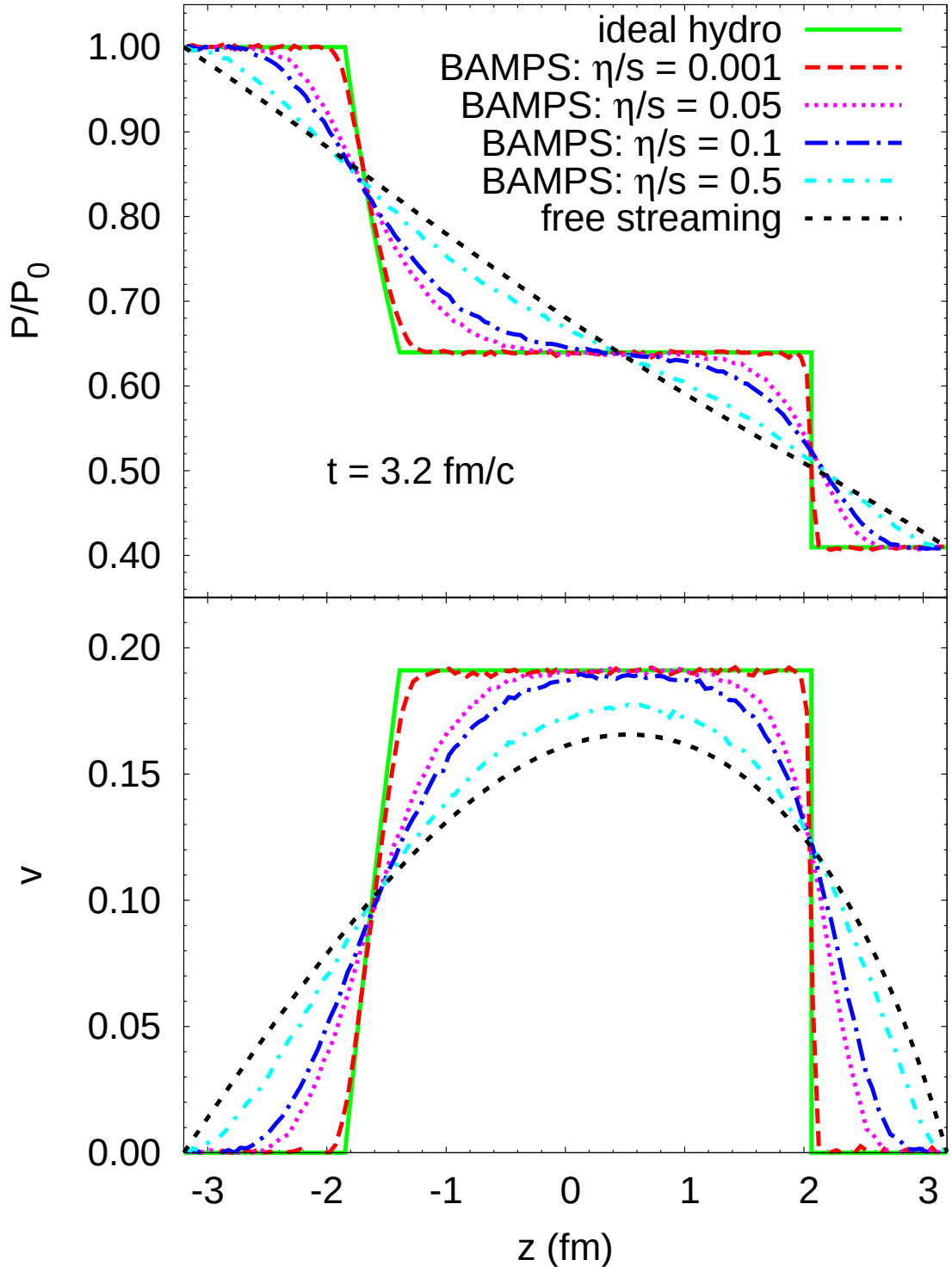

Abbildung 11.2: *Local pressure (top) and velocity (bottom) distribution in a Riemann problem: At z=0 fm (the x-y-plane) there is an initial discontinuity in pressure and energy density of thermalized matter.*

4.2.12 Ab-initio relativistic density functional calculations for spectral line shifts of Alkali atoms in liquid helium

Fachgebiet Theoretische Physik, Universität Kassel
J. Anton, B. Fricke, P. K. Mukherjee, S. Fritzsche

Investigations on the spectral properties of atomic systems embedded inside liquid helium were carried out over several decades [1] and yielded rich information on not only the spectral line shifts, change in line profiles and various other spectroscopic information of the embedded atom but also indicate a possible way of investigating the quantum fluid properties with the impurity atom acting as sensitive external microprobes [1,2]. The impurity atom experiences a strong Pauli type repulsion at the liquid helium boundary resulting in the formation of a nano cavity surrounding the foreign atom. The size and form of the cavity depends on the pair potential between the impurity atom and surrounding He and the detailed electronic structure of the impurity.

Our current aim is to ascertain the applicability and success of the RLDA [3,4] method in interpreting the experimental spectral data of foreign atoms embedded in liquid helium. Here we have performed investigations on Na-He, Rb-He and Cs-He clusters and the shifts of the spectral transition lines D1 and D2 are obtained.

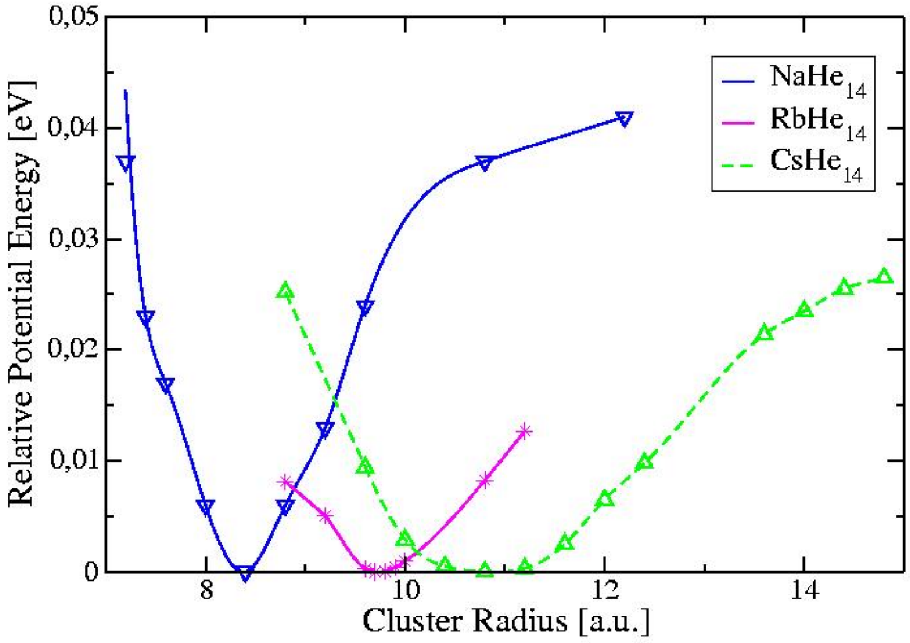

Abbildung 12.1: *Theoretical potential energy curves of the alkali-He clusters plotted against cluster radius*

Tabelle 12.1: *Spectral line shifts of alkali atoms embedded in liquid helium. Experimental values are presented together with our relativistic RLDA as well as other non-relativistic (averaged) results.*

Transition	Shift	
	exp.	Theory [5]
Na		
$s_{\frac{1}{2}} \rightarrow p_{\frac{1}{2}}$	unknown	–22.90
$s_{\frac{1}{2}} \rightarrow p_{\frac{3}{2}}$	unknown	–22.72
Rb		
$s_{\frac{1}{2}} \rightarrow p_{\frac{1}{2}}$	–16.8 ± 0.5 [6]	–14.02
$s_{\frac{1}{2}} \rightarrow p_{\frac{3}{2}}$	–16.0 ± 0.5 [6]	–16.81
Cs		
$s_{\frac{1}{2}} \rightarrow p_{\frac{1}{2}}$	–18.4 ± 0.5 [6]	–15.52
$s_{\frac{1}{2}} \rightarrow p_{\frac{3}{2}}$	–18.1 ± 0.5 [6]	–17.83

Literaturverzeichnis

[1] B. Tabbert, H. Gunther, G. zu Putlitz, *J. Low. Temp. Phys.* **109**, 653 (1997)
[2] B. Tabbert, M. Beau, M. Foerste, et al., *Z. Phys. B* **98**, 399 (1995)
[3] J. Anton, P. K. Mukherjee, B. Fricke and S. Fritzsche, *J. Phys. B* **40**, 2453 (2007)
[4] D. Geschke et al., *Phys. Rev. B* **62**, 15439 (2000)
[5] J. Anton, B. Fricke, P. K. Mukherjee, S. Fritzsche, *Phys. Lett. A* **372**, 4462 (2008)
[6] Y. Takahashi, K. Sano, T. Kinoshita, T. Yabuzaki, *Phys. Rev. Lett.* **71**, 1035(1993)

4.2.13 Boltzmann/Hydrodynamik-Hybridmodell für Schwerionenkollisionen

Hannah Petersen, Jan Steinheimer, Qingfeng Li, Marcus Bleicher
Institut für Theoretische Physik, Goethe Universität Frankfurt,
Max-von-Laue-Strasse 1, 60438 Frankfurt am Main

In hochenergetischen Schwerionenkollisionen werden die Eigenschaften stark wechselwirkender Materie untersucht. Insbesondere ist der Phasenübergang von einem Hadronengas zum Quark-Gluon-Plasma, der bei hohen Temperaturen und/oder hohen Dichten erwartet wird, von großem Interesse. Nur durch die theoretische Beschreibung und vollständige Simulation der Kollision ist es möglich, aus den gemessenen Teilchenverteilungen im Orts- und Impulsraum, Rückschlüsse auf die Hochdichtephase der Reaktion zu ziehen.

Ein sehr erfolgreicher Ansatz für die Beschreibung der Dynamik der Schwerionenrekationen sind sogenannte Hybridmodelle, die hydrodynamische Rechnungen mit mikroskopischen Ansätzen kombinieren. Hierbei werden entweder die Anfangsbedingungen mit einem mikroskopischen Transportmodell generiert und dann eine (3+1)-dimensionale hydrodynamische Rechnung durchgeführt oder die Anfangsbedingungen beispielsweise mit Hilfe einer Glauberrechnung parametrisiert und ein mikroskopisches Transportmodell für die hadronischen Wechselwirkungen in der späten Phase der Reaktion verwendet. Der nächste logische Schritt war nun die Implementierung eines integrierten Zuganges, bei dem die hydrodynamische Phase dynamisch in ein hadronisches Transportmodell integriert wird.

Berechnungen mit verschiedenen Zustandsgleichungen wurden durchgeführt und es wurde systematisch untersucht, welche Effekte durch eine Änderung des Ausfrierprozesses und durch die Änderung der Dynamik hervorgerufen werden. Hierbei wurden die folgenden Observablen im Einzelnen untersucht werden:

Durch Teilchenkorrelationen im Endzustand wurden mit Hilfe der HBT-Analyse die Systemgröße und die Lebenszeit des Feuerballs gemessen. Der Phasenübergang spiegelt sich beispielsweise in längeren Lebenszeiten wider.

Produktion von Teilchen mit seltsamen Quarks als Test zur Erreichung des thermischen Gleichgewichts. Des weiteren wurde die Produktion von metastabiler exotischer mehrfachseltsamer Materie im Rahmen des Hybridmodells untersucht.

Der kollektive transversale Fluss als ideale Beobachtungsgröße für den Druck wurde bei verschiedenen Strahlenergien untersucht. Der gerichtete und vor allem der elliptische Fluss sind sehr gut geeignet, um den Phasenübergang zu detektieren, da diese Größen bei allen Strahlenergien eine Rolle spielen.

Diese Studien haben große Relevanz insbesondere im Hinblick auf zukünftige Experimente am neuen Beschleuniger FAIR, der sich zur Zeit in Planung befindet.

Referenzen

Q. Li et al, Phys.Lett.B659:525-530,2008
J. Steinheimer et al, Phys.Rev.C77:034901,2008
Q. Li, et al, Phys.Lett.B663:395-399,2008
H. Petersen et al, Phys.Rev.C78:044901,2008
J. Steinheimer et al, arXiv:0811.4077

4.2.14 The many-particle scattering system He^{++} on He: A complete unified description

Fachgebiet Theoretische Physik, Universität Kassel
J. Anton, B. Fricke, X. Ma

In recent years we have developed a method which allows to give a complete unified description for a many-particle ion-atom scattering system which is able to calculate all possible processes which occur in such a collision at the same time. In order to describe such highly differential cross sections the theoretical task is to solve the many-particle Dirac equation directly

$$\hat{H}_{\rm el}\ \Psi(\vec{r}_1,\ldots,\vec{r}_N,{\rm t}) = {\rm i}\,\hbar\frac{\partial}{\partial t}\ \Psi(\vec{r}_1,\ldots,\vec{r}_N,{\rm t}).$$

As choice for the electronic Hamilton operator $\hat{H}_{\rm el}$ we include the kinetic energy, the electron-nucleus interaction and the electron-electron interaction in form of the Coulomb part and the exchange part in the form of a local approximation. As ansatz for the total wave function we assume a Slater determinant

$$\Psi(\vec{r}_1,\ldots,\vec{r}_N,{\rm t}) = \frac{1}{\sqrt{\rm N!}}\begin{vmatrix} \psi_1(\vec{r}_1,{\rm t}) & \ldots & \psi_1(\vec{r}_N,{\rm t}) \\ \vdots & \ldots & \vdots \\ \psi_N(\vec{r}_1,{\rm t}) & \ldots & \psi_N(\vec{r}_N,{\rm t}) \end{vmatrix},$$

where we approximate the time-dependent single-particle wave functions $\psi_i(\vec{r},{\rm t})$ as a sum of static molecular functions with expansion coefficients $a_{\rm ij}$. We have applied this method to the system He^{++} on He at 30 keV [1]. Using the method of inclusive probabilities [2] we are able to reconstruct with the knowledge of all expansion coefficients $a_{\rm ij}$ the excitation, transfer and ionization probabilities. They allow to answer the questions which describe the system completely: What is the impact parameter dependent probability of double charge transfer (see Fig. 14.1) or electron capture in the K, L and M-shell of the projectile? Both quantities are experimentally available. The results for all possible processes are given in Table 14.1.

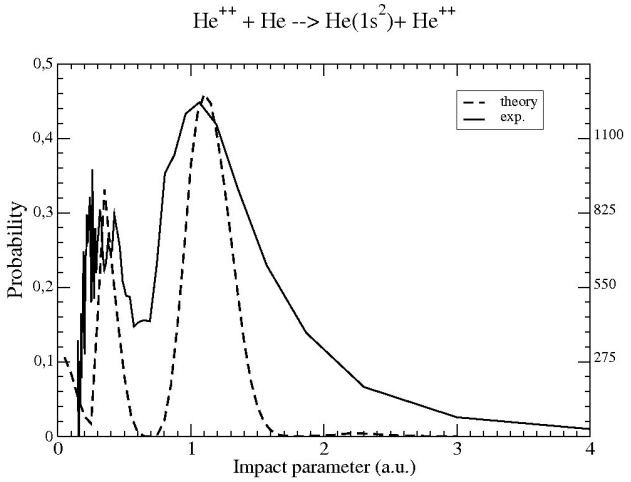

Abbildung 14.1: *Impact parameter dependent probability for the double charge transfer for the scattering system He^{++} on He at 30 keV.*

Tabelle 14.1: *Integral relative probability for charge transfer,transfer and ionization for the system $He^{++} \rightarrow He$ at 30 keV.*

Scattering system	Process	Relative probability for the process	
		exp.	theoret.
$He^{++} + He \rightarrow$	$He + He^{++}$	64.3 %	66 %
	$He^{+}(1s) + He^{+}$	12.1 %	8 %
	$He^{+}\ (n = 2) + He^{+}$	16.4 %	18 %
	$He^{+}\ (n > 2) + He^{+}$	2.9 %	4 %
	$He^{+} + He^{++} + e$	2.9 %	4 %
	$He^{++} + He^{+} + e$	1.4 %	

Literaturverzeichnis

[1] J. Anton et al, *Phys. Lett. A* **369**, 85 (2007)

[2] H.-J. Lüdde, A. Henne, T. Kirchner and R. M. Dreizler, *J. Phys. B* **29**, 4423 (1996)

4.2.15 Solving the 3d Schrödinger Equation for ? Bound States in an Anisotropic Quark-Gluon Plasma

Prof. Dr. Adrian Dumitru, Dipl. Phys. Yun Guo
Institut für Theoretische Physik der Johann Wolfgang Goethe-Universität

To determine the wave functions of bound quarkonium states, we solve the time-independent Schrödinger equation on a three-dimensional lattice in coordinate space with a given potential. To find solutions to the time-independent Schrödinger equation we use the finite difference time domain method (FDTD) [1]. In this method we start with the time-dependent Schrödinger equation which can be solved by expanding in terms of the eigenfunctions. If one is only interested in the lowest energy states (ground state and first few excited states), an efficient way to proceed is to transform the time-dependent Schrödinger equation to Euclidean time by a Wick rotation. For details of the algorithm we refer to ref. [1].

By definition the ground state is the state with the lowest energy eigenvalue. Therefore, at late imaginary time the sum over eigenfunctions is dominated by the ground state eigenfunction. Because of this one can obtain the ground state wavefunction and energy by solving the time-dependent Schrödinger equation starting from a random three dimensional wavefunction and evolving forward in imaginary time. This initial wavefunction should have nonzero overlap with all eigenfunctions of the Hamiltonian; however, due to the damping of higher-energy eigenfunctions at sufficiently late imaginary times we are left with only the ground state. Once the ground state wavefunction (or, in fact, any other wavefunction) is found we can compute its energy eigenvalue by computing the expectation value of the Hamiltonian.

The basic method for finding excited states is to first evolve the initially random wavefunction to large imaginary times, find the ground state wavefunction, and then project this state out from the initial wavefunction and re-evolve the partial-differential equation in imaginary time. However, there are (at least) two more efficient ways to accomplish this. The first is to record snapshots of the 3d wavefunction at a specified interval during a single evolution. After having obtained the ground state wavefunction, one can then go back and extract the excited states by projecting out the ground state wavefunction from the recorded snapshots. An alternative way to select different excited states is to impose a symmetry condition on the initially random wavefunction which cannot be broken by the Hamiltonian evolution. In the anisotropic case this trick can be used to separate the different polarizations of the first excited state of the quarkonium system and to determine their energy eigenvalues with high precision. This high precision allows one to more accurately determine the splitting between polarization states which are otherwise degenerate in the isotropic Debye-Coulomb potential. Whichever method is used, once the wave function of an excited state has been determined one can again determine its energy eigenvalue.

Systemanforderungen

To get a reasonable accuracy we choose lattices with lattice-spacings a approximately 20 times smaller than the root-mean-square radius of the state under consideration. The lattice size L was chosen to be about 6 times larger than the RMS radius. For the temporal step we employed $\Delta\tau = a^2/\ 5$ for a stable simulation and stopped the time evolution when the energy of the state had stabilized to within 10^{-6}. Solving for the ground state requires lattices of size 128^3 but to fit excited states we require up to 512^3 lattice points.

- CPU-Stunden pro Jahr: 500

- Typische Zahl von Prozessoren bei parallelen Rechnungen (sonst 1): 4-8
- Vernetzung (Gigabit oder Myrinet/Infiniband): Gigabit
- Hauptspeicherbedarf pro Prozess: 1 Gbyte
- Plattenplatz zur Datenspeicherung: 40 Gbyte

Mitglieder der Arbeitsgruppe

JProf. Dr. A. Dumitru, Y. Guo (Doktorand).

References

[1] I. W. Sudiarta and D. J. W. Geldart, Journal of Physics A 40 8, 1885 (2007).

4.2.16 Orbital-dependent exchange-correlation energy functionals

H. Jiang, R. Manteufel, E. Engel
Inst. für Theor. Physik, J.W.Goethe-Universität Frankfurt am Main

The success of density functional theory (dft) relies on the quality of the standard approximation for the exchange-correlation (xc) energy functional, the generalized gradient approximation (GGA). However, the GGA fails for some interesting problems, as highly correlated solids and dispersion forces. A systematic improvement over the GGA is offered by xc-functionals which depend on the Kohn-Sham (KS) orbitals, rather than only on the density. In this formalism, the exchange energy can be treated exactly (EXX), which solves the long-standing self-interaction problem. As a consequence, one e.g. obtains a Rydberg series of unoccupied states for neutral atoms, implying the existence of negative atomic ions. Applications to solids point at an improved description of the band gaps of semiconductors, although the convergence of these results has been questioned recently. However, neither the complete neglect of correlation nor the combination of the exact exchange with a conventional correlation functional is adequate. In addition, often relativistic effects play an important role for the electronic structure of solids. The inclusion of orbital-dependent exchange and correlation functionals in a relativistic framework is therefore one of the major goals in dft.

In the present project the concept of the orbital-dependent xc-functionals has been introduced into relativistic spin density functional theory (rsdft), as the appropriate dft approach to magnetic systems (ranging from open-shell atoms to solids). After establishing the formal background for this approach by extension of the optimized potential method (OPM) to rsdft [1,2], the resulting integral equations for the determination of the xc potential has been implemented in two computer codes, a code for open-shell atoms (which serves both as a benchmarking tool and as solver for the core states of solids) and a general purpose KKR code for solids [2,3]. The atomic code has also been used to generate relativistic EXX-pseudopotentials which were then applied to study the electronic structure of semiconductors within the plane-wave pseudopotential scheme [4]. In particular, the size of the band gap resulting from highly converged calculations with the exact exchange has been investigated.

OPM calculations for molecules and solids are still challenging, due to the high computational demands resulting from the solution of the OPM integral equations. Even in the case of atoms the complicated structure of the orbital Green‘s function (which enters into the OPM integral equation) of rsdft and the evaluation of orbital-dependent correlation require more than standard desktop resources. All calculations have therefore been performed on the HPC cluster of the CSC at Goethe University Frankfurt.

The calculations for atoms addressed three topics: (i) the relative importance of exchange splitting and spin-orbit coupling, (ii) the accuracy of atomic hyperfine constants, and (iii) the relative stability of the $3d^{n-1}4s^2$ and $3d^n4s$ configurations of the 3d transition metal elements, i.e. the energy associated with the s-d-transfer process.

It was found that the spin alignment favored by the exact exchange dominates the KS spectrum over a wider range of nuclear charges than observed for conventional density functionals. A prominent example is Pb for which the states of the 6p shell are ordered according to good total angular momentum j in case of the GGA, while this ordering dissolves in the EXX calculation. The modified balance between spin alignment and spin-orbit coup-

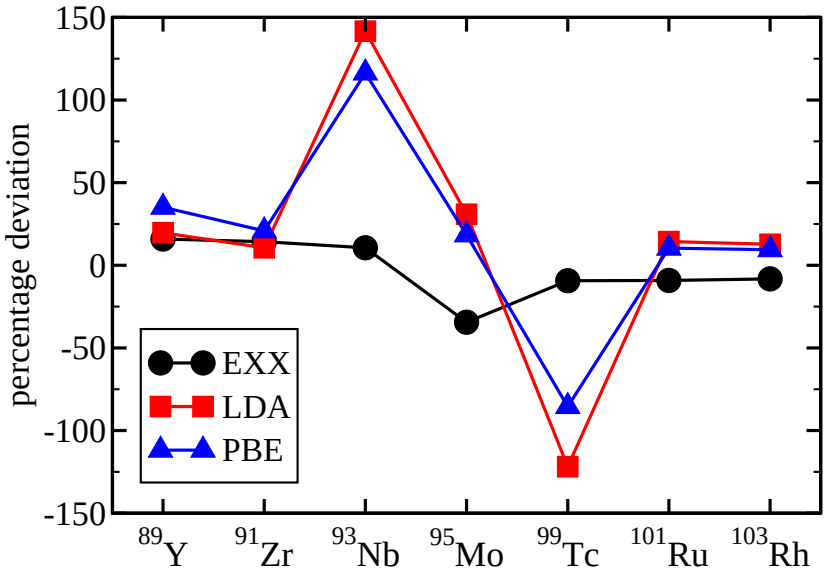

Abbildung 16.1: *Deviation of hyperfine constants a from experimental value: EXX results versus local density approximation (LDA) and GGA data for 4d transition metal elements.*

ling seems to improve in particular the description of the 4d elements: For several of the 4d elements the exact exchange provides a much better description of hyperfine constants than the GGA (see Fig. 16.1). Similarly, the EXX scheme yields improved s-d-transfer energies for the 3d elements. When combined with an orbital-dependent representation of correlation in the form of the RPA [5], the resulting s-d-transfer energies closely follow their experimental counterparts throughout the complete 3d shell (see Fig. 16.2). The agreement between EXX+RPA and experiment is particularly good in the second half of the shell, for which the identification of KS and experimental states is unambiguous (which is non-trivial for the first half). The s-d-transfer energies of the 3d elements thus provide another example for the scientific potential of orbital-dependent xc-functionals.

First results obtained with the plane-wave pseudopotential calculations for semiconductors confirm the improved band gaps resulting from use of the exact exchange: Using large valence spaces and corresponding plane-wave basis sets, one can demonstrate that the core-valence interactions missing in previous EXX-calculations for semiconductors do not affect the band gaps significantly [4]. The HPC computing facilities of the CSC were crucial for the success of this convergence check.

References

[1] D. Ködderitzsch, H. Ebert, E. Engel, Phys. Rev. B **77**, 045101 (2008).
[2] E. Engel, D. Ködderitzsch, H. Ebert, Phys. Rev. B **79** (2009).
[3] D. Ködderitzsch, H. Ebert, H. Akai, E. Engel, J. Phys.: Condens. Matter **21** (2009).

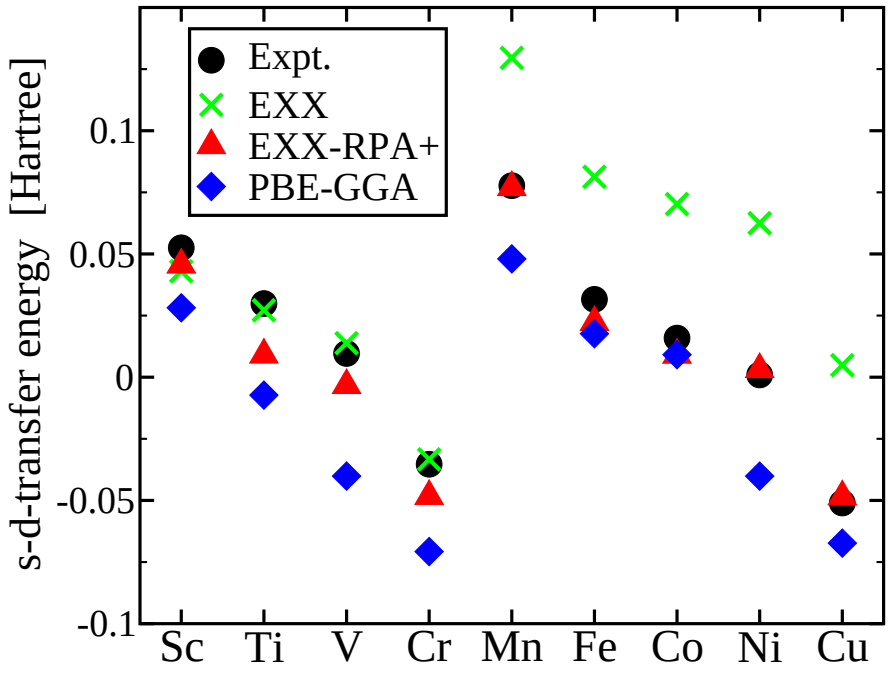

Abbildung 16.2: *s-d-transfer energies of 3d-elements: EXX results versus data obtained from exact exchange plus RPA+ for correlation (EXX-RPA+), GGA (PBE variant) and experimental numbers (RPA+ = RPA + 2nd order exchange within the LDA).*

[4] R. Manteufel, E. Engel, to be published (2008).
[5] H. Jiang, E. Engel, J. Chem. Phys. **127**, 184108 (2007).

4.2.17 Liquid surface model for carbon nanotube energetic

Frankfurt Institute for Advanced Studies, Goethe University, Frankfurt am Main, Germany
Ilia A. Solov'yov, Maneesh Mathew, Andrey V. Solov'yov and Walter Greiner

Carbon nanotubes have been considered as potential candidates for a variety of electrical, mechanical and chemical applications. However, in order to use them commercially, many issues need to be resolved. One of the major issues is the controlling of the chirality of nanotubes during their synthesis.

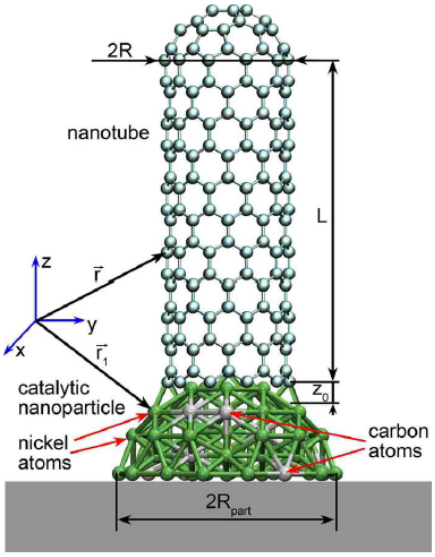

Abbildung 17.1: *Single-wall carbon nanotube atop a catalytic nickel nanoparticle, z_0 is the distance between the nanotube and the catalytic nanoparticle, L is the length of the nanotube, R is the nanotube radius, and R_{part} is the radius of the nanoparticle.*

We have developed a model [1] for calculating the energy of single wall carbon nanotubes of arbitrary chirality (determined by two integer numbers n and m). This model, which we call as the liquid surface model, predicts the energy of a nanotube with relative error less than one percent once its chirality and the total number of atoms are known. The parameters of the liquid surface model and its potential applications are discussed. The model has been suggested for open end and capped nanotubes. The influence of the catalytic nanoparticle, atop which nanotubes grow (see Fig. 17.1), on the nanotube stability is also discussed.

The suggested model gives an important insight in the energetics and stability of nanotubes of different chirality and might be important for the understanding of nanotube growth process. For the computations we use empirical Brenner and Tersoff potentials and discuss their applicability to the study of carbon nanotubes. From the calculated energies we determine the elastic properties of the single wall carbon nanotubes (Young modulus, curvature constant) and perform a comparison with available experimental measurements and earlier theoretical predictions.

The result of comparison of the binding energy per atom predicted by the liquid surface model and that calculated using the Tersoff potential for the open end nanotubes is illustrated in Fig. 17.2 which shows the dependence of the binding energy on the total number of atoms in the system. Different symbols: squares, triangles, stars and dotsrepresent the values calculated using the Tersoff potential and the lines near the corresponding symbols show the predictions of the liquid surface model.

References

[1] Ilia A. Solov'yov, Maneesh Mathew, Andrey V. Solov'yov and Walter Greiner, *Phys. Rev. E* **78**, (2008) 051601.

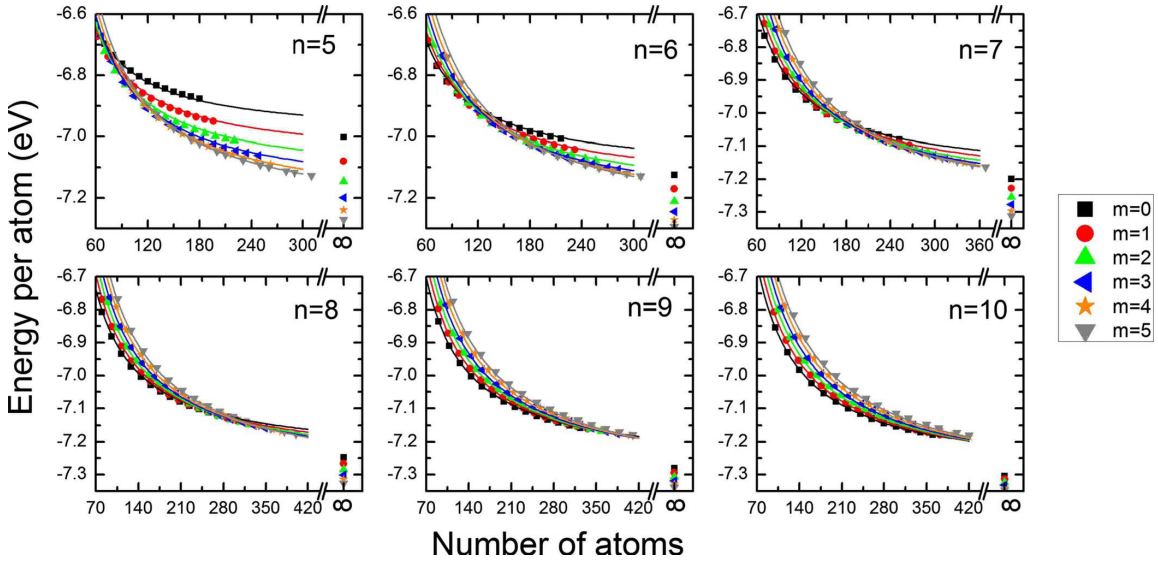

Abbildung 17.2: *Comparison of the binding energy per atom calculated using the Tersoff potential and that obtained from the liquid surface model for the open end nanotubes. The curves show the values predicted by the model and different symbols (squares, triangles, stars, dots) correspond to the calculated values. The plots are shown for n=5-10. Each curve in one plot corresponds to a different m value.*

4.2.18 Towards understanding of C_{60}-based nanowire growth with anomalous anisotropy

[1] *Frankfurt Institute for Advanced Studies, Goethe University, Frankfurt am Main, Germany*
[2] *Department of Chemistry, University of Cambridge, Cambridge, United Kingdom*
Ilia A. Solov'yov[1], Junfeng Geng[2], Andrey V. Solov'yov[1] and Brian F. G. Johnson[2]

The growth of one-dimensional (1D) nanocrystals is an important research topic in crystal engineering for nanotechnology because of the properties associated with the low-dimensionality, quantum confinement effect, and potential magnetic and photonic applications.

In a recent study [1], it was demonstrated that exceptionally long fullerene nanowires, with a length-to-width aspect ratio as large as ˜3000-5000, can be grown from 1,2,4-trimethylbenzene solution of C_{60}.

We perform a thorough theoretical analysis, aimed to explain the exceptionally large aspect ratio of C60-based nanowires. By accounting for different interactions in the system we have calculated the structure of the unit cell and determined the role of the fullerene and of the solvent molecules in the crystallization process of the nanowire [2]. The structure of six energetically favorable isomers of the nanowire unit cell is shown in the figure. We have calculated the adhesion energy of C60 molecules to the nanowire surface and demonstrated that it is related to the anisotropy of the crystal.

To get a more in-depth understanding of the nanowire growth mechanism we have also considered the influence of electron polarization on the anisotropy of the C60-based nanowires [3] and studied the possible polymerization reactions in the system, which likely occur between the C60 and the solvent molecules in the nanowire [4].

References

[1] J. Geng, W. Zhou, P. Skelton, W. Yue, I. Kinloch, A. Windle, and B. Johnson, *J. Am. Chem. Soc.* **130** (2008) 2527.

[2] J. Geng, I. Solov'yov, W. Zhou, A.V. Solov'yov, and B.F.G Johnson, *J. Phys. Chem. C, submitted* (2008).

[3] I. Solov'yov, J. Geng, A.V. Solov'yov, and B.F.G Johnson, *Chem. Phys. Lett., submitted (2008).*

[4] J. Geng,I.A. Solov'yov, D.G. Reid, A.E.H. Wheatley, A.V. Solov'yov and B.F.G. Johnson, *Angew. Chem. Int. Ed., submitted* (2008).

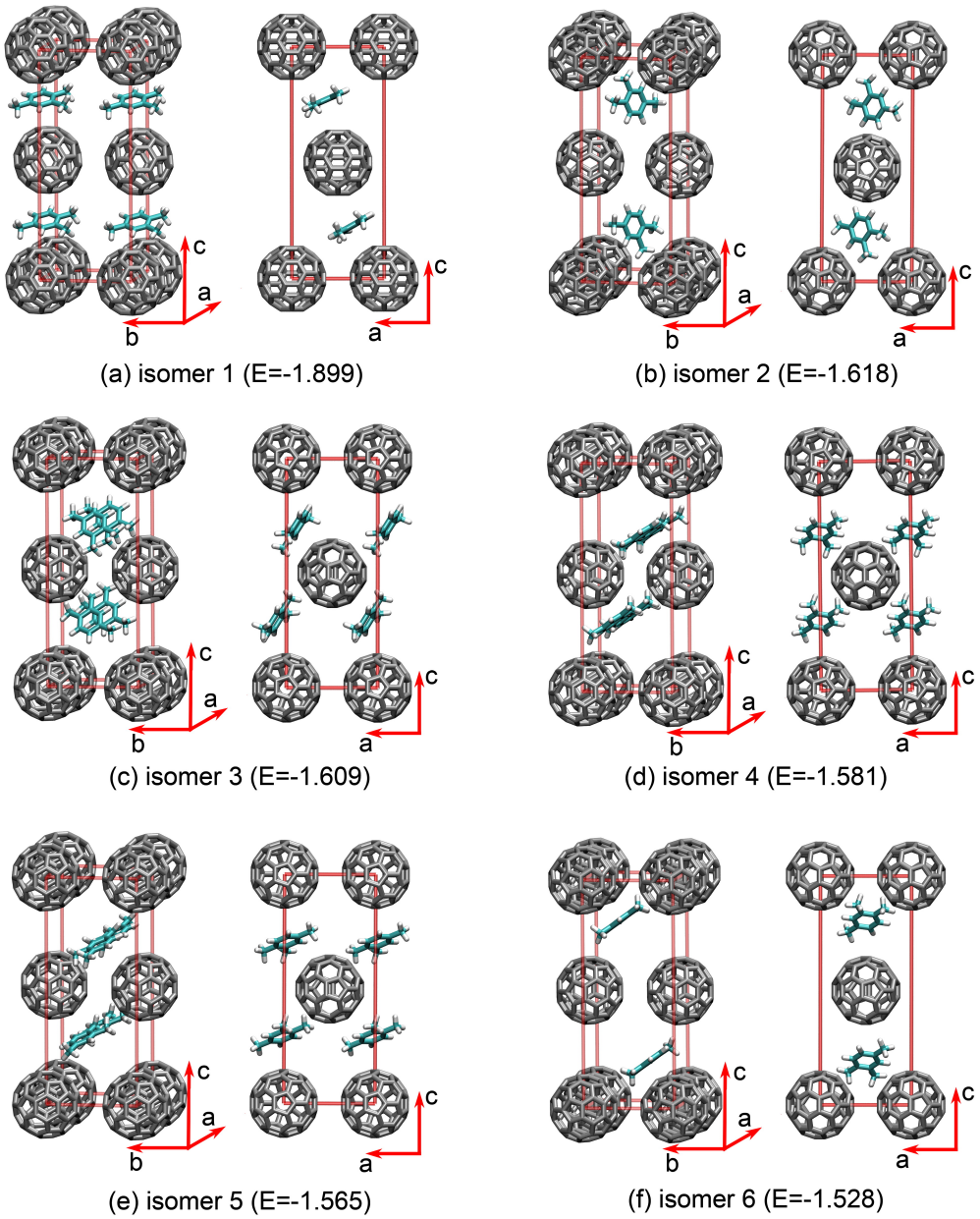

Abbildung 18.1: *Optimized isomeric states in the C_{60}·TMB nanowire unit cell as derived from the calculations. The number in the brackets below each image shows the energy of the structure (in eV). The coordinate frames used in the present work are also indicated.*

4.2.19 Phase transitions in fullerenes

Frankfurt Institute for Advanced Studies, Goethe University, Frankfurt am Main, Germany
Adilah Hussein, Alexander Yakubovich, Andrey Solov'yov and Walter Greiner

The phase transition of fullerenes C_{60} and C_{240} by was investigated by conducting constant-temperature molecular dynamics simulations. We have simulated the self assembly process of the C_{60} from a gaseous phase in the vicinity of the phase transition temperature at which the two phases should coexist. Here, the fullerene system is seen to continuously oscillate between two phases: the solid-like cage and the gas-like state of dimers and short chains. These oscillations correspond to consecutive fragmentation and assembly of the fullerene cage. We have also investigated the temperature-dependent heat capacity of the fullerenes, whose prominent peaks are signatures of the finite system analogue of first-order phase transitions. Our simulations were conducted for 500 ns using a developed topologically constrained pair-wise forcefield and were then supplemented by statistical mechanics analysis to take into account pressure and entropy corrections. These corrections lead to a phase transition temperature of 3800-4200 K, for the pressure range of 10-100 kPa, in good agreement with available experimental values.

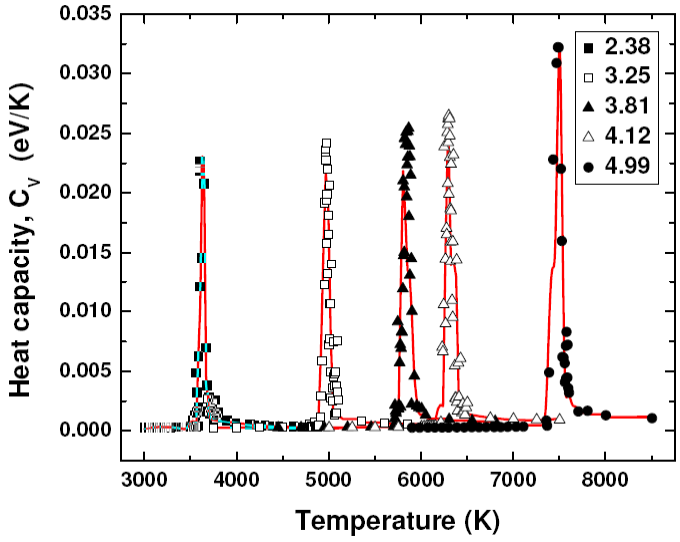

Abbildung 19.1: *C_{60}heat capacity plots obtained for different energies of the single bonds in the system. The temperature at the maximum of each heat capacity curve is denoted the phase transition temperature, T_{PT}: 3500 K (2.38 eV), 4950 K (3.25 eV), 5855 K (3.81 eV), 6450 K (4.12 eV), 7450 K (4.99 eV). The scatter plots are calculated using the fluctuations of the total energy while the thick solid lines were differentiated from the cubic B-spline interpolation of the total energy on temperature dependence.*

References

[1] A Hussien, A Yakubovich, A Solov'yov and W Greiner, http://arxiv.org/abs/0807.4435v1 (2008)

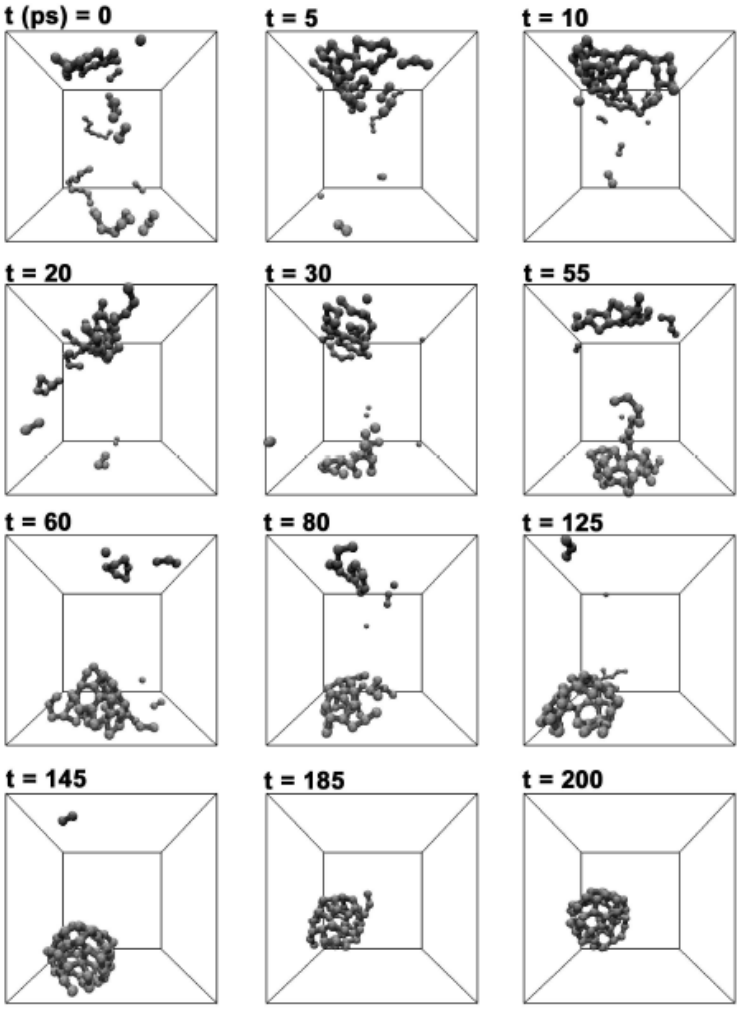

Abbildung 19.2: *Snapshots of the re-assembly process (gas-like phase to solid-like phase) from the coexistence behavior of C_{60} in the phase transition region at $T = 5855$ K. All times are in ps and denote the interval from the first snapshot.*

4.2.20 Phase transitions in polypeptide chains

Frankfurt Institute for Advanced Studies, Goethe University, Frankfurt am Main, Germany
Alexander Yakubovich, Ilia Solov'yov, Andrey Solov'yov and Walter Greiner

The phase transitions in finite complex molecular systems, i.e. the transition from a stable 3D molecular structure to a random coil state or vice versa (also known as (un)folding process), has a long standing history of investigation. The phase transitions of this or similar nature occur or can be expected in many different complex molecular systems and in nano objects, such as polypeptides, proteins, polymers, DNA, fullerenes, nanotubes .They can be understood as first order phase transitions, which are characterized by rapid growth of the system's internal energy at a certain temperature.

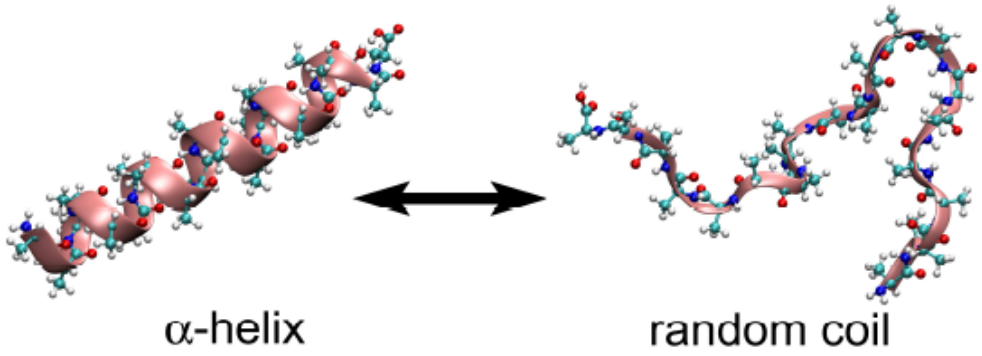

Abbildung 20.1: *The characteristic structural change of alanine polypeptide experiencing an helix- random coil phase transition*

We have calculated the potential energy surfaces of polypeptides with respect to their twisting degrees of freedom and construct a parameter–free partition function of the polypeptide using the suggested method. From the build up partition function we derive various thermodynamical characteristics for alanine polypeptides of different length as a function of temperature. Thus, we analyze the temperature dependence of the heat capacity, latent heat and helicity for alanine polypeptides consisting of 21, 30, 40, 50 and 100 amino acids. Alternatively, we have obtained same thermodynamical characteristics from the use of molecular dynamics simulations and compared them with the results of the new statistical mechanics approach. The comparison proves the validity of the statistical mechanic approach and establishes its accuracy. We have studied the helix-random coil transition in alanine, valine and leucine polypeptides consisting of 30 amino acids *in vacuo.*The calculations were performed using the Langevin molecular dynamics approach. The influence of side chain radicals on internal energy and heat capacity of the polypeptides is discussed. The heat capacity of these polypeptides is calculated as a function of temperature using two different methods. Namely as the derivative of the energy with respect to temperature, and on the basis of energy fluctuations in the system. The convergence of the fluctuations based

approach is analyzed as a function of simulation time. This study provides the comparison of methods for the description of structural transitions in polypeptides.

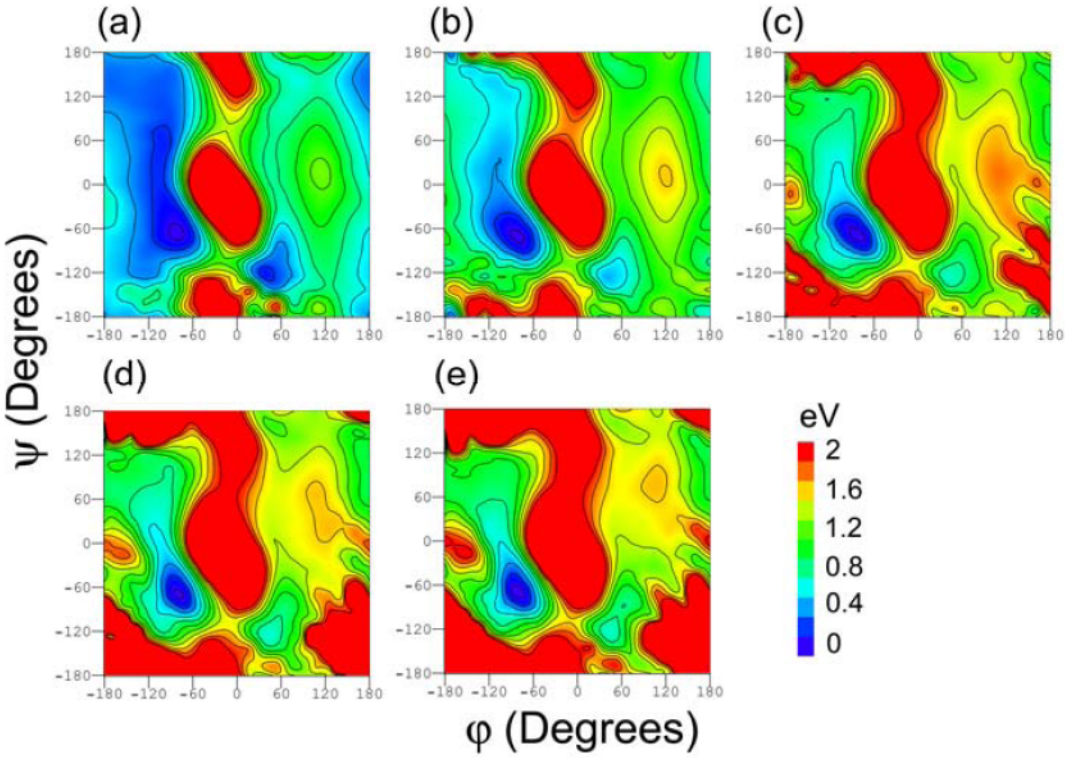

Abbildung 20.2: *Potential energy surfaces for different amino acids of alanine polypeptide consisting of 21 amino acids calculated as the function of twisting dihedral angles φ and ψ in: (a) second alanine, (b) third alanine, (c) fourth alanine (d) fifth alanine and (e) tenth alanine. Amino acids are numbered starting from the NH2 terminal of the polypeptide. Energies are given with respect to the lowest energy minimum of the PES in eV. The equipotential lines are shown for the energies 1.8, 1.6, 1.4, 1.2, 1.0, 0.8, 0.6, 0.4 and 0.2 eV.*

References

[1] A.V. Yakubovich, I.A. Solov'yov, A.V. Solov'yov, W. Greiner, *European Physical Journal D* **46** (2008) 215.

[2] I.A. Solov'yov, A.V. Yakubovich, A.V. Solov'yov, W. Greiner, *European Physical Journal D*, **46** (2008) 227.

[3] A.V. Yakubovich, I.A. Solov'yov, A.V. Solov'yov, W. Greiner, *Europhysics News* **38** (2007) 10.

[4] I.A. Solov'yov, A.V. Yakubovich, A.V. Solov'yov, W. Greiner, *Physical Review E* **75** (2007) 051912.

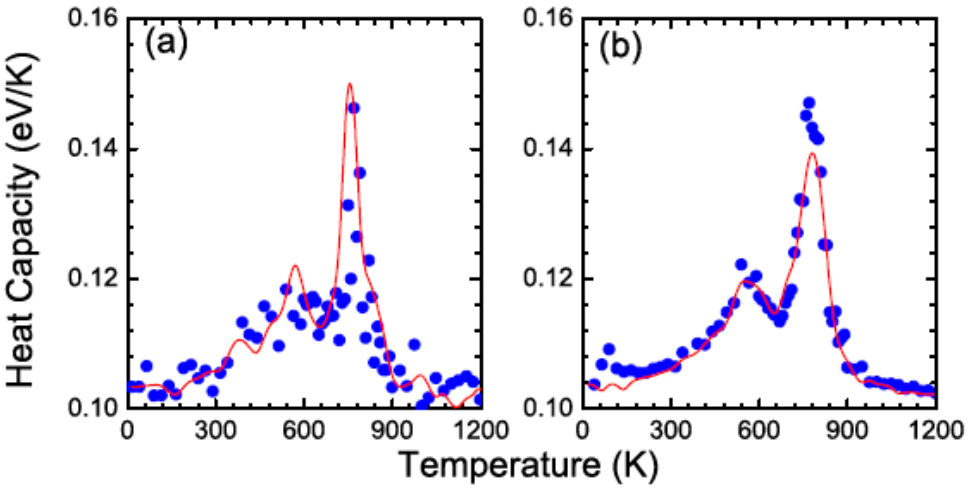

Abbildung 20.3: *Dependence of the heat capacity on temperature calculated for the Val30 polypeptide. Plots (a) and (b) correspond to the energy dependencies obtained from short and long simulations respectively. The dots show dependence of the heat capacity obtained from the analysis of polypeptides energy fluctuations; the solid line corresponds to the derivative of the interpolating functionof the transition energy on temperature.*

4.2.21 The dynamics of antigen-antibody binding

Frankfurt Institute for Advanced Studies, Goethe University, Frankfurt am Main, Germany
Elsa Henriques, and Andrey Solov'yov

Biological processes are driven by interactions between the molecular components of cellular machinery, commonly between proteins and their target molecules (generically termed ligands). Most of these processes portray a cascade of protein-ligand association/dissociation events, and thus, knowledge and control of their energetics and kinetics is of key importance in molecular biology, proteomics, and therapeutic research, to name a few.

The unbinding process of a protein-ligand complex of major biological interest was investigated by means of a computational approach at atomistic classical mechanical level. An energy minimization based technique was used to determine the dissociation paths of the system by probing only a relevant set of generalized coordinates. The complex problem was reduced to a low-dimensional scanning along a selected distance between the protein and the ligand. Orientational coordinates of the escaping fragment (the ligand) were also assessed in order to further characterize the unbinding. Solvent effects were accounted for by means of the Poisson–Boltzmann continuum model. The corresponding dissociation time was derived from the calculated barrier height, in compliance with the experimentally reported Arrhenius-like behavior. The computed results are in good agreement with the available experimental data.

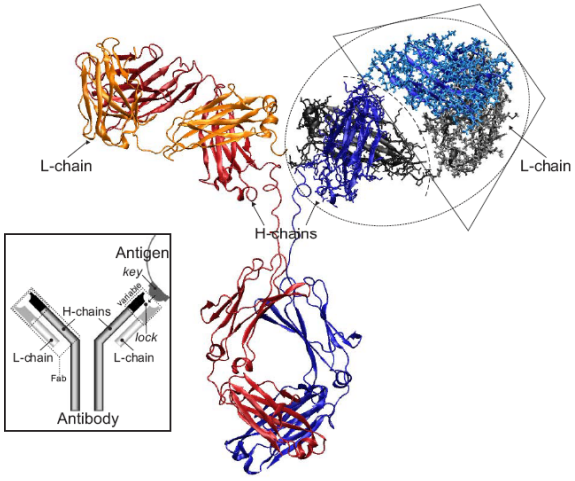

Abbildung 21.1: *Overall ribbon representation of a complete AB structure. The two pairs of H-chains are depicted in red and blue, and the corresponding L-chains in yellow and grey. The dashed ellipse highlights one of the AG-binding fragments (the so-called Fab), in an all-atom representation; the trapezoidal region puts in evidence the Fab variable domains (with added hydrogens), and the dashed arc illustrates the chains' cleavage sections for these variable domains to be detached. A simplified scheme of AB-AG binding is presented in the inset*

[1] E.S. Henriques and A.V. Solov'yov, *European Physical Journal D.* **46** (2008) 471.

4.2.22 Impurity effect on the melting of nickel clusters as seen via molecular dynamics simulations

Frankfurt Institute for Advanced Studies, Goethe University, Frankfurt am Main, Germany
Andrey Lyalin, Adilah Hussien, Andrey V. Solov'yov and Walter Greiner

Doping of Ni147 with a carbon impurity lowers its melting temperature by 30 K due to excessive stress on the cluster lattice. The distortion of the cluster lattice results in the change of the cluster's energetics as well as its entropy. The magnitude of the change induced is dependent upon the parameters of the interaction between the nickel atoms and the carbon impurity. We have demonstrated that an induced contraction of the icosahedral cluster's lattice in the vicinity of the impurity results in an increase of the melting temperature of the cluster; whereas additional strain in the lattice results in the reduction of the melting temperature. Therefore, the melting temperature of atomic clusters can be ffectively tuned by the addition of an impurity of a particular type.

Doping by a C or C2 impurity changes the melting temperature of the cluster, consequently this means that doping affects the mobility of the atoms in the Ni cluster. This effect has to be taken into consideration in particular applications with metal clusters when the entire process depends on the thermodynamic state of the cluster. An example of such experiment is the process of the catalytically activated growth of carbon nanotubes. The kinetics of the carbon nanotube growth depends upon diffusion of carbon atoms through the metal catalyst. Presence of the impurities can considerably change the flux, thereby affecting the growth rate of the carbon nanotube. The additional change in the thermodynamic state of the catalytic particle in the nanotube growth process might also depend on the strength of the interaction of the particle with a substrate.

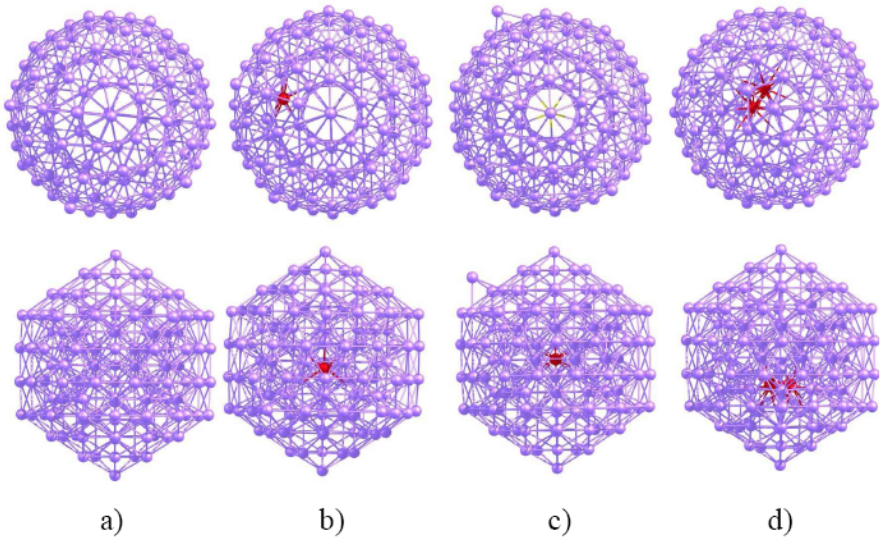

Abbildung 22.1: *(a) Optimized structure of a pure Ni147 cluster; (b) the isomer state structure of the C-doped Ni147 cluster; (c) the ground state structure of the C-doped Ni147 cluster; (d) the optimized structure of the C2-doped Ni147 cluster.*

In the present work [1], we have considered a single C and C2 impurity in the cluster of Ni147. It is interesting to study how several C impurities will influence the thermodynamic properties of the host cluster. In particular, it is important to find the optimum conditions (concentration of C atoms, temperature, thermodynamic state of the particle, etc.) when the C atoms begin aggregating into ordered carbon structures, such as nanotubes. This study requires careful investigation of the reliable many-body potentials for C-C interactions in the host metal cluster. The influence of impurities on properties of finite systems is a general effect. While our results were obtained for free clusters, many interesting problems can be found when one considers the influence of impurities on the phase transitions and stability of clusters deposited on a substrate. Thus, recently it has been experimentally shown that the oxidation of silver clusters deposited on a HOPG surface changes the stability and morphology of cluster formations. Clusters on substrates have important technological applications and the understanding of how these clusters stabilize on the surface are of profound interest.

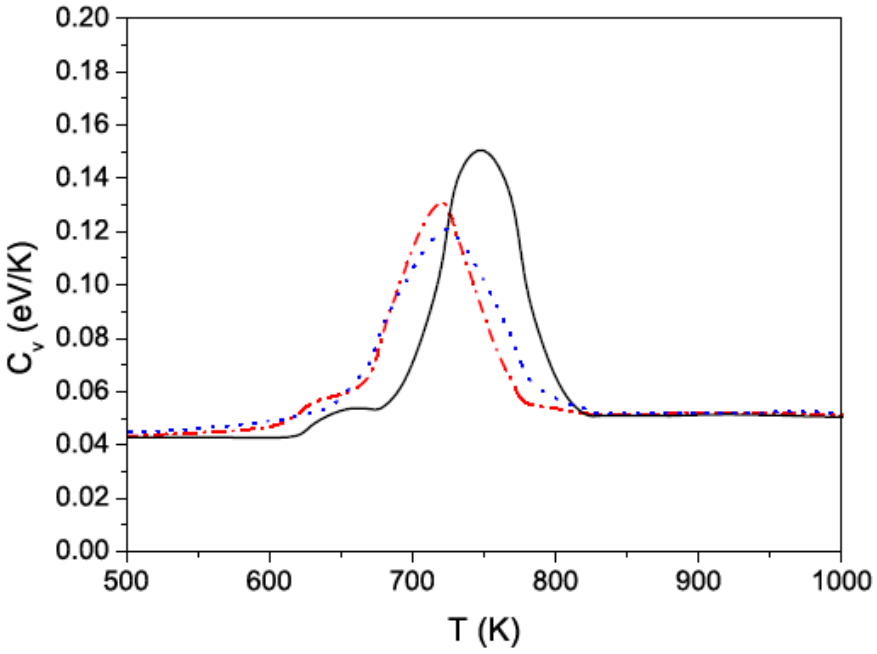

Abbildung 22.2: *Heat capacity for the pure Ni147 cluster (solid line), the C-doped Ni147 cluster. (dashed-dotted line) and the C2-doped Ni147 cluster (dotted line) as a function of T. Temperatures Tm = 750 K, 720 K and 725 K corresponds to the melting temperatures of the pure, the C-doped Ni147 and the C2-doped Ni147 cluster, respectively.*

References

[1] Andrey Lyalin, Adilah Hussien, Andrey V. Solov'yov, Walter Greiner, arXiv:0808.1263v1 (submitted to Phys. Rev. E)

4.2.23 Probing the late stage of heavy ion reactions using resonances

Institut für Theoretische Physik, J.W.Goethe-Universität Frankfurt am Main
Sascha Vogel and Marcus Bleicher

One of the most interesting topics of today's research in physics is the study of properties of nuclear matter under extreme conditions, i.e. very high temperatures and densities. One expects several phase transitions for highly excited nuclear matter, one of them is the chiral phase transition, where chiral symmetry is expected to be (partially) restored. One of the key observables for the restoration of the chiral symmetry is the expected change of the spectral function of the ρ meson and thus the changed mass-spectrum compared to a Breit-Wigner-distribution.

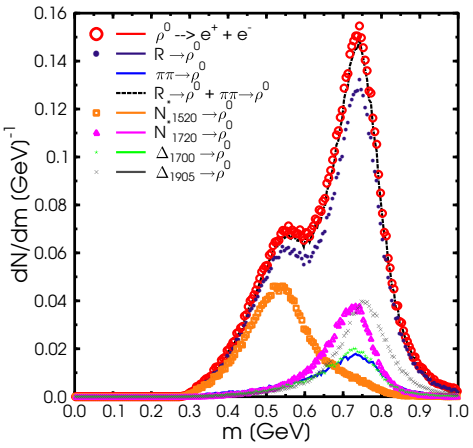

Abbildung 23.1: *Mass spectrum of the ρ^0 meson and the corresponding production channels. One observes that the ρ meson originating from a high mass baryon resonance decay or from $\pi\pi$ annihilation contribute to the high mass part of the spectrum, whereas ρ mesons originating from $N^*(1520)$ decays contribute to the mass regime of about 500 - 600 MeV.*

However, one has to consider kinematical effects which do not imply chiral symmetry restoration and still change the mass distribution of the ρ meson. In order to disentangle kinematical effects from effects originating from chiral symmetry restoration one has to apply a transport model approach to describe the dynamics of the system and to investigate binary hadron hadron collisions. The model used in Frankfurt is the Ultra Relativistic Molecular Dynamics (UrQMD) model, which has been developed over the past decade.

In order to study resonance effects one has to handle complex array structures and large output files, which is impossible without a dedicated scientific computer cluster. In order to compare with experimental results several thousand events for intermediate energies or several million events for low energies are necessary to draw definite and stringent conclusions.

One recent result is depicted in figure 23.1. Shown is the mass spectrum of the ρ^0 meson for a carbon-carbon collision at 2 AGeV and the corresponding production channels of the ρ meson. One observes that the $N^*(1520)$ decay chain $N^*(1520) \rightarrow N + \rho$ contributes strongly into the low mass region, whereas pion pion absorption feeds into the expected pole mass region of 770 MeV.

[1] S. Vogel and M. Bleicher, Reconstructing ρ^0 and ω mesons from non-leptonic decays in C+C collisions at 2 GeV/nucleon in transport model calculations, Phys. Rev. C **74** (2006) 014902

[2] S. Vogel, H. Petersen, K. Schmidt, E. Santini, C. Sturm, J. Aichelin and M. Bleicher, How sensitive are di-leptons from rho mesons to the high baryon density region?, Phys. Rev. C **78** (2008) 044909

4.3 Ingenieurwissenschaften

4.3.1 Modelling and Development of new Methods for Large Eddy Simulation in order to Perform Analysis and Optimization of Reacting and Non-reacting Systems

Pradeep Pantangi// Fachgebiet für Energie- und Kraftwerkstechnik, TU Darmstadt

Mixing Analysis and Optimization in Jet Mixer Systems by Means of Large Eddy Simulation (LES)

To achieve the analysis and optimization of mixing processes by means of Large Eddy Simulation (LES) technique, an advanced subgrid scale (SGS) scalar model package for the description of turbulent in reacting gaseous and liquid flows is developed and validated. This aims to strongly improve the prediction accuracy of the mixing field quantities prior to any mixing modification study.Here both non-reacting and reacting cases are considered. To cover different reaction regimes, the mixing processes with chemical reaction in jet mixer systems under investigation are described in terms of mixture fraction and two reaction progress variables. To assess the accuracy of the SGS model package, the present work is focussed on the high Schmidt-number phenomena.The results of LES are compared with experiments and other numerical results for both a non-reacting jet in channel flow configuration and a confined impinging jets reactor (CIJR) featuring a parallel reaction system. The mixing processes analysed experimentally in the CIJR with respect to the influence of operating conditions (active modification) on mixing properties are evaluated and a quality of measure that is a prerequisite for mixing optimization by means of passive modification is developed.

Towards Innovative Methods for Combustion Prediction in Aero-Engines

The fuel-air mixture preparation, along with the evolution of spray properties strongly influence the formation and emission of pollutants. EKT is now focused on developing a complete model for a reliable description and simulation of gas turbine combustion chamber using the FASTEST-3D code, suitable for complex configurations. This code has already been validated by simulating single-phase combustion configurations using the equilibrium model and the flamelet model. The objective of the project is to further develop existing LES code in FASTEST-3D for calculation of partially premixed turbulent systems in particular swirled pre-vaporised kerosene high-pressure combustion system . The task includes the implementation of advanced combustion models and the appropriate turbulence-chemistry interaction models accounted for by a multivariate presumed-pdf model for LES. Validation of this code will be performed using experimental data provided within the TIMECOP project.

In addition to the flamelet model, a Flamelet Generated Manifold (FGM) method developed by TU-Eindhoven (TUE, P. de Goey) in combination with ILDM method for turbulent conditions will be especially implemented in the FASTEST-3D LES code. The method is based on the laminar flamelet equations and includes ILDM reduction methodology by solving transport equations for a given number of progress variables. The objective is a better prediction of minor species concentrations.

Development and Validation of Advanced Subgrid Scale Models for Large Eddy Simulations (LES) of Scalar Transport in Non-reacting and Combustion Systems

In previous works the subgrid scale (SGS) models assessment was mainly performed through comparisons with Direct Numerical Simulation (DNS) results limited to low Reynolds numbers. Based on a comprehensive, highly resolved experimental database of scalar field and SGS quantities, an assessment of SGS scalar flux models is carried out at both resolved and sub-grid scale levels for configurations characterized by high Reynolds numbers for which DNS-data are not available. For this purpose, various combustion configurations featuring different combustion regimes (premixed, partially premixed) are used. Different SGS scalar flux models are evaluated along with a new developed dynamic algebraic anisotropy model. The new SGS scalar flux model is proved to achieve an overall good agreement with experimental data at both levels in simple configurations. Practical implementation and validation in complex configurations is being performed. Especially a flame surface density (FSD) based combustion model is applied.

4.3.2 Large-Eddy Simulation of Turbulent Combustion using Steady Flamelet and Progress Variable Methods

Clemens Olbricht
Fachgebiet für Energie- und Kraftwerkstechnik, TU Darmstadt

Understanding mixing and combustion dynamics becomes increasingly important, particularly for achieving high efficiency and low emissions. In gas turbine combustion the prevention of global extinction is of significant importance. Therefore, stability of the reaction is ensured by using geometrical flame holders or by aerodynamic flame holding approaches. Such stabilization methods are applied within the Sydney Bluff-Body configuration which was experimentally investigated at the University of Sydney and the Sandia National Labs, [1] and [2]. To stabilize the flame the un-swirled case takes advantage of the Bluff-Body geometry. Some swirling cases of this series are characterized by a vortex breakdown mechanism which induces recirculation above the Bluff-Body wake which serves as a second stabilization zone. In this work several, tabulated chemistry based, combustion models are applied to Large-Eddy Simulation (here: LES with Germano's dynamic approach). Simulations of selected isothermal flow cases provide a basis for further studies of reacting, unswirled and swirled Bluff-Body configurations. A variety of several parameters, like the used SGS model, grid resolution or combustion model is performed.

The Sydney bluff-body configuration with all dimensions and the coordinate system, is shown in Figure 2.1. Here, the rotationally symmetric bluff-body nozzle (diameter D_{bb}=50mm) is located in a square duct. Gas is fed through the centered pipe (diameter D_j = 3.6mm) at a bulk velocity of u_j at ambient conditions. The secondary airstream (ambient conditions, co-flow) between the duct and the burner is fixed at u_e. Swirled air is injected through an annular gap (primary air flow, u_s,w_s, l_s=5mm). The swirl numbers S_g are evaluatedwith the mean bulk velocities (w_s/u_s) within the gap flow. All velocities and velocity fluctuations were measured through Laser Doppler velocimetry (LDV). Scalar measurements were carried out using Raman/Rayleigh/LIF. The measurements were conducted by Dally et al. [2] (HM1E, HM3) and Al-Abdeli and Masri [1] (SM1, SMA2).

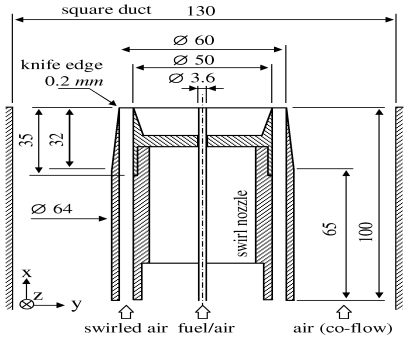

Abbildung 2.1: *Sketch of the Sydney Bluff-Body configuration.*

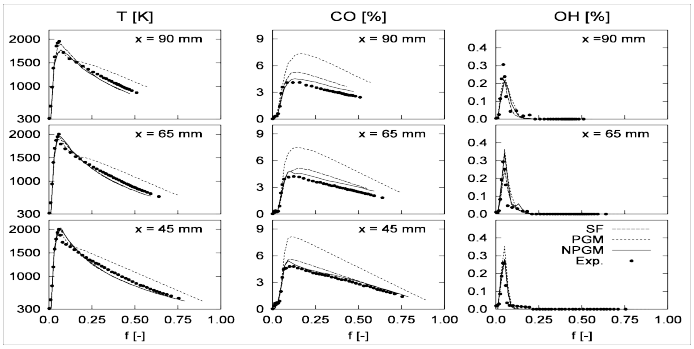

Abbildung 2.2: *Conditional means of the temperature, CO and OH concentrations of HM1E burner.*

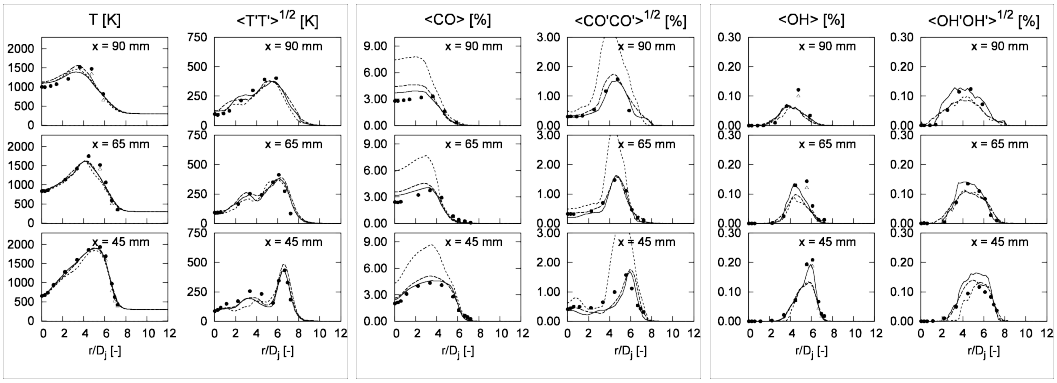

Abbildung 2.3: *Comparison of the time-averaged temperature <T> , <CO> and <OH> concentration and their fluctuations for flow case HM1E (Legend: see Fig. 2.2).*

Three different non-swirling bluff-body flow cases have been considered, the non-reacting NRFC, and the reacting cases HM1E and HM3. The HM-cases use a mixture of CNG and H2 (1 : 1) as fuel. Both Hmcases are simulated with different elliptically smoothed, multi-block meshes (up to $6.6 \cdot 106$) and different PDF/chemistry models. Here, a variation of the used chemistry library is carried out, which utilzes steady flamelets (SF) with one or multiple strain rates (a = 10, ..., $1662s^{-1}$). Aditionally, a progress variable approach (PVA) similar to [3] has been used which applies non-premixed (NPGM) and premixed (PGM) generated manifols, respectively. Results of the temperature and the concentrations of CO and OH conditioned at the mixture fraction for HM1E are shown in Figure 2.2. It can be identified that this flame (50% from extinction) is in principle well described with a multiple strain rate SF approach. Applying PVA with NPGM improves the results of minor species like CO and OH. Conceptual CO is far to high at the rich side using PGM. Deviations of the temperature, which arise for PGM, are caused by linear extrapolation beyond the burning limits. At Figure 2.3 radial temperature, CO and OH-concentration profiles and their fluctuations at different axial positions are shown for the same case and model combination. The spatial plots allow to assess the interplay of the CFD code and the three combustion models. Temperature and OH are predicted with excellent accuracy by all models; even the fluctuations are captured with good accuracy. For CO the best results succeed with the NPGM approach, while the trend to overestimate CO with PGM is confirmed. The simulations of HM3E (90% from extinction) using SF and PVA approaches provided good agreement of the velocities and their fluctuations to experimental data at all positions. The main flow features like recirculation and jet penetration are predicted with good accuracy. Within the sphere of the recirculation zone scalar and species predictions succeed; above this zone local extinction is present. With the PVA the local extinction is too high. Consequently the temperature and species are under predicted in this region.

References

1. Al-Abdeli, Y., Masri, A.: Comb. Theory Modelling, vol. 7 (2003), 731–766
2. Dally, B., Fletcher, D., Masri, A.: Comb. Theory Modelling, vol. 2 (1998), 193–219
3. Vreman, A.W., Albrecht, B.A., van Oijen, J.A.,de Goey, L.P.H., Bastiaans, R.J.M.: Comb. and Flame 153 (2008) 394–416

4.3.3 Hybrid LES/TPDF Methods in Combustion

Jens Kühne
Fachgebiet für Energie- und Kraftwerkstechnik, TU Darmstadt

Motivation

In many technical applications turbulent non-premixed combustion plays a major role, e.g. aircraft engines and furnaces. In order to decrease development costs and periods of named above applications numerical simulation is an important factor. Within this type of combustion an interaction between the occuring turbulent structures and the chemistry is very important and has to be modelled adequately.

Method and Theory

Large Eddy Simulation (LES) is known to be a powerful tool for calculations of non-reacting and reacting turbulent flows. During the past decades a lot of development work was done on this simulation technique.

One basic characteristic of LES is the spatial filtering of the transport equations which in fact decreases the known information within each numerical cell. In reacting flows, especially this information is needed, because the correlations between e.g. the temperature and the mixture fraction is not linear. For this purpose the probability density function (PDF) approach has been developed and is coupled to the LES. A typical way of modelling the sub-grid PDF of a scalar property is the usage of the so called presumed β-PDF ansatz. While using a β-PDF approach for a scalar it is necessary to apply a model for the variance of this property. Generally, the β-PDF approach has some drawbacks like the presumed shape of the distribution, which does not include all possible shapes of the PDF.

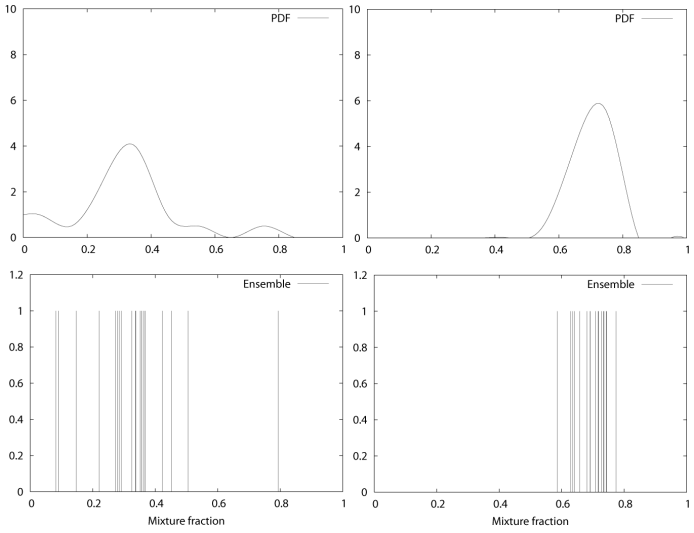

Abbildung 3.1: *Ensemble distribution and corresponding PDF of mixture fraction*

That is why the approach of a transported PDF is used in our method. The transport equation is solved by using an efficient Eulerian particle based Monte-Carlo method. The recent implementation is based on a TVD ansatz and is second order accurate in space and time.

Particle based solvers are very costly in terms of computer ressources. The main idea is to represent a probability density function in each numerical cell by an ensemble of stochastic particles. In order to get reasonable results and to minimize the statistical error an adequate magnitude of the ensemble must be provided. Since typical grid sizes of LES are in the range of million of mesh cells one obtains high total amounts of particles within the computational domain. The minimum amount of particles in a single cell ensemble is about 50 particles and so the total dimension of particles is in the range of ten to a hundred million.

Results

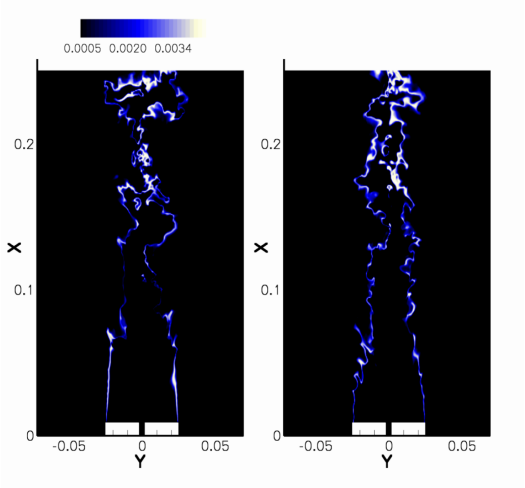

Abbildung 3.2: *Figure 2: Instantaneous distribution of OH mass fraction of the Sydney bluff body burner HM1e; without (left) and with artificial inflow turbulence (right)*

The focus of this work lies on the simulation of turbulent non-premixed flames, especially the well-known target flames of the TNF workshop. Here, the piloted jet flame Sandia Flame D and the Sydney bluff body flame HM1e were simulated successfully.

Simulations of the Sandia Flame D were dedicated to verify the developed adaptive method for Eulerian Monte-Carlo Simulations. Here, the particle density within a numerical cell, which is normally fixed, is varied by a certain distribution function. This function depends on different characteristic flow and mixing properties, e.g. the turbulent Reynolds number and the normalized variance of the mixture fraction.

The Sydney bluff body configuration is used to analyze sensitivities of LES. This configuration consists of a round bluff body with a diameter of 50mm and a coaxial jet of 3.6mm. The fuel, which enters the domain through the main jet, is a mixture of methane and H_2. Several simulations with varying boundary conditions and numerical methods are performed. For instance, the impact of the artificial inflow turbulence generator is investigated. Figure 2 shows instantaneous snapshots of the OH mass fraction of the Sydney bluff body burner HM1e. Left hand side shows the calculation without and on the right hand side with artificial inflow turbulence. As one can easily see both pictures differ in terms of the flame structure. Furthermore, the ability of a β-shaped function representing the real ditribution of the PDF is analyzed by comparing these results with results obtained by the transported Monte-Carlo PDF method. The calculations of this bluff body configuration are performed on a numerical mesh with about $1.2\text{x}10^6$ cells and for the transported PDF method the particle density is 50 particles per cell. Thus, the code uses $60\text{x}10^6$ particles in order to calculate the PDF of the mixture

fraction in the whole domain.

Publications

J.Kuehne, C.Olbricht, A.Sadiki, J.Janicka, EKT TUD, J.-Y. Chen, UC Berkeley
Hybrid LES Monte-Carlo PDF Modeling of Turbulent Piloted Jet Flames
Proc. Turbulence and Shear Flow Phenomena 5, Munich
2007

4.3.4 Large-Eddy-Simulation of Multiphase Flows

Frederik Hahn
Fachgebiet für Energie- und Kraftwerkstechnik, TU Darmstadt

Multiphase flow phenomena are common in nature and technique. One subset of these flow phenomena are conditions where small particles or droplets interact with a gaseous carrier phase. For this type of flow it is characteristic that only one of the (fluid) phases is continuously connected. Technical examples are cyclone dust separators and all kinds of spray systems. Due to the strong interaction of both phases for these conditions, it is evident to accurately calculate the transient behaviour of both phases simultaneously. Especially the prediction of the carrier phase turbulence and its modulation is essential.

The focus of the present project is on the prediction of liquid fuel combustion in gas turbines. Therefor the existing flow solver FASTEST is expanded with a Lagrangian particle tracking module. In this Euler/Lagrangian called approach the gaseous phase is calculated in an Eulerian description whilst for the dispersed phase paths of all particles are computed individually based on Newton's second law. This approach is suited for multiphase flows with dilute or medium dispersed phase loadings. In those cases flow phenomena are strongly dominated by continuous/dispersed phase interactions. This approach is limited in practice, even though it leads to a very detailed description of physical phenomena, due to the fact that numerical effort rises with the number of individually tracked Lagrangian particles. In combination with the standards of LES concerning resolution in space and time the method is not only accurate, it as well requires high computing power. To retain the performance of FASTEST and to fulfill these needs the Lagrange module is parallelized by domain decomposition as well.

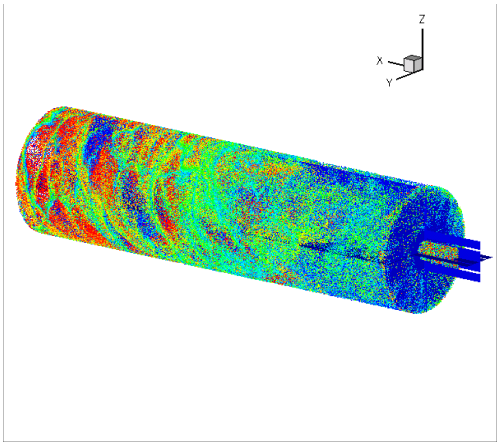

Abbildung 4.1: *Generic two phase swirl configuration. Particles coloured by size in front of orthonormal planes.*

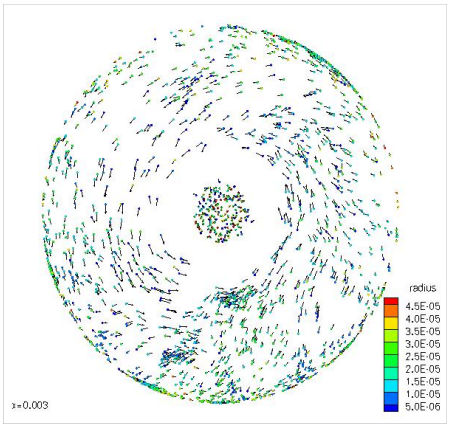

Abbildung 4.2: *Particles in a sheet of 300 µm thickness. Arrows represent direction of movement.*

In the following two applications examples are shown which are computed using the previously described methodology. The first example is a particle laden swirling flow. This configuration allows the investigation of the dispersion behaviour of polydisperse particles in heavily turbulent flow. In figure 4.1 an instantaneous snapshot of the model combustor is shown. Beside the cylindrical combustor itself the inlet pipes are shown. The central

pipe feeds a particle laden jet into the combustor. By an annular gap swirled air enters the combustor. Particles coloured by their sizes are depicted in front of orthonormal intersections of the domain. Unsteady phenomena like separation and clustering of particles can be observed. In figure 4.2 in a sheet of 300µm thickness particles are visualized. Again clustering and separation of particles are obvious.

The second example is an evaporating spray. An isopropyl alcohol spray originating from a hollow cone pressure atomizer evaporates in a preheated turbulent air stream. In figure 4.3 an instantaneous snapshot of the carrier phase velocity field is presented. Easily the strongly turbulent, unsteady nature of the ongoing physical processes can be identified. The plane cutting the symmetry axis of the configuration gives information about the geometry of the three-dimensional setup. In figure 4.4 again an unsteady snapshot is shown. Here the carrier phase mixture fraction is shown in a cutting plane. In addition evaporating droplets in a sheet of 300µm thickness are presented. The dilution of the spray in downstream direction due to evaporation can be identified.

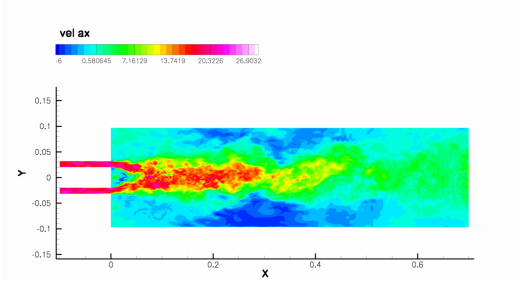

Abbildung 4.3: *Particles in a sheet of 300 µm thickness. Arrows represent direction of movement.*

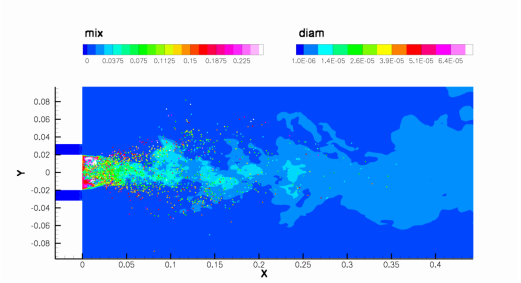

Abbildung 4.4: *Particles in a sheet of 300 µm thickness. Arrows represent direction of movement.*

Publications

F. Hahn, A. Sadiki and J. Janicka, EKT TUD

Large Eddy Simulation of a Particle Laden Swirling Flow Based on an Eulerian-Lagrangian Approach.

Proc. of the ICMF, vol. 6, 2007.

F. Hahn, C. Olbricht, J. Janicka, EKT TUD

Large Eddy Simulation of an Evaporating Spray Based on an Eulerian-Lagrangian Approach.

Proc. of Europ. ILASS Conf. 2008

4.3.5 Hybrid LES/CAA Simulation of a Turbulent Nonpremixed Jet Flame

Christian Klewer
Fachgebiet für Energie- und Kraftwerkstechnik, TU Darmstadt

Introduction

Knowledge on combustion generated noise and especially on combustion instability is of great importance in the design process of stationary gas turbine combustors and aircraft engines. In the presence of walls and therefore enclosed flames, a feedback of the acoustics onto the flame is possible, if the flame drives a resonant mode of the combustion chamber. The combustion instability phenomenon is known to appear prevalent in the context of lean, premixed combustion. As a first step towards the simulation of the combustion instability phenomenon, the noise emission by an open nonpremixed jet flame is studied in this work employing a hybrid approach combining large eddy simulation (LES) with computational aeroacoustics (CAA). In order to simulate combustion induced noise, different hybrid approaches were proposed in the close past.

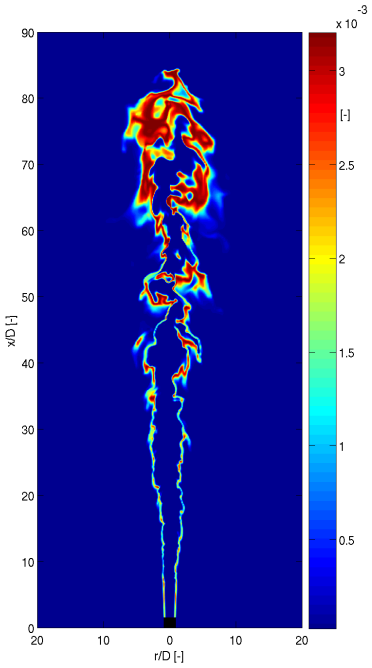

Abbildung 5.1: *Instantaneous OH massfraction*

The proposed hybrid approach is based on a LES of the reactive flow field using a low Mach number formulation. Within the CAA Solver, the equations of linear acoustics with the appropriate combustion noise source term and inhomogeneous fluid properties are solved. The two solvers are combined into a single tool for the description of the acoustics in the vicinity of the flame, exploiting the disparity of scales between the fluid flow and the acoustics. Furthermore, specialized boundary conditions can be applied for both the reacting flow variables and the acoustic quantities. The governing equations are solved within the LES in house code FLOWSI, which has shown to predict jet flames with promising results before. The acoustic wave propagation is described using linearized acoustic equations. The governing equations are solved within a wave propagation algorithm implemented in the open source CLAWPACK software package. Since this solver is a general purpose solver for first order hyperbolic problems with variable coefficient matrices, its use is predestined for the current study.

Experimental Test Case and Numerical Setup

Throughout this work the so called DLR-A flame has been investigated. Since the DLR-A flame is a benchmark flame of the TNF workshop, detailed measurements on the reactive flow field are available. Furthermore, measurements of sound pressure levels exist allowing

for a comparison of the results obtained by the current LES/CAA approach. The DLR-A flame consists of a central methane fuel jet, which is fed coaxially through a round nozzle into a constant coflow of ambient air. The numerical grid for the LES computations consists of 1.9 mio. cells, while the CAA grid consists of 2.9 mio. cells. All computations have been performed on the Hessian High Performance Computer (HHLR).

Results

An instantaneous cross-sectional view of the OH mass fraction is provided in figure 5.1 to give an idea of the instantaneous location of the flame. In figure 5.2, a snapshot of the acoustic pressure is given providing a qualitative insight into the acoustic field. One can observe that the flame acts as a cylindrical acoustic source radiating sound. The most active regions are connected to the location of the flame, where the unsteady heat release is generated.

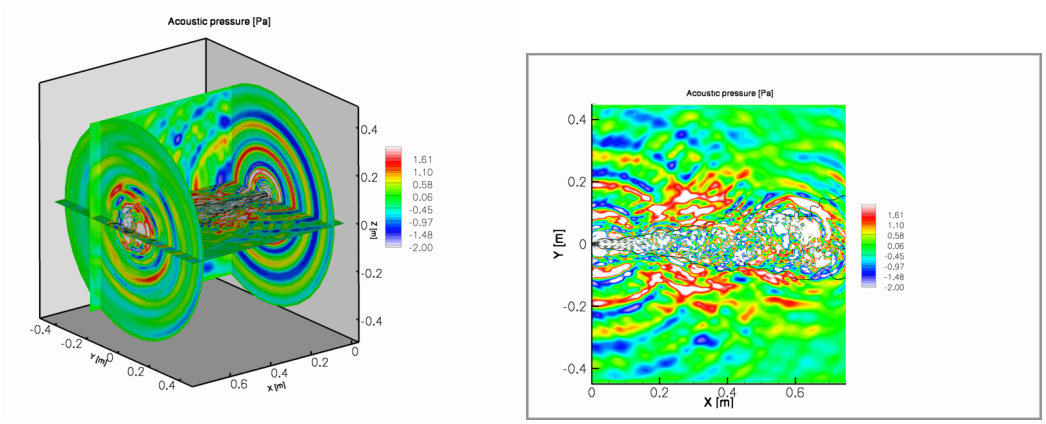

Abbildung 5.2: *View of the acoustic field*

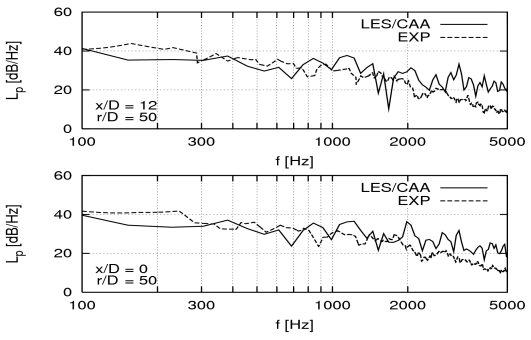

Abbildung 5.3: *Comparison of simulated spectra with experimental investigations*

A spectral analysis of the sound pressure level computed by means of a FFT is presented in figure 5.3. The presented simulated spectrum is obtained via averaging eight individual spectra along the circumference. Promising agreement between simulation and experiment over a range from approximately 100 Hz to 2000 Hz can be observed.

Publications

C. Klewer, F. Hahn, C. Olbricht, J. Janicka, EKT TUD
Hybrid LES/CAA Simulation of a Turbulent Nonpremixed Jet Flame
Direct and Large Eddy Simulation 7, Trieste
2008

4.3.6 Geometrische Struktur kleinskaliger Turbulenz

Prof. Dr.-Ing. Martin Oberlack, Dipl.-Ing. Fettah Aldudak
Fachgebiet für Strömungsdynamik, Fachbereich Maschinenbau, TU Darmstadt

Bei der Turbulenz handelt es sich um ein weit verbreitetes Naturphänomen, das heute noch in vielfacher Hinsicht unverstanden ist. Ihr ausgeprägt chaotischer und dreidimensionaler Charakter tragen zu einem großen Teil hierzu bei.

Turbulenz tritt in vielen Bereichen der Natur und Technik auf, in der Geo- und Astrophysik, in der Meteorologie sowie der Aerodynamik, aber auch in technischen Apparaten und Maschinen sowie teilweise in biologischen Systemen. Bislang beschränken sich die Berechnungsmethoden für die Vorhersage turbulenter Strömungen immer noch größtenteils auf halbempirische Schließungsannahmen und Modelle für sogenannte integrale Größen. Diese sind z.B. das integrale Zeit- und Längenmaß und repräsentieren die großen Strukturen in einem turbulenten Strömungsfeld. Sie werden durch Differentialgleichungen für die turbulente kinetische Energie k únd die Dissipation ε ausgedrückt. Für kleinere Längen- und Zeitskalen bleibt das Verständnis bruchstückhaft. Die einzige durch Experimente und Theorie weitgehend abgesicherte Aussage für kleinere Längenmaße beruht auf einer Dimensionsanalyse von Strukturfunktionen nach Kolmogorov, die besagt, dass die Differenz der Geschwindigkeitsfluktuationen zwischen zwei Punkten im Strömungsfeld proportional zur 1/3-Potenz des Abstandes zwischen den Punkten sein muss.

Die heute verbreitet verwendeten Simulationstechniken lösen, wie im Falle von Large-Eddy-Simulationen, bestenfalls die großen Strukturen numerisch auf, müssen jedoch bei der Betrachtung der kleinen Skalen Gebrauch von Modellen machen, die das Schließungsproblem der Turbulenz somit lediglich zu kleineren Skalen verschieben. Direkte Numerische Simulationen sind die einzige Methode, die turbulente Strukturen bis zu Kolmogorov-Skalen numerisch auflösen können, stellen aber aufgrund ihrer Beschränktheit auf sehr einfache Geometrien und niedrige Strömungsgeschwindigkeiten keine Alternative für anwendungsnahe technische Probleme.

Um die Kolmogorov'schen Skalierungen in die Formulierung von Turbulenzmodellierung einfließen zu lassen, sollte das Augenmerk auf die geometrische Eigenschaft des turbulenten Feldes gerichtet werden. Die Frage nach einer Klassifizierung des turbulenten Skalenspektrums ist hier von besonderer Bedeutung. Um dies zu ermöglichen, bedarf es allerdings einer Methode, die das gesamte turbulente Feld in Gebiete vergleichbarer geometrischer Strukturen aufteilt und Rückschlüsse auf ihre Eigenschaften erlaubt. Bisher war es nicht gelungen, die Geometrie der Turbulenz vollständig durch Objekte endlicher Größe darzustellen und damit das innerhalb der Kaskade veränderliche Längenmaß quantitativ zu erfassen.

Geometrische Strukturen in der Turbulenz können sinnvollerweise nur mit statistischen Methoden beschrieben werden, wobei die beschreibenden Parameter Längen sein werden. In diesem Sinne wird im Rahmen dieses Projektes die Theorie der sogenannten Dissipationselemente behandelt, die auf Wang & Peters [1] zurückgeht. Das Ziel dieser Theorie ist es, das gesamte Strömungsfeld in kleine Einheiten zu zerlegen und aus diesen statistische Informationen der Strömung zu rekonstruieren.

Sie können mit der Methode der Gradienten-Trajektorien bestimmt werden. Gradienten-Trajektorien starten von jeder Gitterzelle im Feld in Richtung steigender und fallender Gradienten, bis sie jeweils einen Maximum- bzw. ein Minimum-Punkt erreichen. Das Feld kann hierbei eine beliebige skalare Größe sein wie die Geschindigkeit, ihre Fluktuation oder

die Dissipation. Alle Punkte im physikalischen Raum, deren Trajektorie an den zwei selben Extrempunkten endet, werden zu einem Element zusammengefasst, das als „Dissipationselement“ bezeichnet wird. Da durch jeden Punkt im Raum genau eine Trajektorie verläuft, kann somit der Raum eindeutig eingeteilt werden. Alle Extrempunkte des Skalarfeldes stellen Endpunkte eines Elementes dar, und somit variiert der Skalar monoton innerhalb des Elements. Die Geometrie eines Dissipationselementes lässt sich zunächst durch den linearen Abstand zwischen den jeweiligen Minimum- und Maximum-Punkten parametrisieren.

An dieser Stelle wird nicht nur die so definierten Elemente mit Hilfe von drei-dimensionalen DNS-Daten betrachtet, sondern auch eine Theorie zur Beschreibung der statistischen Eigenschaften dieser Elemente anhand der Verteilung des Längenmaßes entwickelt werden.

Ein besonderer Schwerpunkt bei diesem Projekt ist die Betrachtung wandgebundener Strömung, was im Zusammenhang mit Dissipationselementen erstmalig behandelt wird. Hierbei wird die von [1] entwickelte Gleichung für die Verteilungsfunktionen der aus den Dissipationselementen gewonnenen Längenmaße um eine Abhängigkeit von wandnormaler Richtung ergänzt. Die einzelnen Terme dieser Gleichung sollen, gestützt auf DNS-Daten, überprüft und gegebenenfalls modifiziert werden. Ein weiteres Ziel ist es, ausgehend von dieser Gleichung eine physikalische Begründung der Gleichung für die Dissipation ε in Zwei-Gleichungs-Modellen für turbulente Strömungen zu liefern.

Das Bild zeigt zwei Beispiele für Dissipationselemente. Die Farbkodierung zeigt den Wert des passiven Skalars an, wobei blau dem Minimum und rot dem Maximum entspricht.

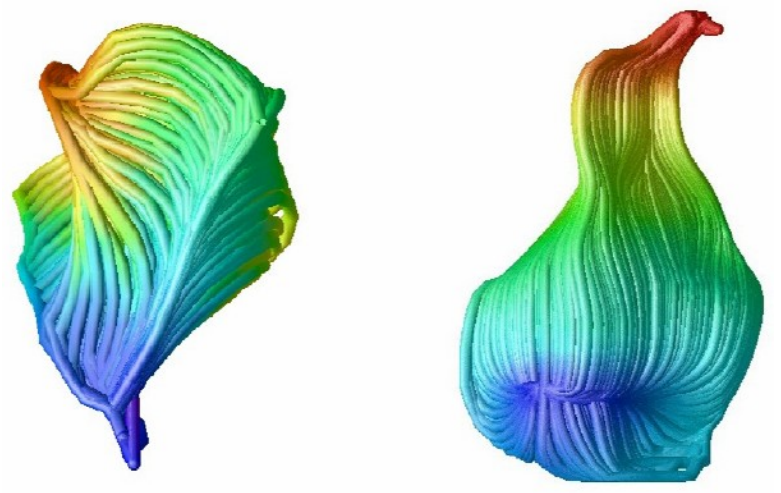

Verweise

1. Wang, L., Peters, N. The length scale distribution function of the distance between extremal points in passive scalar turbulence, J. Fluid Mech. **554**, 457-475 (2006).

4.3.7 Wall Normal Rotating Channel Flow: Direct Numerical Simulation, Modeling and Lie Group Analysis

Mehdizadeh and M. Oberlack
Chair of fluid dynamics

Rotating channel flows are of great importance in many engineering applications. In these flows the structure of turbulence and mechanism of momentum transport are highly affected by additional body forces, namely, Coriolis and centrifugal forces. Turbulent channel flows with the spanwise and the streamwise rotation have been extensively studied by many authors [1], [2] and [3].

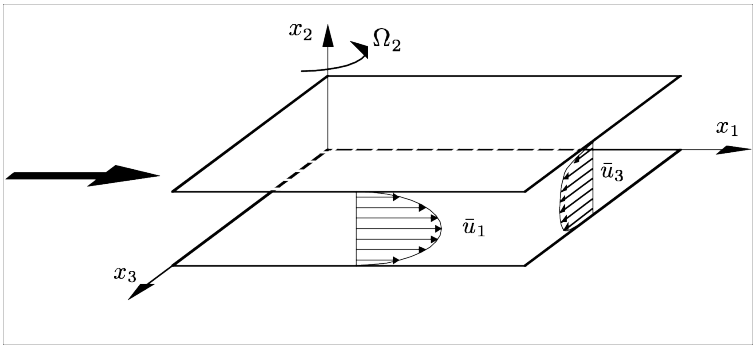

Abbildung 7.1: *Wall normal rotating channel flow*

However, the turbulent channel flows with the wall-normal rotation have been rarely investigated. Since there is no possible experimental approach to the investigation of these flows, the direct numerical simulation (DNS) is the only available method to precisely examine their behaviors. Since a rather complicated analytical solution for the laminar case for arbitrary rotation rate is known we can compare the behavior of the flow in laminar and turbulent state. The flow geometry can be seen in Figure 7.1

The project entirely could be summarized in the following tasks:

1. Provide a reference data base using direct numerical simulation (DNS) for different Reynolds numbers at different rotation rates and analyze the results.
2. Use the DNS data to study the ability of turbulence models to predict the flow under consideration.
3. Use Lie group analysis to find symmetries of the equations of the motion and to derive new scaling laws.

The DNS code which we are using is based on standard spectral method with Fourier decomposition in the streamwise and spanwise directions as well as Chebyshev decomposition in the wall normal direction. The orginal version of the code was developed at KTH in Stockholm. For more detail see [4].

The code is parallelized by OpenMp. The OpenMp application programming interface (API) supports multi-platform shared memory multiprocessing programming. All calculations have been conducted at Hessian High Performance Computer (HHLR).

References

[1] Johanson J.P., Halleen R.M., Lezius D.K.
Effects of the spanwise rotation on the structure of two-dimensional fully developed turbulent channel flow.
J.Fluid Mech., vol. 56, pp. 533-557
1972
[2] Grundestam O., Wallin S., V.Johansson A.
Direct numerical simulation of rotating turbulent channel flow.
J.Fluid Mech., vol. 598, pp. 177-199
2008
[3] Oberlack M., Cabot W., Pettersson Reif B.A., Weller T.
Group analysis, DNS and modeling of a turbulent channel flow with streamwise rotation.
J.Fluid Mech., vol. 562, pp. 383-403
2006
[4] Lundbladh A., Henningson D., Johansson A. Aeronautical Research Institute of Sweden, Bromma.
An efficient spectral integration method for the solution of the Navier-Stokes equation.
Tech. Rep. FFA-TN 1992-28
1992

4.3.8 Strömungsoptimierung durch parallelisierte Sensitivitätenberechnung

Julian Michaelis, Michael Schäfer
Fachgebiet Numerische Berechnungsverfahren im Maschinenbau, TU Darmstadt

Die numerische Strömungssimulation ist heute ein wichtiger Bestandteil des modernen Ingenieurwesens als Ergänzung zum physikalischen Experiment. Durch die stetig steigende Rechnerleistung treten neben der reinen Simulation von Strömungen mittlerweile auch komplexere Probleme wie die Strömungsoptimierung in den Vordergrund. Dabei sollen gegebene Designparameter (Einstromgeschwindigkeit, Temperatur, Geometrie, etc.), die sich direkt oder indirekt auf das Strömungsfeld auswirken so gewählt werden, dass zuvor definierte Zielfunktionale minimiert werden. Eine Methode zur Optimierung geschieht mit Hilfe der Berechnungen der so genannten Strömungssensitivitäten.

Die Sensitivitäten der Strömungsvariablen beschreiben, wie diese sich in Abhängigkeit der Designparameter ändern, also wie z.B. das Geschwindigkeitsfeld beeinflusst wird, wenn die Geometrie variiert wird. Kennt man den Einfluss der Stellgrößen auf die Strömungsvariablen kann man dieses Wissen nutzen und den Gradienten des zu minimierenden Funktionals bestimmen. Der Gradient bildet die Basis für anschließende Optimierungsalgorithmen, die ausgehend von den aktuellen Parameterwerten iterativ verbesserte Werte für die Steuergrößen finden.

Ausgangspunkt für die Berechnung der Strömungssensitivitäten sind die nicht-linearen Navier-Stokes Gleichungen, die das mathematische Modell zu Strömungsberechnung liefern. Ein primitiver Ansatz zur Bestimmung der Sensitivitäten ist ein einfacher Differenzenquotient. Dabei wird das Strömungsfeld zunächst mit einem Strömungslöser berechnet und anschließend ein Parameter leicht modifiziert um das Strömungsfeld dann erneut zu lösen und so den Einfluss des Parameters zu schätzen. Allerdings müssen bei N Steuerparametern dann N+1 Strömungslösungen berechnet werden. Bei einer hohen Anzahl von Parametern und einer komplexen Geometrie bedeutet dies einen erheblichen Rechenaufwand.

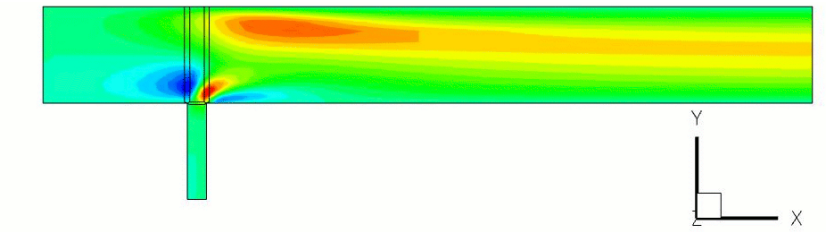

Abbildung 8.1: *Verteilung der Sensitivität der x-Geschwindigkeit in einem T-Kanal in Abhängigkeit der Einlassgeschwindigkeit am unteren Einstrom*

Effizienter ist der Ansatz der Sensitivitätsgleichungen, beschrieben in [1], der wiederum die Navier-Stokes Gleichungen als Ausgangspunkt hat. Allerdings wird bei diesem Ansatz der gesamte Gleichungssatz inklusive seiner Rand- und Anfangswertbedingungen nach den einzelnen Steuerparametern differenziert. Dabei entsteht für jede Designvariable ein eigenständiges Gleichungssystem, das es zu lösen gilt. Zwar müssen für N Steuerparameter auch hier N zusätzliche, unabhängige Gleichungssysteme gelöst werden. Allerdings sind die entstehenden Systeme linear in den Unbekannten, wodurch die Berechnung beschleunigt werden kann.

Eine Implementierung zur Bestimmung der Strömungssensitivitäten ist bereits in den am Institut benutzten Strömungslöser FASTEST eingebaut, beschrieben in [2]. Zur Beschleunigung dieses Lösers liegt ein großes Augenmerk auf dem Entwurf und Implementierung einer Parallelisierung, die auf dem HHLR (Hessischer Hochleistungsrechner) genutzt werden kann. Dabei werden die neu hergeleiteten, linearen Sensitivitätsgleichungen zeitgleich für alle Parameter gelöst. Dadurch soll erreicht werden, auch sehr komplexe Optimierungsprobleme mit schwierigen Geometrien und einer Vielzahl an unterschiedlichen Designvariablen numerisch zu lösen.

Verweise

1. M. D. Gunzburger, "Perspectives in Flow Control and Optimization", siam, Philadelphia, 2003

2. J. Michaelis, "Implementation and Analysis of a Sensitivity Based Optimization Method in FASTEST", Diplomarbeit, FNB, TU Darmstadt, Juli 2008

4.3.9 Numerische Strömungskontrolle und -optimierung

Johannes Siegmann, Michael Schäfer
Fachgebiet Numerische Berechnungsverfahren im Maschinenbau

Die Entwicklung neuartiger, sowie für den jeweiligen Einsatzzweck optimal ausgelegter Bauteile ist ein oftmals langwieriger und somit kostenintensiver Prozess. Neben den Möglichkeiten der experimentellen Bestimmung der Strömungsgrößen steht an dieser Stelle die Methodik der numerischen Strömungssimulation zur Verfügung. Sie bietet neben der Einsparung von Kosten- und Zeitaufwand zur Fertigung von Prototypen sowie der Durchführung von Messungen die Möglichkeit, das Strömungsverhalten auch in schwer bis nichtzugänglichen Bereichen vorherzusagen.

Die bereits entwickelten und in den hauseigenen Strömungslöser FASTEST implementierten numerischen Verfahren bieten die Möglichkeit effizienter Strömungsberechnungen. Zusätzlich soll nun die Möglichkeit gegeben werden optimale Konfigurationen auch bei großer Zahl von Parametern und Nebenbedingungen effizient zu finden. Ziel des Projektes ist die Implementierung und Validierung eines auf der Berechnung von Sensitivitäten basierenden Optimierungsalgorithmus (siehe auch Abbildung 9.1). Durch die enge Verknüpfung der Sensitivitätsbestimmung mit der Lösung des Strömungsmodells innerhalb eines Softwarepakets wird eine hocheffiziente Gesamtlösung angestrebt.

Ansätze zur Lösung von Minimierungsproblemen lassen sich generell in Strategien ohne und mit Bestimmung der Ableitung des Zielfunktionals unterteilen. Bei Ersteren erfolgt eine Abbildung des Zielfunktionals über ein Polynommodell welches anschließend unter relativ geringem Aufwand zu differenzieren ist. Der zweite Ansatz sieht hingegen die Bestimmung des Differentials des realen Zielfunktionals vor. Zur Ermittlung des Differentials stehen mehrere Methoden zur Verfügung. Beispiele sind Finite Differenzen, Lösen der adjungierten Gleichung sowie die Bestimmung der Sensitivitäten. Diese stellen ein Maß für die Änderung der Zustandsgrößen in Abhängigkeit von Veränderungen der Designparameter dar. Die Bestimmung der Sensitivitäten erfolgt über die Lösung der nach den Designparametern abgeleiteten Navier-Stokes-Gleichun-gen, welche die Zustandsgleichungen für das Fluid darstellen.

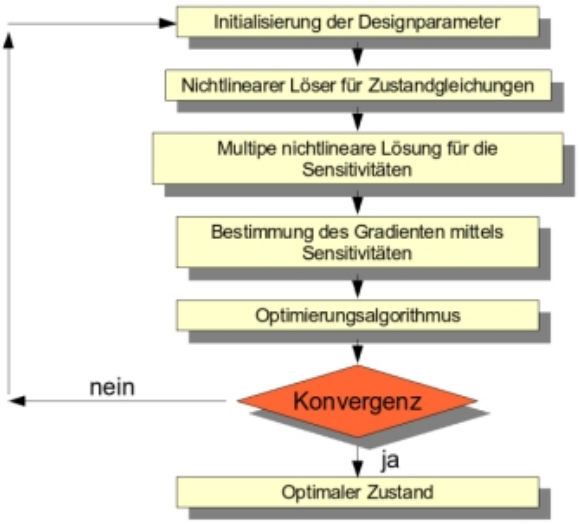

Abbildung 9.1: *Ablauf des Algorithmus*

Das ermittelte Differential wird anschließend an einen Optimierungsalgorithmus (Line-Search oder Trust-Region) übergeben, welcher mit dessen Hilfe das Minimum des Zielfunktionals ermittelt. Gerade auf die Ermittlung der Strömungsgrößen sowie der zugehörigen Sensitivitiäten entfällt hierbei ein großer Rechenaufwand. Um an dieser Stelle vertretbare Rechenzeiten zu erzielen wird auf Seiten der Strömungslösung bereits auf das parallele Hochleistungsrechnen zurückgegriffen. Diese Techniken sollen nun auch zur Beschleunigung

der Sensitivitätsberechnung eingesetzt werden. Es ist hierbei denkbar entweder analog zur Strömung die gesamte Rechnung sequentiell auf alle Prozessoren zu verteilen, oder die Gleichungssysteme der jeweiligen Designparameter zeitgleich verschiedenen Prozessoren zuzuordnen.

4.3.10 A Local Adaptive Grid Refinement Strategy for Flow Computations

Friederike Gauß, Michael Schäfer
Fachgebiet Numerische Berechnungsverfahren im Maschinenbau, TU Darmstadt

Computational fluid dynamics (CFD) is becoming more and more important in computational engineering. As the complexity of applications increases, there is a need of highly efficient computer codes to solve these problems.

A major problem when dealing with complex flows is the occurrence of largely different scales, e.g. in case of turbulent flows or for chemically reacting flows (e.g. involving combustion phenomena). When generating the computational grid, an orientation on the smallest scales leads to a very high number of grid cells and thus to high memory requirement and CPU time.

To overcome this problem, an algorithm, which adapts the grid spacing locally to the needs in different parts of the computational domain, was developed and implemented in the existing flow solver FASTEST [1]. With this approach a large number of grid cells can be saved while maintaining the desired accuracy.

The refinement algorithm is embedded into a geometric multigrid method. Multigrid algorithms are well developed and have proven to be a powerful tool to significantly accelerate flow computations [2]. Combining those two strategies, a highly efficient algorithm is created.

To illustrate the adaptive algorithm, a flow through a channel with a cube obstacle is shown in the figure. The first picture shows the flow field. The second one shows regions with refined grid (red) embedded the original grid (blue).

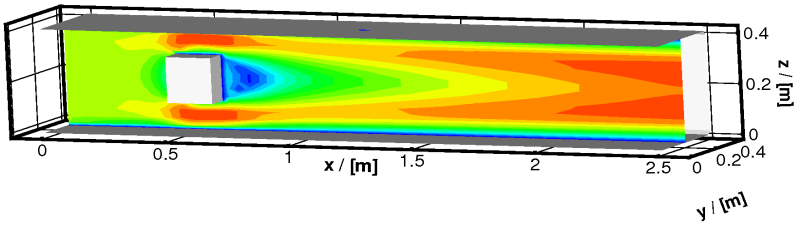

The adaptive algorithm can be used to accelerate the CFD computations performed on parallel high-performance computers. For this purpose, the adaptive algorithm has to be combined with a suitable dynamic load balancing strategy. The method gives the possibility to calculate highly complex applications in complex geometries in an efficient way. In particular, the advantages of block-structured grids with respect to numerical efficiency can be maintained.

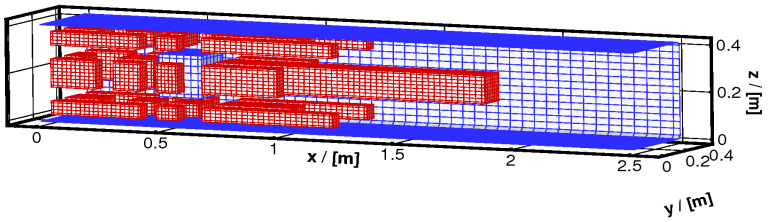

Literature

[1] D. C. Sternel (ed.), *FASTEST-Manual*, Fachgebiet Numerische Berechnungsverfahren im Maschinenbau, TU Darmstadt, 2005

[2] F. Durst and M. Schäfer. A Parallel Blockstructured Multigrid Method for the Prediction of Incompressible Flows. Int. J. for Numerical Methods in Fluids, 22:549–565, 1996.

4.3.11 Numerical conditioning of non-linear phenomena during phase change processes in foundry engineering

Tomasz Wacławczyk, Michael Schäfer, Dörte Sternel
Fachgebiet Numerische Berechnungsverfahren im Maschinenbau, TU Darmstadt

During numerical modelling of the solidification in binary alloys physical properties of the transition zone between solid and fluid, i.e. the mushy layer, must be reconstructed, see Ref. (1-2). Unlike porosity based solidification models, in this project we consider an alternative approach where the viscosity is a material parameter responsible for the influence of the local solidified alloy morphology on the flow field. Assumptions about a functional dependence of the viscosity and the density on the solid fraction allows for the approximation of the material properties across the mushy layer. Since the viscosity of a partially solidified alloy might be measured in a laboratory (viscosity measurements in the cylindrical rheometer) the experimental evidence is used for calibration of the solidification viscosity model. A second part of the project deals with numerical modelling of the oxide and bi-oxide layers. Initially, an algorithm for detection of the reconnection regions was developed, see Fig. 11.1. Localisation of the bulk reconnection is a signal for the passive scalar initialisation that is interpreted as the bi-oxide layer. Because Eulerian tracking of the initialised scalar leads to its unphysical numerical diffusion further work will be focused on implementation of the Lagrangian oxide and bi-oxide tracking model.

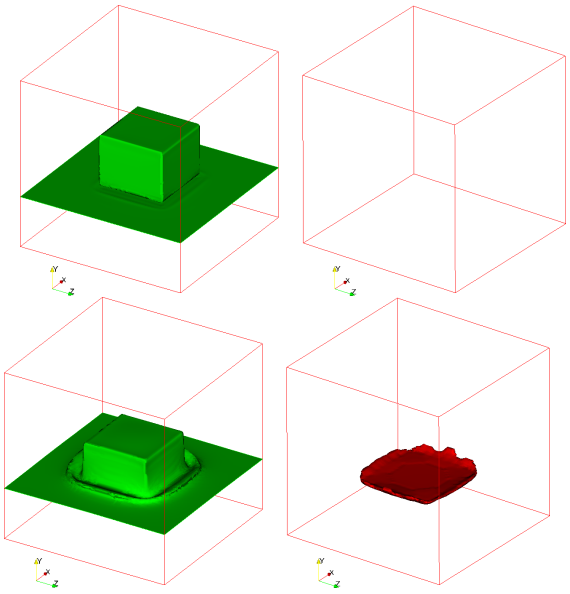

Abbildung 11.1: *Detection of the reconnection during collision of the liquid metal (model of the bi-oxide skin), two time moments t1 < t2 top and bottom, respectively.*

The simulation of phase change process requires a very large computational effort due to the complexity of the physical model and the large scale of the industrial systems used in foundry engineering i.e. large Reynolds numbers of the liquid metal flows (discretization grids with several millions of control volumes). Moreover, the presence of a deformable interface and the bi-oxide tracking algorithm makes the employment of parallel high-performance computing a necessity.

References

1. H. E. Huppert, M. G Worster, Dynamic solidification of the binary melt, *Nature,* Vol. 314, pp. 703-708, 1985
2. M. Le Bars, M. G. Worster, Solidification of a binary alloy: Finite-element, single-domain simulation and new benchmark solutions, *J. Comp. Phys.,* Vol. 216, pp. 247-253, 2006

4.3.12 Parallel Computation of Fluid Structure Interaction in Labyrinth Seals

Yu Du, Michael Schäfer
Fachgebiet Numerische Berechnungsverfahren im Maschinenbau, TU Darmstadt

The numerical simulation of fluid structure interaction (FSI) has become increasingly important in the worldwide community of computational engineering [1]. It is one of the main research fields at the Institute of Numerical Methods in Mechanical Engineering at TU Darmstadt for the recent years, e.g. [2,3]. The project "Fluid Structure Interaction in Labyrinth Seals" is supported by DFG and Rolls-Royce.

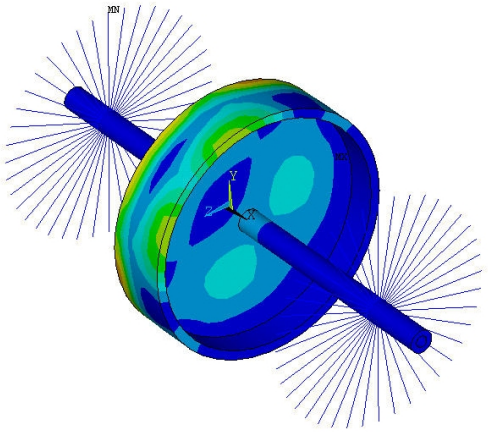

Fig. 1 Displacement of the structure of a labyrinth seal

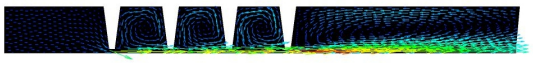

Fig. 2 Velocity vector of the fluid field of a labyrinth seal

Labyrinth seals are a type of non-contacting seal. They are widely used in gas turbine engines to control internal leakage, thereby increase engine performance and decrease operating costs. To provide sealing across a stationary/rotating interface, the seals have to be non-contacting to avoid excessive heat production or even engine failure. However, their sealing capacities are limited by the need to maintain a clearance between the seal and the rotating surface. Hence the optimization of labyrinth seals consists in finding the compromise between minimum leakage and non-contacting characteristics. For such seals with small clearance, high pressure, high flow speed and high rotational speed, fluid structure interaction (FSI) plays an important role and complex mechanical effects are aroused.

The project is focused on the numerical simulation of the FSI in labyrinth seals. A series of systematic simulations and parameter studies provide insight into the complex fluid and structural physics inside labyrinth seals. Based on the knowledge acquired by numerical simulations, the theories of labyrinth seals are examined and complemented. Finally, an optimized shape of labyrinth seals is established.

Comparing to traditional CFD or CSM, the computations of FSI are more demanding of computer resources in terms of memory size, CPU speed and storage space. Both of the fluid field and the solid physics need to be modeled and, moreover, coupled. Therefore FSI is not only the summation of CFD and CSM, but also requires more time steps and iterations to converge. If run serially, one simulation could last several months. To limit wall clock times in an acceptable range, FSI simulations are usually run in parallel. Here, a high communication speed among the processors is a crucial issue with respect to a high parallel performance.

Literature

1. H.-J. Bungartz and M. Schäfer (Editors). Fluid-Structure Interaction. Springer, LNCSE 53, Berlin, 2006.

2. S. Yigit, M. Schäfer, and M. Heck. Grid Movement Techniques and Their Influence on Laminar Fluid-Structure Interaction Computations. Journal of Fluids and Structures, 24:819-832, 2008.

3. S. Yigit, D. Sternel, and M. Schäfer. Efficiency of fluid-structure interaction simulations with adaptive under relaxation and multigrid acceleration. Int. Journal of Multiphysics, 1:85–99, 2007.

4.3.13 Fluid-Structure Interaction in Turbulent Flows

Plamen Pironkov, Michael Schäfer, Dörte Sternel
Fachgebiet Numerische Berechnungsverfahren im Maschinenbau, TU Darmstadt

Fluid-structure interaction (FSI) occurs in many engineering applications, as for example in the design of aircraft turbines, car engines or in biomechanical applications. In all these cases a full set of interaction phenomena between the fluid and the solid is observed. This includes flow acting on a solid (during drag, lift or movement), as well as solid acting on flow (during deformation or/and movement). Moreover, in most cases the fluid flow is turbulent. For this purpose, the simulations should be done in respect to the time resolved prediction of wall forces and the moving structure, inside the flow field. Large Eddy Simulation (LES) with a high spatial resolution near the wall is the most promising way to get results for the turbulent flow of required accuracy.

In this project we use an implicit partitioned ALE approach, which tries to combine the advantages of weakly and strongly coupled schemes. Every time step consists of a nested iteration procedure for the velocity-pressure coupling. The coupling is realized via the finite-volume flow solver FASTEST, the finite-element structural solver FEAP, and the quasi-standard coupling interface MpCCI. The coupled solver is fully parallelized for an efficient use on high-performance computers – a necessary prerequisite in order to be able to cope with the tremendous computational effort required for high-resolutioon LES.

An important aspect of this project is the verification and the validation of the numerical algorithm. For this purpose a simulation of a test case for which experimental data are available, has been carried out. We investigate the effects of the different subgrid scale turbulence models (Germano, Smagorinsky) and compare them with those from a standard k-epsilon RANS model.

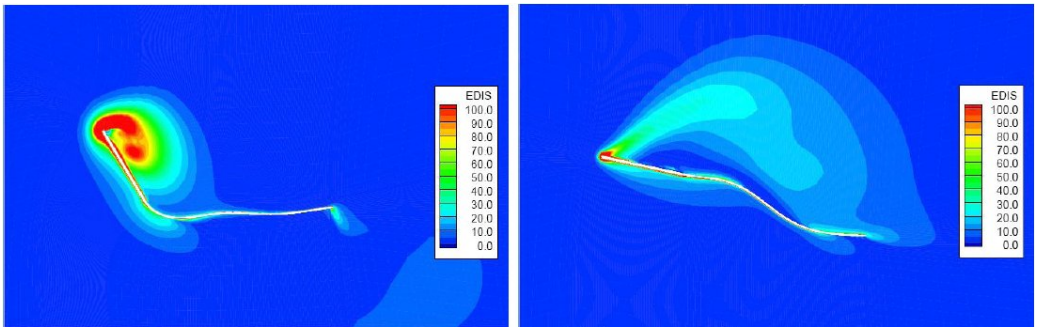

Abbildung 13.1: *Snapshotsof turbulent dissipation at two different time steps.*

Literature

1. H.-J. Bungartz and M. Schäfer (Editors). Fluid-Structure Interaction. Springer, LNCSE 53, Berlin, 2006.

2. D.C. Sternel, M. Schäfer, M. Heck, and S. Yigit. Efficiency and accuracy of fluid-structure interaction simulations using an implicit partitioned approach. Computational Mechanics, online first, Doi: 10.1007/s00466-008-0278-y, 2008.

4.3.14 Evolutionary Algorithms for Flow Shape Optimization

Hongtao Sun, Michael Schäfer
Fachgebiet Numerische Berechnungsverfahren im Maschinenbau, TU Darmstadt

Evolutionary Algorithms (EAs) have been widely used for shape design optimization in engineering. A distinct advantage of EAs is that they are capable of dealing with global and multi-objective optimization problems. They are at the same time derivative free optimization methods, which make them attractive for solving fluid flow optimization problems. However, as stochastic optimization methods EAs usually involve large number of function evaluations that are very time consuming. The objective of this research focuses on improving the efficiency of the evolutionary optimization process. To this respect different approaches are considered and investigated.

A parallel genetic algorithm is firstly implemented in a master-slave model. It is used in particular in the case where the cost of function evaluations computationally is much higher compared with the communication time. One master processor controls the optimization procedure and inside each generation the objective functions are evaluated independently on several parallel processors. This parallelization model doesn't affect the behaviour of the algorithm and the computational time can be ced at most by N times with N slave processors. Meanwhile, some low-cost approximation models such as Radial basis function network (RBFN) model and the reduced-order model based on proper orthogonal decomposition (POD) are constructed to substitute the expensive function evaluations. These surrogated models are adaptively updated during the optimization process in order to assure the optimization accuracy. Furthermore, considering the poor convergence rate of EA at the near optima region, the deterministic optimization method is combined with EA for the local refinement, therefore to further accelerate the optimization process. This whole optimization procedure is illustrated in Figure 14.1.

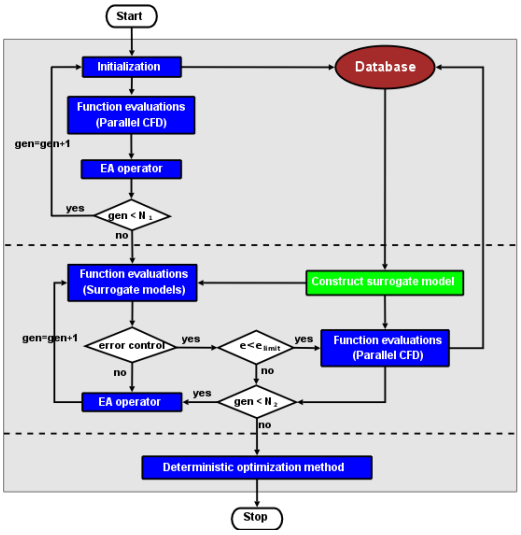

Abbildung 14.1: *Flowchart of efficient evolutionary optimization procedure*

The approaches have been tested on several single or multi-objective flow shape optimization problems. The comparison of the optimization results indicates that it leads to a significant reduction of the computational cost retaining the optimization performance.

Literature

1. Z. Harth, H. Sun, M. Schäfer, Comparison of Trust-region-based and Evolutionary Methods for Optimization of Flow Geometries, Engineering Optimization, 39:797-810, 2007.

2. H. Sun, Z. Harth, M. Schäfer, Efficiency improvement of Evolutionary Algorithms for Flow Shape Optimization, World Congr. on Structure & Multidiscipl. Optimization, Korea, 2007.

4.3.15 Parallel Non-Linear Finite Elements for Micropolar Continua

Steffen Bauer, Michael Schäfer
Fachgebiet Numerische Berechnungsverfahren im Maschinenbau, TU Darmstadt

The classical continuum theory is based on the hypothesis of continuously distributed mass densities in material bodies, irrespective of their inherent discrete molecular or atomistic structure. This assumption holds for the majority of practical applications in the field of engineering sciences, since structures of interest can be considered as large in relation to their sub-microscopic assembly. However, there exist various experimental works describing phenomena at the nano-scale with growing industrial relevance due to a sustaining trend towards miniaturization. In brief, this works state that considerable effects arise whenever the wavelength of deformation is near the material's intrinsic length scale [e.g. 2]. In regard to structures at the nano-scale this implies: "the smaller, the stronger". Classical continuum theory solutions are not able to resolve these effects at all. However, the theoretical framework of so called enhanced continua in general, and micropolar continuum theory in particular, offer a phenomenological approach to model this interesting material behavior entirely. Casting the theoretical framework into a numerical scheme such as the finite element (FE) method is inevitable for solving real life engineering problems.

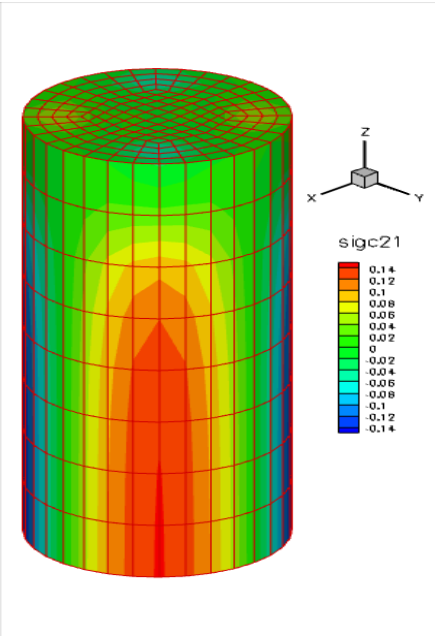

Abbildung 15.1: *Exemplary FE results for micropolar rod under torsional load; contours of couple-stress distribution*

Non-linear FE applications, suitable for spatial micropolar configurations undergoing large deformations as given in [2], entail drastically increased computational effort in comparison to conventional formulations. Non-symmetric global tangent stiffness arrays, a sophisticated numerical treatment of additionally appearing microrotational degrees of freedom and the presence of a large number of history variables are main features that challenge an effective computation. An exemplary discretization is given in Figure 1. In comparison to standard finite elements, the solution process for micropolar meshes consumes up to a hundredfold of wall clock time and up to 10 times more of computer memory. Further improvement of algorithms, both on the element and on the solver level, may increase the size of manageable configurations on serial computers. However, this approach is limited. A treatment of micropolar structures with practical relevance and according mesh sizes on serial machines is not possible.

Therefore, parallel finite elements and the access to a sufficient amount of high-performance computing resources play a pivotal role for such studies. Initial analysis with a parallel version of the FE code FEAP show promising results in regard to accuracy, speed-up and scale-up [3]. These studies were restricted to the application of conventional elements, and

a further pending issue is the adaption and expansion of the parallel build to handle micropolar elements efficiently.

References

1. M.R. Begley and J.W. Hutchinson, The mechanics of size-dependent indentation, Journal of the Mechanics and Physics of Solids 46 (1998) 2049-2068

2. S. Bauer et al., Three-dimensional finite elements for large displacement micropolar elasticity, Computer Methods in Applied Mechanics and Engineering (2008), submitted for review

3. B. Müller, Parallel Finite Element Method with FEAP8.2, B.Sc.-Thesis, Fachgebiet Numerische Berechnungsverfahren im Maschinenbau, TU Darmstadt, August 2008

4.3.16 Time dependent shape optimization with higher-order surfaces in consideration of FSI

Gerrit Becker, Michael Schäfer
Fachgebiet Numerische Berechnungsverfahren im Maschinenbau, TU Darmstadt

Fluid-structure interactions (FSI) arise in many disciplines and applications, e.g. elastic artery modeling, airfoil flutter or wind loads on structures. Therefore, the significance of efficient numerical methods to solve these problems has increased steadily. Thus, the demand for shape optimization has arisen, e.g. the drag and lift force optimization of airfoils. Throughout the last years, researchers have improved the numerical methods concerning fluid-structure interactions. Efficient codes are available now. Furthermore, in the field of structural mechanics shape optimization is already commercially receivable and fluid mechanics researchers make good progress. However, simulations combining fluid-structure interactions and shape optimizations have not been deeply investigated yet.

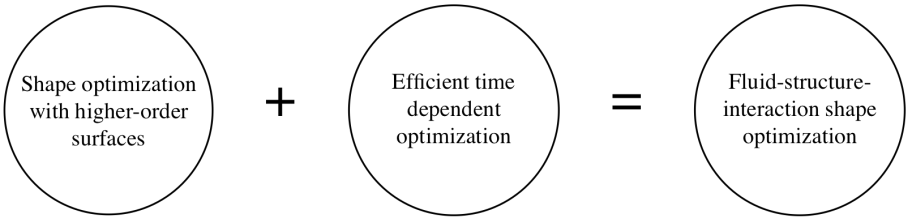

Abbildung 16.1: *Classification of this project's content within the context of FSI optimization*

Therefore, it is aspired to establish shape optimizations within fluid-structure interaction applications. Since the optimal shape is calculated, numerical shape optimization of coupled problems may reduce the costs of time-consuming experiments.

Within this project a new deformation approach for optimizing shapes is developed. It allows a straightforward application towards coupled problems, i.e. the coupled code's routines for grid deformation and generation are utilized for the shape movement within the optimization process as well. The new method is implemented within the fluid region and works aside the fluid-structure coupling surfaces. Because of the time dependence in fluid-structure interactions, an efficient time dependent optimization approach needs to be considered. The implementation into the FSI environment is shown in Fig. 16.2

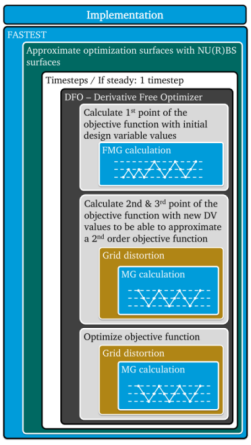

Abbildung 16.2: *Implementation into the FSI environment*

The applied code solves fluid-structure interactions via an implicit partitioned approach. It is based on FASTEST, a parallel multigrid flow solver, utilizing an entirely conservative finite-volume method to solve the incompressible Navier-Stokes equation on a non-staggered, block structured and cell centered grid. Furthermore, FEAP is used as a finite-element based structural solver. The coupling interface

is realized via MpCCI, which sends forces of the flow region to the structural solver and returns resulting deformations. For these, an efficient block-based grid deformation tool is implemented for the fluid region, allowing large grid movements by algebraic and elliptic mesh generation techniques. Work on an efficient parallelization of the whole FSI optimization code is in progress.

4.3.17 Algebraische Mehrgitterlöser zur Berechnung turbulenter Strömungen in komplexen Geometrien

Christine Baur, Michael Schäfer
Fachgebiet Numerische Berechnungsverfahren im Maschinenbau, TU Darmstadt

Nach wie vor ist es schwieriges Problem komplexe turbulente Strömungen mit hinreichender Genauigkeit zu simulieren. Ein vielversprechender Ansatz ist die Methode der Grobstruktursimulation (LES), bei der nur die kleinen turbulenten Skalen modelliert und die großen direkt gelöst werden. Die LES ist als Mittelweg zwischen direkter Simulation und statistischen Modellen zu verstehen. Allerdings nimmt die Grobstruktursimulation immer noch sehr hohe Rechenzeiten und sehr viel Speicherplatz in Anspruch [2,3].

Im Rahmen dieses Projekts wird zur LES der auf der Finite-Volumen-Methode basierte Strömungslöser FASTEST verwendet [1], der auf einer randangepassten, dreidimensionalen, blockstrukturierten räumlichen Diskretisierung basiert. Aus der Finite-Volumen-Diskretisierung der Erhaltungsgleichungen erhält man große dünn besetzte Gleichungssysteme, bei deren Lösung klassische Lösungsverfahren an ihre Grenzen stoßen und deswegen hierarchische Verfahren zur höheren numerischen Effizienz eingesetzt werden. Bereits umfangreich getestet ist die Anwendung von geometrischen Mehrgitterverfahren. Für die Simulationen turbulenter Strömungen mit algebraischen Mehrgitterlösern fehlen hingegen umfassende Effizienzuntersuchungen. Vorteil der algebraischen Verfahren ist die Unabhängigkeit von der Problemgeometrie, weil die Vergröberung der Gitter allein durch die Anordnung der Systemmatrix entsteht, während geometrische Verfahren von der räumlichen Diskretisierung abhängig sind. Anhand eines Testproblems wird der in FASTEST implementierte algebraische Mehrgitterlöser SAMG für unterschiedlich komplexe Geometrien auf seine Effizienz hin untersucht. Es handelt sich um eine Kanalgeometrie, durch welche die Strömung labyrinthartig geführt wird. Eine höhere Komplexität wird durch die Variation der Anzahl und Länge der Hindernisse erreicht. Abbildung 17.1 zeigt den Konturplot für das Geschwindigkeitsprofil des Testfalls mit der höchsten Komplexität. Es wird der algebraische Mehrgitterlöser anhand der Rechenzeiten mit dem geometrischen Mehrgitterlöser verglichen. Ergebnisse für Berechnungen mit laminarer Strömung zeigen, dass der algebraische Mehrgitterlöser bei hoher Komplexität der Geometrie hinsichtlich der Rechenzeit gegenüber dem geometrischen Mehrgitterverfahren deutlich besser abschneidet.

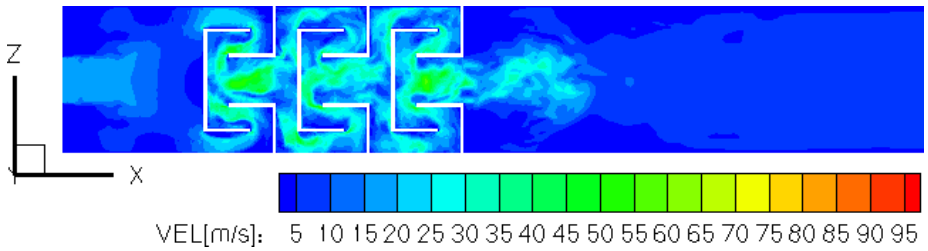

Abbildung 17.1: *Strömung durch Kanal: Geschwindigkeitsprofil in der x-z-Ebene bei y=0.1m*

Literatur

1. D. C. Sternel, FASTEST-Manual, Fachgebiet Numerische Berechnungsverfahren im Maschinenbau, TU Darmstadt, 2005.

2. T. Lehnhäuser, S. Ertem-Müller, M. Schäfer, and J. Janicka. Advances in Numerical Methods for Simulating Turbulent Flows. Progress in Computational Fluid Mechanics, 4:208–228, 2004.

3. M. Kornhaas, D.C. Sternel, M. Schäfer. Influence of time step size and convergence criteria on large eddy simulations with implicit time discretization. In J. Meyers, B.J. Guerts, and P. Sagaut (eds.), Quality and Reliability of Large-Eddy Simulations, pages 119-130, Springer, Berlin, 2008.

4.3.18 Strömungs-Akustik-Kopplung auf Basis der Grobstruktursimulation

Michael Kornhaas, Michael Schäfer, Dörte Sternel
Fachgebiet Numerische Berechnungsverfahren im Maschinenbau, TU Darmstadt

Ein wesentlicher Teil des Geräuschaufkommens in unserem täglichen Umfeld wird von turbulen- ten Strömungen verursacht. Dazu zählt beispielsweise das Geräusch fahrender Autos, Fluglärm oder der Lärm von Lüftern aller Art. Obwohl vor allem im urbanen Umfeld die Vermeidung und Minimierung von Lärm immer wichtiger wird, sind die physikalischen Mechanismen, die zur Schallentstehung in turbulenten Strömungen beitragen, noch immer nicht vollständig verstanden. Aufgrund der stetig wachsenden Rechenleistung moderner Computersysteme besteht erstmalig die Möglichkeit der vorhersagenden Simulation turbulenter Strömungen für größere Reynoldszahlen und komplexere Geometrien durch die „Direkte Numerische Simulation (DNS)“ oder die „Grobstruktursimulation (engl. Large Eddy Simulation, LES)“, bei der die großen energiereichen Skalen aufgelöst und nur die kleinen vom Gitter nicht erfassten Skalen modelliert werden.

Diese beiden Verfahren zeichnen sich neben ihrer hohen Genauigkeit auch dadurch aus, dass die zeitlichen Schwankungen der Strömungsgrößen erfasst werden. Aus dem so erhaltenen instationären Strömungsfeld lassen sich akustische Quellterme bestimmen und anschließend die Ausbreitung des Schalls berechnen.

Im Rahmen dieses Projekts wird das instationäre Strömungsfeld mittels Grobstruktursimulation berechnet und aus den Schwankungen werden akustische Quellterme für die linearisierten Eulergleichungen bestimmt, mit deren Hilfe dann die Schallsausbreitung berechnet wird.

Aufgrund der für die Grobstruktursimulation benötigten hohen räumlichen und zeitlichen Auflösung und dem damit einhergehenden Bedarf an Arbeitsspeicher und Rechenleistung, lassen sich solche Problemstellungen derzeit nur auf parallelen Hochleistungsrechnern simulieren.

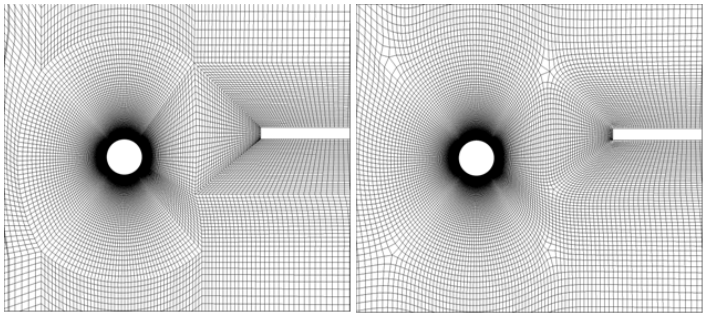

Abbildung 18.1: *Optimierung der Gitterqualität durch elliptisches Glätten. Links: ohne Glättung; rechts: geglättet*

Außer zur eigentlichen numerischen Simulation kommt der HHLR im Rahmen dieses Projekts auch bei der Generierung der Berechnungsgitter und deren Optimierung zum Einsatz. So werden beispielsweise die verwendeten Gitter zur Minimierung des Diskretisierungsfehlers elliptisch geglättet. Abbildung 18.1 zeigt einen Ausschnitt eines geglätteten sowie eines nicht optimierten Gitters für den Akustik-Testfall einer *„Platte im turbulenten Nachlauf eines Kreiszylinders“*.

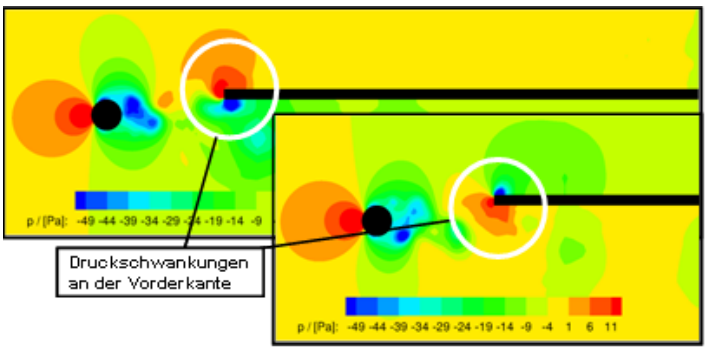

Abbildung 18.2: *Instationäre Druckverteilung im Zylindernachlauf und dem Vorderkantenbereich der Platte*

Im konkreten Fall wurde für die Gitter-glättung 25 GB RAM benötigt, so dass diese nicht auf einer herkömmlichen Workstation durchgeführt werden kann. Das Berechnungsgitter besteht aus ca. 20 Mio. Kontrollvolumen.

Die eigentliche Berechnung wurde auf 32 Prozessoren durchgeführt. Abbildung 18.2 zeigt die instationäre Druckverteilung für zwei Zeitschritte im Bereich der Platten-vorderkante. Es treten starke Druck-schwankungen auf, welche als akustische Quelle wirken.

4.3.19 Automated Aerodynamic Optimisation of a Transonic Compressor Stage by Application of non-axisymmetric Endwalls

Steffen Reising, Heinz-Peter Schiffer
Fachgebiet für Gasturbinen, Luft- und Raumfahrtantriebe, Fachbereich Maschinenbau

Introduction

In the last few decades the development of axial aircraft compressors has led to extremely high stage loadings to reduce the entire engine size and weight. Stage loading is recognized to be the single most important design decision due to its influence on the overall performance and on the engine size. However, this trend also promotes several disadvantages as e.g. the risk of separation on the suction side and higher secondary flow due to the increased circumferential static pressure gradient in the blade channel. The application of non-axisymmetric endwalls is one approach to reduce blade loading in the hub region and to control endwall flow with the main objectives of increasing the component efficiency and the total pressure ratio. The challenge hereby is to find the optimal non-axisymmetric endwall shape which results in the largest benefit in performance. In this report an approach is presented to find a fully 3D endwall geometry that satisfies the mentioned requirements. This approach is based on an optimization chain using the commercial CFD Software FINE^{TM}/Turbo and FINE^{TM}/Design3D. This procedure is applied on the known Configuration I of the Darmstadt Transonic Compressor, limited to the hub endwall of the stator. The numerical results show a high benefit in overall performance resulting in a rise in stage efficiency of 1.65% and a slight improvement in total pressure ratio.

Optimisation chain

The idea of the presented method, of which a flow chart is shown in Figure 19.1, is to accelerate the design of new endwall contours by using the knowledge acquired during the previous designs of similar contours.

The core of the design system is the database containing the results of all Navier-Stokes computations performed during the generation of the initial databases. This database contains three kinds of data for each sample: The fluid properties and flowfield boundary conditions, the parameters to define each sample geometry and each sample's aerodynamic performance characterised e.g. by efficiency. After a sufficiently large initial database of arbitrary samples has been generated in an automated way, an iterative procedure is used which is structured as follows:

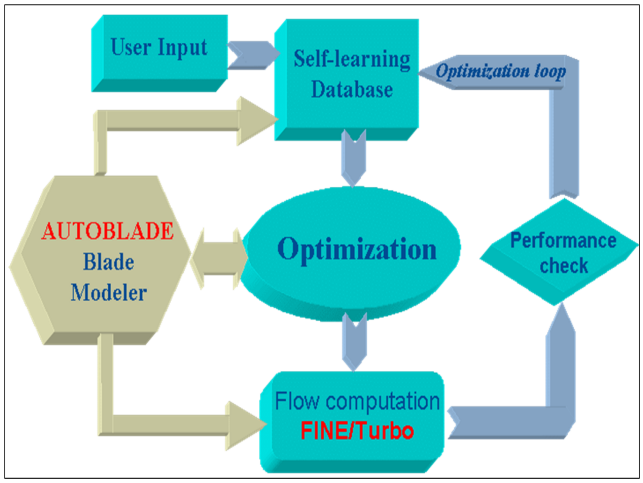

Abbildung 19.1: *Schematic of optimisation process*

A learning process is used to build the neural network based on the examples stored in the initial database. The network contains free parameters that are to be adapted to fit the database samples. A fitting process is performed by back-propagation of the errors. After the mapping of the database samples, the neural network is able to predict the aerodynamic performance of endwall contours that are not part of the database. The next step is to find a new design by using the mentioned optimisation procedure formed by a genetic algorithm. The performance of this new design is evaluated by means of the trained neural network. To quantify performance, an objective function is used which transfers all user-imposed constraints into a single number. The result of this optimisation is a point which is expected to be close to the global optimum of the design space. This new geometry is now evaluated by the 3D Navier-Stokes flow solver and added to the database. The comparison of the performance obtained by CFD with the one predicted by the neural network permits to evaluate the accuracy of the network. The new sample's performance is also compared to the design goals. If these have not been achieved another design iteration is started repeating the same process until the optimum geometry has been reached. As this process proceeds, the database grows after each iteration leading to improvements of the approximate relation and therefore to a better prediction of the real optimum.

Results

In Figure 19.2 one can notice that the optimisation did not only lead to improvements for design conditions but also for the entire speed line. Figure 19.3 shows the surface subsidence of the non-axisymmetric endwall combined with the static pressure distribution. Between the middle of the blade channel and the pressure side, the optimisation led to convex curvature involving an acceleration of the flow and a reduction in static pressure. On the other hand, the contour plot of the endwall shows a concave curvature at the suction side which decelerates the flow increasing the static pressure like in a diffuser.

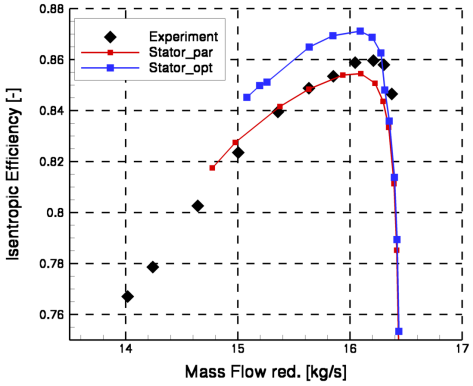

Abbildung 19.2: *Speedlines of original and optimized design*

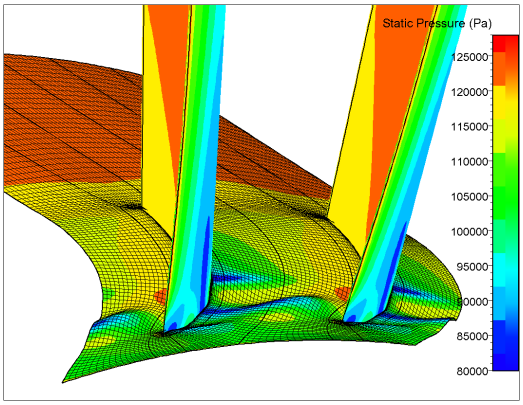

Abbildung 19.3: *Static pressure distribution on endwall*

Having a closer look at the flow characteristics at design conditions, it becomes clearly apparent that the major part of the improvement results from the decrease of the separation zone. Figure 19.4 displays the suction side of the initial stator showing a huge separation

bubble reaching from the hub to approximately 30% channel height. According to the streaklines on the blade surface in Figure 19.5, the radial extension of the separation area is limited to 10% relative channel height.

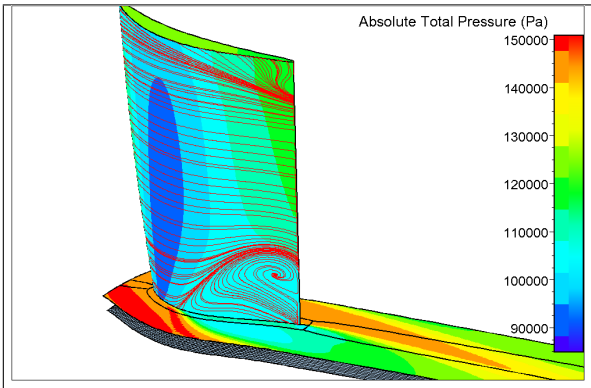

Abbildung 19.4: *Separation zone of original design*

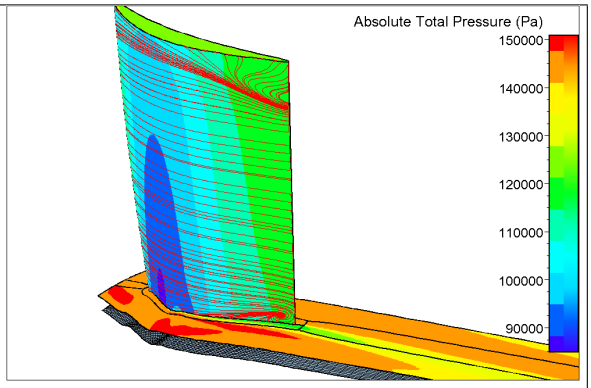

Abbildung 19.5: *Reduced separation zone of optimised design*

4.3.20 Drop impact onto a liquid layer: cavity shape and propagation of a solitary wave

Edin Berberovic, Nils P. van Hinsberg, Suad Jakirlic, Ilia V. Roisman and Cameron Tropea
Technische Universtität Darmstadt
Chair of Fluid Mechanics and Aerodynamics, Petersenstraße 30, 64287 Darmstadt, Germany

A complementary experimental and numerical investigations of a normal drop impact onto a liquid film of finite thickness are presented. The effects of various influencing parameters such as drop impact velocity, liquid film thickness and physical properties of the liquids, including viscosity and surface tension, on the time evolution of the crater formation are investigated. Numerical simulation solving the Navier-Stokes equations for unsteady, incompressible flow are performed using an advanced free-surface capturing model based on a two-fluid formulation of the classical volume-of-fluid (VOF) model in the framework of the finite volume numerical method. In this model an additional convective term, referred to as the compression term originating from the convective velocity modelling in terms of a weighted average of the corresponding liquid and gas velocities, is introduced into the transport equation for the phase fraction, providing a sharper interface resolution. Utilizing the detailed database resulted from experiments and numerical predictions the dynamics of drop impact on liquid surfaces, the shape of the cavity and the formation and propagation of a solitary wave in the crater are determined and analyzed.

In the modified approach, based on a two-fluid formulation of the equation for volume fraction., the contributions of the liquid and gas velocities to the evolution of the free surface are assumed proportional to the corresponding phase fraction, and accordingly the velocity of the effective fluid in a VOF model is defined as a weighted average.

The additional convective term, referred to as the compression term ensures a strong coupling between a classical VOF and a two-fluid model. The additional convective term provides the necessary compression of the interface, thus avoiding the need to devise a special compressive scheme for convection. This term is active only within the interface region and vanishes at both limits of the phase fraction. Therefore it does not affect the solution out-side this region.

The momentum equation is modified in order to account for the effects of surface tension. The surface tension at the liquid-gas interface generates an additional pressure gradient resulting in a force, which is evaluated per unit volume using the Continuum Surface Force (CSF) model.

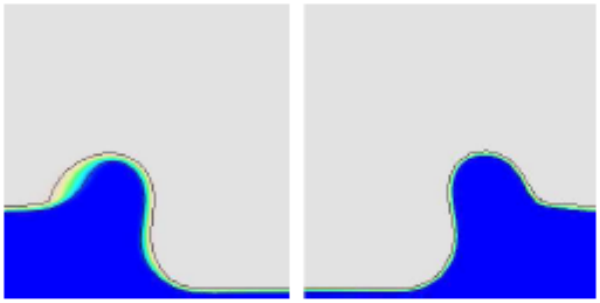

Abbildung 20.1: *Crater shape for drop impact of glycerin/water mixture, classical VOF model (left) and advanced model (right). $H = 1$, $We = 329$, $Re = 428$, tU/D=9.89.*

All computations are performed using a cell-center-based finite volume method on a fixed unstructured numerical grid and employing the solution procedure based on the PISO algorithm for coupling between pressure and velocity in transient flows. The grid is adaptively refined in the region of the crater development. The transient and source terms are discretized using the mid-point rule and integrated over cell volumes. Time derivative terms are discretized using an implicit Euler scheme. The terms comprising spatial derivatives, as diffusion and convective terms, are converted into integrals over surfaces bounding each cell using Gauss's theorem. The integration is performed by summing values at cell faces, obtained by interpolation. For the evaluation of gradients a linear face interpolation is used.

The numerical simulations demonstrate not only the good predictive capabilities of the advanced algorithm. They help also to understand the mechanisms of crater evolution. In particular the formation and propagation of the solitary wave along the cavity surface is explained using the results of the numerical predictions of the pressure field in the liquid.

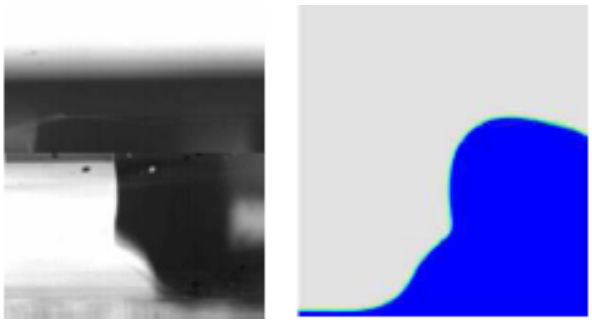

Abbildung 20.2: *Crater shape for drop impact of isopropanol, experiment (left) and simulations (right). H= 2, We = 392, Re = 1730, tU/D=31:44*

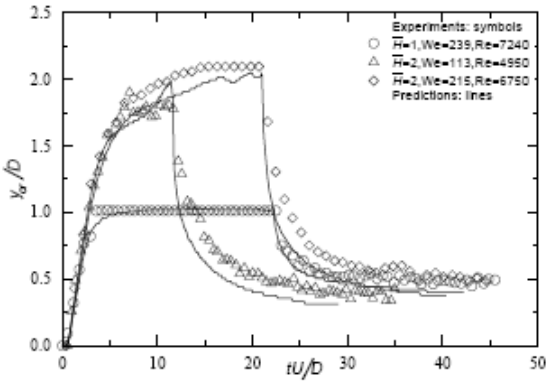

Abbildung 20.3: *Dimensionless crater depth for drop impact of distilled water.*

4.3.21 Experimental and computational investigations of flow and mixing in a single annular combustor configuration

B. Kniesner,G. Kadavelil, M. Gnirß, S. Jakirlić and C.Tropea
Chair of Fluid Mechanics and Aerodynamics, Petersenstr. 30, 64287 Darmstadt
Technische Universität Darmstadt, Germany

A complementary experimental and computational study of the flow and mixing in a single annular gas turbine combustor has been carried out. The object of the investigation is a generic mixing chamber model, representing an unfolded segment of a simplified Rich-Quick- Lean (RQL) combustion chamber operating under isothermal, non-reacting conditions at ambient pressure, Fig. 21.1. Two configurations without and with secondary air injection were considered.

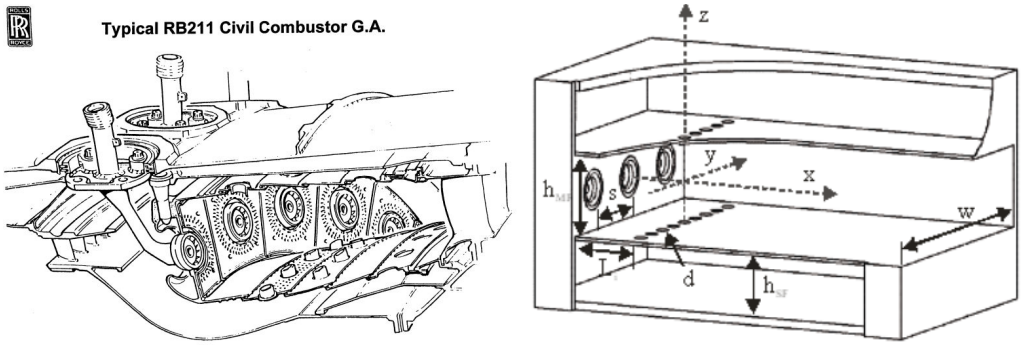

Abbildung 21.1: *Exampleof a single-annular combustor (left) and its appropriate simplification (right) pertinent to the present experimental and computational investigations*

To provide an appropriate reference database several planar optical measurement techniques (time-resolved flow visualisation, PIV, QLS) were used. The PIV measurements have been performed providing profiles of all velocity and Reynolds-stress components at selected locations within the flue. Application of a two-layer hybrid LES/RANS (HLR) method coupling a near-wall k$-\varepsilon$ RANS model with true LES in the core flow was the focus of the computational work. In addition to the direct comparison with the experimental results, the HLR performance is comparatively assessed with the results obtained by using conventional LES using the same (coarser) grid as HLR and two eddy-viscosity-based RANS models. The HLR model reproduced all important flow features, in particular with regard to the penetrating behaviour of the secondary air jets, their interaction with the swirled main flow, swirl-induced free recirculation zone evolution and associated precessing-vortex core phenomenon in good agreement with experimental findings. Selected results obtained by computing both configurations without (*J=0*) and with secondary air injection (*J=100*) are illustrated in next figures. Figs. 21.2 display the comparison of the experimentally obtained axial velocity profiles and streamwise stress components and corresponding computational results at six streamwise locations in the horizontal *x-y* plane. The velocity profile evolution exhibiting regions with negative velocity values in the flue is a typical representative of a flow in a swirl combustor. The results, especially those obtained by the present HLR model follow closely the experimental ones. Proper capturing of the velocity profiles with respect to their local maxima and minima indicate the correctly predicted rate of spreading of the swirling jets and the form, size and intensity of the flow reversal zone.

It is also in accordance with the rate of entrainment of the curved, annular swirling stream into the core flow. Fig. 21.3 displays the experimentally and computationally obtained evolution of the profiles of the axial velocity in the vertical mixing chamber plane ($y=0$) for the case with secondary air injection (J=100). Characteristic streamwise locations ahead of and after the injection plane were selected. One should note that the experimental data are not available in the immediate wall vicinity ($z/H \geq 0.45$). The profile shapes of all quantities characterized by local minima and maxima and sign changes are well reproduced by both computational methods applied.

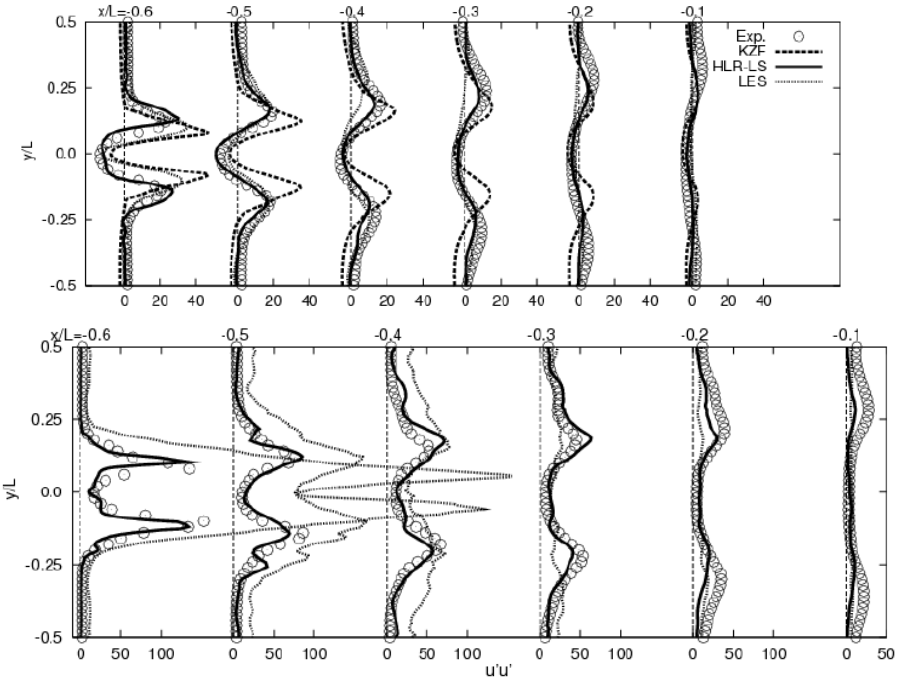

Abbildung 21.2: *Evolution of axial velocity profiles and streamwise stress components at selected streamwise positions in the horizontal plane (z=0) of the mixing chamber for the case without secondary air injection (J=0)*

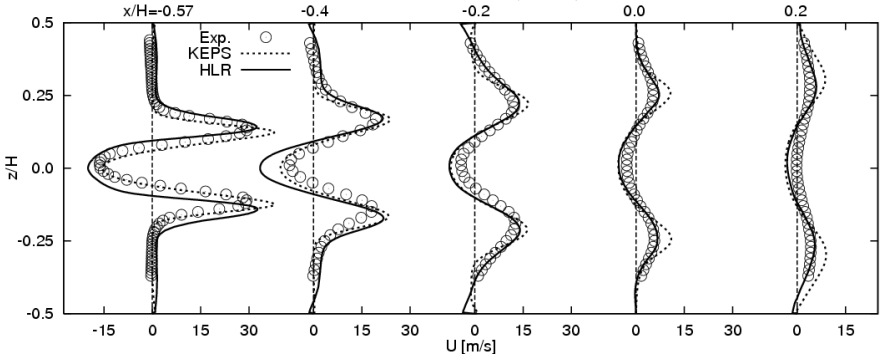

Abbildung 21.3: *Computationally obtained profiles of the axial mean velocity component at selected streamwise positions in the vertical mixing chamber plane y=0 (upper) for the case with secondary air injection (J=100)*

4.3.22 Swirl intensity influence on interaction between non-swirling and swirling co-axial jets in a combustor configuration: LES and modelling study

Sanjin Šarić, Björn Kniesner, Paul Altenhöfer, Suad Jakirlić,Cam Tropea[1], Dalibor Čavar[2], Branislav Basara[3]

[1]Chair of Fluid Mechanics and Aerodynamics, Petersenstr. 30, 64287 Darmstadt Technische Universität Darmstadt, Germany

[2] Fluid Mechanics Section, Department of Mechanical Engineering, Technical University of Denmark, Nils Koppels Alee 403, 2800 Kgs. Lyngby, Denmark

[3]Advanced Simulation Technology, AVL List GmbH, Hans-List-Platz 1, A-8020 Graz, Austria

Structural characterization of flow and turbulence in the model of a tubo-annular combustion chamber is investigated computationally using LES (Large Eddy Simulation) method and the ζ-f RANS (Reynolds-averaged Navier-Stokes) model of Hanjalić et al. (2004). The latter model, representing a robust eddy-viscosity-based model of turbulence, is used in conjunction with the universal wall treatment combining the integration up to the wall and wall functions. Reference LDA (inlet section including central and annular pipes) and PIV (combustor) measurements were performed by Palm (2006). The focus of the investigation was on the swirl intensity influence on the interaction between central non-swirling stream and a swirling co-axial jet issuing from an annular inlet section in the near-field of the flue. The results obtained demonstrate gradual expansion of the free flow reversal zone into the radial direction with corner (wall-bounded) bubble being substantially suppressed. The increasing swirl intensity contributes significantly to the intensification of the radial movement associated with strong turbulence level increase in the region of the swirling shear layer, thus promoting the mixing. The overall agreement between simulations and measurements is good. This is particularly the case in the shear layer and the outer, wall-affected flow region. . All computations have been performed on the supercomputer HHLR using the in-house code FASTEST-3D (Flow Analysis by Solving Transport Equations Simulating Turbulence) which uses a finite volume method for block-structured, body-fitted, non-orthogonal, hexahedral meshes.

References

1. Hanjalić, K., Popovac, M. and Hadziabdić, M., 2004, "A robust near-wall elliptic-relaxation eddy-viscosity turbulence model for", Int. J. Heat Fluid Flow, Vol. 25, p. 1047-1051

2. Palm, R., 2006, "Experimentelle Untersuchung der Strömung und Vermischung in einem Drallbrennermodell", Ph.D. Thesis, Darmstadt University of Technology

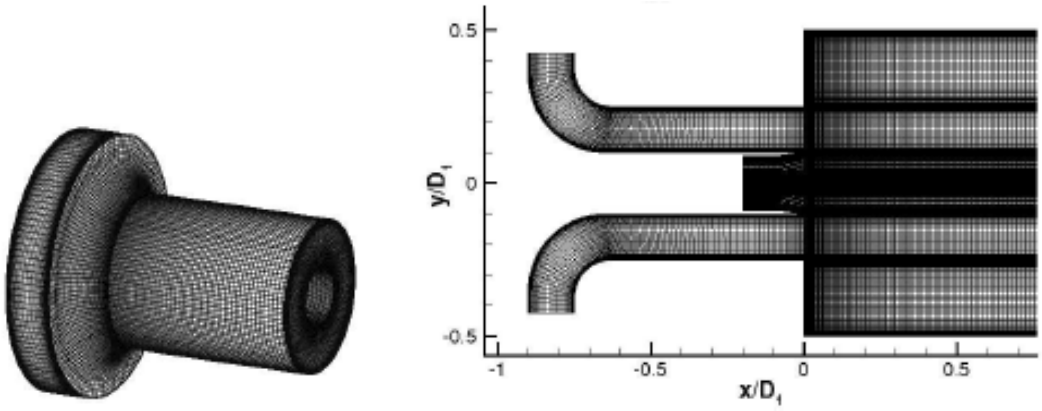

Abbildung 22.1: *Asimplified swirl generator (left) including the combustor flue used for LES (right, a grid slice in the x-y plane)*

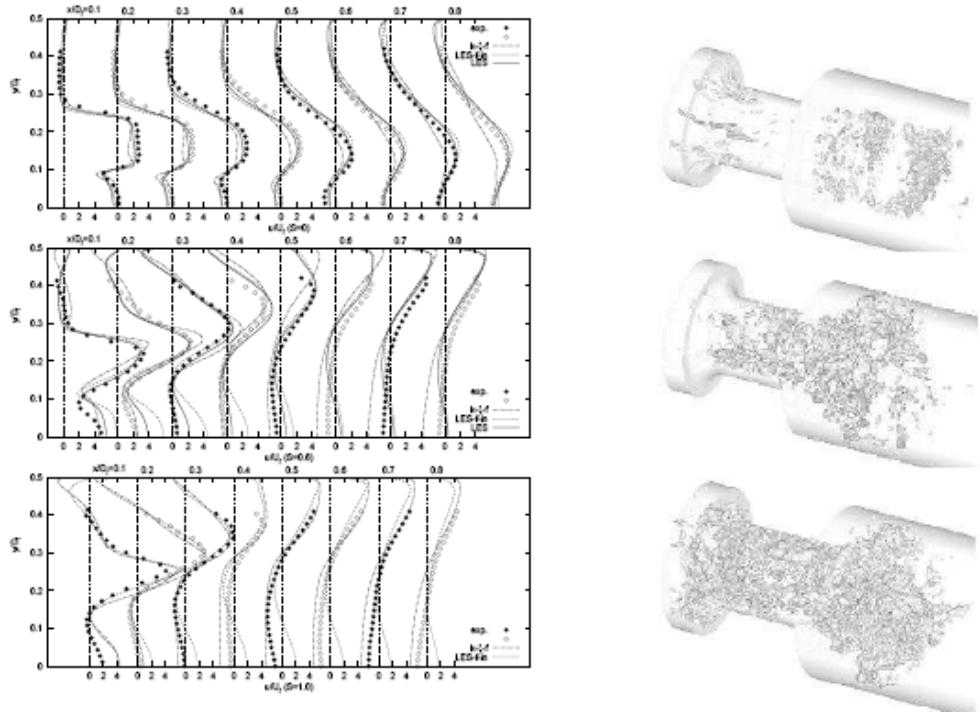

Abbildung 22.2: *RANS and LES predictions of the mean streamwise velocity for various swirl intensities. U_f represents the bulk velocity within the flue (left). Visualization of coherent flow structures in LES of swirling flow in the combustor - isosurface of the instantaneous pressure fluctuation p' for various swirl intensities (right).*

4.3.23 Computational study of the separated flow in a 3D-diffuser

G. Kadavelil[1], M. Kornhaas[2], S. Šarić[1], D. Sternel[2], S. Jakirlić[1] and M. Schäfer[2]
[1] Chair of Fluid Mechanics and Aerodynamics, Petersenstr. 30, 64287 Darmstadt
Technische Universität Darmstadt, Germany
[2] Chair of Numerical Methods in Mechanical Engineering, Dolivostr. 15, 64293 Darmstadt
Technische Universität Darmstadt, Germany

An incompressible flow in a 3-D diffuser with deflected upper wall (with an angle of expansion $\alpha = 11.3^{\mathrm{o}}$) and one side wall (with an angle of expansion $\alpha = 2.56^{\mathrm{o}}$) at the inlet-duct-height-based Reynolds number of $\mathrm{Re_h} = 10000$ (Fig. 23.1), for which the experimentally obtained reference database was provided by Cherry et al. (2008), was studied computationally by using the LES (Large Eddy Simulation), DES (Detached Eddy Simulation) and HLR (Hybrid LES/RANS) methods. The focus of the investigation was on the adverse pressure gradient effects evoked by the duct expansion on the size and shape of the three-dimensional flow separation pattern. The computations were performed with:

- LES (Large Eddy Simulation): the sub-grid scales were modelled by the Smagorinsky (1963) formulation utilizing the dynamic determination of the model coefficient proposed by Germano et al. (1991)
- DES (Detached Eddy Simulation): a seamless hybrid LES/RANS approach employing the one-equation turbulence model by Spalart and Allmaras (S-A, 1994), based on the transport equation for turbulent viscosity ν_{t}, to model the influence of the smallest, unresolved scales on the resolved ones (e.g. Travin et al., 2002) in the LES sub-region of the solution domain. The same (RANS) model was used to model the near-wall layer. The smooth transition from the near-wall RANS layer to the off-wall LES region was achieved by switching the wall distance d in the destruction term in the ν_{t}-equation to the representative grid spacing Δ_{DES}.
- HLR (Hybrid LES/RANS): a zonal (with a variable interface), two-layer hybrid approach combining LES method in the outer layer and RANS method in the near-wall layer. In the latter method, the low-Reynolds number $\mathrm{k} - \varepsilon$ model due to Launder and Sharma (1974) was applied in the near-wall region. The subgrid-scale model due to Smagorinsky is used in the core flow. The model coupling is realised via the turbulent viscosity, representing an approach which enables the solution obtained by using one system of equations. Depending on the flow zone, the turbulent viscosity is either computed from the RANS formulation or from the Smagorinsky model. More details about the HLR method are given in Jakirlić et al. (2006) and Kniesner et al. (2007).

All computational results were obtained by using the in-house code FASTEST-3D (Flow Analysis by Solving Transport Equations Simulating Turbulence) which uses a finite volume method for block-structured, body-fitted, non-orthogonal, hexahedral meshes.

Following figures display selected results obtained by different hybrid LES/RANS modelling approaches: DES and a zonal hybrid LES/RANS scheme (HLR) in the vertical plane in the diffuser section aiming at comparative analysis of their features and performances in such a complex flow configuration featured by a three-dimensional separation pattern.

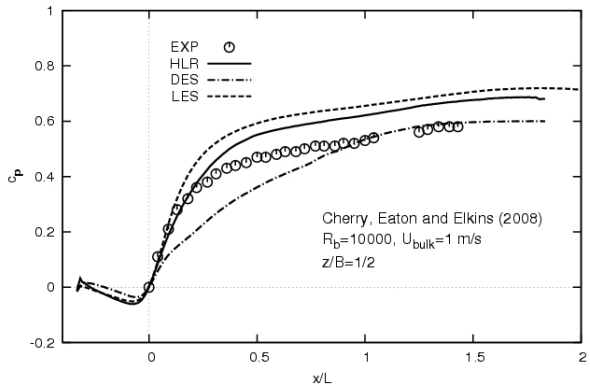

Abbildung 23.1: *Pressure coefficient evolution along the lower diffuser wall*

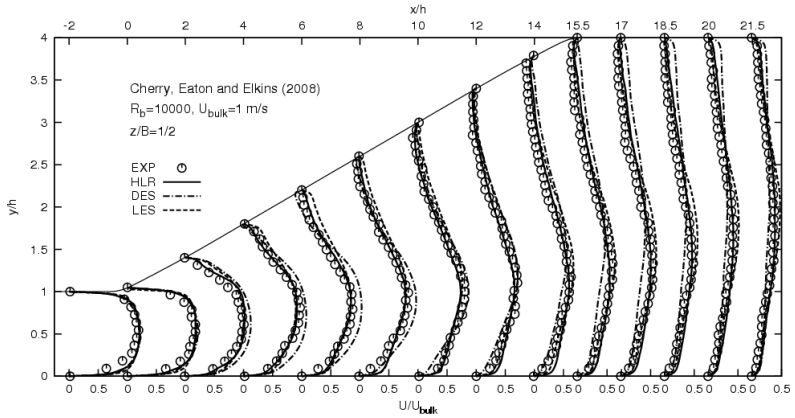

Abbildung 23.2: *Evolution of the axial velocity profiles in the vertical plane at z/B=0.5*

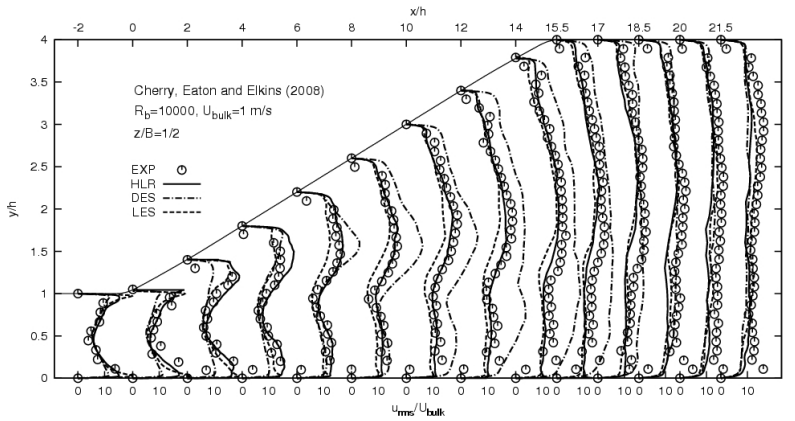

Abbildung 23.3: *Evolution of the streamwise stress component profiles in the vertical plane at z/B=0.5*

4.3.24 Computational analysis of locally forced flow over a wall-mounted hump at high-Re number

S. Šarić[1], S. Jakirlić[1], A. Djugum[2], C. Tropea[1]
[1]Chair of Fluid Mechanics and Aerodynamics, Petersenstr. 30, 64287 Darmstadt Technische Universität Darmstadt, Germany
[2]Department of Mechanical Engineering, University of Sarajevo, Omladinsko Šetalšte 9,71000 Sarajevo, Bosnia and Herzegovina

An incompressible, high-Reynolds number flow (slightly less then 1 Mio. per chord) over a smoothly contoured, asymmetric, wall-mounted hump was computationally studied using the LES (large eddy simulation) and DES (detached eddy simulation) methods. In addition, several second-moment and eddy-viscosity closures within the RANS (Reynolds-averaged Navier–Stokes) framework were tested. The focus of the investigation was on the effects of local perturbation of the hump boundary layer introduced by spatially uniform (in the spanwise direction) steady suction and oscillatory suction/blowing through a narrow opening (1.7 mm) situated at the hump crest immediately upstream of the natural separation point. Reference experiments have shown that both flow control mechanisms cause a shortening of the recirculation bubble relative to the baseline configuration with no flow control. All statistical turbulence models used in the RANS framework resulted in a substantially larger recirculation zone independent of the modelling level, being a consequence of a too low turbulence level in the separated shear layer. Accordingly, the effect of the steady suction, namely the reduction of the reattachment length, was underpredicted. The LES method, despite a relatively coarse mesh (with a total of 4 Mio. cells) for such a high-Reynolds number, wall-bounded flow, was capable of capturing important effects of the flow control qualitatively and quantitatively. DES failed to do so in the suction case, despite good results in the baseline and oscillatory blowing/suction cases, indicating that a shallow separation from curved surfaces poses a challenge to this hybrid RANS/LES strategy. A sensitivity study of the RANS/LES interface position within the DES approach shows that a RANS region chosen too thin (with the interface situated at the very beginning of the logarithmic layer) can lead to a strong reduction of the turbulent viscosity causing a low turbulence level within the shear layer region aligned with the recirculation zone, which in turn leads to a larger separation bubble. All computations have been performed on the supercomputer HHLR using the in-house code FASTEST-3D (Flow Analysis by Solving Transport Equations Simulating Turbulence) which uses a finite volume method for block-structured, body-fitted, non-orthogonal, hexahedral meshes.

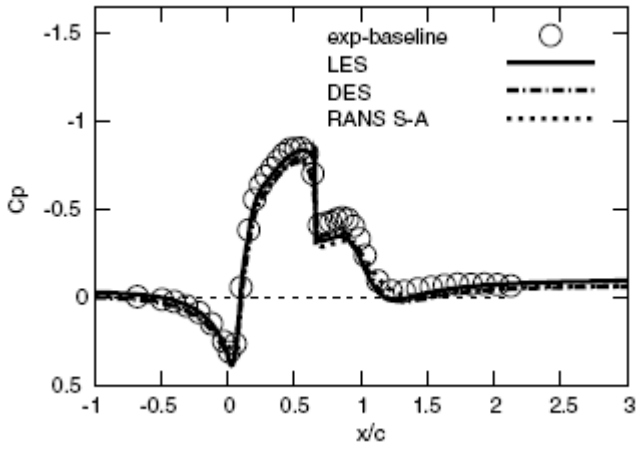

Abbildung 24.1: *Pressure coefficient for the baseline configuration.*

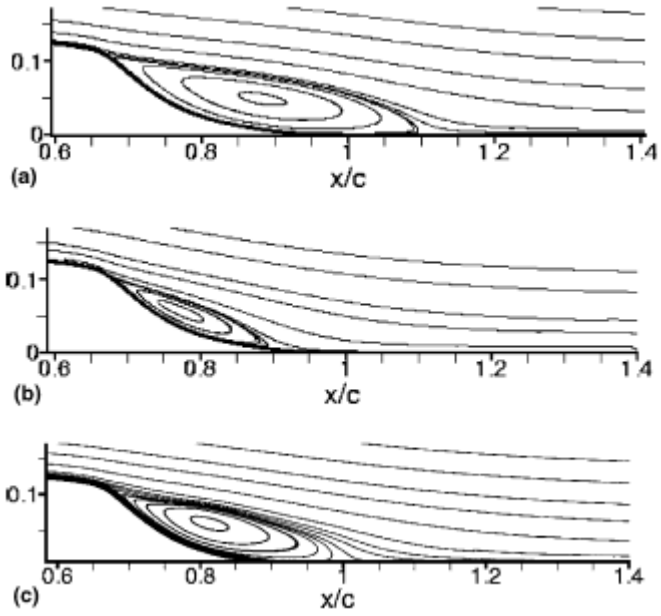

Abbildung 24.2: *Time-averaged streamlines obtained by LES method. (a) Baseline, (b) steady suction and (c) oscillatory suction/blowing configuration*

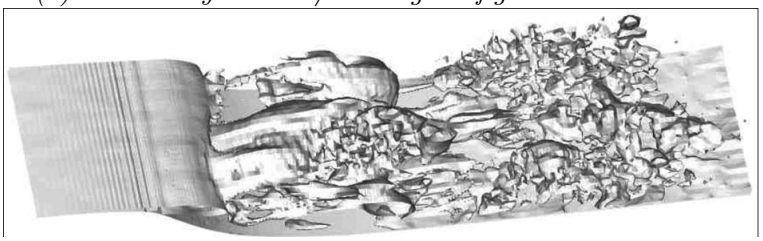

Abbildung 24.3: *Iso-surfaces of the spanwise vorticity obtained by DES of oscillatory suction/blowing flow control case.*

4.3.25 Solid nitrogen under pressure

Jani Kotakoski, Karsten Albe
Fachgebiet Materialmodellierung, FB 11, Material- und Geowissenschaften,
Petersenstr 23, D-64287 Darmstadt, e-mail: albe@mm.tu-darmstadt.de

Experiments have recently confirmed[1] the theoretical predictions[2,3] on nitrogen forming a polymeric solid under pressure, although nitrogen is traditionally considered as chemically inert due to the strong tripple bonds in dimers, which form the conventional solid nitrogen structures. After the original prediction for the atomic structure of polymeric nitrogen, cubic gauche (N-cg) [3], which was confirmed by the experiments[1], several theoretical groups have proposed new possible structures which could be more stable or easier to synthesize than N-cg. However, a consistent comparison reviewing all the suggested phases has been lacking.

In our studies[5], we have used first principles calculations within the density-functional theory in trying to provide an overview on the pressurized solid nitrogen structures. For example, we have found that the N-cg with another insulating phase[4] with covalent bonds in all three dimensions are thermodynamically favored at pressures 50-200 GPa, after the molecular structures have become higher in enthalpy. At 200 GPa, the black phosphorus phase, which has previously been described as the high-pressure phase of nitrogen, becomes the lowest in enthalpy. However, according to our results, this phase exhibits imaginary phonon frequencies at 200 GPa (see figure 25.1), which indicates instability of the structure. In fact, this phase seems to be metastable only at pressures of 100-150 GPa.

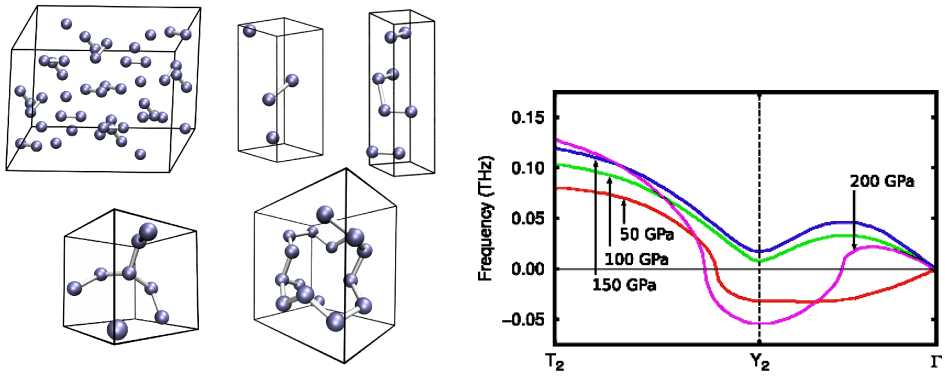

Abbildung 25.1: *(Left) Different solid nitrogen structures. (Right) The imaginary branch of the phonon dispersion relation of black phosphorus phase at different pressures.*

As the experiments on polymeric nitrogen are performed under high pressures using diamond anvil cells, we have also studied the effect of pressure on the electronic band structure and density of states of the most interesting polymeric nitrogen phases. The band gaps of the two insulating phases were seen to respond differently to the applied pressure - for N-cg the band gap increases up to at least 100 GPa, and again decreases after this, whereas for the other phase the band gap always decreases with increasing pressure (see figure 25.2).

Because of the difficulties in synthesizing the polymeric structures by starting from the molecular phases, we have also studied the possibility of using other precursor materials.

One group of possible candidates for this are the alkali metal azides as in these structures the nitrogen atoms form N3 molecules with bonds weaker than the dimer bond. Hence, one could expect that breaking these bonds would be easier in order to form the single-bonded polymeric nitrogen network, as compared to the case of molecular nitrogen.

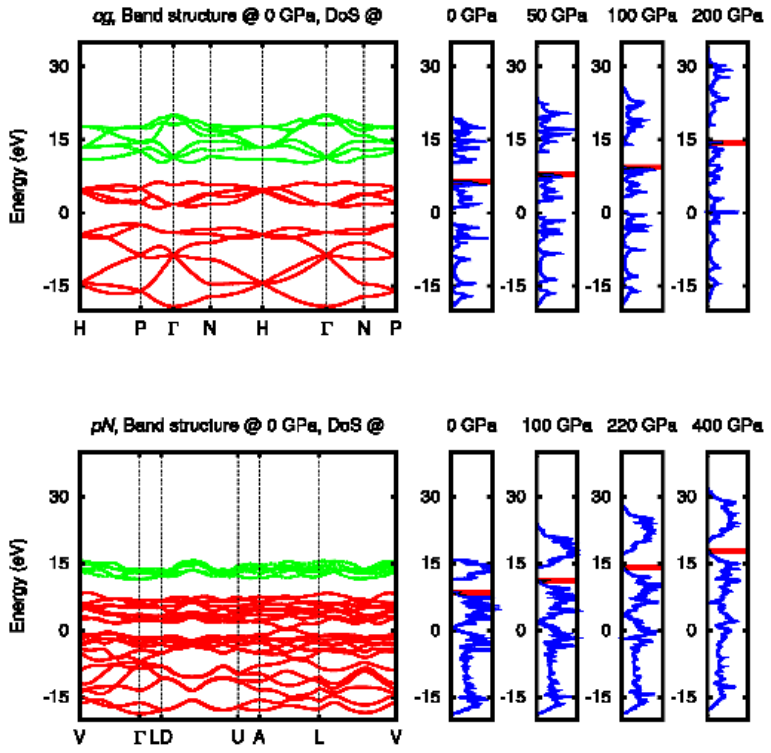

Abbildung 25.2: *Electronic band structures of the two insulating polymeric nitrogen phases with electronic density of states at different pressures.*

According to our results, the solubility of lithium to N-cg is significantly lower than that of H or Na. Although the azide structures remain thermodynamically stable with respect to phase-separated polymeric nitrogen and metal, this gives hope in forming the polymeric nitrogen with mixed lithium impurities when pressurizing the lithium azide, whereas less hope is given for sodium or hydrogenic azides.

In conclusion, we have improved the understanding on the various nitrogen phases under pressure, as well as investigated the possibility of using different precursor materials for the synthesis of these structures. These studies serve as a starting point towards obtaining the high-T,P phase diagram of solid nitrogen and can help experimentalists on their task in trying to realize the potential of these materials.

Literature

1. Eremets et at., Nature Mater. 558, **3,** 2004
2. McMahan and LeSar, Phys. Rev. Lett. 1929, **54,** 1985

3. Mailhiot et al., Phys. Rev. B 14419, **46**,1992

4. Oganov and Glass, J. Chem. Phys. 244704, **126**, 2006

5. J. Kotakoski and K. Albe, *First-principles calculations on solid nitrogen: A comparative study of high-pressure phases*, Rev. B 144109, **77,** 2008

4.3.26 Defect chemistry of transparent conducting oxides: Oxygen interstitial defects in zinc oxide

Paul Erhart and Karsten Albe
Fachgebiet Materialmodellierung, FB 11, Material- und Geowissenschaften,
Petersenstr 23, D-64287 Darmstadt, e-mail: albe@mm.tu-darmstadt.de

Zinc oxide is a transparent semiconductor with a direct bandgap of 3.4 eV. It can be doped degenerately n-type and free electron concentrations in excess of 10^{21} cm^{-3} can be reached. In the last couple of years p-type doping of zinc oxide has been reported by a number of groups. Ambipolar dopability in conjunction with its high exciton binding energy render ZnO a highly interesting material for transparent electronics and blue light emitting devices. Often ambipolar dopability of wide bandgap materials is impeded by self-compensation which is related to the dependence of the defect formation enthalpies on the position of the Fermi level. In that case adding dopants will not lead to the generation of free carriers but to the generation of compensating defects such as in insulators. In order to achieve p-type conductivity in zinc oxide, however, the Fermi level needs to be close to the valence band whose energy is $>\tilde{}7.0$ eV below the vacuum level as determined by photoelectron spectroscopy. Taking 4.5 eV as reference for the standard hydrogen electrode on an absolute energy scale, a Fermi level position at the valence band maximum corresponds to a redox potential of $>\tilde{}2.5$ eV. Chemically such large redox potentials will lead to oxidation of the oxygen atoms, which implies changing the oxidation state from O^{2-} to O^{-} or even further to O^{0}. Under such conditions nominally ${O^{2-}}_2$ ions might occupy O^{2-} lattice sites as in zinc peroxide ZnO_2. Hitherto, to the best of our knowledge such a peroxo-like defect structure has not been considered in the literature of zinc oxide. Nevertheless we anticipate this defect to play a key role in the defect physics of this material.

In order to test our proposition, we have conducted a detailed analysis of the geometry and the electronic structure of several oxygen interstitial configurations in zinc oxide based on density functional theory (DFT) calculations within the local density approximation (LDA). In order to identify the most stable structure for the oxygen interstitial defect, we have generated a number of initial configurations. The atomic positions were then relaxed using conjugated-gradient minimization.

For neutral and positive charge states we find a "dumbbell"-like configuration to be signifcantly more stable than any of the high-symmetry configurations considered previously. In fact, our calculations suggest that oxygen interstitials are abundant defects under oxygen-rich conditions when the Fermi level is relatively close to the valence band maximum.

The dumbbell geometry is characterized by two oxygen atoms sharing to equal parts a regular oxygen lattice site and forming a rather strong bond. The interstitial configuration is shown in Fig. 26.1 Its geometry changes only slightly as the charge state varies between $2+$ and $2-$. The accumulation of electron density between the oxygen atoms is indicative for covalent bonding opposed to the predominantly ionic character of the oxygen-zinc bonds. The analysis of the net charges using the schemes due to Bader and Hirshfeld suggests that as the charge state changes from 0 to $2+$ the surplus charge is compensated virtually exclusively by the two oxygen atoms. The partial charges of second and farther neighbors do not display any significant deviation from their ideal bulk values. We infer that the oxygen-oxygen bond is the major reason for the remarkable capability of this defect to

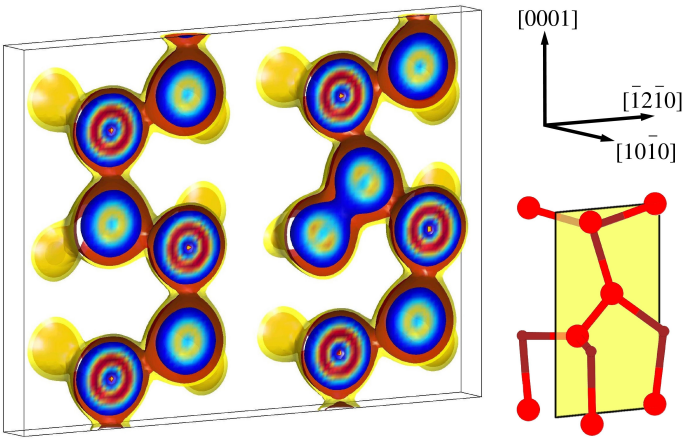

Abbildung 26.1: *Geometry and electron density of the dumbbell interstitial configuration. The electron density isosurface plot shows a cut parallel to the (10-10) plane. The figure demonstrates the strong covalent bond between the two oxygen atoms of the dumbbell.*

compensate positive surplus charges and is therefore accountable for the low formation energies of the neutral and positive charge states.

For negative charge states a different equilibrium geometry is observed. The configuration can be considered as two interstitial oxygen atoms associated with one oxygen vacancy. Each oxygen atom is bonded to four zinc atoms but no oxygen-oxygen bond is formed. The Bader and Hirshfeld analyses yield further insight. For the $2-$ and $1-$ charge states the net charge on each oxygen atom of the defect pair is equivalent to an oxygen atom on an ideal lattice site.

In summary, we have carried out DFT calculations on oxygen interstitials and identified two configuratons with particular low formation energies under oxygen-rich conditions. For the negative charge states one observes a tendency of the system to minimize oxygen-oxygen interactions accompanied by a preference for oxygen-zinc bonding while the opposite behavior occurs for positive charge states which favor oxygen-oxygen bonding. The latter behavior is related to the ability of the oxygen-oxygen bond to compensate positive surplus charges. The dumbbell interstitial defect actually displays to a certain extent the per-oxo-like behavior anticipated in the introduction.

Acknowledgement

We acknowledge financial support through the Collaborative Research Center (SFB) 595 of the DFG.

Literature

1. P. Erhart, N. Juslin, O. Goy, K. Nordlund, R. Müller, K. Albe, *Analytic bond-order potential for atomistic simulations of zinc oxide*, J. Phys.: Cond. Matter 8565-6605, **18**, 2006

2. P. Erhart, K. Albe, *Diffusion of zinc vacancies and interstitials in zinc oxide,* Appl. Phys. Lett. 201918**, 88,** 2006

3. P. Erhart, K. Albe, A. Klein, *First-principles study of intrinsic point defects in ZnO: Role of band structure, volume relaxation and finite size effects,* Phys. Rev. B 205203, **73**, 2006 Download

4. P. Erhart, K. Albe, *First-principles study of migration mechanisms and diffusion of oxygen in zinc oxide,* Phys. Rev. B 115207, **73**, 2006

5. Erhart, A. Klein, R.G. Egdell, K. Albe, *Band structure of indium oxide: Indirect versus direct band gap,* Phys. Rev. B 153205, **75**, 2007

4.3.27 Structural stability of multiply twinned FePt nanoparticles

Michael Müller, Karsten Albe
Fachgebiet Materialmodellierung, FB 11, Material- und Geowissenschaften,
Petersenstr 23, D-64287 Darmstadt, e-mail: albe@mm.tu-darmstadt.de

The prospect of realizing magnetic nanoparticles that can be applied in high-density recording or medical applications has driven a large number of research activities in recent years. Among all candidate materials FePt in the face centered tetragonal $L1_0$ phase has attracted much attention. This structure is characterized by alternating Fe and Pt layers in c-direction and possesses a high uniaxial magneto-crystalline anisotropy energy (MAE). Because of the high MAE, single crystalline FePt nanoparticles with a diameter as small as 4 nm can maintain a stable magnetization direction on a time scale of 10 years. When prepared by gas-phase synthesis processes, however, no single crystalline FePt particles are obtained. Instead, multiply twinned shapes in the form of icosahedral or decahedral particles are predominant. In order to understand the occurrence of the different structural motives, a detailed knowledge of the energetics of FePt particles in the various conformations is necessary. In our work we investigated the structural stability of FePt nanoparticles by atomic scale and continuum model calculations.

In conjunction with a recently developed interatomic FePt potential, the molecular statics method has been applied for calculating the fully relaxed energy of FePt nanoparticles in single crystalline, multiply twinned icosahedral and multiply twinned decahedral morphologies. The particle energy as a function of size is shown in Fig. 27.1. In general, even for the smallest particle sizes studied, the single crystalline shapes are energetically favored over multiply twinned particles by at least 10 meV/atom. Also, icosahedral particles exhibit a much higher energy than decahedral ones because of their higher internal strain and larger twin boundary areas. The large energy differences between single crystalline particles on the one hand and icosahedral and decahedral particles on the other hand, however, can mainly be attributed to a large twin boundary energy predicted by the interatomic potential. Compared to electronic structure calculations, an overestimation of the twin boundary energy by a factor of two is possible.

In order to assess the influence of the uncertainty of the twin boundary energy, a more versatile continuum description of particle energies has been employed. In this continuum model, the energy of a nanoparticle is approximated by the sum of volume, surface and twin boundary energy terms:

$$E(N)=\mathrm{N}\,(E_c+\mathrm{W})+\mathrm{A_{twin}}(N)\gamma_{\mathrm{twin}}+\sum_{\mathrm{hkl}}A_{\mathrm{hkl}}(N)\gamma_{\mathrm{hkl}}. \quad (1)$$

Here, E_c is the cohesive energy per atom in the bulk phase and W is an average strain energy per atom, which is zero for single crystalline particles. A_{twin} and γ_{twin} denote the twin boundary area and its energy. Furthermore, A_{hkl} and γ_{hkl} denote the total area and energies of the *hkl* facets terminating the particle surface. For validating the continuum model, its predictions on particle energies when provided with materials parameters from the interatomic potential are compared with the atomistic calculations in Fig. 27.1, where an excellent agreement is found.

By varying the surface and twin boundary energies, Eq. (1) has now been used for evaluating the boundaries between stability domains of decahedral, icosahedral and single crystalline particles as is shown in Fig. 27.2.

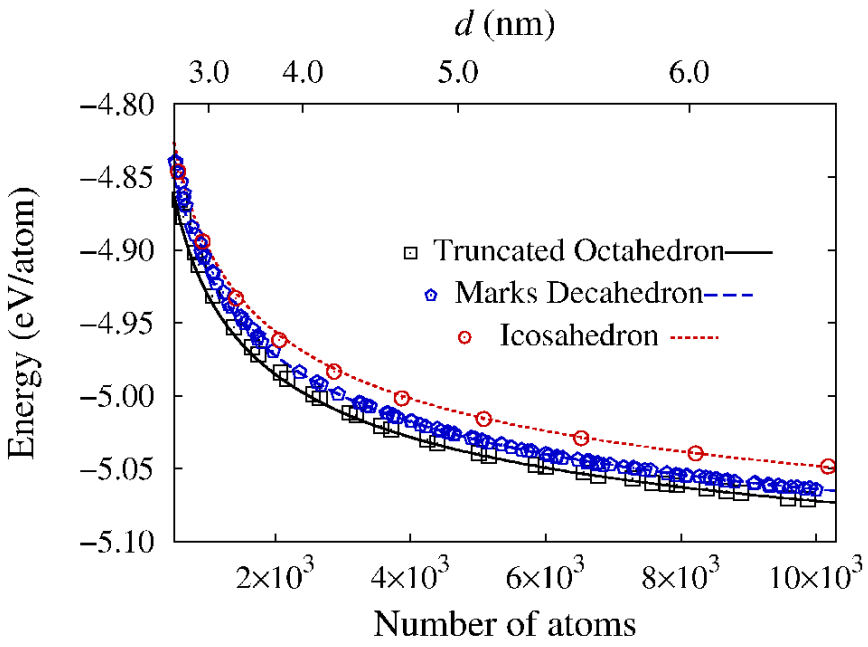

Abbildung 27.1: *Average potential energy for FePt nanoparticles in different morphologies. Data points denote molecular statics calculations, curves are predictions of the continuum model Eq. (1).*

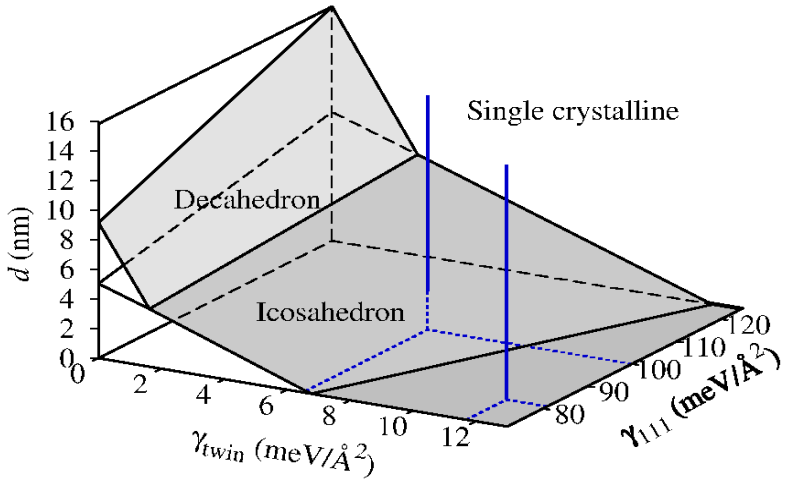

Abbildung 27.2: *Stability of FePt particles in multiply twinned and single crystalline morphologies as obtained from Eq. (1) by varying surface and twin boundary energies. The vertical lines indicate surface and twin boundary energies predicted by the interatomic potential used in Fig. 1 and values estimated on the basis of first principles calculations.*

For estimating which set of surface and twin boundary energies best describes reality, reference values from first principles calculations have been considered, which amount to 100 meV/Å^2 and 6.5 meV/Å^2, respectively. For this set of energies, Fig. 2 reveals that icosahedral particles are stable up to a diameter of 2.6 nm.

The calculations on particle energies provide a reasonable explanation for the predominance of icosahedral FePt nanoparticles prepared by inert gas condensation. Since icosahedral particles are energetically most stable for small sizes below 2.6 nm, it is likely that icosahedral seeds evolve during the nucleation stage of inert gas condensation. When growing further, kinetic trapping of the particles in the metastable morphology can then lead to the presence of icosahedral particles even at larger sizes.

Literature

1. Müller, K. Albe, *Structural stability of multiply twinned FePt nanoparticles*, Acta Mat. 6617-6626, **55**, 2007

2. M. Müller, P. Erhart, K. Albe, *Thermodynamics of $L1_0$ ordering in FePt nanoparticles studied by Monte Carlo simulations based on an analytic bond-order potential,* Phys. Rev. B 155412, **76,** 2007

3. M. Müller, K. Albe, *Lattice Monte Carlo simulations of FePt nanoparticles: Influence of size, composition, and surface segregation on order-disorder phenomena,* Phys. Rev. B 094203, **72,** 2005

4.3.28 Phase diagram of the Pt-Rh alloy studied with a refined BOS mixing model

Johan Pohl and Karsten Albe
Fachgebiet Materialmodellierung, FB 11, Material- und Geowissenschaften,
Petersenstr 23, D-64287 Darmstadt, e-mail: albe@mm.tu-darmstadt.de

The Pt-Rh alloy is used in automotive exhaust gas converters as a three-way catalyst. It has attractedttracted much attention from the scientific community due to its catalytic applications. But although many studies have been performed on the bulk, surface and nanoparticulate properties of this alloy, some features still remain puzzling. An answer to the question whether Pt-Rh phase separates or not could only recently be given. The phase diagram commonly given in phase diagram collections for Pt-Rh is wrong (see for example [1]). It shows a miscibility gap and gives a critical temperature of 1033K. This phase diagram is based on a prediction by E. Raub [2] dating back to 1959. He inferred from the experimentally confirmed phase separation in Ir-Pt, Ir-Pd and Pd-Rh, that Pt-Rh would also phase separate. The critical temperature was estimated from the difference in the melting points of the two constituents. Although the phase diagram was reprinted many times since, a miscibility gap has never been observed in experiment. Recent ab-inito density functional theory (DFT) studies [3] indicate that Pt-Rh does not phase separate, but that various ordered compounds form at temperatures below 300K. These studies have been corroborated by experimental results using diffuse x-ray scattering in order to measure the amount of short-range order present in the alloy at a temperature as high as 923K [4].

Although it is possible to map out the phase diagram from the formation energies calculated by DFT, it can not be considered a standard method. A new phase diagram for Pt-Rh that incorporates the findings of the last 10 years has not been available so far. Therefore, we developed a new theoretical model based on the bond-order simulation (BOS) mixing model for Metropolis Monte-Carlo simulations, which, in conjunction with thermodynamic integration in the grand-canonical ensemble, enables us to calculate the total free energy of any binary alloy including the configurational part of the entropy. Our approach allows for a fast and easy calculation of the bulk phase diagram. The calculated phase diagram for Pt-Rh is shown in Fig. 28.1.

Our model can be described as follows: Each atom on a fixed lattice site i will be given a site energy $\varepsilon_{Z_i}^{T_i}\left(M_i^{(n)}\right)$ depending on the type of atom T_i, its total coordination Z_i and its number of unequal first to fourth nearest neighbors $M_i^{(n)}$ (n=1,...,4). From the total energy of the sytem, which is just the sum of the site energies over all sites $\mathrm{E}=\sum_i \varepsilon_{Z_i}^{T_i}\left(M_i^{(n)}\right)$, the energy differences of two configurations needed for Metropolis Monte-Carlo simulations can be calculated. The expression for the site energies of A and B type atoms is

$$\varepsilon_Z^A\left(M_n\right) = \varepsilon_Z^A + \tfrac{1}{2}\sum_{\mathrm{n}=1}^{4} M_n \Delta \mathrm{E}_{(n)}^{\mathrm{AB}} + \tfrac{1}{2} M_1\left(M_1 - 1\right)\lambda^A$$

$$\varepsilon_Z^B\left(M_n\right) = \varepsilon_Z^B + \tfrac{1}{2}\sum_{\mathrm{n}=1}^{4} M_n \Delta \mathrm{E}_{(n)}^{\mathrm{AB}} + \tfrac{1}{2} M_1\left(M_1 - 1\right)\lambda^B$$

Our model thus involves 6 mixing parameters $\Delta \mathrm{E}_{(n)}^{\mathrm{AB}}$ with n=1,...,4 , λ^A and λ^B. These parameters are sufficient for all bulk calculations in which no under-coordinated atoms are

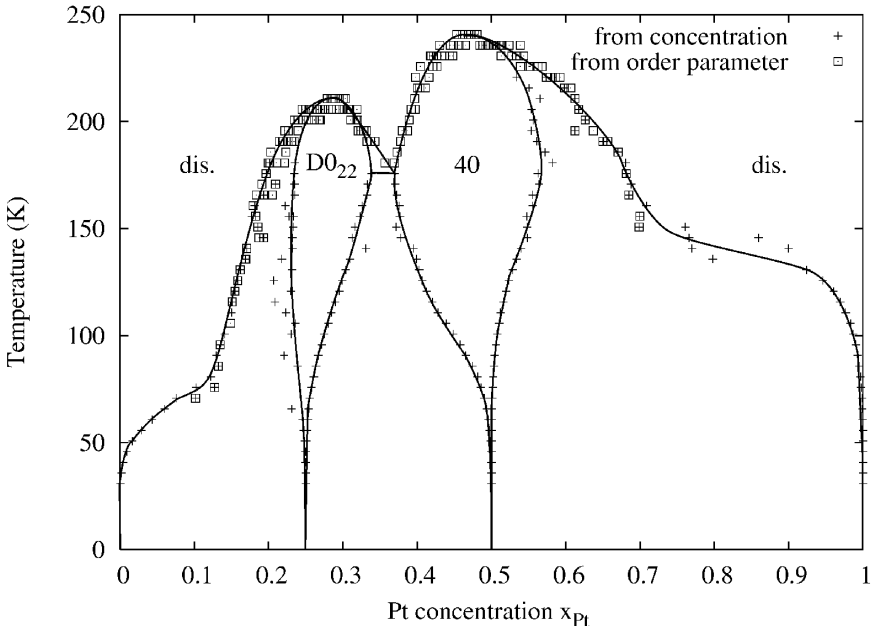

Abbildung 28.1: *The phase diagram of Pt-Rh based on our calculations, the 40 and $D0_{22}$ structures are the stable compounds that are found at low temperatures, above 240K there are no stable ordered structures, no miscibility gap is present in the system [8].*

present. In this case the site-energy constants ε_Z^A and ε_Z^B, that depend only on total nearest neighbor coordination, can be set to zero. In any other case we have to make us of these constants in order to model for example the surface energy of surfaces with different coordination. In case of modelling particles we have to make use of a complete set of site energy constants. In case of a face-centered cubic parent lattice we would need to fix 12 site energy constants (Z=1,...,12) for A and B type atoms correspondingly.

In order to map out the complete free energy surface of an alloy, we applied the thermodynamic integration method using Monte Carlo simulations in the semi-grand canonical ensemble. This method was proposed by van de Walle et al. [5]. In the semi-grand canonical ensemble the total number of atoms is fixed, while the difference between the number of A and B type atoms is allowed to fluctuate. The method provides us with an accurate calculation of the thermodynamic potential surface as well as the free energy surface, dependent on temperature and on the concentration.

It is possible to deduce the temperature-composition phase diagram from the calculated free energy surface. However, it is more convenient to calculate it from the discontinuities of the order parameter and of the concentration. This approach was followed when calculating the phase diagram of Pt-Rh presented in illustration 1.

In addition, we examined the short range order of Pt-Rh at high temperatures applying our model in canonical Monte Carlo simulations. Agreement with experiments performed at 923K [4] was obtained for the Warren-Cowley short range order parameters up to sixth nearest neighbors.

Literature

1. T. Massalski, Binary Alloy Phase Diagrams (ASM, International, Materials Park, Ohio) 1990
2. E. Raub, J. Less-Common Met 1, 3 (1959)
3. Z. Lu, B. Klein and A. Zunger, J. Phase Equilib. 16, 36 (1995)
4. C. Steiner et al., Phys. Rev. B 71, 104204 (2005)
5. A. van de Walle and M. Asta, Modelling Simul. Mater. Sci. Eng. 10, 521 (2002)
6. L.Zhu and A. DePristo, J. Chem. Phys. 102, 5342 (1995)

1. A. Kohan, P. Tepesch, G. Ceder and C. Wolverton, Comp. Mat. Sci. 9, 389 (1998)
2. J. Pohl, K. Albe, submitted to Acta Materialia

4.3.29 Molecular dynamics simulation of deformation mechanisms in nanocrystalline fcc metals

Yvonne Ritter, Alexander Stukowski, Karsten Albe
Fachgebiet Materialmodellierung, FB 11, Material- und Geowissenschaften,
Petersenstr 23, D-64287 Darmstadt, e-mail: albe@mm.tu-darmstadt.de

Materials with a grain size of less than 100nm exhibit unique mechanical properties: nanocrystalline (nc) metals are characterized by an extraordinary strength and the occurrence of superplasticity; enhanced ductility is found for ceramics at nano grain sizes and nc-coatings stand out due to highly improved wear, friction and corrosion behavior. The outstanding mechanical properties found for nc metals are a result of the mechanisms relevant for plastic deformation at small grain sizes, which fundamentally differ from those present in coarse grained metals. Plastic deformation of nanostructured metals is thought to arise from the intricate interplay between dislocation and grain boundary (GB) processes. The underlying concepts and fundamental mechanisms of this complex interplay, however, have still not been fully exposed [1], although nc metals have been studied intensively since the synthesis of the first nc metals in bulk form about 20 years ago [2]. The interest in the mechanical properties of nc metals has been highly increasing over the last years, which is as well attributed to the enhanced computer performance allowing more and more realistic numerical models. In the past, molecular dynamics (MD) simulations lead to substantial progresses in understanding plastic deformation of nc metals [3].

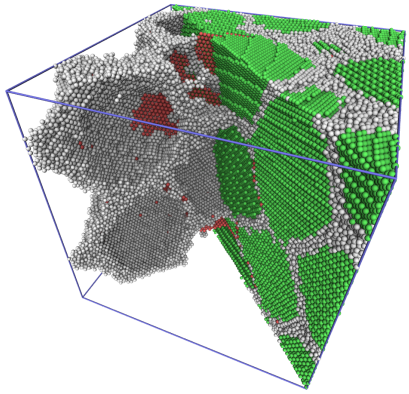

Abbildung 29.1: *Nanocrystalline model structure generated by Voronoi tesselation.*

In this study we investigated the plastic deformation of nc materials by MD simulations using bicrystal models of face centered cubic (fcc) metals (Al and Cu) containing different high angle CSL (coincidence site lattice)-boundaries.Grain boundary sliding, induced by an applied shear deformation with a constant strain rate, has been shown to occur by the cooperative movement of all GB atoms for a $\Sigma 7$ (111) twist boundary. The barriers for the process were found to be rather high, a sliding mechanism carried by intrinsic GB dislocations, however, appeared to be even less favorable for the system. The relative movement of the two grains was observed to occur on different paths resulting in different sliding barriers (see Fig. 29.2). Furthermore it has been shown that, depending on the stacking fault energy, the GB slides from one distinct minimum energy to another (like for Al with a high SF energy), or the GB slides over a smooth energy hypersurface with several local minima (like for Cu with a low SF energy). For a $\Sigma 33$ (225) tilt boundary with a dissociated boundary structure, GB sliding has not been observed. Instead intrinsic stacking fault facets were found to be emitted from the boundary, when the bicrystals were exposed to a shear deformation. When the ISF facets reached their maximum elongation, stress-induced grain growth occurred. The atomistic mechanisms during the dissociation process

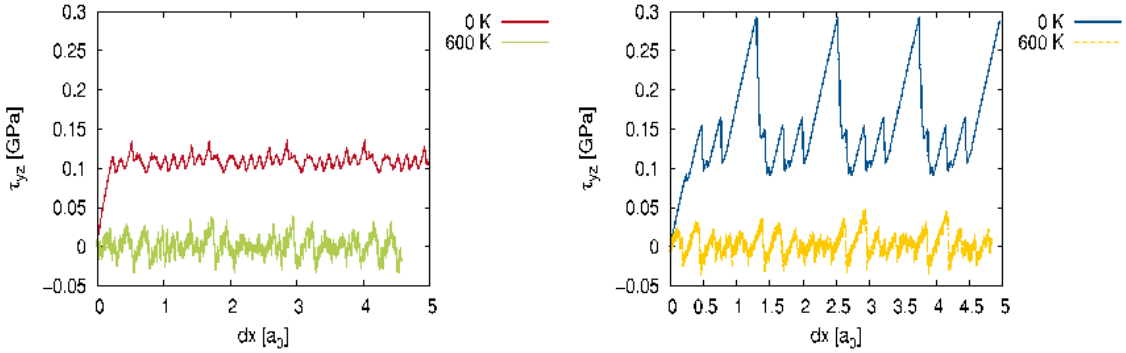

Abbildung 29.2: *Stick-slip character of GB sliding for (left) Cu and (right) Al bicrystals containing a Σ7 (111) twist boundary.*

and the structural changes in the interface due to the shear deformation were monitored and the influence of the SF energy was analyzed. When subjected to a tensile deformation, a statistical dislocation nucleation process was found for the Σ7 (111) twist boundary. The effect of thermal activation has been investigated and the nucleation mechanism has been studied on an atomic scale. It has been found, that Shockley partial dislocations were emitted from the boundary on the (11-1), (1-11) and (-111) slip planes building tetrahedra of stacking faults (see Fig. 4.3.29).

The emission of partial dislocations has been observed for the Σ33(225) interface as well, the nucleation sites, however, were not occurring randomly. The structural units within the interface due to the GB dissociation served as preferred locations for the emission of dislocations. Hence, the stresses required for the nucleation of the first partial dislocation were found to be lower than for the Σ 7 boundary.

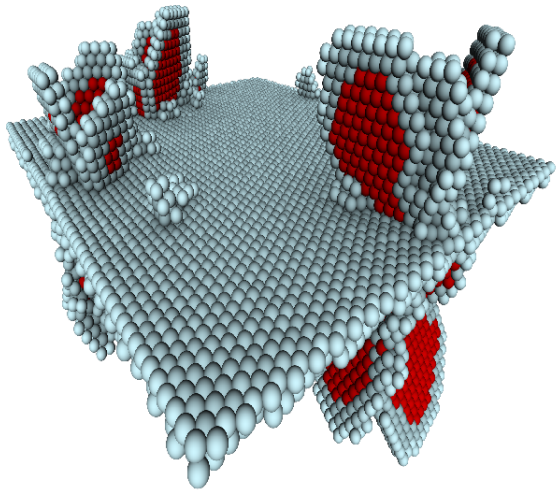

Abbildung 29.3: *Dislocation nucleation at a Σ (111) copper bicrystal interface under tensile deformation; Atoms in an fcc environment are deleted, black = hcp environment, grey = unordered environment.*

Acknowledgements

This work is supported by DFG-Forschergruppe 714 “Plasticity of nanocrystalline metals and alloys”

Literature

1. Yamakov, D. Wolf, S. R. Phillpot et al., Nature Materials, 45-48, **1,** 2002
2. D. Wolf, V. Yamakov, S. R. Phillpot et al., Acta Mat., 1-40, **53,** 2005
3. D. E. Spearot, K. I. Jacob and D. L. McDowell, Acta Mat., 3579-3589, **53,** 2005
4. A. Stukowski, J. Markmann, J. Weißmüller, K. Albe, Acta Mat., i*n print*

4.4 Mathematik & Informatik

4.4.1 Hierarchische Steuerung und gemischt-ganzzahlige Optimierung hybrider, diskret-kontinuierlicher nichtlinearer dynamischer Systeme

P. Bales, B. Geißler, O. Kolb, J. Lang, A. Martin, A. Morsi
Technische Universität Darmstadt, Fachbereich Mathematik

In diesem Forschungsprojekt werden vernetzte Transportsysteme am Beispiel von Flussproblemen in Gasnetzwerken im Rahmen einer Theorie der hierarchischen Steuerung und gemischt-ganzzahligen Optimierung hybrider, diskret-kontinuierlicher nichtlinearer dynamischer Systeme modelliert, analysiert, simuliert und optimiert. Die Beschäftigung mit Gasnetzwerken ist zum einen durch konkrete aktuelle Problemstellungen in der Industrie und zum anderen durch den exemplarischen Charakter der zugrundeliegenden Problemstruktur motiviert. Es ergeben sich dabei Strukturanalogien zu anderen Anwendungskontexten wie etwa die optimale Steuerung von Bewässerungs- und Abwassersystemen, Straßenverkehrsnetzen und vernetzten Servicesystemen. Auf der Modellebene führt die Betrachtung vernetzter Systeme auf eine Graphenstruktur. Die Dynamik auf dem Graphen wird durch eine Hierarchie lokaler Dynamiken (gewöhnliche und partielle Differentialgleichungen) auf den Kanten und Transmissionsbedingungen an den Knoten beherrscht. Die Dynamik wird mittels Entscheidungsvariablen und kontinuierlichen Steuerungen gemäß einer Zielfunktion optimiert. Die Entscheidungsvariablen werden im Zuge der kombinatorischen gemischt-ganzzahligen Optimierung auf den Knoten ermittelt, sodann wird die Dynamik auf der durch die Wahl der Entscheidungsparameter festgelegten Steuerungsstruktur einer lokalen Optimierung und numerischen Simulation unterzogen, deren Ergebnis im Rückfluss als Korrektor verwendet wird. Das globale Optimierungs- und Steuerungsproblem wird durch eine Hierarchisierung von kombinatorischen und kontinuierlichen Ansätzen gelöst.
Bereits bei in der Praxis auftretenden Netzen moderater Größe ergeben sich Optimierungsprobleme mit Hunderttausenden von Variablen und Nebenbedingungen, deren Lösung den Einsatz von Hochleistungsrechnern erfordert.

4.4.2 Computer Vision with Probabilistic Methods

Christian Wojek, Paul Schnitzspan, Mario Fritz, Bernt Schiele
Multimodal Interactive Systems, Computer Science Department, TU Darmstadt

Object detection and scene understanding are among the most fundamental problems in computer vision. In recent years significant progress has been achieved and several successful methods for object detection and scene understanding have emerged. Applications such as autonomous driving, driving assistance, robotics and image retrieval will benefit from this branch of research. Currently, our research group is at the forefront of this research area further advancing the state of the art.

Common to many of the most successful and in particular to our methods are the application of probabilistic modeling and inference mechanisms. Those typically consist of a two-stage process. While in the first stage models are learned from a feature representation of training images, the second step applies those models to unknown test images. Both steps are computationally highly demanding but for different reasons.

During model training an optimization problem in a high dimensional feature space has to be solved. Feature space representations up to several thousand dimensions are common and require (depending on the probabilistic model) lot of computational resources to solve the optimization problem and also to calculate features. In many cases parameter choices are non-trivial and require systematically exploring the space of possible settings.

Also the testing step is computational demanding. Today's benchmarking databases often consist of several thousands images and they are widely used by the research community to compare different methods. Even though the computation per image is not too demanding and might be even in the order of several seconds per image the size of the databases makes the evaluation of our models computationally intensive.

In 2008 we have worked on problems of dynamic scene recognition and object detection and published our work in national and international conferences. In computer vision there exist three major international conferences (CVPR, ICCV, ECCV) with highly competitive acceptance rates. Three of the four publications mentioned here are published at those events (ECCV, CVPR).

In [1] conditional random fields (CRF) were successfully applied to the problem of scene segmentation. Here, we used wavelet features together with a boosting classifier in order to obtain an initial segmentation of images, which were taken from a driving car. Using these initial segmentation together with an object detector (developed in [2]) as input for a CRF we were able to refine the results in a novel graphical model. Figure 2.1 shows some sample detections and a sample segmentation.

Abbildung 2.1: *Scene segmentation in an automotive domain [1]*

Also we have explored the direct application of CRFs to object detection. In [3] we worked on a hierarchical formulation of CRFs that combines local and global image information. It exploits recent HOG features, which are computed from 2D image gradients and represent objects as histograms of gradients. Figure 2.2 shows the hierarchical model applied to the class of motorbikes.

Abbildung 2.2: *Hierarchical CRF for object detection of [3] and sample application to motorbikes*

In [4] we explored topic models for applications in image classification, for re-ranking of image search results (by Google image search) and also for object detection. Those models are in particular interesting as they allow a very compact object representation and thus very few training instances are required. Figure 2.3 shows visual topics of a bicycle with a histograms of gradient feature representation.

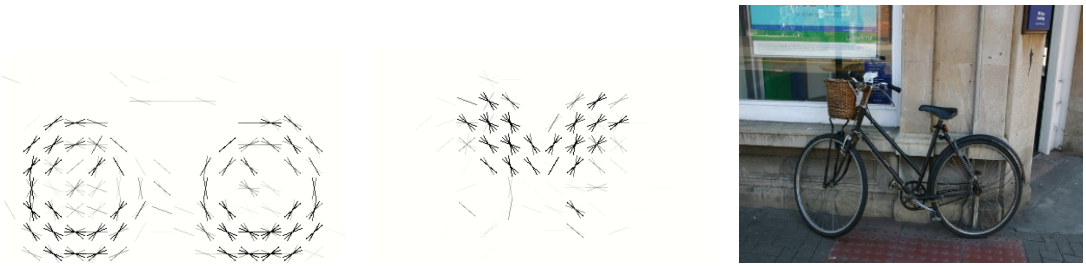

Abbildung 2.3: *Two visual topics learned from training data and sample image to be classified*

All applied methods heavily relied on the availability of computational resources at CSC Frankfurt to exploit a large number of possible configurations of features and models. For future work we would like to use multiple combinations of features in conjunction with more elaborate and realistic models. Both, additional features and new probabilistic models will require the availability of sufficient computing power and recent computer hardware.

References

[1] Christian Wojek and Bernt Schiele: *A Dynamic Conditional Random Field Model for Joint Labeling of Object and Scene Classes* in European Conference on Computer Vision (ECCV 2008), Oct. 13-16 2008, Marseille, France, 2008

[2] Christian Wojek and Bernt Schiele: *A Performance Evaluation of Single and Multi-Feature People Detection* in 30th DAGM Symposium (DAGM 2008), June 9-13 2008, Munich, Germany, 2008

[3] Paul Schnitzspan, Mario Fritz and Bernt Schiele: *Hierarchical Support Vector Random Fields: Joint Training to Combine Local and Global Features* in European Conference on Computer Vision (ECCV 2008), Oct. 13-16 2008, Marseille, France, 2008

[4] Mario Fritz and Bernt Schiele: *Decomposition, Discovery and Detection of Visual Categories Using Topic Models* in IEEE Conference on Computer Vision and Pattern Recognition (CVPR 2008), June 24-26 2008, Anchorage, USA, 2008

4.5 Sonstige

4.5.1 Epileptogenesis due to glia-mediated synaptic scaling

Cristina Savin, Jochen Triesch and Michael Meyer-Hermann
Frankfurt Institute for Advanced Studies

Homeostatic regulation of neuronal activity is fundamental for stable functioning of the cerebral cortex. One form of homeostatic synaptic scaling was recently shown to be mediated by glial cells that interact with neurons through the diffusible messenger TNF-alpha. Interestingly, TNF-alpha is also used by the immune system as a pro-inflammatory messenger, suggesting potential interactions between immune system signalling and the homeostatic regulation of neuronal activity.

We have developed a first computational model of neuron-glia interaction by TNF-alpha mediated synaptic scaling. The model shows how under normal conditions the homeostatic mechanism is effective in balancing network activity. After chronic immune activation or TNF-alpha overexpression by glia, however, the network develops seizure-like activity patterns. This may explain why under certain conditions brain inflammation increases the risk of seizures. Additionally, the model shows that TNF-alpha diffusion may be responsible for epileptogenesis after localised brain lesions.

References:

1. Savin, C., Triesch, J. and Meyer-Hermann, M., *Epileptogenesis due to Glia-Mediated Synaptic Scaling,* Journal of the Royal Society Interface (*in press*), 2008.

2. Savin, C., Triesch, J. and Meyer-Hermann, M., *A computational model of glia-mediated seizure induction,* In Proc. Workshop on Seizure Prediction, Freiburg, 2007.

3. Savin, C., Triesch, J. and Meyer-Hermann, M., *Seizure Induction by Glia-Mediated Synaptic Scaling,* Cosyne, Salt Lake City, USA, February 2007.

4.5.2 Global water resources in a changing world

Petra Döll
AG Hydrologie, Institut für Physische Geographie, Goethe-Universität Frankfurt

To achieve a sustainable development of the planet Earth, water resources need to be managed well. This requires an assessment of the current water situation, an understanding of historic developments and the generation of scenarios of the future. A global-scale freshwater assessment helps to understand the global water system and how it is impacted by humans, as in a globalized world, freshwater assessments can no longer be restricted to the river basin scale.

To support these tasks, we have developed the global-scale water model WaterGAP that computes both water resources and water use with a spatial resolution of 0.5° x 0.5° (55 km at the equator). WaterGAP has recently been improved with respect to lateral flow velocities and the storage dynamics of man-made reservoirs. Together with new data sets, including data on the Earth's dynamic gravity field, precipitation, reservoirs and land use, new analyses regarding certain aspects of the global water system have been performed. These include the alteration of natural river flow regimes by human water withdrawals and reservoir construction, with its impacts on aquatic ecosystems. Another focus is the assessment of the impact of climate change on water resources. The figure below shows, as an example, the possible impact of climate change on groundwater resources (This figure was included in the Fourth Assessment Report of the IPCC, Kundzewicz et al., 2007).

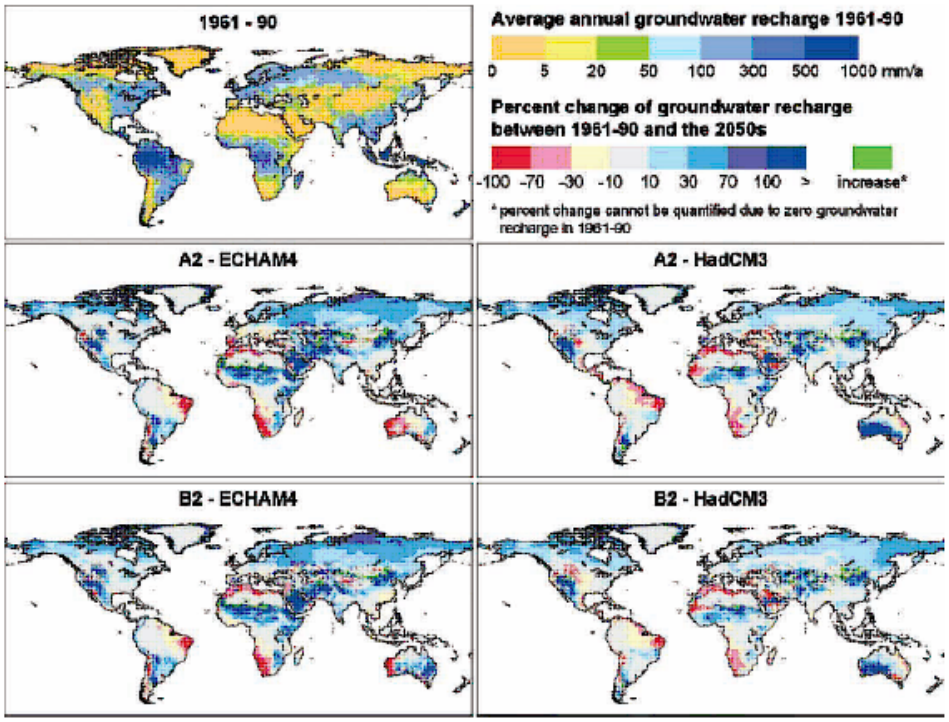

Figure 3.5. *Simulated impact of climate change on long-term average annual diffuse groundwater recharge. Percentage changes of 30 year averages groundwater recharge between present-day (1961 to 1990) and the 2050s (2041 to 2070), as computed by the global hydrological model WGHM, applying four different climate change scenarios (climate scenarios computed by the climate models ECHAM4 and HadCM3), each interpreting the two IPCC greenhouse gas emissions scenarios A2 and B2 (Döll and Flörke, 2005).*

To better understand the link between food and water, water use for the production of crops was computed, with a spatial resolution of 5 arc-minutes (8 km at the equator), using the new Global Crop Water Model. To achieve reliable modelling results, we developed a land use data set that differentiates 26 irrigated and rainfed crop types. This allowed, for the first time, to differentiate the use of blue water (irrigation water) from the use of green water (precipitation) (see figure below).

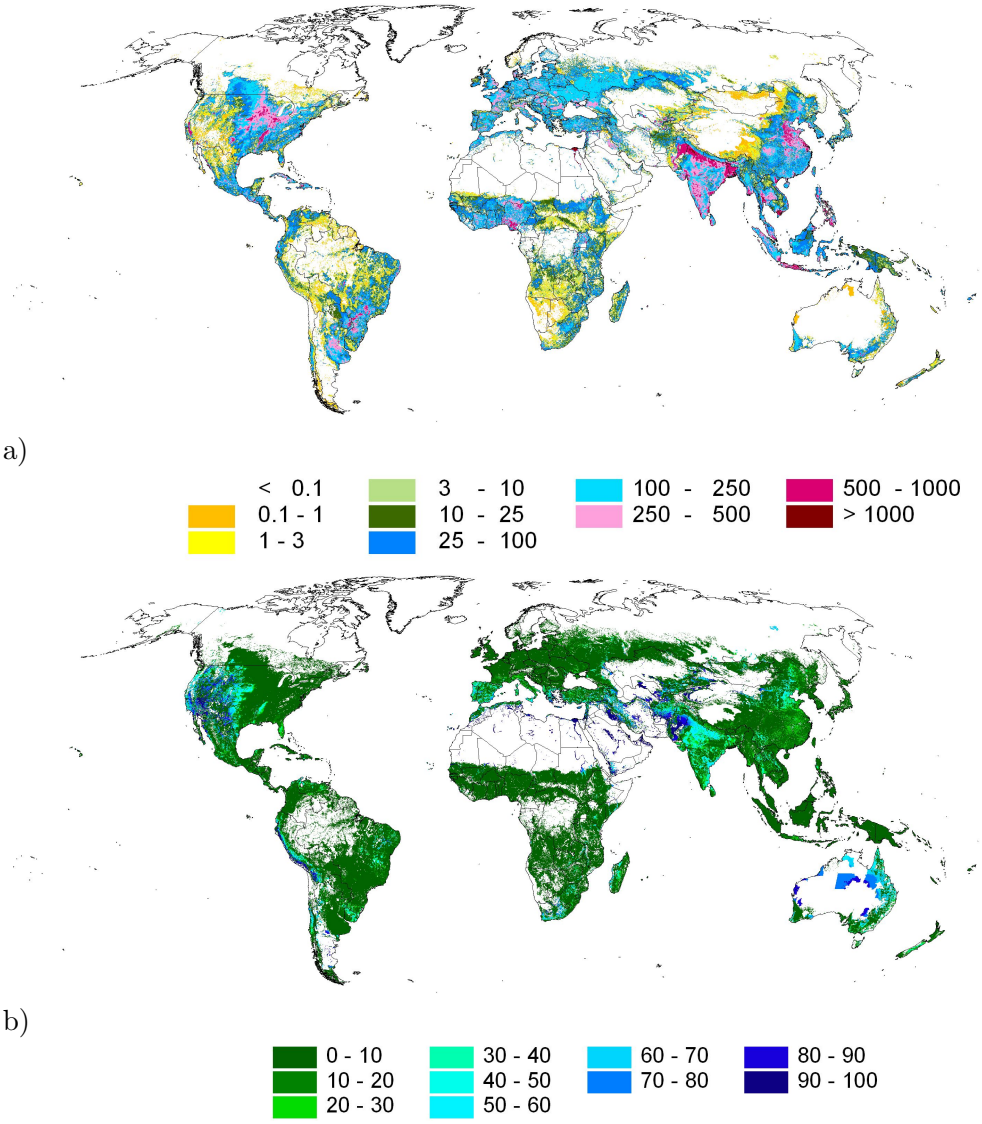

Abbildung 2.1: *Consumptive water use for crop production around 2000. a) Total water use, in mm/a, b) fraction of blue (irrigation) water, in %.*

References

Kundzewicz, Z.W., L.J. Mata, N.W. Arnell, P. Döll, P. Kabat, B. Jiménez, K.A. Miller, T. Oki, Z. Sen and I.A. Shiklomanov (2007): Freshwater resources and their management. Climate Change 2007: Impacts, Adaptation and Vulnerability. Contribution of Working Group II to the Fourth Assessment Report of the Intergovernmental Panel on Climate

Change, M.L. Parry, O.F. Canziani, J.P. Palutikof, P.J. van der Linden and C.E. Hanson, Eds., Cambridge University Press, Cambridge, UK, 173-210.

4.5.3 Regional climate projections in different regions of the world

Bodo Ahrens, Andreas Dobler, Steffen Kothe
Institut für Atmosphäre und Umwelt, Goethe-Universität Frankfurt

Simulations from current global circulation models (GCMs) feature a grid resolution of about 200km and a downscaling to a grid resolution of 50km or less is necessary to assess regional patterns. These are for instance important for investigations on climate predictions of the water balance of regional watersheds or of heavy precipitation changes.

Using the regional climate model CLM (see http://www.clm-comunity.eu), a regionalization is carried out in different areas of the world. Through the application in different climate regions, uncertainties in the model system can be better identified and the adaptability of the projections can be increased. For the EC-Project BRAHMATWINN regional climate simulations have been carried out in a South Asian and a European domain as shown in Figs. 1 and 2. These simulations are carried for the time periods 1960-2100. The IPCC SRES scenarios A1B, A2, B1, Commitment as well as 20th century control runs have been simulated. Currently an additional target domain in Western Africa is planned. All these climate model runs require a high amount of computational resources which can only be provided by high-performance computing centers such as the CSC.

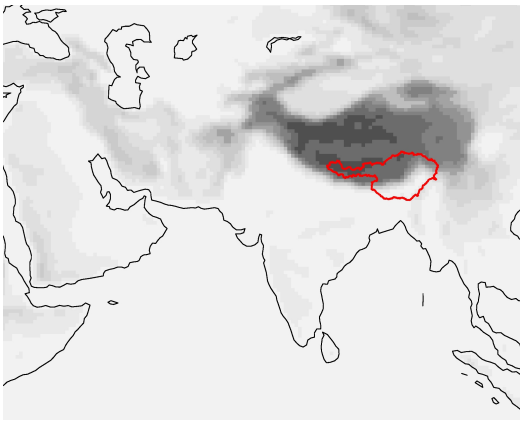

Abbildung 3.1: *The South Asian simulation domain including the Upper Brahmaputra river basin (red).*

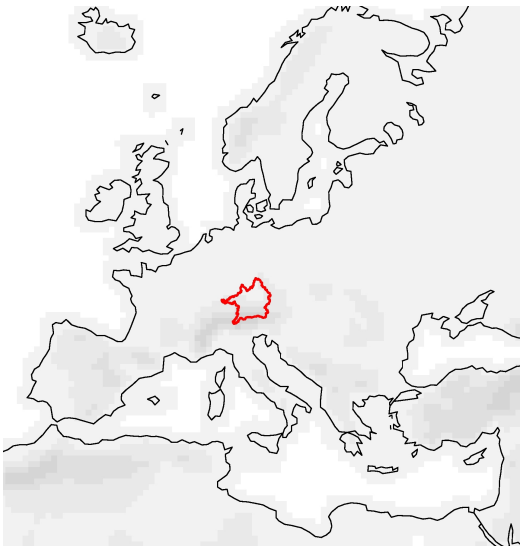

Abbildung 3.2: *The European simulation domain including the Upper Danube river basin (red).*

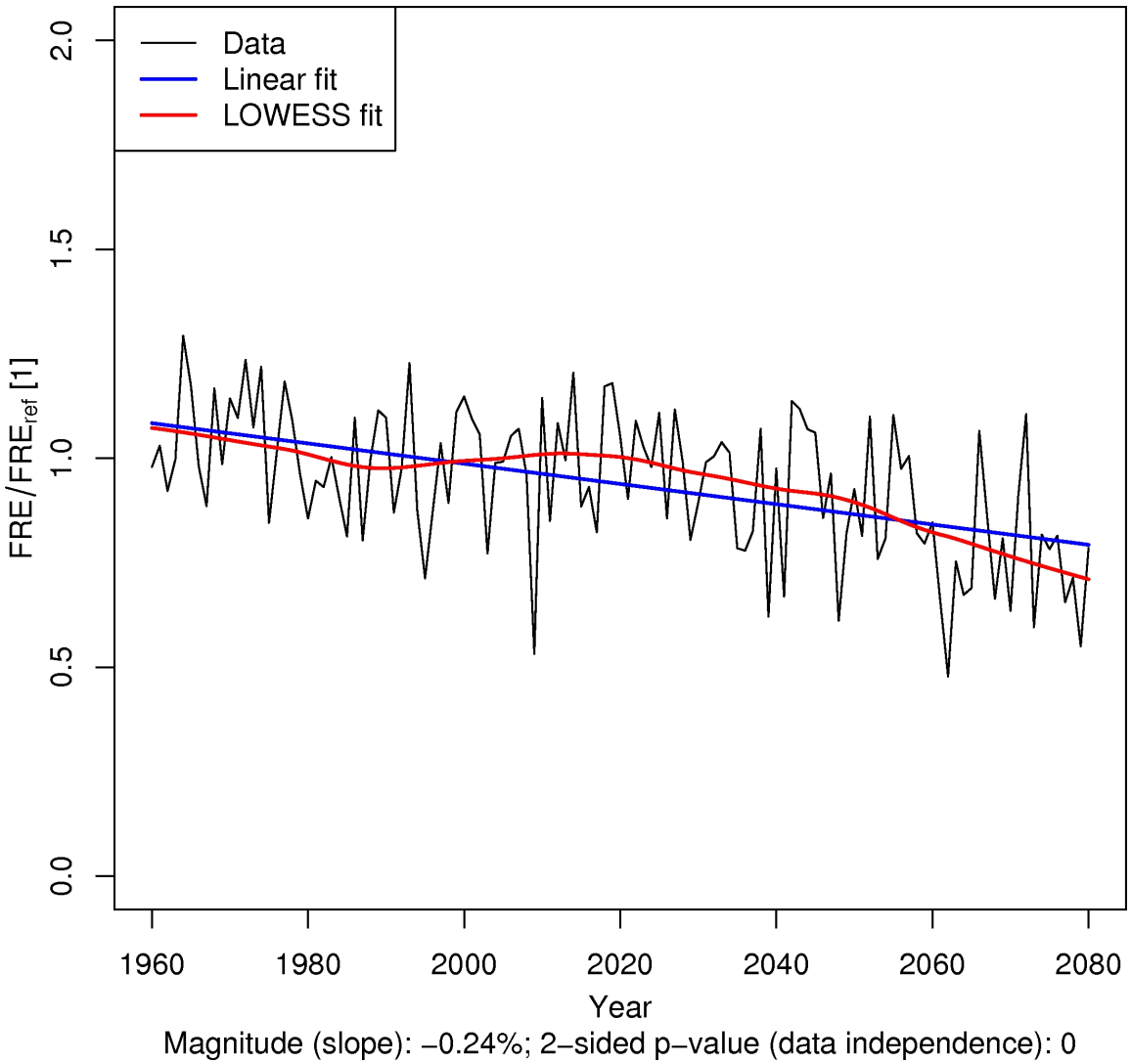

Abbildung 3.3: *Changes of rain day frequency during summer (JJA) in the Upper Danube river basin as projected within the CLM SRES A1B scenario run in reference to the time period 1971-2000. The graph includes a linear and a locally-weighted polynomial regression fit to the CLM projection.*

The data resulting from the CLM runs may for instance be used to project trends of daily precipitation statistics in the target regions. An example is shown in Fig. 3

Veröffentlichungen:

A. Dobler, B. Ahrens, Institut für Atmosphäre und Umwelt, Goethe-Universität Frankfurt
Precipitation by a regional climate model and bias correction in Europe and South Asia
Meteorol. Z., 17(4): 499-509
2008

4.5.4 Learning Efficient Representations in Low-Level Vision

Cornelius Weber
Frankfurt Institute for Advanced Studies

In our work we are trying to understand function and structure formation in the lower visual cortex V1. Even though we are far from attempting to simulate an entire cortical area, the simulation of a tiny patch of cortical tissue requires intensive computations for which we used the CSC computer cluster.

We have successfully integrated two strands of prior models of the lower visual system: work on developing V1 simple-cell like receptive fields from generative sparse coding models and work on integrating in a biologically plausible fashion a mechanism of short-term neuronal plasticity to maintain firing rate homeostasis. Key idea was to enforce the required sparse coding of the generative model by the same mechanism that maintains firing rate homeostasis. The combination of these strands of research has led to a model that develops simple-cell like receptive fields from natural images and at the same time accounts for a short-term perceptual finding: the tilt aftereffect, see (Weber and Triesch, 2008).

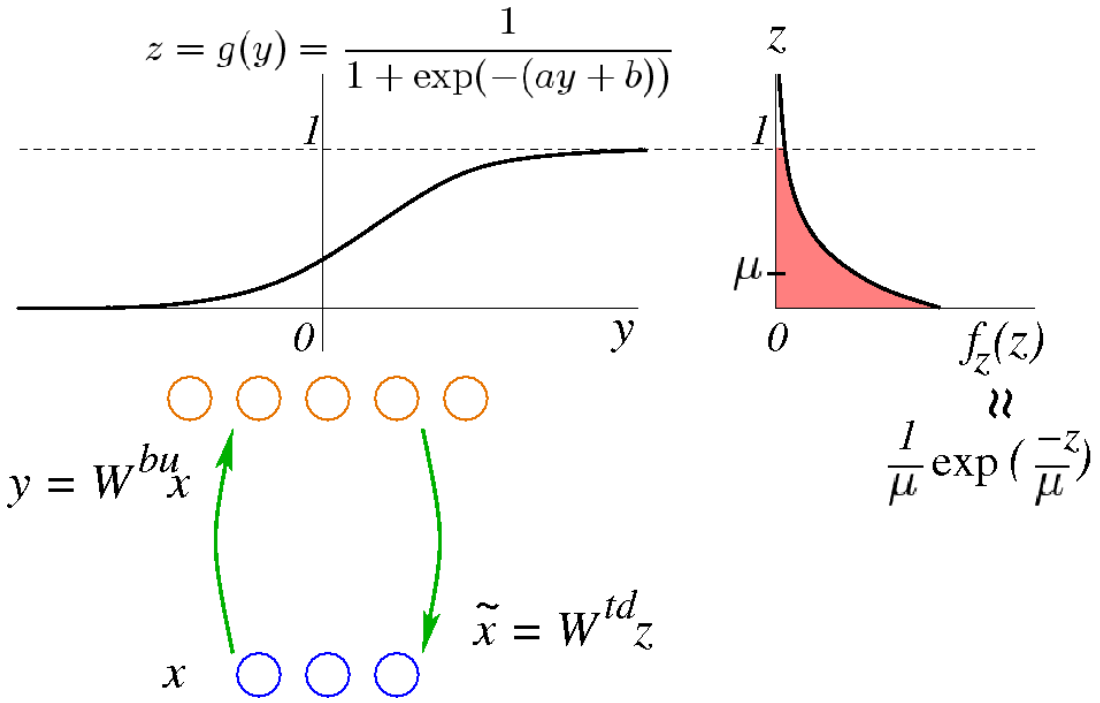

Abbildung 4.1: *The lower left part shows the model architecture. An input vector x, which is a natural image patch, is represented by the input units and is conveyed via the bottom-up weights to the ``net input'' $y = W^{bu}\,x$ of the hidden units. The transfer function g on the hidden neurons is shown at the top of the figure. This function computes the output z of these hidden units.*

This transfer function has two modifiable parameters: a scales the input and resembles a gain, or slope, and b shifts the curve along the input axis and resembles a threshold. The hidden variables z are subject to an exponential prior density function $f_z(z)$ on z in the

range [0,1], as shown to the right of the figure. This function imposes sparseness on the hidden units' activations, and it is parameterized by the mean μ.

The reconstruction $\tilde{x}$ of the input is computed from the hidden variables z using the top-down weights: $\tilde{x} = W^{td} z$, as shown in the lower part of figure 4.1. This feedback architecture together with the reconstruction error that is used for learning makes this model a generative model. The top-down generative weights W^{td} are trained to generate the data with minimal reconstruction error while the bottom-up recognition weights W^{bu} are trained to functionally invert the generative weights.

Trained weights are shown in figure 4.2.

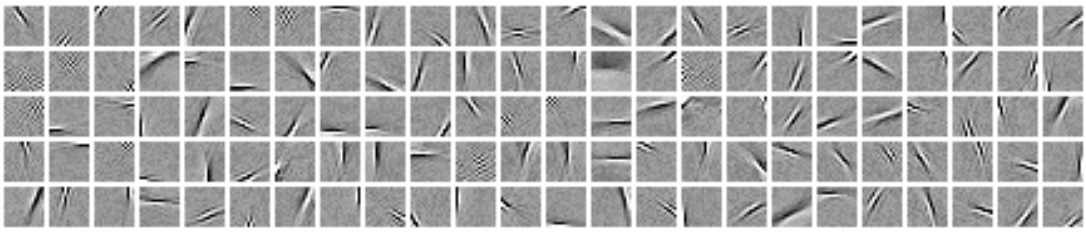

Abbildung 4.2: *Receptive fields of 5x24 hidden units, which is one quarter of all trained cells in this specific simulation (Weber and Triesch, 2007). Each small square corresponds to the receptive field of one hidden unit, which corresponds to one row of the bottom-up weight matrix W^{bu}. The square is an area in the visual field where positive weights (responding to light on-set) are displayed dark and negative weights (responding to light off-set) displayed light. One can see that the largest regions in most input areas are grey (zero weights), meaning that the receptive field (non-zero weights) is confined to a small region. The receptive fields have a characteristic shape that makes the units respond to oriented edges. These are efficient codes for natural images (Barlow, 1994).*

In addition to the neuronal unit activations y and the adjustable weights W^{td} and W^{bu}, this model has the transfer function parameters a and b as further adjustable parameters. These adjust the statistics of the activations z to match the desired exponential, hence they have to average over z and must therefore be slower in their dynamics. However, they should be faster than the weight dynamics, since their development relies on the sparse activations. We chose to regard the time course of transfer function parameter changes as matching visual after-effects that occur in the range of tens of seconds, and so modelled the tilt aftereffect (TAE). Figure 4.3 shows the TAE model result.

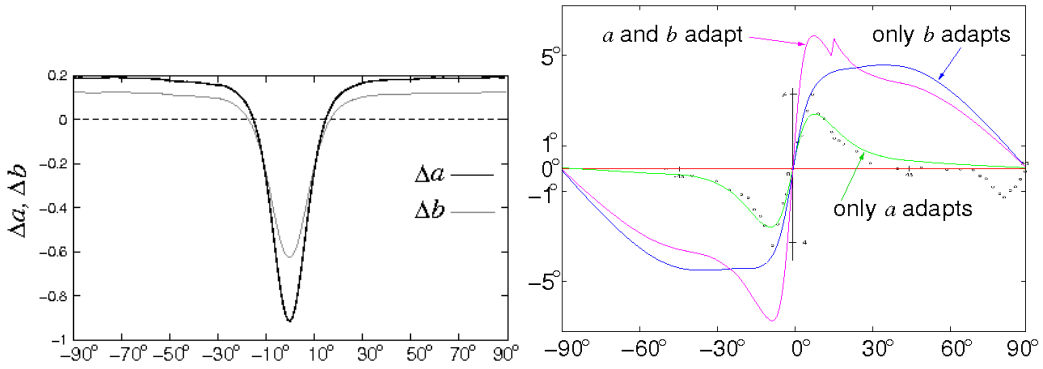

Abbildung 4.3: *A vertical grating (zero degrees on the x-axes in each plot) was presented to the model for a few hundreds of data points, corresponding to a few seconds. The left plot shows that the transfer function parameters have changed dependent on the orientation of the neurons: neurons with an orientation like the grating (near zero degrees) have decreased both their gain a, and also the threshold parameter b has become more negative. Thus, they will respond less to a grating that is near zero degrees. A consequence is the TAE, shown in the right plot: the y-axis shows the model's perceived deviation of its orientation estimation of a test pattern of given orientations. For example, a test pattern of +30 degrees angle will be perceived as if tilted a few more positive degrees. The dots correspond to human data, and our results show that the green model curve matches these data well. The green curve marks a model in which only the gain parameter a adapts during presentation of the grating. We conclude that if the threshold b is variable, then it must adapt on a much slower time scale, for example accounting for firing rate homeostasis on a 24-hour time scale [Turrigiano and Nelson, 2004].*

References:

Barlow, H. (1994). What is the computational Goal of the Neocortex? In: Large Scale Neuronal Theories of the Brain, pp. 1-22, MIT Press.

Turrigiano, G.G. and Nelson, S.B. (2004). Homeostatic Plasticity in the Developing Nervous System. Nature Rev Neurosci., 5, pp. 97-107.

Weber, C. and Triesch, J. (2007). Intrinsic plasticity in a generative model of V1. In: Proc. Dynamic Brain Forum.

Weber, C. and Triesch, J. (2008). A Sparse Generative Model of V1 Simple Cells with Intrinsic Plasticity. Neural Computation, 20, pp. 1261-84.

4.5.5 Weiterentwicklung und Implementation von Methoden der Kopplungsanalyse für die genetische Kartierung komplexer Krankheiten

Prof. Dr. Konstantin Strauch, Dipl.-Math. Thomas Künzel, Dipl.-Stat. Antònia Flaquer
Institut für Medizinische Biometrie und Epidemiologie, Philipps-Universität Marburg

Die Genetische Epidemiologie befaßt sich mit der Identifizierung und Charakterisierung von Genen, die ursächlich an der Entstehung von Krankheiten beim Menschen beteiligt sind. Der erste Schritt dazu ist die Lokalisierung oder Kartierung der Gene. Mittels der Kopplungsanalyse läßt sich untersuchen, ob bestimmte Markerausprägungen und Krankheitsphänotypen in Familien überproportional häufig gemeinsam vererbt werden. Ist dies der Fall, so spricht dies für die Existenz eines krankheits(mit)verursachenden Gens in der chromosomalen Region. Die genetische Kartierung stellt insbesondere bei komplexen Krankheiten eine besondere Herausforderung dar, da solche Krankheiten meist durch mehrere Gene und möglicherweise Umweltfaktoren verursacht werden. Dabei ist der Effekt eines einzelnen Gens im Vergleich zu Mendelschen Krankheiten, die einem klaren dominanten oder rezessiven Erbgang folgen, nur gering. Dementsprechend schwierig ist die Kartierung eines einzelnen Gens (geringe Power). Ziel dieses Projekts ist die Weiterentwicklung von Methoden der Kopplungsanalyse für die genetische Kartierung komplexer Krankheiten. Die methodischen Entwicklungen werden in Software implementiert, so daß sie bei der Genkartierung angewendet werden können, beispielsweise im Rahmen von Untersuchungen zu Volkskrankheiten wie Diabetes, Adipositas, Allergie/Asthma oder neuropsychiatrischen Krankheiten. Der methodische Schwerpunkt des Projekts liegt auf der adäquaten Modellierung der Krankheitsparameter, d.h. der Penetranzen (Erkrankungswahrscheinlichkeiten bei bestimmten Genotypkonfigurationen) sowie der Krankheitsallelfrequenzen (Häufigkeit der krankheitsverursachenden Genvarianten in der Bevölkerung). Dadurch wird die Power (Trennschärfe) bei der Gen-Identifizierung erhöht, also die Wahrscheinlichkeit, ein krankheitsverursachendes Gen bei der Analyse auch tatsächlich zu finden. Bei der sogenannten MOD-Score-Analyse wird der parametrische LOD-Score, der als Stärke des Signals für die Existenz eines krankheitsverursachenden Gens in der jeweiligen chromosomalen Region fungiert, über die Krankheitsmodellparameter (also Penetranzen und Krankheitsallelfrequenz) maximiert. Anders als bei der einfachen LOD-Score-Analyse müssen die Krankheitsmodellparameter, die bei komplexen Krankheiten meist unbekannt sind, daher beim MOD-Score-Verfahren nicht vorgegeben werden. Dadurch wird nicht nur die Power der Kopplungsanalyse erhöht, sondern es können auch Informationen über die Wirkungsweise und den Erbgang der krankheitsverursachenden Genvarianten gewonnen werden. Das Verfahren stellt jedoch hohe Anforderungen an die Rechenkapazitäten, da der Score für viele verschiedene Parameterkombinationen berechnet werden muß. Unsere Gruppe hat die MOD-Score-Analyse für autosomale Genorte und dichotome Phänotypen (betroffen / nicht betroffen) in das Programm GENEHUNTER-MODSCORE implementiert [1-3] und auf verschiedenste genetisch komplexe Krankheiten angewendet. Der MOD-Score-Ansatz wird im Rahmen dieses Projekts weiterentwickelt und algorithmisch optimiert. Die geplanten Neuentwicklungen beinhalten MOD-Score-Verfahren für quantitative Merkmale sowie für Genorte auf den Geschlechtschromosomen, auch unter Berücksichtigung geschlechtsspezifischer Penetranzen sowie des genomischen Imprintings (bei diesem epigenetischen Effekt hängt die Erkrankungswahrscheinlichkeit davon ab, ob das Krankheitsallel vom Vater oder von der Mutter geerbt wurde).

Ein weiterer Schwerpunkt ist die Kopplungsanalyse mit expliziter Modellierung zweier Krankheitsgenorte. Es ist naheliegend, dieses Verfahren bei genetisch komplexen Krankheiten anzuwenden, die durch mindestens zwei Genorte bestimmt werden. Die Kopplungsanalyse mit zwei Krankheitsgenorten wurde von unserer Gruppe in das Programm GENEHUNTER-TWOLOCUS implementiert [4]. Der LOD-Score, der die Stärke des Kopplungssignals angibt, ist in diesem Fall eine Funktion der genetischen Positionen zweier Krankheitsgenorte, die sich auf zwei verschiedenen Chromosomen befinden, wie in der folgenden Abbildung dargestellt. Bei diesem Beispiel konnten zwei genetische Regionen auf den Chromosomen 5 und 11 identifiziert werden, die gemeinsam das Risiko für die Entstehung von venösem Thromboembolismus beeinflussen [5].

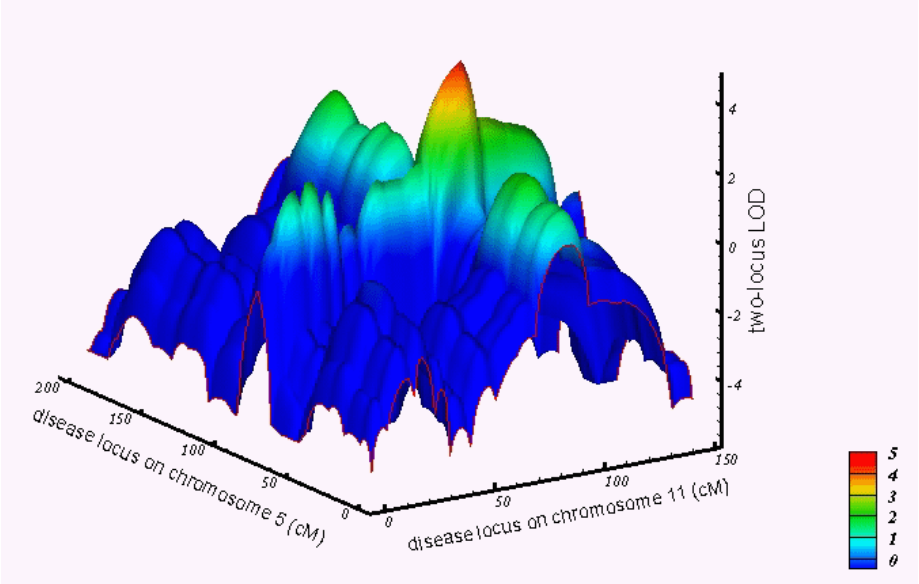

Die Zwei-Genort-Kopplungsanalyse erreicht in vielen Fällen eine höhere Power bei der genetischen Kartierung komplexer Krankheiten als eine Analyse mit nur einem Krankheitslocus, allerdings ist der Rechenzeitbedarf auch um eine Größenordnung höher. Aus diesem Grund haben wir das Programm GENEHUNTER-TWOLOCUS optimiert und parallelisiert [6]. Auf diese Weise sind die umfangreichen Berechnungen, die zur Identifizierung bisher unbekannter krankheitsverursachender Gene führen, auf großen Parallelrechnern oder Clustern durchführbar. Die erfolgreiche Bearbeitung dieses und anderer Projekte am Institut für Medizinische Biometrie und Epidemiologie hängt entscheidend von der Verfügbarkeit von Ressourcen wie dem Marburger Rechencluster (MaRC) des Marburger Hochschulrechenzentrums ab, auf den im Rahmen dieses Projektes in erheblichem Maße zugegriffen wird.

1. Strauch K(2003): Parametric linkage analysis with automatic optimization of the disease model parameters. American Journal of Human Genetics 73(Suppl1):A2624.

2. Dietter J, Mattheisen M, Fürst R, Rüschendorf F, Wienker TF, Strauch K (2007): Linkage analysis using sex-specific recombination fractions with GENEHUNTER-MODSCORE. Bioinformatics 23:64-70.

3. Mattheisen M, Dietter J, Knapp M, Baur MP, Strauch K (2008): Inferential testing for linkage with GENEHUNTER-MODSCORE: the impact of the pedigree structure on the null distribution of multipoint MOD scores. Genetic Epidemiology 32:73-83.

4. Strauch K, Fimmers R, Kurz T, Deichmann KA, Wienker TF, Baur MP (2000): Parametric and nonparametric multipoint linkage analysis with imprinting and two-locus-trait models: application to mite sensitization. American Journal of Human Genetics 66:1945-1957.

5. Berger M, Mattheisen M, Kulle B, Schmidt H, Oldenburg J, Bickeböller H, Walter U, Lindner T, Strauch K, Schambeck CM (2005): High factor VIII levels in venous thromboembolism show linkage to imprinted loci on chromosomes 5 and 11. Blood 105:638-644.

6. Dietter J, Spiegel A, an Mey D, Pflug HJ, Al-Kateb H, Hoffmann K, Wienker TF, Strauch K (2004): Efficient two-trait-locus linkage analysis through program optimization and parallelization: application to hypercholesterolemia. European Journal of Human Genetics 12:542-550.

5 Veröffentlichungen

2007

1. *A. Ivanov and S. Kantorovich and E. Reznikov and C. Holm and A. Pshenichnikov and A. Lebedev and A. Chremos and P. Camp, FIAS Frankfurt*
   Magnetic properties of polydisperse ferrofluids: A critical comparison between experiment, theory and computer simulation
   Phys. Rev. E 75(061405),

2. *A. Lyalin, I.A. Solov'yov, A.V. Solov'yov, and W. Greiner, Frankfurt Institute for Advanced Studies, Ruth-Moufang-Str. 1, Frankfurt am Main, Germany*
   Interplay of electronic and geometry shell effects in properties of neutral and charged Sr-clusters
   Phys. Rev. A. 75, 053201 (2007).

3. *A. Tolvanen, J. Kotakoski, A. V. Krasheninnikov, K. Nordlund*
   Relative abundance of single and double vacancies in irradiated single-walled carbon nanotubes
   Appl. Phys. Lett. 173109 91

4. *A.V. Yakubovich, I.A. Solov'yov, A.V. Solov'yov, W. Greiner, Frankfurt Institute for Advanced Studies, Ruth-Moufang-Str. 1, Frankfurt am Main, Germany*
   Ab initio description of phase transitions in finite bio- nano-systems
   Europhysics News 38, 10 (2007).

5. *Balzani, D., Schröder, J., Gruttmann, F., Fachgebiet Statik, TU Darmstadt,*
   Polyconvex energy densities with applications to anisotropic thin shells,
   PAMM- 7, 4060027-4060028, 2007 / DOI 10.1002/pamm.200700437.

6. *Basara, B., Aldudak, F., Schrefl, M., Jakirlić, S., Hanjalić, K. Tropea, C. and Mayer, J. AVL List GmbH, Graz, Austria, Fachgebiet Strömungslehre und Aerodynamik, Technische Universität Darmstadt und BMW AG, München*
   Experimental Investigations and Computations of Unsteady Flow past a Real Car Using a Robust Elliptic Relaxation Closure with a Universal Wall Treatment.
   SAE Technical Paper Series, Paper No. 2007-01-0104, pp. 1-11, (also in SAE 2007 Transactions, Journal of Passenger Cars – Mechanical Systems, March 2008; Vol. V116-6, ISBN 978-0-7680-1985-8)

7. *Bela E. Bode, Jörn Plackmeyer, Thomas F. Prisner and Olav Schiemann, Institute of Physical and Theoretical Chemistry and Center for Biomolecular Magnetic Resonance, Max-von-Laue-Strasse 7, J. W. Goethe-University, 60438 Frankfurt am Main, Germany.*

PELDOR Measurements on a Nitroxide-Labeled Cu(II) Porphyrin: Orientation Selection, Spin-Density Distribution, and Conformational Flexibility
J. Phys. Chem. A, 2008, 112 (23), 5064–5073.

8. *Benjamin Koch (Frankfurt U., FIAS & Frankfurt U.) , Marcus Bleicher (Frankfurt U., FIAS) , Horst Stoecker (Frankfurt U., FIAS & Frankfurt U.) .*
Black Holes at LHC?
Published in J.Phys.G34:S535-542,2007. e-Print: hep-ph/0702187

9. *Benjamin Lungwitz (Frankfurt U., Inst. Kernphys.) , Marcus Bleicher (Frankfurt U.) .*
Searching for the Critical Point of QCD: Theoretical Benchmark Calculations.
Published in Phys.Rev.C76:044904,2007. e-Print: arXiv:0707.1788 [nucl-th]

10. *C. Olbricht, F. Hahn, A. Sadiki, J. Janicka, EKT TUD*
Analysis of Subgrid Scale Mixing Using a Hybrid LES-Monte-Carlo PDF Method
International Journal of Heat and Fluid Flow, 28/6 :1215-1226

11. *C. Olbricht, F. Hahn, J. Kühne, A. Sadiki, J. Janicka, F. Bake, I. Röhle, EKT TUD*
Flow and mixing in a model GT combustor investigated by LES and Monte-Carlo filtered pdf methods
ASME Turbo Expo GT2007-27270

12. *D. Antypov and C. Holm, FIAS Frankfurt*
Osmotic Coefficient Calculations for Dilute Solutions of Short Stiff-Chain Polyelectrolytes
Macromolecules 40(3)(731-738),

13. *D. Zschiesche, G. Zeeb and S. Schramm, CSC, ITP and FIAS Frankfurt*
Phase structure in a hadronic chiral model
J. Phys. G 34, 1665

14. *Daniel Krieg, Marcus Bleicher (Frankfurt U.) .*
Decreasing elliptic flow at the LHC: Calculations in a parton recombination approach.
Published in Phys.Rev.C78:054903,2008. e-Print: arXiv:0708.3015 [nucl-th]

15. *Debora Mahlke, Alexander Martin, Susanne Moritz, Technische Universität Darmstadt, Fachbereich Mathematik*
A Simulated Annealing Algorithm for Transient Optimization in Gas Networks,
Mathematicals Methods of Operations Research, 66:99 - 166,

16. *E. Czinki, A. G. Csaszar, G. Magyarfalvi, P. R. Schreiner, W. D. Allen,*
Secondary structures of peptides and proteins via NMR chemical-shielding anisotropy (CSA) parameters,
J. Am. Chem. Soc. 2007, 129, 1568.

17. *E. D. Butova, A. A. Fokin, P. R. Schreiner,*
Beyond the Corey Reaction; One-Step Diolefination of Cyclic Ketones,
J. Org. Chem. 2007, 72, 5689.

18. *E. L. Bratkovskaya, O. Linnyk (FIAS, Frankfurt U.), W. Cassing (Giessen U.), and H. Stöcker (ITP & FIAS, Frankfurt U.)*
Charmed signatures for phase transitions in heavy-ion collisions
Contributed to 4th International Workshop on Critical Point and Onset Deconfinement, Darmstadt, Germany, 9-13 Jul 2007. arXiv:0709.2185 [nucl-th].

19. *E. Lussetti, T. Terao, and F. Müller-Plathe, Eduard-Zintl-Institut fuer Anorganische und Physikalische Chemie, Technische Universität Darmstadt, Petersenstrasse 20, D-64287 Darmstadt, Germany*
Non-equilibrium molecular dynamics calculation of the thermal conductivity of amorphous polyamide-6,6
J. Phys. Chem. B 111, 11516-11523

20. *E.L. Bratkovskaya (FIAS, Frankfurt U.),*
Signals of the QGP phase transition - a view from microscopic transport models, Proceedings of the CRIMEA-2007 Conference on "New Trends in High-Energy Physics:Experiment, Phenomenology, Theory", Yalta, Crimea, Ukraine, 15-22 Sep 2007;
arXiv:0710.5756 [nucl-th].

21. *E.S. Henriques and A.V. Solov'yov, Frankfurt Institute for Advanced Studies, Ruth-Moufang-Str. 1, Frankfurt am Main, Germany*
A Rational Method for Probing Macromolecules Dissocation: the Antibody-Hapten system
European Physical Journal D. 46, 471 (2007).

22. *Fiedler, K., Döll, P.*
Global modelling of continental water storage changes – sensitivity to different climate data sets
Advances in Geosciences, 11, 63-68

23. *G. I. Lykasov (JUNR, Dubna) and W. Cassing (Giessen U.),*
Charmonium dissociation by mesons in heavy-ion collisions.
Nucl. Phys. A782 (2007) 396-399.

24. *G. Santangelo, A. Di Matteo, F. Müller-Plathe, and G. Milano, Eduard-Zintl-Institut fuer Anorganische und Physikalische Chemie, Technische Universität Darmstadt, Petersenstrasse 20, D-64287 Darmstadt, Germany*
From Mesoscale back to Atomistic Models: A Fast Reverse-Mapping Procedure for Vinyl Polymer Chains
J. Phys. Chem. B 111, 2765-2773

25. *George Chagelishvili, George Khujadze, Martin Oberlack, Abastumani Astrophysical Observatory, Tbilisi, Georgia, Group of Fluid Dynamics, Department of Mechanics, Darmstadt, Germany*

DNS of stochastically forced laminar plane Couette flow: peculiarities of hydrodynamic fluctuations
Fifth International Symposium on Turbulence and Shear Flow Phenomena,TSFP-5

26. *George Khujadze, Martin Oberlack, Group of Fluid Dynamics, Department of Mechanics, Darmstadt, Germany*
New Scaling Laws in ZPG Turbulent Boundary Layer Flow
Fifth International Symposium on Turbulence and Shear Flow Phenomena,TSFP-5

27. *Gruttmann, F., Fachgebiet Statik, TU Darmstadt,*
On non-linear FE-formulations for thin shells using a three-field variational principle,
in: J. Soric, F. Gruttmann, W. Wagner (eds.), Advanced Numerical Analysis of Shell-like Structures, 15-29,

28. *Güntner, A., Schmidt, R., Döll, P.*
Supporting large- scale hydrogeological monitoring and modelling by time-variable gravity data
Hydrogeology Journal, 15(1), 167- 170, DOI: 10.1007/s10040-006-0089-1

29. *Güntner, A., Stuck, J., Werth, S., Döll, P., Verzano, K., Merz, B.*
A global analysis of temporal and spatial variations in continental water storage
Water Resources Research, 43, W05416, DOI:10.1029/2006WR005247

30. *H. Petersen, M. Bleicher (Frankfurt U.) .*
Studying the energy dependence of elliptic and directed flow within a relativistic transport approach.
Published in Eur.Phys.J.C49:91-96,2007.

31. *H. Sun and M. Schäfer, Department for Numerical Methods in Mechanical Engineering, Technische Universität Darmstadt*
A Proper Orthogonal Decomposition Based Reduced Model for Improving Evolutionary flow Shape Optimization
In Proceedings, Eurogen 2007 Evolutionary methods for Design, Optimization and Control, Jyvaskyla, Finland

32. *H. Sun and Z. Harth and M. Schäfer, Department for Numerical Methods in Mechanical Engineering, Technische Universität Darmstadt*
Efficiency improvement of Evolutionary Algorithms for Flow Shape Optimization
in Proceedings, 7th World Congress on Structure and Multidisciplinary Optimization, Seoul, Korea

33. *Horst Stocker, Benjamin Koch (Frankfurt U., FIAS & Frankfurt U.) , Marcus Bleicher (Frankfurt U.)*
An introduction to mini black holes at LHC.
Published in Braz.J.Phys.37:836-839,2007.

34. *I.A. Solov'yov, A.V. Yakubovich, A.V. Solov'yov, W. Greiner, Frankfurt Institute for Advanced Studies, Ruth-Moufang-Str. 1, Frankfurt am Main, Germany*
Two center multipole expansion method: application to macromolecular systems
Physical Review E 75, 051912 (2007).

35. *I.A. Solov'yov, D.E. Chandler and K.Schulten, Frankfurt Institute for Advanced Studies, Ruth-Moufang-Str. 1, Frankfurt am Main, Germany*
Magnetic Field Effects in Arabidopsis thaliana Cryptochrome-1
Biophys. J. 92, 2711 (2007).

36. *I.A. Solov'yov, and W. Greiner, Frankfurt Institute for Advanced Studies, Ruth-Moufang-Str. 1, Frankfurt am Main, Germany*
Theoretical Analysis of an Iron Mineral-Based Magnetoreceptor Model in Birds
Biophys. J. 93, 1493 (2007).

37. *I.C. Arsene, L.V. Bravina, W. Cassing (Giessen U.) et al.,*
Dynamical phase trajectories for relativistic nuclear collisions.
Phys. Rev. C75 (2007) 034902.

38. *J. Dietter, M. Mattheisen, R. Fürst, F. Rüschendorf, T. F. Wienker, K. Strauch, Universität Marburg, Universität Bonn, Gene Mapping Center, Max-Delbrück-Center for Molecular Medicine, Berlin*
Linkage analysis using sex-specific recombination fractions with GENEHUNTER-MODSCORE
Bioinformatics 23(1), 64-70

39. *J. Kühne, C. Olbricht, A. Sadiki, J. Janicka, J.-Y. Chen, EKT TUD*
Hybrid LES Monte-Carlo PDF Modeling of Turbulent Piloted Jet Flames
5th International Symposium on Turbulence and Shear Flow Phenomena

40. *J. Steinheimer, M. Bleicher (Frankfurt U.) , H. Petersen (Frankfurt U. & Frankfurt U., FIAS) , S. Schramm (Frankfurt U.) , H. Stocker (Frankfurt U. & Frankfurt U., FIAS & Darmstadt, GSI) , D. Zschiesche (Frankfurt U.) .*
(3+1)-dimensional hydrodynamic expansion with a critical point from realistic initial conditions.
Published in Phys.Rev.C77:034901,2008. e-Print: arXiv:0710.0332 [nucl-th]

41. *Jakirlić, S., Eisfeld, B., Jester-Zürker, R. and Kroll, N. Fachgebiet Strömungslehre und Aerodynamik, Technische Universität Darmstadt und DLR Braunschweig*
Near-wall, Reynolds-stress model calculations of transonic flow configurations relevant to aircraft aerodynamics.
Int. J. Heat and Fluid Flow, Vol. 28, No. 4, pp. 602-615

42. *Jörg Fritscher, Peter Hrobárik, and Martin Kaupp, Institute of Physical and Theoretical Chemistry and Center for Biological Magnetic Resonance, J. W. Goethe University of Frankfurt, Max-von-Laue-Str. 7, D-60438 Frankfurt, Germany, Institute of Inorganic Chemistry, Slovak Academy of Sciences, Dúbravská cesta 9, SK-84536*

Bratislava, Slovakia, and Institut für Anorganische Chemie, Universität Würzburg, Am Hubland, D-97074 Würzburg, Germany.
Computational Studies of EPR Parameters for Paramagnetic Molybdenum Complexes. II. Larger MoV Systems Relevant to Molybdenum Enzymes
Inorg. Chem., 2007, 46 (20), 8146–8161.

43. *Joerg Fritscher, Peter Hrobarik, and Martin Kaupp, Institute of Physical and Theoretical Chemistry, J. W. Goethe University of Frankfurt, and Center for Biological Magnetic Resonance, Max-von-Laue-Strasse 7, D-60438 Frankfurt, Germany, Institute of Inorganic Chemistry, Slovak Academy of Sciences, Dubravska cesta 9, SK-84536 Bratislava, Slovakia, and Institut für Anorganische Chemie, Universitaet Wuerzburg, Am Hubland, D-97074 Wuerzburg, Germany*
Computational Studies of Electron Paramagnetic Resonance Parameters for Paramagnetic Molybdenum Complexes. 1. Method Validation on Small and Medium-Sized Systems
J. Phys. Chem. B, 2007, 111 (17), 616–4629

44. *Kniesner, B., Jester-Zürker, R., Jakirlić, S. and Hanjalić, K. Fachgebiet Strömungslehre und Aerodynamik, Technische Universität Darmstadt*
RANS-SMC and hybrid LES/RANS of a backward-facing step flow subjected to increasingly enhanced wall heating.
5th International Symposium on Turbulence and Shear Flow Phenomena (TSFP5), Munich, Germany, August 27-29

45. *Kniesner, B., Šarić, S., Mehdizadeh, A., Jakirlić, S., Hanjalić K., Tropea, C., Sternel, D., Gauß, F. and Schäfer, M. Fachgebiete Strömungslehre und Aerodynamik/Numerische Berechnungsverfahren im Maschinenbau, Technische Universität Darmstadt*
Wall treatment in LES by RANS: method development and application to aerodynamic flows and swirl combustors.
ERCOFTAC Bulletin, No. 72, pp. 33-40

46. *Kundzewicz, Z.W., Mata, L.J., Arnell, N.W., Döll, P., Kabat, P., Jiménez, B., Miller, K.A., Oki,, T., Sen, Z., Shiklomanov, I.A.*
Freshwater resources and their management
In: Parry, M.L., Canziani, O.F., Palutikof, J.P., van der Linden, P.J. and Hanson, C.E. (eds.): Climate Change 2007: Impacts, Adaptation and Vulnerability. Contribution of Working Group II to the Fourth Assessment Report of the Intergovernmental Panel on Climate Change, 173-210, Cambridge University Press, Cambridge, UK

47. *L. Bravina, I. Arsene, M.S. Nilsson, K. Tywoniuk (Oslo U.) , E. Zabrodin (Oslo U. & Moscow State U.) , M. Bleicher (Frankfurt U.) , H. Stocker (Frankfurt U. & Frankfurt U., FIAS) , W. Greiner (Frankfurt U., FIAS) .*
Equilibration of matter in relativistic heavy-ion collisions.
Published in Int.J.Mod.Phys.E16:777-786,2007.

48. *M. Bleicher (Frankfurt U.) , X. Zhu (Frankfurt U., FIAS & Tsinghua U., Beijing) .*
Is constituent quark scaling a unique sign of parton recombination?
Published in Eur.Phys.J.C49:303-308,2007.

49. *M. Bröring, F. Brégier, E. Cónsul Tejero, C. Hell, M. C. Holthausen*
Revisiting the Electronic Ground State of Copper Corroles
Angew. Chem. 119, 449

50. *M. D. Wodrich, C. Corminboeuf, P. R. Schreiner, A. A. Fokin, P. v. R. Schleyer,*
How accurate are DFT treatments of organic energies?,
Org. Lett. 2007, 9, 1851.

51. *M. Heck and M. Schäfer and D. C. Sternel and S. Yigit, Department for Numerical Methods in Mechanical Engineering, Technische Universität Darmstadt*
Efficient and Robust Simulation of Fluid-Structure Interaction
in Proceedings, ECCOMAS, Computational Methods in Marine Engineering II, Barcelona

52. *M. Kotke, P. R. Schreiner,*
Generally Applicable Organocatalytic Tetrahydropyranylation of Hydroxy Functionalities with Very Low Catalyst Loading,
Synthesis 2007, 779.

53. *M. Müller, K. Albe*
Concentration of thermal vacancies in metallic nanoparticles
Acta Mat. 3237-3244 55

54. *M. Müller, P. Erhart, K. Albe*
Analytic bond-order potential for bcc and fcc iron—comparison with established embedded-atom method potentials
J. Phys.: Condens. Matter 326220 19

55. *M. Müller, P. Erhart, K. Albe*
Thermodynamics of L10 ordering in FePt nanoparticles studied by Monte Carlo simulations based on an analytic bond-order potential
Phys. Rev. B 155412 76

56. *Martin Kober, Benjamin Koch, Marcus Bleicher (Frankfurt U. & Frankfurt U., FIAS)*
.
First Order Calculation of the Inclusive Cross Section pp to ZZ by Graviton Exchange in Large Extra Dimensions.
Published in Phys.Rev.D76:125001,2007. e-Print: arXiv:0708.2368 [hep-ph]

57. *O. Linnyk, E. L. Bratkovskaya (FIAS, Frankfurt U.), W. Cassing (Giessen U.), and H. St¨ocker (ITP&FIAS, Frankfurt U.),*
Charmonium dynamics in nucleus-nucleus collisions at SPS and FAIR energies,
Nucl. Phys. A 786 (2007) 183-200 [nucl-th/0612049].

58. *Oliver Kolb, Jens Lang, Pia Bales, Technische Universität Darmstadt, Fachbereich Mathematik*
Adaptive linearized models for optimization of gas networks
PAMM, Proc. Appl. Math. Mech. 7, 1061301-1061302,

59. *Omori, T., Jakirlić, S., Obi, S. and Tropea, C. Fachgebiet Strömungslehre und Aerodynamik, Technische Universität Darmstadt und Keio University, Yokohama, Japan*
Computational analysis of the shear-induced lift force on a cylindrical particle by means of LES with relevance to particle-laden liquid flow in an upward duct.
International Conference on Multiphase Flows, ICMF 2007, Leipzig, Germany, July9–13

60. *P. Erhart, A. Klein, R.G. Egdell, K. Albe*
Band structure of indium oxide: Indirect versus direct band gap
Phys. Rev. B 153205 75

61. *P. Erhart, K. Albe*
Thermodynamics of mono- and di-vacancies in barium titanate
J. Appl. Phys. 084111 102

62. *P. Erhart, R. A. Eichel, P. Träskelin, K. Albe*
Association of oxygen vacancies with impurity metal ions in lead titanate: First principles calculations
Phys. Rev. B 174116 76

63. *P. R. Schreiner,*
Relative Energy Computations with Approximate Density Functional Theory - A Caveat!,
Angew. Chem. Int. Ed. 2007, 23, 4217.

64. *Pham, V.D., Gruttmann, F., Fachgebiet Statik, TU Darmstadt,*
A few typical delamination patterns of compressed thin films,
PAMM- 7, 4040023-4040024, 2007 / DOI 10.1002/pamm.200700349.

65. *Qingfeng Li (Frankfurt U., FIAS) , Marcus Bleicher (Frankfurt U.) , Horst Stocker (Frankfurt U., FIAS & Frankfurt U. & Darmstadt, GSI) .*
The Effect of pre-formed hadron potentials on the dynamics of heavy ion collisions and the HBT puzzle.
Published in Phys.Lett.B659:525-530,2008. e-Print: arXiv:0709.1409 [nucl-th]

66. *Qingfeng Li (Frankfurt U., FIAS) , Marcus Bleicher (Frankfurt U.) , Horst Stocker (Frankfurt U., FIAS & Frankfurt U.) .*
Pion freeze-out as seen through HBT correlations in heavy ion collisions from FAIR/AGS to RHIC energies.
Published in J.Phys.G34:2037-2044,2007. e-Print: arXiv:0706.2091 [nucl-th]

67. *R. Haunschild, C. Loschen, S. Tüllmann, D. Cappel, M. Hölscher, M. C. Holthausen, G. Frenking*
Theoretical Studies of Ethylene Addition to Transition Metal Compounds with Carbene and Oxo Groups LnM(=CH2)(=O)
J. Phys. Org. Chem. 20, 11

68. *S. Foxon, J.-Y. Xu, S. Turba, M. Leibold, F. Hampel, F. W. Heinemann, O. Walter, C. Würtele, M. C. Holthausen, S. Schindler*

Syntheses, Characterization and Reactivity of Iron(II), Nickel(II), Copper(II) and Zinc(II) Complexes of the Ligand N,N,N',N'-Tetrakis(2-pyridylmethyl)-1,3-benzenediamine (1,3-tpbd) and its phenol derivative N,N,N^3,N^3-Tetrakis(2-pyridylmethyl)-2,6-p-cresolediamine (2,6-tpcd)
Eur. J. Inorg. Chem. 429

69. *S. Tayefeh, T. Kloss, G. Thiel, B. Hertel, A. Moroni, S. M. Kast, TU Darmstadt, Universität Mailand*
Molecular Dynamics Simulation Study of the Cytosolic Mouth in Kcv-type Potassium Channels
Biochemistry 46, 4826-4839

70. *S. Tayefeh, TU Darmstadt*
Computational Study of the Kcv Potassium Channel
Dissertation

71. *S. Tyagi and A. Arnold and C. Holm, FIAS Frankfurt*
ICMMM2D: An accurate method to include planar dielectric interfaces via image charge summation
J. Chem. Phys. 127(154723),

72. *S. Vogel, H. Petersen, K. Schmidt, E. Santini, C. Sturm (Frankfurt U.) , J. Aichelin (SUBATECH, Nantes) , M. Bleicher (Frankfurt U.)*
How sensitive are di-leptons from rho mesons to the high baryon density region?
Published in Phys.Rev.C78:044909,2008. e-Print: arXiv:0710.4463 [hep-ph]

73. *S. Yigit and M. Heck and D. C. Sternel and M. Schäfer, Department for Numerical Methods in Mechanical Engineering, Technische Universität Darmstadt*
Efficiency of Fluid-Structure Interaction Simulations with Adaptive Underrelaxation and Multigrid Acceleration
International Journal of Multiphysics, Vol. 1/1, pp. 85-99

74. *S. Yigit and M. Heck and M. Schäfer and D. C. Sternel, Department for Numerical Methods in Mechanical Engineering, Technische Universität Darmstadt*
An Enhanced Implicit Partitioned ALE Approach for Fluid-Structure Interaction Simulations
in Proceedings, ECCOMAS, Computational Methods for Coupled Problems in Science and Engineering II, Ibiza

75. *S. Yigit and M. Heck and M. Schäfer, Department for Numerical Methods in Mechanical Engineering, Technische Universität Darmstadt*
Numerical Investigation of Structural Behavior During Fluid Excited Vibrations
Revue Européenne de Mécanique Numérique, Vol. 16/3, pp. 491-519

76. *Siebert, S., Döll, P.*
Irrigation water use - A global perspective
In Lozán, J.L., Graßl, H., Hupfer, P., Menzel, L., Schönwiese, C-D. (eds.): Global Change: Enough Water for all? University of Hamburg, Hamburg, 104-107

77. *Stephane Haussler, Stefan Scherer (Frankfurt U., FIAS) , Marcus Bleicher (Frankfurt U.) .*
The Effect of Dynamical Parton Recombination on Event-by-Event Observables.
Published in Phys.Lett.B660:197-201,2008. e-Print: hep-ph/0702188

78. *T. I. Kückmann, F. Dornhaus, M. Bolte, H.-W. Lerner, M. C. Holthausen, M. Wagner*
Broadening the Scope of Ancillary Phosphane-Type Ligands: A Systematic Comparison of PR3, PR2BH3-, and SiR3- and Their Chalcogen Derivatives
Eur. J. Inorg. Chem. 1989

79. *T. Järvi, A. Kuronen, K. Meinander, K. Nordlund, K. Albe*
Contact epitaxy by deposition of Cu, Ag, Au, Pt, and Ni nanoclusters on (100)-surfaces: Size limits and mechanisms
Phys. Rev. B 115422 75

80. *T. Järvi, A. Kuronen, K. Nordlund, K. Albe*
Structural modification of multiply twinned nanoparticles by ion irradiation: a molecular dynamics study
J. Appl. Phys. 124304 102

81. *T. Kloss, TU Darmstadt*
Quantitative Berechnung thermodynamischer Observablen mittels dreidimensionaler Integralgleichungstheorien
Dissertation

82. *T. Spyriouni, C. Tzoumanekas, D. Theodorou, F. Müller-Plathe, and G. Milano, Eduard-Zintl-Institut fuer Anorganische und Physikalische Chemie, Technische Universität Darmstadt, Petersenstrasse 20, D-64287 Darmstadt, Germany*
Coarse-Grained and Reverse-Mapped United-Atom Simulations of Long-Chain Atactic Polystyrene Melts
Macromolecules 40, 3876-3885

83. *T. Terao, E. Lussetti, and F. Müller-Plathe, Eduard-Zintl-Institut fuer Anorganische und Physikalische Chemie, Technische Universität Darmstadt, Petersenstrasse 20, D-64287 Darmstadt, Germany*
Non-equilibrium molecular dynamics methods for computing the thermal conductivity: Application to amorphous polymers
Phys. Rev. E 75, 057701

84. *V. Dexheimer, S. Schramm and H. Stöcker, CSC, ITP and FIAS Frankfurt*
Neutron Stars in a Chiral Model with Temperature
J. Phys. G 35 014060

85. *V. Lobaskin and B. Dünweg and M. Medebach and T. Palberg and C Holm, FIAS Frankfurt*
Electrophoresis of Colloidal Dispersions in the Low-Salt Regime".
Phys. Rev. Lett. 98(176105),

86. *V. P. Konchakovski (H-QM, Frankfurt U.),*
Dynamical study of fluctuations in relativistic nuclear collisions,
PoS CPOD07 (2007) 021.

87. *V. P. Konchakovski (H-QM, Frankfurt U.), M. I. Gorenstein (BITP, Kiev), and E. L. Bratkovskaya (FIAS, Frankfurt U.),*
Multiplicity Fluctuations in Proton-Proton and Nucleus-Nucleus Collisions,
Phys. Lett. B 651 (2007) 114-118.

88. *W. Cassing (Giessen U.),*
QCD thermodynamics and confinement from a dynamical quasiparticle point of view.
Nucl. Phys. A791 (2007) 365-381.

89. *W. L. Cavalcanti, X. Chen and F. Müller-Plathe, Eduard-Zintl-Institut fuer Anorganische und Physikalische Chemie, Technische Universität Darmstadt, Petersenstrasse 20, D-64287 Darmstadt, Germany*
Shear Viscosity Calculations through a Reverse Nonequilibrium Method
Phys. Stat. Sol. A 204, 935-939

90. *Wei Zhao, Hossein Eslami, Welchy Leite Cavalcanti, and Florian Müller-Plathe, Eduard-Zintl-Institut fuer Anorganische und Physikalische Chemie, Technische Universität Darmstadt, Petersenstrasse 20, D-64287 Darmstadt, Germany*
A Refined All-Atom Model for the Ionic Liquid 1-n-Butyl 3-Methylimidazolium bis(Trifluoromethylsulfonyl)imide [bmim][Tf2N]
Zeitschrift für Physikalische Chemie, 221, 1647-1662

91. *X.Y. Chen, P. Carbone, W.L. Cavalcanti, G. Milano, F. Müller-Plathe, Eduard-Zintl-Institut fuer Anorganische und Physikalische Chemie, Technische Universität Darmstadt, Petersenstrasse 20, D-64287 Darmstadt, Germany*
Viscosity and Structural Alteration of a Coarse-grained model of Polystyrene under Steady Shear Flow Studied by Reverse Nonequilibrium Molecular
Macromolecules 40, 8087-8095

92. *Y. Huai, B. Kniesner, A. Sadiki and S. Jakirlić Fachgebiete Energie- Und Kraftwerkstechnik/Strömungslehre und Aerodynamik, Technische Universität Darmstadt*
Large Eddy Simulations of Passive-scalar Mixing using a Tensorial Eddy Diffusivity-based SGS-Modeling.
11th EUROMECH European Turbulence Conference, June 25-28, Porto, Portugal

93. *Z. Harth and H. Sun and M. Schäfer, Department for Numerical Methods in Mechanical Engineering, Technische Universität Darmstadt*
Comparison of Trust-region-based and Evolutionary Methods for Optimization of Flow Geometries
Engineering Optimization, Vol. 39/7, pp. 797-810

94. *Z. Harth and H. Sun and M. Schäfer, Department for Numerical Methods in Mechanical Engineering, Technische Universität Darmstadt*

Comparison of derivative free Newton-based and evolutionary methods for shape optimization of flow problems
Int. Journal for Numerical Methods in Fluids, 53:753–775

95. *Šarić S., Kniesner, B., Altenhöfer, P., Jakirlić, S., Tropea, C., Čavar, D. and Basara, B. Fachgebiet Strömungslehre und Aerodynamik, Technische Universität Darmstadt, Technical University of Denmark, Lyngby und AVL List GmbH Graz, Austria*
Swirl intensity influence on interaction between non-swirling and swirling co-axial jets in a combustor configuration: LES and modelling study.
5th International Symposium on Turbulence and Shear Flow Phenomena (TSFP5), Munich, Germany, August 27-29

96. *Šarić, S., Jakirlić, S., Breuer, M., Jaffrezic, B., Deng, G., Chikhaouui, O., Fröhlich, J., von Terzi, D., Manhart, M. and Peller, N. DFG-CNRS Research Group (Darmstadt, Erlangen, Nant, Karlsruhe, München)*
Evaluation of Detached Eddy Simulations for predicting the flow over periodic hills.
ESAIM Proceedings, Vol. 16 (February), E. Cances and J.-F. Gerbeau (Eds.), pp. 133-145, EDP Sciences, France

97. *Šarić, S., Jakirlić, S., Čavar, D., Kniesner, B., Altenhöfer P. and Tropea, C. Fachgebiet Strömungslehre und Aerodynamik, Technische Universität Darmstadt und Technical University of Denmark, Lyngby*
Computational study of mean flow and turbulence structure in inflow system of a swirl combustor.
Notes on Numerical Fluid Mechanics and Multidisciplinary Design, Vol. 96, Tropea,, C., Jakirlić, S., Heinemann, H.-J., Henke, R. and Hönlinger; H. (Eds.), pp. 462-470, Springer Verlag (ISBN: 978-3-540-74458-0)

98. *F. Hahn, A. Sadiki, J. Janicka, EKT TUD*
Large Eddy Simulation of a Particle Laden Swirling Flow Based on an Eulerian-Lagrangian Approach.
Proc. of the ICMF, vol. 6

99. *P. Carbone, F. Negri, and F. Müller-Plathe, Eduard-Zintl-Institut fuer Anorganische und Physikalische Chemie, Technische Universität Darmstadt, Petersenstrasse 20, D-64287 Darmstadt, Germany*
A Coarse-grained Model for Polyphenylene Dendrimers: Switching and Backfolding
Macromolecules 40, 7044-7055

2008

1. *A. Dobler, B. Ahrens, Institut für Atmosphäre und Umwelt, Goethe-Universität Frankfurt*
Precipitation by a regional climate model and bias correction in Europe and South Asia
Meteorol. Z., 17(4): 499-509

2. *A. Hussien, A. Yakubovich, A. Solov'yov and W. Greiner, Frankfurt Institute for Advanced Studies, Ruth-Moufang-Str. 1, Frankfurt am Main, Germany*
Phase transitions in fullerenes: Fragmentation and reassembly of the carbon cage
http://arxiv.org/abs/0807.4435v1 (2008), Submitted to Phys. Rev. A

3. *A. Mehdizadeh, M. Oberlack, Department of Mechanical Engineering, TU-Darmstadt.*
Study of effects of wall-normal rotation on the turbulent channel flow using DNS.
Proceedings in the iTi Conference on Turbulence III.

4. *A. Mishra, A. Kumar, S. Sanval, S. Schramm, IIT Delhi, CSC and FIAS Frankfurt*
Kaon and antikaon optical potentials isospin asymmetric hyperonic matter
preprint arXiv:0808.1937, submitted to Phys. Rev. C.

5. *A. Mishra, S. Schramm, W. Greiner, IIT Delhi, CSC and FIAS Frankfurt*
Kaons and antikaons in asymmetric nuclear matter
arxiv/nucl-th/0802.363, Phys. Rev. C. in print

6. *A. Nemirowski, H. P. Reisenauer, J. Romanski, G. Mloston, P. R. Schreiner,*
Prototypical Triplet Alkyl Phosphonatocarbenes,
J. Phys. Chem. A 2008, 112, in press.

7. *A.V. Yakubovich, I.A. Solov'yov, A.V. Solov'yov, W. Greiner, Frankfurt Institute for Advanced Studies, Ruth-Moufang-Str. 1, Frankfurt am Main, Germany*
Towards the understanding of structure formation and dynamics in bio-nano systems
European Physical Journal D DOI: 10.1140/epjd/e2008-00126-y (2008).

8. *Akos Rapp, Walter Hofstetter*, and Gergely Zarand*
Trionic phase of ultracold fermions in an optical lattice: A variational study
Phys. Rev. Lett. B 77, 144520

9. *Andrea Nören-Müller, Wolfram Wilk, Krishna Saxena (Goethe Universität Frankfurt), Harald Schwalbe (Goethe Universität Frankfurt), Markus Kaiser, and Herbert Waldmann*
Discovery of a New Class of Mycobacterium tuberculosis Protein Tyrosine Phospatase B Inhibitors by Biology Oriented Synthesis (BIOS)
Angew. Chem. Int Ed Engl., 47, 5973-5977

10. *Andrey Lyalin, Adilah Hussien, Andrey V. Solov'yov, Walter Greiner, Frankfurt Institute for Advanced Studies, Ruth-Moufang-Str. 1, Frankfurt am Main, Germany*
Impurity effects on the melting of Ni clusters
arXiv:0808.1263v1, submitted to Phys. Rev. E

11. *Arnold, A. and Holm, C., FIAS Frankfurt*
Interactions of like-charged rods at low temperatures: Analytical theory vs. simulations.
The European Physical Journal E 27(1)(21-29)

12. *Balzani, D., Gruttmann, F., Schröder, J., Fachgebiet Statik, TU Darmstadt,*
Analysis of thin shells using anisotropic polyconvex energy densities,
Comp. Meth. Appl. Mech. Engrg., 197, 1015-1032

13. *Basara, B., Girimaji, S., Jakirlić, S., Aldudak, F. and Schrefl, M. AVL List GmbH, Graz, Austria, Fachgebiet Strömungslehre und Aerodynamik, Technische Universität Darmstadt, BMW AG, München*
Experiments and calculations relevant to aerodynamic effects during highway passing manoeuvres.
In "The Aerodynamics of Heavy Vehicles II: Trucks, Buses and Trains". Lecture Notes in Applied and Computational Mechanics, Vol. 41, R. McCallen, F. Browand and J. Ross (Eds.), pp. 433-447, Springer Verlag (ISBN: 978-3-540-85069-4)

14. *Bates, B.C., Kundzewicz, Z.W., Wu, S., Palutikof, J.P. (eds.):*
Climate Change and Water. Technical Paper of the Intergovernmental Panel on Climate Change,
IPCC Secretariat, Geneva, 210 pp. (Petra Döll is one of 26 lead authors)

15. *C. Klewer, F. Hahn, C. Olbricht, J. Janicka, EKT TUD*
Hybrid LES/CAA Simulation of a Turbulent Non-Premixed jet Flame
Direct and Large-Eddy Simulations 7

16. *C. Olbricht, F. Hahn, J. Janicka, EKT TUD*
Detailed Numerical Investigation of Sydney Bluff-Body Flames
ETMM 7, pp. 713-718,

17. *Cornelius Weber und Jochen Triesch; Frankfurt Institute for Advanced Studies (FIAS), Johann-Wolfgang Goethe University*
A Sparse Generative Model of V1 Simple Cells with Intrinsic Plasticity
Neural Computation 20:1261-1284

18. *D. Maiti, D.-H. Lee, K. Gaoutchenova, C. Würtele, M. C. Holthausen, A.A. Narducci Sarjeant, J. Sundermeyer, S. Schindler, K. D. Karlin*
Reactions of a Copper(II) Superoxo Complex Lead to C-H and O-H Substrate Oxygenation: Modeling Copper-Monooxygenase C-H Hydroxylation
Angew. Chem. 120, 88

19. *David Roosen*, Maarten Wegewijs and Walter Hofstetter**
Non-equilibrium dynamics of anisotropic large spins in the Kondo regime: Time-dependent numerical renormalization group analysis
Phys. Rev. Lett. 100, 087201

20. *Dommert, Florian and Schmidt, Jochen and Qiao, Baofu and Zhao, Yuanyuan and Krekeler, Christian and Site, Luigi Delle and Berger, Robert and Holm, Christian, FIAS Frankfurt*
A comparative study of two classical force fields on statics and dynamics of [EMIM][BF_4] investigated via molecular dynamics simulations
J. Chem. Phys. 129(22)(224501),

21. *Döll, P., Berkhoff, K., Bormann, H., Fohrer, N., Gerten, D., Hagemann, S., Krol, M.*
Advances and visions in large- scale hydrological modelling: findings from the 11th Workshop on Large-Scale Hydrological Modelling
Adv. Geosci., 18, 51- 61

22. *Döll, P., Fiedler, K.*
Global-scale modeling of groundwater recharge
Hydrol. Earth Syst. Sci., 12, 863–885

23. *Döll, P., Petschel-Held, G., Leemans, R.*
Scale issues in scenario development
In Alcamo, J. (ed.): Environmental Futures: The Practice of Environmental Scenario Analysis. Developments in Integrated Environmental Assessment, 3, Elsevier, 151-168

24. *E. L. Bratkovskaya (FIAS, Frankfrut U.) and W. Cassing (Giessen U.),*
Dilepton production and off-shell transport dynamics at SIS energies,
Nucl. Phys. A 807 (2008) 214-250.

25. *E.L. Bratkovskaya (FIAS, Frankfurt U.), S.M. Kiselev, and G.B. Sharkov (ITEP, Moscow),*
Direct photon production from hadronic sources in high-energy heavy-ion collisions'
Phys. Rev. C 78 (2008) 034905 (10 pages).

26. *E.L. Bratkovskaya (FIAS, Frankfurt U.), W. Cassing (Giessen U.), and O. Linnyk (FIAS, Frankfurt U.),*
Low mass dilepton production at ultrarelativistic energies,
Phys. Lett. B (2008) in press (doi:10.1016/j.physletb.2008.11.034).

27. *F. Hahn, C. Olbricht, J. Janicka, EKT TUD*
Study of Two Swirl Stabilized GT Combustor Devices
ETMM 7, pp. 780-785

28. *Freydank, K. and Siebert, S.*
Towards mapping the extent of irrigation in the last century: time series of irrigated area per country
Frankfurt Hydrology Paper 08. Institute of Physical Geography, University of Frankfurt, Frankfurt am Main, Germany

29. *George Khujadze, Martin Oberlack and George Chagelishvili, Group of Fluid Dynamics, Department of Mechanics, Darmstadt, Germany, Abastumani Astrophysical Observatory, Tbilisi, Georgia*
Stochastically forced laminar plane Couette flow
iTi Conference on Turbulence III, October 12-15, 2008, Italy, ITI2008

30. *George Khujadze, Martin Oberlack, George Chagelishvili, Group of Fluid Dynamics, Department of Mechanics, Darmstadt, Germany, Abastumani Astrophysical Observatory, Tbilisi, Georgia*

DNS of stochastically forced laminar plane Couette flow: peculiarities of hydrodynamic fluctuations
Proceedings in Applied Mathematics and Mechanics, 30 May 2008, GAMM2008

31. *Grass, K. and Böhme, U. and Scheler, U. and Cottet, H. and Holm, C., FIAS Frankfurt*
Importance of Hydrodynamic Shielding for the Dynamic Behavior of Short Polyelectrolyte Chains".
Physical Review Letters 100(096104),

32. *Groll, R., Jakirlić, S. and Tropea, C. ZARM, Universität Bremen und Fachgebiet Strömungslehre und Aerodynamik, Technische Universität Darmstadt*
Comparative study of Euler/Euler and Euler/Lagrange approaches simulating evaporation in a turbulent gas-liquid flow.
Int. J. Numerical Methods in Fluids (published online: www.interscience.wiley.com, DOI: 10.1002/fld.1844)

33. *Gruttmann, F., Pham, V.D., Fachgebiet Statik, TU Darmstadt,*
A finite element model for the analysis of buckling driven delamination of thin films on rigid substrates
Computational Mechanics, 41 (3), 361-370

34. *Hannah Petersen (Frankfurt U., FIAS & Frankfurt U.) , Jan Steinheimer, Gerhard Burau, Marcus Bleicher (Frankfurt U.) , Horst Stocker (Frankfurt U. & Darmstadt, GSI & Frankfurt U., FIAS) .*
A Fully Integrated Transport Approach to Heavy Ion Reactions with an Intermediate Hydrodynamic Stage.
Published in Phys.Rev.C78:044901,2008. e-Print: arXiv:0806.1695 [nucl-th]

35. *Hirabayashi, Y., Kanae, S., Motoya, K., Masuda, K., Döll, P.*
A 59-year (1948-2006) global near-surface meteorological data set for land surface models. Part I: Development of daily forcingand assessment of precipitation intensity
Hydrological Research Letters 2, 36-40

36. *Hosein Ali Karimi-Varzaneh, Paola Carbone, and Florian Müller-Plathe, Eduard-Zintl-Institut für Anorganische und Physikalische Chemie, Technische Universität Darmstadt, Petersenstrasse 20, D-64287 Darmstadt, Germany*
Fast dynamics in coarse-grained polymer models: The effect of the hydrogen bonds
The Journal of Chemical Physics 129, 154904.

37. *Hosein Ali Karimi-Varzaneh, Paola Carbone, and Florian Müller-Plathe, Eduard-Zintl-Institut für Anorganische und Physikalische Chemie, Technische Universität, Darmstadt, Petersenstrasse 20, D-64287 Darmstadt, Germany*
Transferability of coarse-grained force-fields: The polymer case
The Journal of Chemical Physics 128, 064904

38. *Hunger, M., Döll, P.*
Value of river discharge data for global-scale hydrological modeling

Hydrol. Earth Syst. Sci., 12, 841-861

39. *I. Solov'yov, J. Geng, A.V. Solov'yov, and B.F.G Johnson, Frankfurt Institute for Advanced Studies, Ruth-Moufang-Str. 1, Frankfurt am Main, Germany*
On the possibility of the electron polarization to be the driving force for the C60-TMB nanowire growth
Chem. Phys. Lett., submitted (2008).

40. *I. Titvinidze*, M. Snoek*, and W. Hofstetter**
Supersolid Bose-Fermi Mixtures in Optical Lattices
Phys. Rev. Lett. 100, 100401

41. *I.A. Solov'yov, A.V. Yakubovich, A.V. Solov'yov, W. Greiner, Frankfurt Institute for Advanced Studies, Ruth-Moufang-Str. 1, Frankfurt am Main, Germany*
(\)*alpha*-**helix—random coil phase transition: analysis of ab initio theory predictions**
European Physical Journal D 46, 227 (2008).

42. *Ilia A. Solov'yov, Maneesh Mathew, Andrey V. Solov'yov and Walter Greiner, Frankfurt Institute for Advanced Studies, Ruth-Moufang-Str. 1, Frankfurt am Main, Germany*
Liquid surface model for carbon nanotube energetic
Phys. Rev. E 78, 051601 (2008).

43. *J. Geng, I. Solov'yov, W. Zhou, A.V. Solov'yov, and B.F.G Johnson, Frankfurt Institute for Advanced Studies, Ruth-Moufang-Str. 1, Frankfurt am Main, Germany*
Uncovering a Solvent-Controlled Preferential Growth of Buckminsterfullerene (C60) Nanowires
J. Phys. Chem. C, submitted (2008).

44. *J. Geng, I.A. Solov'yov, D.G. Reid, A.E.H. Wheatley, A.V. Solov'yov and B.F.G. Johnson, Frankfurt Institute for Advanced Studies, Ruth-Moufang-Str. 1, Frankfurt am Main, Germany*
The Fullerene-Based C60 TMB Nanowires: Transition from Single Nanocrystals to 1D Nanopolymers
Angew. Chem. Int. Ed., submitted (2008).

45. *J. Kühne, F. Hahn, J.-Y.Chen, J. Janicka, EKT TUD*
Efficient Coupled LES / Transported PDF Approach Using a Second Order Accurate Eulerian Monte-Carlo Scheme
Twelfth International Conference on Numerical Combustion

46. *J. Markmann, V. Yamakov, A. Stukowski, K. Albe and J. Weissmuller*
Intrinsic microstrain in nanocrystalline metals
TMS Proceedings 175 1

47. *J. Steinheimer, M. Bleicher, H. Petersen, S. Schramm, H. Stöcker, D. Zschiesche, CSC, ITP and FIAS Frankfurt*
(3+1)-Dimensional Hydrodynamic Expansion with a Critical Point from Realistic Initial Conditions
Phys. Rev. C 77, 034901

48. *Juan J. Cerdà and Sofia Kantorovich and Christian Holm, FIAS Frankfurt*
Aggregate formation in ferrofluid monolayers: simulations and theory".
J.Physics-Condensed Matter 20(204125),

49. *Juan J. Cerdà and Tomás Sintes and C. Holm and C.M. Sorensen and A.Chakrabarti, FIAS Frankfurt*
Shear effects on crystal nucleation in colloidal suspensions
Phys Rev E 78(031403),

50. *Juan J. Cerdà and V. Ballenegger and O. Lenz and Ch. Holm, FIAS Frankfurt*
P3M algorithm for dipolar interactions.
J. Chem. Phys. 129(234104)

51. *K. Byczuk, W. Hofstetter*, and D. Vollhardt*
Competition between Anderson localization and antiferromagnetism in correlated lattice fermionsystems with disorder
preprint. [arXiv:0810.2958]

52. *K. Ruth, S. Tüllmann, H. Vitze, M. Bolte, H.-W. Lerner, M. C. Holthausen, M. Wagner*
Copper Complexes of Mono- and Ditopic [(Methylthio)methly]borates: Missing Links and Linked Systems En Route to Copper Enzyme Models
Chem. Eur. J. 14, 6754

53. *K. Yapici and B. Karasözen and M. Schäfer and Y. Uludag, Department for Numerical Methods in Mechanical Engineering, Technische Universität Darmstadt*
Numerical Investigation of the Effect of the Rushton Type Turbine Design Factors on Agitated Tank Flow Characteristics
Chemical Engineering & Processing, 47:1346-1355

54. *Klinkel, S., Gruttmann, F., Wagner, W., Fachgebiet Statik, TU Darmstadt,*
A mixed shell formulation accounting for thickness strains and finite strain 3d material models,
Int. J. Num. Meth. Engng., 74, 945-970

55. *Kniesner, B. and Jakirlić, S. Fachgebiet Strömungslehre und Aerodynamik, Technische Universität Darmstadt*
Interface issues in LES/RANS coupling strategies: location, variables exchange and turbulence level adjustment.
5th European Congress on Computational Methods in Applied Sciences and Engineering - ECCOMAS 2008, Venice, Italy, June 30 – July 5

56. *Kundzewicz, Z.W., Mata, L.J., Arnell, N.W., Döll, P., Jimenez, B., Miller, K., Oki, T., Sen, Z., Shiklomanov, I.*
The implications of projected climate change for freshwater resources and their management
Hydrological Sciences Journal, 53(1), 3-10

57. *L.V. Bravina et al.*

Microscopic models and effective equation of state in nuclear collisions at FAIR energies.
Published in Phys.Rev.C78:014907,2008. e-Print: arXiv:0804.1484 [hep-ph]

58. *Lenz, O. and Holm, C., FIAS Frankfurt*
Simulation of charge reversal in salty environments: Giant overcharging?.
Eur. Phys. J. E 26(191-195),

59. *M. Harmata, C. Huang, P. Rooshenas, P. R. Schreiner,*
An Interrupted [4+3] Cycloaddition Reaction: A Hydride Shift (Ene Reaction) Intervenes13,
Angew. Chem. 2008, 120, 8824.

60. *M. Heck, Department for Numerical Methods in Mechanical Engineering, Technische Universität Darmstadt*
Mehrgitterverfahren zur effizienten numerischen Simulation von Fluid-Struktur-Wechselwirkungen
Dissertation

61. *M. Kornhaas and D. C. Sternel and M. Schäfer, Department for Numerical Methods in Mechanical Engineering, Technische Universität Darmstadt*
Influence of time step size and convergence criteria on large eddy simulations with implicit time discretization
In Collection, Quality and Reliability of Large-Eddy Simulations, Berlin

62. *M. Snoek*, I. Titvinidze*, C. Toke*, K. Byczuk, and W. Hofstetter**
Antiferromagnetic Order of Strongly Interacting Fermions in a Trap: Real-Space Dynamical Mean-Field Analysis
New J. Phys. 10, 093008

63. *M.I. Gorenstein (BITP, Kiev), M. Hauer, V.P. Konchakovski (H-QM, Frankfurt U.) , E.L. Bratkovskaya (FIAS, Frankfurt U.),*
Fluctuations of the K/ Ratio in Nucleus-Nucleus Collisions: Statistical and Transport Models,
submitted to Phys. Rev. C (2008) arXiv:0811.3089 [nucl-th].

64. *Maurizio Pellecchia, Ivano Bertini, David Cowburn, Claudio Dalvit, Ernest Giralt, Wolfgang Jahnke, Thomas L. James, Steve W. Homans, Horst Kessler, Claudio Luchinat, Bernd Meyer, Hartmut Oschkinat, Jeff Peng, Harald Schwalbe (Goethe Universität Frankfurt), Gregg Siegal*
Perspectives on NMR in Drug Discovery: A Technique Comes of Age
Nature Rev. Drug Discovery, 7, 758-745

65. *Mohammad Alagemandi, Elena Algaer, Michael C. Böhm, and Florian Müller-Plathe, Eduard-Zintl-Institut fuer Anorganische und Physikalische Chemie, Technische Universität Darmstadt, Petersenstrasse 20, D-64287 Darmstadt, Germany*
Thermal Conductivity and Thermal Rectification of Carbon Nanotubes by Reverse Non-equilibrium Molecular Dynamics Simulations
Submitted to Nanotechnology.

66. *N. Armesto, (ed.) et al.*
Heavy Ion Collisions at the LHC - Last Call for Predictions.
Published in J.Phys.G35:054001,2008. e-Print: arXiv:0711.0974 [hep-ph]

67. *O. Linnyk, E.L. Bratkovskaya (FIAS, Frankfurt U.), W. Cassing (Giessen U.),*
Charmed hadron signals of partonic medium,
Proceedings of the International Conference Strangeness in Quark Matter, 6 - 10 Oct 2008, Beijing, China, J. Phys. G 35 (2008) in press, arXiv:0810.4257 [nucl-th].

68. *O. Linnyk, E.L. Bratkovskaya (FIAS, Frankfurt U.), W. Cassing (Giessen U.), H. Stoecker (FIAS, Frankfurt Uni. & GSI),*
Charmonium dynamics in heavy ion collisions,
Proceedings of the International Conference Strangeness in Quark Matter, 24 - 29 June 2007, Levoca, Slovakia. J. Phys. G 35 (2008) 044037.

69. *O. Linnyk, E.L. Bratkovskaya (FIAS, Frankfurt U.), and W. Cassing (Giessen U)*
Open and hidden charm in proton-nucleus and heavy-ion collisions
Int. J. Mod. Phys. E 17 (2008) 1367-1439.

70. *O. Linnyk, E.L. Bratkovskaya (FIAS, Frankfurt U.), and W. Cassing (Giessen U.),*
Evidence for non-hadronic interactions of charm degrees of freedom in heavy-ion collisions at relativistic energies,
Nucl. Phys. A 807 (2008) 79-104.

71. *O. Sander, A. Henß, C. Näther, C. Würtele, M. C. Holthausen, S. Schindler, F. Tuczek*
Aromatic Hydroxylation in a Copper Bis(imine) Complex Mediated by a -2-2 Peroxo Dicopper Core: A Mechanistic Scenario
Chem. Eur. J. 14, 9714

72. *Oliver Kolb, Jens Lang, Pia Bales, Technische Universität Darmstadt, Fachbereich Mathematik*
Adaptive linearization for the optimal control problem of gas flow in pipeline networks
Technische Universität Darmstadt, FB Mathematik, Preprint Nr. 2553,

73. *Oliver Kolb, Pia Bales, Jens Lang, Technische Universität Darmstadt, Fachbereich Mathematik*
Moving Penalty Functions for Optimal Control with PDEs on Networks
Technische Universität Darmstadt, FB Mathematik, Preprint Nr. 2562,

74. *Omori, T., Jakirlić, S., Tropea, C. and Obi, S. Fachgebiet Strömungslehre und Aerodynamik, Technische Universität Darmstadt und Keio University, Yokohama, Japan*
Shearless and sheared flow past a circular cylinder: comparative analysis by means of LES.
Int. J. Heat and Fluid Flow, Vol. 29, No. 3, pp. 703-720

75. *P. Carbone, H. A. Karimi Varzaneh, X.Y. Chen and F. Müller-Plathe, Eduard-Zintl-Institut fuer Anorganische und Physikalische Chemie, Technische Universität Darmstadt, Petersenstrasse 20, D-64287 Darmstadt, Germany*

Transferability of coarse-grained force fields: the polymer case
J. Chem. Phys. 128, 064904(1-11)

76. *P. Milko, J. Roithová, D. Schröder, J. Lemaire, H. Schwarz, M. C. Holthausen*
The Phenoxy/Phenol/Copper Cation: A Minimalistic Model of Bonding Relations in Active Centers of Mononuclear Copper Enzymes
Chem. Eur. J. 14, 4318

77. *P. Pironkov and M. Schäfer and K. Krastev, Department for Numerical Methods in Mechanical Engineering, Technische Universität Darmstadt*
Properties of discrete Chebychev collocation differential operators in curvilinear geometries
Numerical Linear Algebra with Applications, 15:701-716

78. *P. R. Schreiner, H. P. Reisenauer,*
Spectroscopic Identification of Dihydroxycarbene,
Angew. Chem. Int. Ed. 2008, 47, 7071.

79. *P. R. Schreiner, H. P. Reisenauer, F. Pickard, A. C. Simmonett, W. D. Allen, E. Matyus, A. G. Csaszar,*
Capture of Elusive Hydroxymethylene and its Fast Disappearance through Tunnelling,
Nature 2008, 453, 906.

80. *Pia Bales, Björn Geißler, Oliver Kolb, Jens Lang, Alexander Martin, Antonio Morsi, Technische Universität Darmstadt, Fachbereich Mathematik*
Comparison of Linear and Nonlinear Optimization of Transient Gas Networks
Technische Universität Darmstadt, FB Mathematik, Preprint Nr. 2552,

81. *Pia Bales, Oliver Kolb, Jens Lang, Technische Universität Darmstadt, Fachbereich Mathematik*
Hierarchical modelling and model adaptivity for gas flow on networks
Technische Universität Darmstadt, FB Mathematik, Preprint Nr. 2554,

82. *Portmann, F., Siebert, S., Bauer, C. and Döll, P.*
Global data set of monthly growing areas of 26 irrigated crops
Frankfurt Hydrology Paper 06. Institute of Physical Geography, University of Frankfurt, Frankfurt am Main, Germany

83. *Qiao, B. and Krekeler, C. and Berger, R. and DelleSite, L. and Holm, C., FIAS Frankfurt*
Effect of Anions on Static Orientational Correlations, Hydrogen Bonds, and Dynamics in Ionic Liquids: A Simulational Study.
J. Phys. Chem. B 112(6)(1743-1751),

84. *Qingfeng Li (Frankfurt U., FIAS) , Marcus Bleicher (Frankfurt U.) , Horst Stocker (Frankfurt U., FIAS & Frankfurt U. & Darmstadt, GSI) .*
Transport model study of the m(T)-scaling for Lambda, K, and pi HBT-correlations.
Published in Phys.Lett.B663:395-399,2008. e-Print: arXiv:0802.3618 [nucl-th]

85. *R. Pasquetti and E. Severac and E. Serre and P. Bontoux and M. Schäfer, Department for Numerical Methods in Mechanical Engineering, Technische Universität Darmstadt*
From stratified wakes to rotor-stator flows by a SVV-LES method
Theoretical and Computational Fluid Dynamics, 22:261-273

86. *Reising S., Schiffer H.-P.: Fachgebiet Gasturbinen, Luft- und Raumfahrtantriebe, Fachbereich 16, TU-Darmstadt*
Automated Aerodynamic Optimisation of a Transonic Compressor Stage by Application of non-axisymmetric endwalls
DGLR Jahrestagung, Dokument ID81252

87. *S. Haussler, S. Scherer (Frankfurt U., FIAS) , M. Bleicher (Frankfurt U.) .*
Correlations and fluctuations of conserved charges in a dynamical recombination approach.
Published in J.Phys.G35:044066,2008.

88. *S. M. Kast, T. Kloss, TU Darmstadt*
Closed-Form Expressions of the Chemical Potential for Integral Equation Closures with Certain Bridge Functions",
J. Chem. Phys., in press

89. *S. Tayefeh, T. Kloss, M. Kreim, M. Gebhardt, D. Baumeister, B. Hertel, C. Richter, H. Schwalbe, A. Moroni, G. Thiel, S. M. Kast, TU Darmstadt, Universität Frankfurt, Universität Mailand*
Model Development for the Viral Kcv Potassium Channel,
Biophys. J., in press

90. *S. Yigit and M. Schäfer and M. Heck, Department for Numerical Methods in Mechanical Engineering, Technische Universität Darmstadt*
Grid movement techniques and their influence on laminar fluid structure interaction computations
Journal of Fluids and Structures, Vol. 24/6, pp. 819 – 832

91. *Schürg, M., Gruttmann, F., Fachgebiet Statik, TU Darmstadt,*
A finite element formulation for the analysis of interlaminar shear stresses in layered composite plates,
PAMM-Proceedings in Applied Mathematics and Mechanics, submitted,

92. *Siebert, S. and Döll, P.*
The Global Crop Water Model (GCWM): Documentation and first results for irrigated crops
Frankfurt Hydrology Paper 07. Institute of Physical Geography, University of Frankfurt, Frankfurt am Main, Germany

93. *Sofia Kantorovich and Juan J. Cerdà and Christian Holm, FIAS Frankfurt*
Microstructure analyisis of monodisperse ferrofluid monolayers: theory and simulation.
Physical Chemistry Chemical Physics 10(14)(1883-1895),

94. *T. J. Müller, M. Al-Samman, and F. Müller-Plathe, Eduard-Zintl-Institut fuer Anorganische und Physikalische Chemie, Technische Universität Darmstadt, Petersenstrasse 20, D-64287 Darmstadt, Germany*
The influence of thermostats and manostats on reverse non-equilibrium molecular dynamics calculations of fluid viscosities
J. Chem. Phys. 129, 014102

95. *T. Kloss, J. Heil, S. M. Kast, TU Darmstadt*
Quantum Chemistry in Solution by Combining 3D Integral Equation Theory with a Cluster Embedding Approach
J. Phys. Chem. B 112, 4337-4343

96. *T. Kloss, S. M. Kast, TU Darmstadt*
Treatment of Charged Solutes in Three-dimensional Integral Equation Theory
J. Chem. Phys. 128, 134505

97. *T. Weil, M. Kotke, C. M. Kleiner, P. R. Schreiner,*
Cooperative Bronsted Acid-Type Organocatalysis: Alcoholysis of Styrene Oxides,
Org. Lett. 2008, 10, 1513.

98. *Titz, A., Döll, P.*
Actor modelling and its contribution to the development of integrative strategies for management of pharmaceuticals in drinking water
Social Science & Medicine. (in press)

99. *U. Bissbort* and W. Hofstetter**
Stochastic Mean-Field Theory for the Disordered Bose-Hubbard Model
preprint. [arXiv:0804.0007]

100. *V. Ballenegger and J. J. Cerdà and O. Lenz and Ch. Holm, FIAS Frankfurt*
The optimal P3M algorithm for computing electrostatic energies in periodic systems
J. Chem. Phys. 128(3)(034109),

101. *V. Dexheimer and S. Schramm, CSC and FIAS Frankfurt*
Proto-Neutron and Neutron Stars in a Chiral SU (3) Model
Astrophys. Journal, in print.

102. *V. Dexheimer, G. Pagliara, L. Tolos, J. Schaffner-Bielich, S. Schramm CSC and FIAS Frankfurt*
Neutron Stars within the SU(2) Parity Model
arxiv/nucl-th/0805.3301, Eur. Phys. J., accepted for publication

103. *V. Dexheimer, S. Schramm, and D. Zschiesche, CSC, ITP and FIAS Frankfurt*
Nuclear Matter and Neutrons Stars in a Parity Doublet Model
Phys. Rev. C 77, 025803

104. *V. P. Konchakovski (H-QM, Frankfurt U.), B. Lungwitz (Frankfurt U.), M. I. Gorenstein (BITP, Kiev), and E. L. Bratkovskaya (FIAS, Frankfurt U.),*
Multiplicity Fluctuations in Nucleus-Nucleus Collisions: Dependence on Energy and Atomic Number,
Phys. Rev. C 78 (2008) 024906 (14 pages).

105. *W. Cassing (Giessen U.) and E.L. Bratkovskaya (FIAS, Frankfurt U.),*
Parton transport and hadronization from the dynamical quasiparticle point of view,
Phys. Rev. C 78 (2008) 034919 (8 pages).

106. *W. Cassing (Giessen U.),*
From Kadanoff-Baym dynamics to off-shell parton transport,
lecture notes of the Schladming Winter School on 'Nonequilibrium Aspects of Quantum Field Theory'; to be published in a special issue of Eur. Phys. J, arXiv:0808.0715 [nucl-th]

107. *W. Cassing (Giessen U.), E.L. Bratkovskaya (FIAS, Frankfurt U.), Y.-.Z. Xing (Tianshui Normal Coll.),*
Parton dynamics and hadronization from the sQGP,
Proceedings of the Erice School/Workshop on Nuclear Physics 2008, Sep. 2008, Erice, Italy, Prog. Part. Nucl. Phys. (2008) in press, arXiv:0810.2804 [nucl-th]

108. *Wackerfuß, J., Gruttmann, F., Fachgebiet Statik, TU Darmstadt,*
A mixed hybrid finite beam Element with an interface to arbitrary three-dimensional material models,
Comp. Meth. Appl. Mech. Engrg., submitted,

109. *Wei Zhao, Frederic Leroy, Sundaram Balasubramanian, and Florian Müller-Plathe, Eduard-Zintl-Institut fuer Anorganische und Physikalische Chemie, Technische Universität Darmstadt, Petersenstrasse 20, D-64287 Darmstadt, Germany*
Shear Viscosity of the Ionic Liquid 1-n-Butyl 3-Methylimidazolium Hexafluorophosphate [bmim][PF] Computed by Reverse Nonequilibrium Molecular Dynamics
Journal of Physical Chemistry B, 112(27), 8129-8133.

110. *Z. Harth, Department for Numerical Methods in Mechanical Engineering, Technische Universität Darmstadt*
Automated Numerical Shape Optimization of 3-dimensional Flow Geometry Configurations
Dissertation

111. *Zhang, J., Döll, P.*
Assessment of ecologically relevant hydrological change in China due to water use and reservoirs
Adv. Geosci., 18, 25-30

112. *van Hinsberg, N.P., Berberović, E., Roismann, I., Jakirlić, S. and Tropea, C. Fachgebiet Strömungslehre und Aerodynamik, Technische Universität Darmstadt*

Complementary experimental and computational study of a drop impacting a shallow pool.
23th Annual Int. Conf. on Liquid Atomization and Spray Systems - ILASS, Como Lake, Italy, September 6-8

113. *Šarić, S, Kniesner, B., Mehdizadeh, A., Jakirlić, S., Hanjalić, K. and Tropea, C. Fachgebiet Strömungslehre und Aerodynamik, Technische Universität Darmstadt*
Comparative assessment of hybrid LES/RANS models in turbulent flows separating from smooth surfaces.
In Ädvances in Hybrid RANS-LES Modelling". Notes on Numerical Fluid Mechanics and Multidisciplinary Design, Vol. 97, S.-H. Peng and W. Haase (Eds.), pp. 142-151, Springer Verlag (ISBN: 978-3-540-77813-4)

114. *D. C. Sternel and M. Schäfer and M. Heck and S. Yigit, Department for Numerical Methods in Mechanical Engineering, Technische Universität Darmstadt*
Efficiency and accuracy of fluid-structure interaction simulations using an implicit partitioned approach
Computational Mechanics, DOI: 10.1007/s00466-008-0278-y

115. *Stefan Scherer, Marcus Bleicher (Frankfurt U.) , Stephane Haussler (Frankfurt U., FIAS) , Horst Stocker (Frankfurt U. & Frankfurt U., FIAS) .*
Population of multi-quark states in exotic multiplets and thermalization in ultra-relativistic heavy ion collisions.
Published in Int.J.Mod.Phys.E17:965-1014,2008.

116. *J. Kotakoski, K. Albe*
First-principles calculations on solid nitrogen: A comparative study of high-pressure phases
Phys. Rev. B 144109, 77

117. *P. Erhart, K. Albe*
Modeling the electrical conductivity in BaTiO3 on the basis of first-principles calculation
J. Appl. Phys. 044315, 04

118. *R.A. Eichel, P. Erhart, P.Träskelin, K. Albe, H. Kungl, M.J. Hoffmann*
Defect-dipole formation in copper-doped PbTiO3 ferroelectrics
Phys. Rev. Lett. 095504 100

119. *Z.-H. Jin, P. Gumbsch, K. Albe, E. Ma, K. Lu, H. Gleiter, H. Hahn*
Interactions between non-screw lattice dislocations and coherent twin boundaries in face-centered cubic metals
Acta Mat. 1126 56

120. *V. Dexheimer, S. Schramm, H. Stöcker, CSC and FIAS Frankfurt*
Neutron Stars in a Chiral Model with Finite Temperature
J.Phys.G35:014060

2009 (in print)

1. *A. Stukowski, J. Markmann, J. Weissmuller K. Albe*
   Atomistic origin of microstrain broadening in diffraction data of nanocrystalline solids
   Acta Materialia, accepted

2. *Basara, B., Jakirlić, S., Aldudak, F. and Tropea, C. Fachgebiete Strömungslehre und Aerodynamik/Strömungsdynamik, Technische Universität Darmstadt*
   Truck interference effects on a car during an overtaking manoeuvre: a computational study.
   Notes on Numerical Fluid Mechanics and Multidisciplinary Design (under consideration for publication)

3. *Berberović, E., van Hinsberg, N.P., Jakirlić, S., Roismann, I. and Tropea, C., Fachgebiet Strömungslehre und Aerodynamik, Technische Universität Darmstadt*
   Drop impact onto a liquid layer: cavity shape and propagation of a solitary wave.
   Physical Review Letter E (under consideration for publication)

4. *Jakirlić, S. Šarić, S., Kadavelil, G., Sirbubalo, E., Basara, B. and Chaouat, B. Fachgebiet Strömungslehre und Aerodynamik, Technische Universität Darmstadt, AVL List GmbH Graz, Austria, ONERA Paris*
   SGS modelling in LES of wall-bounded flows using SMC and related RANS closures: towards a seamless hybrid LES/RANS method.
   6th International Symposium on Turbulence and Shear Flow Phenomena (TSFP6), Seoul, Korea, June 22-24

5. *Jakirlić, S., Eisfeld, B. and Basara, B. Fachgebiet Strömungslehre und Aerodynamik, Technische Universität Darmstadt, DLR Braunschweig und AVL List GmbH Graz, Austria*
   Performance Assessment of Some Popular RANS Models by Relevance to High-lift Aerodynamics.
   47th AIAA Aerospace Sciences Meeting, Orlando, FL, USA, January 5-8, Paper No. AIAA-2009-0049

6. *Jakirlić, S., Eisfeld, B., Jester-Zürker, R., Tropea, C. and Kroll, N. Fachgebiet Strömungs¸-lehre und Aerodynamik, Technische Universität Darmstadt und DLR, Braunschweig*
   Computational Modelling of Transonic Aerodynamic Flows using Near-Wall, Reynolds Stress Transport Models.
   In "MEGADESIGN and MegaOpt - Aerodynamic Simulation and Optimization in Aircraft Design". Notes on Numerical Fluid Mechanics and Multidisciplinary Design, Kroll, N., Schwamborn, D., Becker, K., Rieger, H., Thiele, F. (Eds.), Springer Verlag (in press)

7. *Jakirlić, S., Manceau, R., Šarić, S., Fadai-Ghotbi, A., Kniesner, B., Carpy, S., Kadavelil, G., Friess, C., Tropea, C. and Boree, J. Fachgebiet Strömungslehre und Aerodynamik, Technische Universität Darmstadt und LEA, University of Poitiers, France*

LES, Zonal and Seamless Hybrid LES/RANS: Rationale and Application to Free and Wall-Bounded Flows involving Separation and Swirl.
Notes on Numerical Fluid Mechanics and Multidisciplinary Design (in press)

8. *Kniesner, B., Kadavelil, G., Gnirß, M., Jakirlić, S. and Tropea, C.Fachgebiet Strömungslehre und Aerodynamik, Technische Universität Darmstadt*
Experimental and computational investigations of flow and mixing in a single-annular combustor configuration.
Flow, Turbulence and Combustion (under consideration for publication)

9. *Sirbubalo, E., Kinzel, M. Jakirlić, S. and Tropea, C. Fachgebiet Strömungslehre und Aerodynamik, Technische Universität Darmstadt*
Experimental and modelling study of turbulence diffusion under zero-mean-flow conditions.
6th International Symposium on Turbulence and Shear Flow Phenomena (TSFP6), Seoul, Korea, June 22-24

10. *Sridhar Sreeamulu, Hendrik R.A. Jonker, Thomas Langer, Christian Richter, C. Roy D. Lancaster, Harald Schwalbe (Goethe Universität Frankfurt)*
The human CDC37-HSP90 Complex studied by heteronuclear NMR spectroscopy
J. Biol. Chem., in press

11. *T.T. Järvi, D. Pohl, K. Albe, B. Rellinghaus, L. Schultz, J. Fassbender, A. Kuronen and K. Nordlund*
From multiply twinned to fcc nanoparticles via irradiation-induced transient amorphization
Europhysics Letters, accepted